2016

Ecological-Hydrological Feedback in Forested Wetlands

Scott Thomas Allen
Louisiana State University and Agricultural and Mechanical College

ECOLOGICAL-HYDROLOGICAL FEEDBACK IN FORESTED WETLANDS

A Dissertation

Submitted to the Graduate Faculty of the
Louisiana State University and
Agricultural and Mechanical College
in partial fulfillment of the
requirements for the degree of
Doctor of Philosophy

in

The School of Renewable Natural Resources

by
Scott T. Allen
B.S., University of Maryland, 2009
M.S., Oregon State University, 2012
August 2016

ACKNOWLEDGEMENTS

Numerous individuals, funders, institutions have made this dissertation possible. This work was completed under advisement by Richard F. Keim, with committee: Michele L. Reba, Thomas J. Dean, Sammy L. King, and Ken W. Krauss. Components of the field data presented here were by efforts of J. Wesley Cochran, Brandon L. Edwards, and Blake Amos. Colleagues Mary Grace T. Lemon, Yu-Hsin Hsueh, Erin L. Johnson, Whitney A. Kroschel, Clay Lovelace, Margaret Whitsell, Emily Oakman, Marcus Rutherford, Jim L. Chambers, William H. Conner, Jamie A. Duberstein, April L. Hiscox, Alex G. McCombs, Mike Kaller, and Kevin Armbrust have also have helped in lab work, field work, discussions, and other elements of the process. Several anonymous reviewers have helped improve upon some of the work presented here. I have benefited from the luxury of a life situation that enabled me to pursue this degree with my fullest effort; this is due to contributions from friends and family that are too many to count, but I do not discount any.

Funding has been provided primarily by the Lucius W. Gilbert Foundation, but also by CUAHSI, Sigma Xi, The Wetland Foundation, and the U.S. Army Corps of Engineers, Memphis District. The USGS Climate and Landuse Change R&D Program and USGS Environments Program also provided equipment and personel support. I also thank Louisiana Department of Wildlife and Fisheries, Williams Inc, Natural Resources Professionals LLC, Arkansas Natural Heritage, and the Dale Bumpers White River National Wildlife Refuge for facilitating research site access. I also thank the faculty and staff of LSU and the School of Renewable Natural Resources for support.

TABLE OF CONTENTS

LIST OF TABLES

LIST OF FIGURES

ABSTRACT

In forested wetlands, the biotic and abiotic consequences of water level variability is not well understood. The effects of flooding on carbon and water exchanges are important knowledge gaps where progress could benefit management of natural resources and predicting of changes in surface geophysical cycles. Two specific needs are a better understanding of (1) wetland tree responses to hydrologic variations, and (2) the effects of the forest and associated tree stressors on surface energy and water fluxes. Objectives were to determine effects of flooding on evaporation rates and energy dynamics, tree water use and growth responses to river-floodplain connectivity and water level variability, and interactions between tree-level and site-level effects of flooding. Energy-balance measurements in the understory of a permanently flooded swamp showed nearly all energy was partitioned to latent heat, yielding evaporation rates of 0.9-2.0 mm day^{-1} among months assessed; the seasonal pattern of canopy senescence superimposed upon the pattern of heat storage in the floodwater resulted in highest evaporation rates in October and November, out of phase with above-canopy solar forcing. Evaporation from open water was similar to that from floating vegetation. Tree sapflow measurements in a floodplain forest showed increased transpiration in response to a late season flood pulse at a more flooded site, while, concurrently, transpiration declined at a drier site. The more flood tolerant species (*Quercus lyrata*) benefited more from flooding than did the less tolerant species (*Celtis laevigata*), but neither species showed flood stress. To examine radial growth responses to water levels in forested wetlands, a model (VSL-Wet) was developed and calibrated across six baldcypress chronologies. Best model fits were obtained with parameters that suggest permanently flooded trees may benefit from deeper flooding. Last, measurements across differently flooded sites showed that more flooded sites had sparser forests but with higher growth efficiency trees, demonstrating the need to consider tree-level responses separate from stand-level patterns. Consistent with common assumptions, this work shows that abiotic and biotic parameters of forested wetlands, including carbon and water fluxes, are influenced by hydrologic variations; however, consequences of hydrologic influences are not universal across scales.

CHAPTER 1: INTRODUCTION

1.1 BACKGROUND

In wetlands, hydrologic variability and ecosystem functions are related; for example, this relationship has been demonstrated in coastal marshes (Gedan et al., 2010), freshwater marshes (Odum, 1988), swamps (Mitsch and Ewel, 1979), and floodplain forests (Wharton et al., 1982). Much interest in wetland ecosystem functions arises from the ecosystem services provisioned by those functions (e.g., biogeochemical processing, primary productivity, and landscape structure result in carbon storage, nutrient removal, habitat value, and coastal resilience). Perhaps the majority of wetland research has focused on quantifying these system functions, and relating them to patterns in environmental stimuli—especially hydrologic variability. However, without identifying mechanistic links between drivers and responses, predictive capability of ecosystem functions is limited. Thus, to complement measurements of net effects of ecological functions, we need to understand the underlying mechanisms for such effects and at what spatial and temporal scales they are important. This research need includes responses to hydrologic variability but also the factors responsible for hydrologic variability.

Vegetation exerts strong control over water and carbon dynamics in wetlands, at multiple spatial and temporal scales. Evapotranspiration (ET) is often the largest water efflux in wetlands (Linacre et al., 1970; Mitsch and Gosselink, 2007). Globally, transpiration is the largest component of ET (Schlesinger and Jasechko, 2014). As the predominant primary producer, vegetation is obviously important to carbon dynamics. Thus water and carbon exchanges are linked through vegetation. Both of these exchanges mostly occur at the leaf, through stomata that simultaneously affect the rate of water leaving leaves and the rate of carbon dioxide entering. Environmental variability, and particularly stress responses, can result in changes to the conductance through stomata, governing exchange rates.

For wetland vegetation, relatively little is known about stress responses or growth responses to water variability. Most of our conceptual understanding of plant-water dynamics is with respect to the premise that increasing water tension reduces conductance and limits transpiration (Slatyer, 1967); such models unlikely apply in wetlands where water excess can be a stressor. Several early studies using lysimeters found ET rates from wetland vegetation exceeded open-water ET (reviewed by Abtew and Melesse, 2013; Allen et al., 1997; Crundwell, 1986), suggesting weak stomatal control of fluxes. Idso (1981) concluded that these rates are not good indicators of actual ET and were an artifact of experimental design. Even extensive wetlands in arid regions may not show especially high ET (Baldocchi et al., 2016; Nagler et al., 2003). Regardless, results of those lysimeter studies exhibit a potential for wetland plants to have high conductance. However, effects by and controls over carbon and water exchanges for an ecosystem or a landscape are moderated by energy, atmospheric exchange, and a complex suite of ecophysiological processes (Chapin et al., 2002; Oke, 1988).

In forested wetlands, it has been posited that flooding can limit plant exchange of water and carbon, and, consequently, reduce growth. Wetland trees must be relatively flood tolerant and may persist though long periods of deep flooding or drought, often facilitated by morphologic adaptations (Kozlowski, 1997). However, as in upland plants, gas exchange and leaf conductance measurements of wetland tree seedlings have shown that flooding or drought can decrease stomatal conductance and physiological functions (Anderson and Pezeshki, 2001; Gardiner and Hodges, 1996; McLeod et al., 1986; Nash and Graves, 1993; Pezeshki and Anderson, 1996; Pezeshki and Chambers, 1986, 1985). Tree ring studies have shown both

positive and negative correlations between growth and water level variations at annual and longer time scales (Copenheaver et al., 2007; Golet, 1993; Ford and Brooks, 2002; Keim and Amos, 2012; Mitsch and Rust, 1984; Young et al., 1995). Deep or sustained flooding often results in reduced stand production (e.g., Conner et al., 2014; Megonigal et al., 1997; Mitsch et al., 1991). Synthesis of the evidence above, obtained from multiple approaches at multiple scales, ostensibly suggests that flooding can be an important stimulus to tree function, often with inhibitory effects.

While these prior studies are useful for understanding hydrologic effects on wetland trees at certain scales, there are limitations to inferring controls over carbon and water exchanges from them. Regarding tree responses to hydrologic variability, seedling stress responses do not necessarily parallel those of mature trees, analytical approaches of tree rings do not account for the likely nonlinear responses to flooding, and stand-level production measurements do not necessarily indicate ecophysiological responses to environmental conditions. Regarding ET specifically, the likelihood of extreme rates may be theoretically dismissable, but deeper understanding requires identifying what drivers spatial and temporal variability in ET. Previous characterizations of the general magnitudes of these terms are coarse (Brown, 1981; Liu, 1996, and others reviewed in Mitsch and Gosselink 2007).

This dissertation focuses on tree responses to water variability and how the trees and forests affect water level variability in forested wetlands. While wetland vegetation has other effects on wetland hydrological processes (e.g., surface hydraulic resistances; Kadlec, 1990), tree responses and ET are my focus here. In addition to tree responses being unlike upland forests, the hydrologic characteristics also directly affect energy storage and fluxes. Wetland evaporation likely shares commonalities with both upland understory energy budgets (Baldocchi et al., 2000; Wilson et al., 2000) and lake energy budgets (Ragotzkie, 1978), but with neither as an appropriate base model. Interception loss by wet canopy evaporation also occurs (Carlyle-Moses and Gash, 2011) but are not focused on because concepts from upland forests are likely transferrable.

Understanding of controls over both carbon and water dynamics is particularly important in forested wetlands, but these processes are complex and are a product of countless feedbacks in the soil-plant-atmosphere-continuum. Positive feedbacks are particularly important because a small perturbation to any of the components involved could result in large effects, including trending towards a different stable state. For example, a particularly important and relevant feedback could be between water levels and vegetation water use. If flood stress could result in lower evapotranspiration, and evapotranspiration is a control over water levels, there is potential for an unstable feedback cycle with a trajectory towards wetter conditions in that wetland. The objective of this dissertation is to further our understanding of water-vegetation interactions in forested wetlands, approaching this task from a physical, biological, and ecological viewpoint.

Progress on the basic questions of how wetland conditions cause tree stress and and how these factors integrate into system-level moisture and carbon exchanges are critical for predicting effects of climate change, managing water resources, and understanding the consequences of perturbations to the hydrologic or ecologic landscape. Consideration of this potrentialunderlying feedback cycles between flooding, vegetation stress, and evaporation and transpiration fluxes provides impetus to focus on how the functions and controls over individual components define aggregated effects.

Specific objectives of this research are:

- to develop a physical understanding of the subcanopy energy budget, microclimatic conditions, and resulting ET dynamics in a flooded forested wetland (Chapter 2);

- to determine the role of floating vegetation on subcanopy evaporation (Chapter 3);

- to investigate how connectivity driven water table variations and species differences (between a more flood-tolerant species and less flood-tolerant wetlands species) affect tree water use and phenology (Chapter 4);

- to investigate the characteristics and generalizability of hydrologic controls over wetland tree growth through developing a model for extracting hydrologic growth response functions from dendrochronological records of wetland trees (Chapter 5);

- to provide base-line measurements of baldcypress leaf, crown, and canopy morphometrics (Chapter 6); and

- to examine effects of flooding on stand production with separating tree-level effects from stand-level effects (Chapter 7)

1.2 REFERENCES

Abtew, D.W., Melesse, P.D.A., 2013. Wetland Evapotranspiration, in: Evaporation and Evapotranspiration. Springer Netherlands, pp. 93–108.

Allen, L.H., Jr., Sinclair, T.R., Bennett, J.M., 1997. Evapotranspiration of vegetation of Florida: perpetuated misconceptions versus mechanistic processes. Proc. - Soil Crop Sci. Soc. Fla. 56, 1–10.

Anderson, P.H., Pezeshki, R., 2001. Effects of flood pre-conditioning on responses of three bottomland tree species to soil waterlogging. J. Plant Physiol. 158, 227–233. doi:10.1078/0176-1617-00267

Baldocchi, D.D., Knox, S., Dronova, I., Verfaillie, J., Oikawa, P., Sturtevant, C., Matthes, J.H., Detto, M., 2016. The impact of expanding flooded land area on the annual evaporation of rice. Agric. For. Meteorol. 223, 181–193. doi:10.1016/j.agrformet.2016.04.001

Baldocchi, D.D., Law, B.E., Anthoni, P.M., 2000. On measuring and modeling energy fluxes above the floor of a homogeneous and heterogeneous conifer forest. Agric. For. Meteorol. 102, 187–206. doi:10.1016/S0168-1923(00)00098-8

Bond, B.J., Meinzer, F.C., Brooks, J.R., 2008. How trees influence the hydrological cycle in forest ecosystems, in: Lecturer, P.J.W.S., Lecturer, D.M.H.S., Reader, J.P.S. (Eds.), Hydroecology and Ecohydrology. John Wiley & Sons, Ltd, pp. 7–35.

Brown, S., 1981. A Comparison of the Structure, Primary Productivity, and Transpiration of Cypress Ecosystems in Florida. Ecol. Monogr. 51, 403–427. doi:10.2307/2937322

Carlyle-Moses, D.E., Gash, J.H., 2011. Rainfall interception loss by forest canopies, in: Forest Hydrology and Biogeochemistry. Springer Netherlands, pp. 407–423.

Chapin, F.S., Matson, P.A., Mooney, H.A., 2002. Principles of Terrestrial Ecosystem Ecology. Springer, New York, NY, USA.

Conner, W.H., Duberstein, J.A., Jr, J.W.D., Hutchinson, S., 2014. Impacts of Changing Hydrology and Hurricanes on Forest Structure and Growth Along a Flooding/Elevation Gradient in a South Louisiana Forested Wetland from 1986 to 2009. Wetlands 34, 803–814. doi:10.1007/s13157-014-0543-0

Copenheaver, C.A., Yancey, M.W., Pantaleoni, E., Emrick, V.R., 2007. Dendroclimatic Analysis of a Bottomland Hardwood Forest: Floodplain vs. Terrace Responses [1]. J. Torrey Bot. Soc. 134, 505–511. doi:10.3159/07-RA-010.1

Crundwell, M.E., 1986. A review of hydrophyte evapotranspiration. Rev. Hydrobiol. Trop. 19, 215–232. doi:Crundwell M.E. A review of hydrophyte evapotranspiration. Revue d'Hydrobiologie Tropicale, 1986, 19 (3-4), p. 215-232.

F. C. Golet, A.J.K.C., 1993. Ecology of red maple swamps in the glaciated northeast: A community profile.

Ford, C.R., Brooks, J.R., 2002. Detecting forest stress and decline in response to increasing river flow in southwest Florida, USA. For. Ecol. Manag. 160, 45–64. doi:10.1016/S0378-1127(01)00440-6

Gardiner, E., Hodges, J., 1996. Physiological, morphological and growth responses to rhizosphere hypoxia by seedlings of North American bottomland oaks. Ann. Sci. For. 53, 303–316. doi:10.1051/forest:19960213

Gedan, K.B., Kirwan, M.L., Wolanski, E., Barbier, E.B., Silliman, B.R., 2010. The present and future role of coastal wetland vegetation in protecting shorelines: answering recent challenges to the paradigm. Clim. Change 106, 7–29. doi:10.1007/s10584-010-0003-7

Idso, S.B., 1981. Relative Rates of Evaporative Water Losses from Open and Vegetation Covered Water Bodies1. JAWRA J. Am. Water Resour. Assoc. 17, 46–48. doi:10.1111/j.1752-1688.1981.tb02587.x

Kadlec, R.H., 1990. Overland Flow in Wetlands: Vegetation Resistance. J. Hydraul. Eng. 116, 691–706. doi:10.1061/(ASCE)0733-9429(1990)116:5(691)

Keim, R.F., Amos, J.B., 2012. Dendrochronological analysis of baldcypress (Taxodium distichum) responses to climate and contrasting flood regimes. Can. J. For. Res. 42, 423–436. doi:10.1139/x2012-001

Kozlowski, T.T., 1997. Responses of woody plants to flooding and salinity. Tree Physiol. 17, 490–490. doi:10.1093/treephys/17.7.490

Linacre, E.T., Hicks, B.B., Sainty, G.R., Grauze, G., 1970. The evaporation from a swamp. Agric. Meteorol. 7, 375–386. doi:10.1016/0002-1571(70)90033-6

Liu, S., 1996. Evapotranspiration from Cypress (Taxodium ascendens) Wetlands and Slash Pine (Pinus elliottii) Uplands in North-Central Florida (Dissertation). University of Florida, Gainesville, FL, USA.

McLeod, K.W., Donovan, L.A., Stumpff, N.J., Sherrod, K.C., 1986. Biomass, photosynthesis and water use efficiency of woody swamp species subjected to flooding and elevated water temperature. Tree Physiol. 2, 341–346. doi:10.1093/treephys/2.1-2-3.341

Megonigal, J.P., Conner, W.H., Kroeger, S., Sharitz, R.R., 1997. Aboveground production in southeastern floodplain forests: A test of the subsidy–stress hypothesis. Ecology 78, 370–384. doi:10.1890/0012-9658(1997)078[0370:APISFF]2.0.CO;2

Mitsch, W.J., Ewel, K.C., 1979. Comparative Biomass and Growth of Cypress in Florida Wetlands. Am. Midl. Nat. 101, 417–426. doi:10.2307/2424607

Mitsch, W.J., Gosselink, J.G., 2007. Wetlands, 4th ed. John Wiley & Sons, Inc., New York, NY, USA.

Mitsch, W.J., Rust, W.G., 1984. Tree growth responses to flooding in a bottomland forest in northeastern Illinois. For. Sci. 30, 499–510.

Mitsch, W.J., Taylor, J.R., Benson, K.B., 1991. Estimating primary productivity of forested wetland communities in different hydrologic landscapes. Landsc. Ecol. 5, 75–92. doi:10.1007/BF00124662

Nagler, P.L., Glenn, E.P., Lewis Thompson, T., 2003. Comparison of transpiration rates among saltcedar, cottonwood and willow trees by sap flow and canopy temperature methods. Agric. For. Meteorol. 116, 73–89. doi:10.1016/S0168-1923(02)00251-4

Nash, L.J., Graves, W.R., 1993. Drought and flood stress effects on plant development and leaf water relations of five taxa of trees native to bottomland habitats. J. Am. Soc. Hortic. Sci. 118, 845–850.

Odum, W.E., 1988. Comparative Ecology of Tidal Freshwater and Salt Marshes. Annu. Rev. Ecol. Syst. 19, 147–176.

Oke, T.R., 1988. Boundary Layer Climates, 2 edition. ed. Routledge.

Pezeshki, S.R., 2001. Wetland plant responses to soil flooding. Environ. Exp. Bot. 46, 299–312. doi:10.1016/S0098-8472(01)00107-1

Pezeshki, S.R., Anderson, P.H., 1996. Responses of three bottomland species with different flood tolerance capabilities to various flooding regimes. Wetl. Ecol. Manag. 4, 245–256. doi:10.1007/BF02150538

Pezeshki, S.R., Chambers, J.L., 1986. Variation in Flood-Induced Stomatal and Photosynthetic Responses of Three Bottomland Tree Species. For. Sci. 32, 914–923.

Pezeshki, S.R., Chambers, J.L., 1985. Stomatal and photosynthetic response of sweet gum (Liquidambarstyraciflua) to flooding. Can. J. For. Res. 15, 371–375. doi:10.1139/x85-059

Ragotzkie, R.A., 1978. Heat Budget of Lakes, in: Lakes: Chemistry, Geology, Physics. Springer-Verlag, New York, NY, USA.

Schlesinger, W.H., Jasechko, S., 2014. Transpiration in the global water cycle. Agric. For. Meteorol. 189–190, 115–117. doi:10.1016/j.agrformet.2014.01.011

Slatyer, R., 1967. Plant-water Relationships. Academic Press Inc, New York, NY, USA.

van der Valk, A.G., 2012. The Biology of Freshwater Wetlands, 2 edition. ed. Oxford University Press, Oxford ; New York.

van der Valk, A.G., 1981. Succession in Wetlands: A Gleasonian Approach. Ecology 62, 688–696. doi:10.2307/1937737

Wharton, C.H., Kitchens, W., Pendleton, E.C., Sipe, T.W., 1982. Ecology of bottomland hardwood swamps of the southeast: a community profile, FWS/OBS-81/37. US Department of the Interior, Washington, DC.

Wilson, K.B., Hanson, P.J., Baldocchi, D.D., 2000. Factors controlling evaporation and energy partitioning beneath a deciduous forest over an annual cycle. Agric. For. Meteorol. 102, 83–103. doi:10.1016/S0168-1923(00)00124-6

Young, P.J., Keeland, B.D., Sharitz, R.R., 1995. Growth response of baldcypress [Taxodium distichum (L.) Rich.] to an altered hydrologic regime. Am. Midl. Nat. 133, 206–212. doi:10.2307/2426385

CHAPTER 2: EVAPORATION AND THE SUBCANOPY ENERGY ENVIRONMENT IN A FLOODED FOREST

2.1 INTRODUCTION

A prominent difference of forested wetlands from upland forests is seasonal or permanent flooding. Many have investigated how the aquatic-terrestrial interface of wetlands structures the ecological communities (e.g., Junk et al., 1989; van der Valk, 1981), but there has been little attention on how floodwater structures the microclimate and energy dynamics in forested wetlands. The energy balance at the water-air interface results in important features of the physical environment, including the temporal variability of water temperature profiles, air temperature and humidity profiles (i.e., the microclimate), and latent and sensible heat exchanges between the atmosphere and the water. Although the energy balance below the canopy has been well described in boreal (e.g., Blanken, 1998; Iida et al., 2009), temperate (Schaap and Bouten, 1997; Sun et al., 2016, 2014; Wilson et al., 2000), and arid (Raz-Yaseef et al., 2010; Scott et al., 2003) upland forests, the energy balance has not been investigated in forested wetlands likely differ because of the presence of surface water has tremendous effects on energy storage and partitioning (Oke, 1988; Ragotzkie, 1978). Flooded forests may be similar to lakes, in which energy storage can cause peak evaporation (*E*) to lag behind peak insolation at both daily and annual timescales (Rouse et al., 2005) but it is unknown whether the same is true in flooded forests where the canopy can decouple the understory from the ambient atmosphere. Shoemaker et al. (2005) showed a similar effect is important in shallowly flooded marshes, but with focus on diel storage fluxes. In forested wetlands, investigation of energy components is needed for not only quantifying heat fluxes, especially evaporation, but also for understanding the feedback between these fluxes and the below canopy environment.

It is likely that *ET* partitioning in wetland forests differs from upland forests. In general, transpiration (*T*) composes the majority of *ET* in closed-canopy forests (Baldocchi and Ryu, 2011; Schlesinger and Jasechko, 2014). Wetland forest structure can be highly variable, but closed canopy wetland forests can have transpiration rates that are similar (2 to 4 mm day^{-1}; Bosch et al., 2014; Krauss et al., 2014) to upland forests in the same region (e.g., Domec et al., 2012). We do not know of studies directly comparing upland and wetland forest *T* or *E* separately, however, Shoemaker et al., (2011) compared total *ET* in forested wetlands to total *ET* in a pine upland, and found baldcypress *ET* was, on average, ~20% higher with a mean of 4 and 5 mm day^{-1} in summer months. The understory differs fundamentally between upland and wetland forests, likely affecting proportional contributions of *E* versus *T*. Floodwater effects on *E* and humidity gradients may be an important factor distinguishing wetland energy and water budgets from those of upland environments.

Although evaporation (*E*) is often a small component of terrestrial water budgets, in wetlands it is often assumed that *ET* rates are higher than in uplands because of higher *E*. Past investigations just measuring *E* (i.e., no other energy budget terms) in forested wetlands found *E* of 1.6 mm day^{-1} (Brown, 1981) and up to 3 mm day^{-1} (Liu, 1996), averaging approximately 30% of the total *ET*. Estimating *E* in flooded forests requires a better understanding of physical limitations on *E*. In upland systems, *E* is limited by surface dryness, and vapor fluxes are impeded by diffusion through high resistance soil and litter layers (e.g., Schaap and Bouten, 1997). While these resistances may be irrelevant in flooded wetlands, limitations imposed by the canopy above still apply. A closed forest canopy may intercept the majority of solar radiation with a small fraction transmitted or re-emitted downward (Gay and Knoerr, 1975). The canopy is

also a physical impedance to vapor transport from the understory because it offers substantial resistance to turbulent exchange (Wilson et al., 2000).

The objective of this study is to develop a mechanistic understanding of the energy budget and the sub-canopy *ET* dynamics in a flooded forested wetland during the leaf-on season. Rigorous empirical measurements are needed to validate hypothesized controls over *E* in a forested wetland understory, and, in general, to better understand the sub-canopy microclimate. We hypothesize that peak *E* occurs with canopy senescence in fall because of increased radiation transmission and aerodynamic conductance; also, we expect there to be concurrent effects of stored energy released from floodwater as temperatures patterns shift. Our approach was to measure energy fluxes and identify seasonal changes co-occurring with changing meteorological and phenological conditions from summer to fall.

2.2 METHODS

2.2.1 Site Description

Measurements were conducted between 16-June and 13-November, 2014 in Maurepas Swamp in southeast Louisiana (30°06'03"N, 90°37'29"W). This forested wetland is extensive, with nearly continuous cover for 2.5 km in all directions from the study site. The canopy is predominantly water tupelo (*Nyssa aquatica*) and ash species (*Fraxinus* spp.), with some baldcypress (*Taxodium distichum*). Top of canopy height was 22 m, with a canopy base height of 14 m. There were scattered swamp red maple (*Acer rubrum* var. *drummondii*) in the midstory, with mean height of 6 m with crowns extending nearly to the water surface. Basal area at the study site was 44 m^2 ha^{-1} and fairly homogeneous (basal area at the instrumentation location was within 3% of the mean of four random measurement points) as measured with horizontal point sampling (BAF10 wedge prism). Late-June measurements with a plant canopy analyzer (LAI-2000, LI-COR, Lincoln, NE, USA) with a 76° view angle yielded values from 3.58 to 4.85 (4.18 ± 0.13 m^2 m^{-2}; mean ± std. dev.) along a 60-m transect intersecting the site location with readings taken every 3 m (n = 21). LAI was highly uniform, with a coefficient of variation of 3%. Considering the LAI-2000 underestimates leaf area index (LAI) in unthinned broadleaf forests by ~10-20% (Cutini et al., 1998) and by substantially more for baldcypress forests (Allen et al., 2016), we estimate actual LAI is 5 m^2 m^{-2}.

All trees were deciduous, but baldcypress maintained most of its senesced foliage through the end of the study; senescence of the other species began in mid-September and trees were leafless by the beginning of November. The climate (Table 1) is humid subtropical with monthly mean temperatures ranging from 10 to 27 °C. Mean precipitation (annual mean of 160 cm) is similar among months, although lower in fall of the study year (National Climatic Data Center, Asheville, NC, USA).

The site is permanently flooded and impounded by roads and levees, with relatively stable water depths (measured by pressure transducer; Hobo, Onset). During the study period, water depth was between 0.4 and 0.6 m, aside from two large precipitation events at the beginning of the measurement period (Figure 2.1), with a mean water level (mwl) of 0.52 m,. Typical of impounded, blackwater wetlands in this region, water was dark and tannic and soils had a thick, nebulous, semi-fluid organic layer at the ground surface.

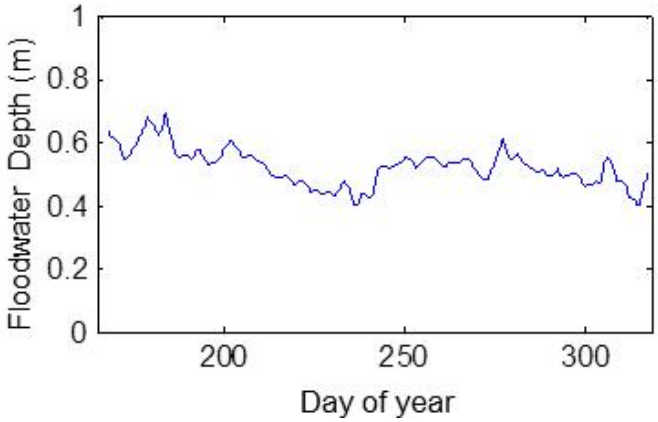

Figure 2.1 Depth of floodwater over the measurement period.

Floating aquatic vegetation covered the water surface, composed of common salvinia (*Salvinia minima*) and duckweed (*Lemna* spp.) with few water hyacinth (*Eichhornia crassipes*). Both *Salvinia* and *Lemna* are low stature plants (< 1 cm) with small fronds and permanently open stomata (Andersen et al., 1985; de la Sota and Pazos, 1990; Tillberg et al., 1981). The floating vegetation was always in a dense mat, but it seemed to begin senescing in November. While vapor fluxes from this surface include both direct *E* and *T* through permanently open stomata, we defined all vapor flux from the understory surface as *E*, to distinguish from canopy *T*. This convention is typical for understory water balance research; other non-wetland studies have similarly lumped the forest layer flux components, including *E* from soil, litter, or bryophytes and *T* from seedling or herbaceous vegetation (e.g., Kettridge et al., 2013; Scott et al., 2003; Sun et al., 2016).

2.2.2 Instrumentation and Measurements

Net radiation was measured 2 m above mwl with two single-component net radiometers (Kipp Zonen NR-lite2, Delft, Netherlands) placed adjacently 0.6 m apart horizontally. The two values were averaged for energy balance calculations; there was a spatial bias between sensors likely related to sunflecks, resulting in a high RMSE (48 W m^{-2}) but mean deviation of 7.6 W m^{-2} between the two radiometers.

Air temperature (t_A) and relative humidity (RH) were measured (CS-215, Campbell Scientific, Inc., Logan, UT, USA) at two heights, 2.1 m and 0.7 m above mwl. Water surface temperature (t_{surf}) was measured using four fine thermocouples floating at the surface, within the floating vegetation layer. Water temperature (t_W) was also measured at two depths using thermocouples: one 12 cm below mwl ($t_{W\text{-}mid}$; 2 cm below the surface when water depth was lowest) and one at the soil-water boundary, 52 cm below mwl ($t_{W\text{-}soil}$). Instrumentation was scanned every five seconds and logged as five minute averages. Wind velocity and sonic temperature were measured at 10 Hz with a 3-dimensional sonic anemometer (CSAT3, Campbell Scientific, Inc., Logan, UT, USA) mounted 1.7 m above mwl.

Wind speed and solar radiation were measured at a conventional meteorological station (at 3 m height in a clearing surrounded by agricultural fields) near Baton Rouge, LA (57 km west of the study site), available through the Louisiana Agriclimatic Information System (http://weather.lsuagcenter.com/). Data were used as an indicator of regional conditions for comparison to below-canopy observations. Canopy phenology was documented during approximately weekly site visits and quantified by a remotely sensed vegetation index (NDVI)

estimated by MODIS satellite data on a 16-day interval for the mostly uniform pixel containing the site.

2.2.3 Analyses

2.2.3.1 Eddy-Covariance Processing

Sensible heat fluxes (H) were calculated by eddy covariance of sonic temperature ($\mathcal{T}$) and vertical wind velocity (w), using EddyPro software (version 5.1.1, LI-COR, Lincoln, NE, USA), calculated as covariance of instantaneous deviations ($\mathcal{T}_i'$, w_i') of individual measurements ($\mathcal{T}_{si}$ and w_i) from 30-minute means ($\bar{\mathcal{T}}, \bar{w}$) such that

$$\mathcal{T} = \mathcal{T}_i' + \bar{\mathcal{T}} \,, \tag{2.1}$$

$$w_i = w_i' + \bar{w} \,, \text{ and} \tag{2.2}$$

$$H = \rho C_p \, \overline{w_i' \mathcal{T}_i'}, \tag{2.3}$$

where H is the sensible heat flux for an averaging interval, ρ = air density, and C_p is the specific heat capacity of the air. Similarly, friction velocity (u_*), an index of momentum flux and the eddy velocity, was calculated from the covariance of w and horizontal wind velocity (u) as

$$u_*^2 = \overline{w_i' u_i'} \,. \tag{2.4}$$

Covariances were calculated on half hour intervals, with planar fit axes rotation for wind measurements (Wilczak et al., 2001), and corrections for high pass (Moncrieff et al., 2004) and low pass filtering (Moncrieff et al., 1997) as implemented in EddyPro; corrected H of 'high quality' data were similar to uncorrected H (R^2 = 1.00; RMSE = 0.26 W m^{-2}). Processed data were flagged based on coherence with steady-state and turbulence requirements (Mauder and Foken, 2004); data flagged as low quality ('2' by the Mauder and Foken method) were removed.

2.2.3.2 Energy Budget Calculations

With H calculated by eddy covariance, latent heat exchange, λE (or E, in units mm day^{-1}), was quantified as the residual of the energy balance,

$$R_n - G - \Delta S = H + \lambda E \,, \tag{2.5}$$

where R_n is net radiation as the average of the two net radiometers, ΔS is change in heat storage in floodwater, and G is heat conducted from water to the soil, all with units W m^{-2}. This eddy-covariance-energy-budget (ECEB) approach enables avoiding the effects of t_A and RH profile inversions on short-interval Bowen Ratio (β) energy balance calculations (Foken, 2008a). However, ECEB is vulnerable to some of the same uncertainties as all methods using energy budget closure, particularly at sub-daily temporal precision (Foken, 2008b; Wilson et al., 2002).

The sum of left-hand side of eq. 2.5 is the available energy (AE) that is partitioned between λE and H. G was calculated as

$$G = -k \frac{\Delta t_W}{\Delta z} \,, \tag{2.6}$$

with assumed thermal conductivity, k, of 0.57 W m^{-1} k^{-1} (Van Wijk and de Vries, 1963) and Δz (sensor separation) of 0.4 m. ΔS was calculated from change in mean t_W (dos Reis and Dias, 1998) half hourly (i.e., $\Delta\tau$ = 30 minutes) with mean t_W approximated as the mean of the two depth intervals such that

$$\Delta S = \frac{C_p}{2\Delta\tau} [(\Delta t_{surf} + \Delta t_{W\text{-}mid}) \Delta z_{surf\text{-}mid} + (\Delta t_{W\text{-}mid} + \Delta t_{W\text{-}soil}) \Delta z] \,, \tag{2.7}$$

with Δz of 0.4 m and $\Delta z_{surf\text{-}mid}$ equal to the difference 0.4 m from the time-varying water depth. For comparison to results from eq. 2.7, mean t_W was also approximated by a power-law model fit with data at three water temperature measurement depths on a half hourly interval. This model yielded an estimate of that was 92% of ΔS by eq. 2.7, with a similar temporal pattern (R^2 = 0.95).

To examine partitioning between E and T, β was calculated as

$$\beta = \frac{H}{\lambda E} \approx \gamma \frac{\Delta t}{\Delta e} , \quad (2.8)$$

directly, where γ is the psychrometric constant ,and either H and λE from ECEB (β_{ECEB}), or calculated from the temperature (Δt) and vapor pressure (Δe) gradients from the water surface (t_{surf}, e_S) to the air at 2.1 m (t_A, e_A) above the mwl. The water surface, with assumed RH of 100%, was used for the lower control because air data at 0.7 m and 2.1 m heights were too similar. Monthly and daily mean gradients were used to evaluate β_{month} and β_{day}, respectively. Long-interval calculations of β are accurate (Webb, 1960) and circumvent conditions where β is indeterminate or not meaningful (Perez et al., 1999). As an alternate calculation of λE also derived from the energy balance,

$$\lambda E_{\beta} = \frac{AE}{1+\beta} , \quad (2.9)$$

was solved for E using both β_{month} and β_{day}, yielding both mean daily ($E_{\beta\text{-day}}$) and mean monthly ($E_{\beta\text{-month}}$) estimates for comparison to the ECEB approach.

In general, analyses were based on ECEB, but E calculated by Eq. 2.5 was compared to E estimated in other ways. Where unspecified, β and λE refer to products of the ECEB method. From the ECEB approach, another alternate calculation of E ($E_{ECEB\text{-reduced}}$) was calculated by reducing the energy balance terms with the assumption that $AE = R_n$ (i.e., neglecting ΔS or G). All E calculations were also compared to E measured directly from water levels in a partially sunken evaporation pan (E_{pan}) at the site with the same floating macrophyte cover as the wetland (Allen et al, 2016).

2.2.3.3 Postprocessing and Analysis

Data during precipitation, indicated by pan water levels, and a period of six hours after were removed from ECEB analysis. This mask, as well as data logger malfunction, resulted in removal of 21% of time between 16-June and 13-November. Data removed because of failure to meet turbulence and steady state requirements comprised another 21% of the remaining data (27% removed during day and 16% during night). All energy budget terms were calculated during the same periods as the eddy covariance H calculations. For other climate data (i.e., t_A and RH, and t_W when not used in calculating ΔS), periods with precipitation were removed but not periods with inadequate eddy covariance conditions.

To analyze across days with variable segments of missing data, ensemble mean diel patterns of variation (Papale, 2012) were used for assessing partitioning of energy budgets, comparing temperature and vapor gradients, and intercomparison of meteorological conditions. This averaging approach was executed in two ways. First, for each month of the study, means for each half-hour increment of the day were calculated for all meteorological variables and energy balance terms. These monthly mean-day calculations were used for comparison of seasonal trends in diel cycles. Second, to investigate variations at intervals shorter than monthly but to avoid averaging across gaps, 3-day ensemble averages were used and averaged for single 'daily' values.

Only daily ensembles with complete hourly coverage were used in analyses. Thus, no gap filling was needed which was preferable because of erratic variations in R_n. Three days was the optimal window length for ensemble averages to yield the largest total number of gap-free, 24-hour periods (e.g., 2-day intervals would yield more intervals, but disproportionately more intervals with gaps). The 3-day ensembles were then averaged across the hourly increment to

yield a single 'daily mean' value; these daily mean ensembles were used for plotting trends and exploring correlations among variables.

To investigate the effects of aerodynamic forcing and surface controls to total sub-canopy E, aerodynamic conductance, g_a, was calculated from wind speed (u) and friction velocity ($u*$) as

$$g_a = \frac{u_*^2}{u}. \quad (2.10)$$

The surface conductance, g_s, was estimated from λE calculated by Eq. 2.5, with the potential gradient defined as $e_S - e_A$ and a total conductance of $(g_s^{-1} + g_a^{-1})^{-1}$, as

$$g_s^{-1} = \frac{\rho C_p}{\gamma \lambda E}(e_s - e_a) - g_a^{-1}. \quad (2.11)$$

The contribution towards E by the potential-gradient driven flux, E_{imp}, can be separated from energy-driven equilibrium E_{eq} as

$$E_{imp} = \frac{\rho C_p}{\gamma \lambda} g_s \times (e_A - e_S), \text{ and} \quad (2.12)$$

$$E_{eq} = \frac{\Delta A E}{\lambda(\Delta+\gamma)}, \quad (2.13)$$

where Δ is the slope of the saturation vapor pressure curve. Respective theoretical contributions of E_{imp} and E_{eq} to total E are defined as:

$$E = \Omega \times E_{eq} + (1 - \Omega) \times E_{imp}, \quad (2.14)$$

where the boundary layer decoupling coefficient, Ω (Jarvis and McNaughton, 1986), can also be estimated as

$$\Omega = \frac{\Delta/\gamma+1}{\Delta/\gamma+1+g_a/g_s}. \quad (2.15)$$

The mean values of 3-day composites were used to evaluate eq. 2.11-15.

2.3. RESULTS

2.3.1. The sub-canopy physical environment

Seasonal changes to sub-canopy R_n and other physical parameters aligned with changes in canopy phenology. The months with highest R_n in the understory were September and October (Figure 2.2A), correlating negatively with NDVI ($R = -0.32$, $p = 0.05$; Figure 2.2B) and overstory solar radiation (R_{sol}), which decreased in fall because of shorter day length and lower sun angle (Figure 2.2C). Wind speed at the external site increased in the fall, as did subcanopy u and $u*$ (Figure 2.2 C, D). The external wind speeds explained much of the variation in sub-canopy wind conditions, with a positive relationship with both sub-canopy u ($R^2 = 0.40$, $p < 0.001$), and sub-canopy $u*$ ($R^2 = 0.38$, $p < 0.001$).

Temperature patterns followed seasonal and diel radiative forcing, and diel air and water temperature variability increased in October and November (Figure 2.3), coincident with canopy senescence. Mean diel temperature variation was 8.8 °C for June through Sept and 12.8 °C for October and November. Temperature differences between 0.7 and 2.1 m heights were generally small (mean difference of 0.15 °C), but the 0.7 m temperature was slightly higher near midday (monthly mean $t_{A\text{-}0.7} - t_{A\text{-}2.4}$ differences from 12:00 to 16:00 were: -0.05, 0.01, 0.16, 0.24, 0.26, and 0.20 °C for June through November respectively). The daily mean air-surface temperature difference ($t_{A\text{-}S}$) generally ranged between 0.0 and -1.0 °C until DOY 270, after which variability increased and mean difference became more negative (Figure 2.2F). Aside from the surface, water temperature showed little diel variation: mean diel variation was 0.39 °C at the soil-water boundary and 0.88 °C at ~10 cm below the water surface.

Table 2.1 Mean daily meteorological data measured below canopy at the study site and measured off site in Baton Rouge, LA, USA: maximum and minimum air temperature (t_A), maximum and minimum relative humidity (RH), maximum vapor pressure deficit (VPD), net radiation under canopy and over floating vegetation (R_{net}), total precipitation (P), and downward shortwave radiation (R_{sol}).

	On site, below canopy						Off site, in clearing						
Month	t_A Max, °C	t_A Min, °C	RH Max, %	RH Min; %	VPD Max; kPa	R_{net}[b] Mean; W m^{-2}	t_A Max; °C	t_A Min; °C	RH Max %	RH Min; %	VPD Max; kPa	P Sum; cm	R_{sol} Mean; W m^{-2}
Jun[a]	30.8	22.4	100	68	1.45	33.8	31.1	22.1	96	53	2.14	9	114
Jul	31.3	22.5	100	64	1.71	36.8	31.9	21.9	95	48	2.49	13	122
Aug	32.3	23.0	100	66	1.71	39.9	32.5	22.6	96	51	2.45	19	103
Sep	31.1	21.9	100	67	1.55	40.3	31.1	21.1	96	50	2.28	6	94
Oct	28.5	15.8	100	52	1.85	47.3	27.7	14.2	96	41	2.15	6	86
Nov[a]	20.5	8.9	99	57	1.07	33.8	20.5	7.9	91	44	1.37	2	62

[a] Measurement did not include entire month (started 6 June, ended 13 November 2014)
[b] Values do not match values of Table 2 which were adjusted to omit gaps from quality control flags

Relative humidity was high, with vapor pressures frequently at saturation. Over the entire period, mean RH was 89%. Vapor pressure deficit (VPD) was zero for 28% of the study period (excluding periods with rain); 6% of the time, saturated conditions coincided with positive *AE* (not shown). In fall, minimum RH was lower (Table 2.1) although daily mean VPD was fairly static (Figure 2.2E). For June, July, and August, saturated conditions were frequent ($t_{dew} \approx t_A$) from 24:00 to 8:00 (Figure 2.3). These high humidity conditions coupled with temperature variations of the water that lagged air temperature variations (Fig 3) resulted in vapor pressure gradients indicating diffusion towards the water surface. Although not always apparent by the t_{dew} versus t_A in the monthly ensembles (Figure 2.3), a downward humidity gradient (i.e., positive $e_A - e_S$) occurred frequently between 8:00 to 12:00 (and occasionally later) over the entire study period (Figure 2.4). By mid-afternoon, conditions reveresed to strong upward humidity gradients (Figure 2.4) which grew even more prominent later in the study. By November, ensemble mean t_{dew} was below t_A all day (Figure 2.3F).

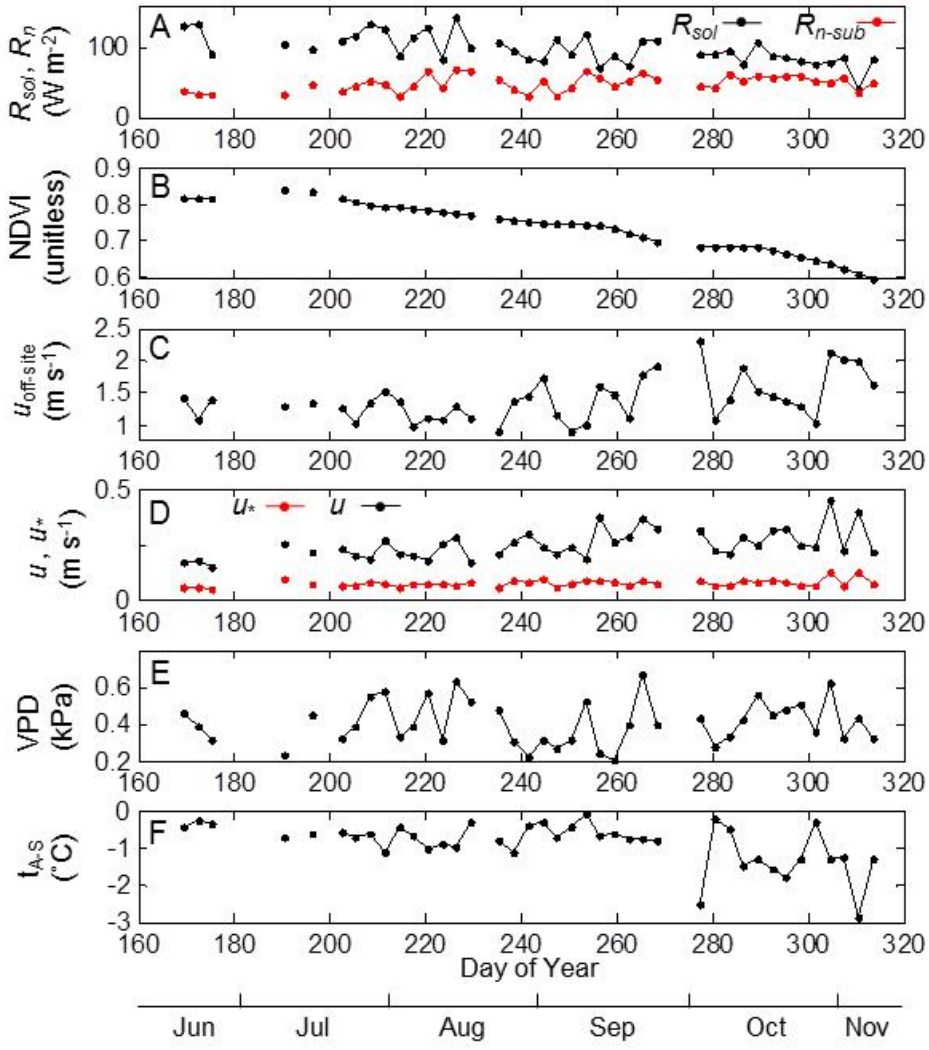

Figure 2.2 Mean of 3-day ensembles for (A) net radiation (below canopy) and solar radiation (external site); (B) canopy cover proxy as measured by NDVI; (C) wind speed, measured at 3 m (external site); (D) wind speed and friction velocity (below canopy); (E) Vapor pressure deficit (below canopy); and, (F) Temperature of water surface minus air temperature.

The energy fluxes reflected the same seasonal transitions in temperatures and canopy conditions. The warm air temperatures from June through September (Figure 2.3) resulted in increased energy storage in the floodwater and flux to the underlying storage (Figure 2.5; Table 2.2). With a greater decline in t_A than in t_W from September to November, both ΔS and G became negative (upward) on average (Figure 2.5; Table 2.2). Not only was mean t_W greater than mean t_A after September, the variability was also greater, which resulted in fall having a more pronounced diel pattern of energy storage and release from the floodwater (Figure 2.6). This was concomitant with increasing R_n and increasing variation in R_n as well (Figure 2.6).

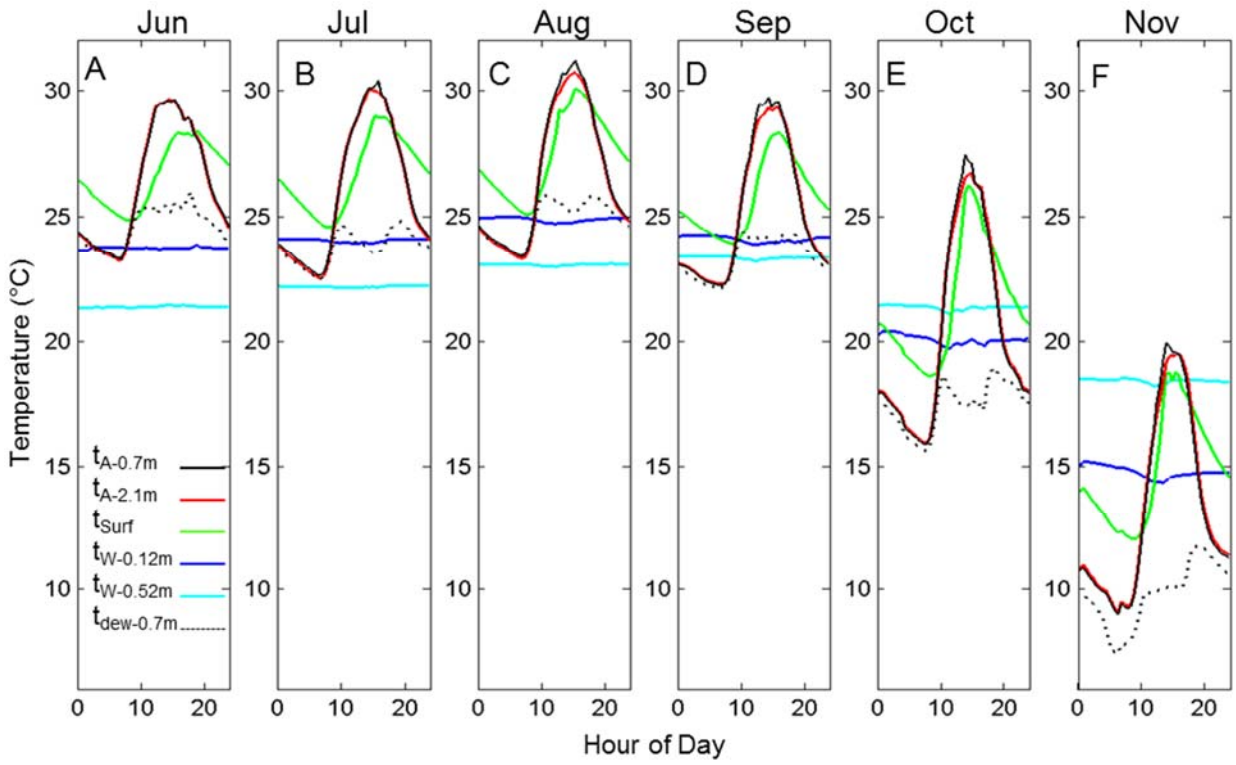

Figure 2.3 Monthly ensembles of half-hourly mean air temperature (t_A) at 0.7 m and 2.1 m above mean water level (mwl), water surface temperature (t_{surf}), water temperature (t_W) at 0.12 m below mwl and 0.52 m below mwl and air dew point temperature (t_{dew}) at 0.7 m above mwl for June-November (A-F).

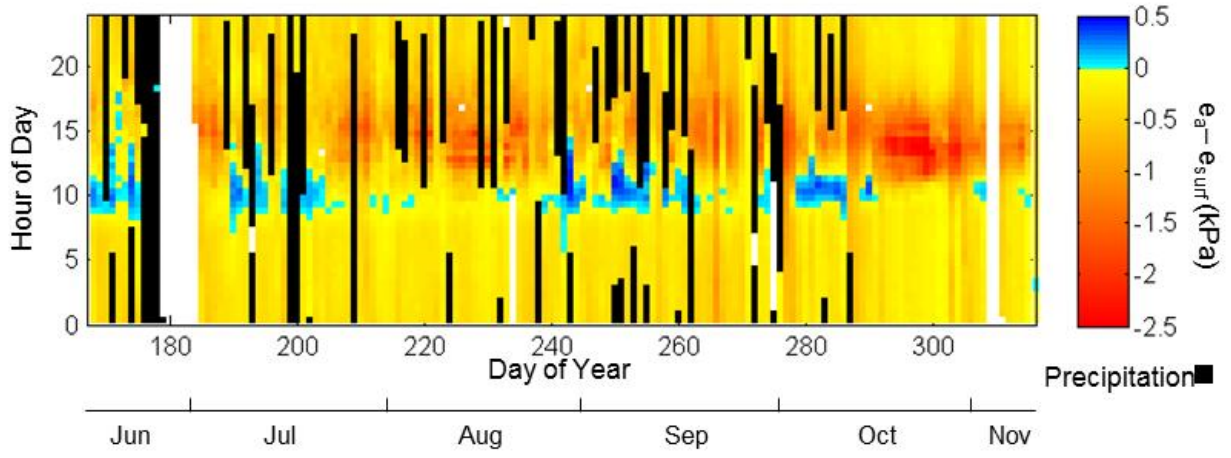

Figure 2.4 Difference between air vapor pressure e_a (at 0.7 m above mean water level) and vapor pressure e_s at the surface temperature (kPa) over the study period; white indicates gaps.

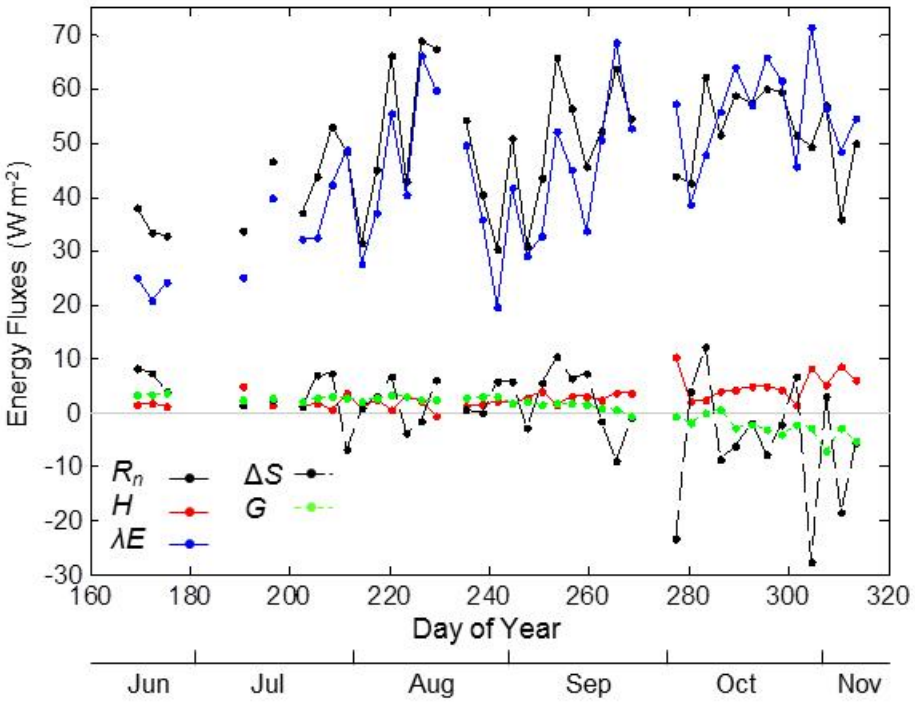

Figure 2.5 Mean of 3-day ensembles for energy budget terms sensible heat flux (H), latent heat flux (λE), net radiation (R_n), heat storage flux (ΔS), and ground heat flux (G). Gray indicates zero line.

Table 2.2 Monthly mean energy budget components, in units of W m^{-2}, calculated for available data that met quality control specification for eddy covariance.

Month	R_n	ΔS	G	λE	H
Jun[a]	33.5	4.2	3.3	24.5	1.5
Jul	42.0	0.9	2.6	36.1	2.4
Aug	49.4	2.2	2.6	43.1	1.5
Sep	49.1	0.4	1.0	44.8	2.8
Oct	52.6	-4.7	-1.9	55.0	4.2
Nov[a]	43.1	-12.5	-5.2	53.7	7.0

[a] Measurement did not include entire month (started 6 June, ended 13 November 2014)

Although R_n was the dominant component of AE at both sub daily and seasonal timescales, G and ΔS both caused the timing of AE to lag R_n. At the seasonal time scale, AE was 78%, 92%, 90%, and 97% of R_n in June, July, August, and September, respectively (Table 2.2). Both G and ΔS fluxes augmented AE in Oct and Nov such that AE was 112% and 141% of R_n (Table 2.2). Diel G variations were small. However, ΔS had large diel variability that increased contemporaneously with increasing R_n diel variability (Figure 2.6), presumably related to canopy

senescence. Throughout much of the measurement period, R_n and ΔS mirrored each other, although R_n was substantially higher during the day (Figure 2.6B). On lower energy 3-day periods, both ΔS and R_n were low (e.g., Figure 2.6J). The temperature and gradients were such that the downward ΔS flux increased more rapidly than downward R_n in the morning (Figure 2.6A) yielding a negative energy balance. This was most apparent at the time of day and time of year (Figure 2.6) associated with downward vapor gradients (Figure 2.4). In the evening, as t_A declined more rapidly than t_W but R_n was still positive, ΔS augmented AE above R_n.

2.3.2 Energy partitioning and sensible heat

Over the study period, almost all AE was partitioned to λE. Overall mean β_{ECEB} was 0.07, whether calculated as a mean across either monthly or 3-day ensembles. Values independently calculated from the temperature and RH gradients were similar, with mean $\beta_{day} = 0.09$ and $\beta_{month} = 0.11$. Gradient and ECEB β followed the same seasonal trend (Table 2.3). All three methods yielded highly collinear results with (evaluated at the monthly scale, n = 6) for β_{month} versus β_{ECEB} ($R = 0.86$, $p = 0.03$), for β_{month} versus β_{day} ($R = 0.93$, $p = 0.007$), and for β_{day} versus β_{ECEB} ($R = 0.70$, $p = 0.12$). As a consequence of consistently low β, there was a close relationship between AE and λE (Figure 2.7E; $R^2 = 0.98$, $\lambda E = 0.92AE + 0.73$ W m^{-2}). Other variables tested—VPD, u_*, and t_{A-S}—were poorly related to λE and the weak relationships seemed mostly driven by day of year (Figure 2.7F,G,H).

Corresponding with the low β, all months had low but net positive H. At longer timescales, H was similar magnitude to G or ΔS (Table 2.2). Partitioning to H increased in the late season (Tables 2 and 3). For June through August, other than a general decrease in H during the day, diel patterns of H fluxes through June-August were weak (Figure 2.6). Later in the year, H was slightly negative in mid morning, positive in early afternoon, positive or near zero in the evening, and near zero through the night; for example, the sign of H changed four times throughout some ensemble days (Figure 2.6E,F,K,J). H was negatively related to t_{A-S} (Figure 2.7D; $R^2 = 0.65$; $H = -3.1 \times t_{A-S} + 0.4$) and the relationship was not just an effect of time of year (time-detrended H [not shown] was also negatively related to t_{A-S}, $R^2 = 0.39$, $p < 0.001$). H was more closely (positively) related with u_* (Figure 2.7C; $R^2 = 0.35$) than was λE, and was less related to AE than was λE (Figure 2.7A; $R^2 = 0.28$); time-detrended H (not shown) was also positively related to u_* ($R^2 = 0.20$, $p = 0.004$) but not AE ($R^2 = 0.02$, $p = 0.42$). Because of the relationship of H with both t_{A-S} and u_*, both were also related to β (Figure 2.7K,L; $R^2 = 0.32$, $p < 0.001$ and $R^2 = 0.22$, $p < 0.003$, respectively) and related to deviations from the λE -AE regression line (Figure 2.7O,P; $R^2 = 0.35$, $p < 0.001$ and $R^2 = 0.19$, $p = 0.005$, respectively).

2.3.3 Evaporation rates

The five estimates of evaporation rates—E_{ECEB}, $E_{ECEB\text{-}reduced}$, $E_{\beta\text{-}day}$, $E_{\beta\text{-}month}$, E_{pan}—were similar in magnitude but there were some predictable differences in seasonal trends. Monthly E ranged from 0.9 to 2 mm day^{-1}, increasing from June and peaking in October and November (September for E_{pan}; Table 2.4). Because these estimates depended on AE, there was high correlation between E_{ECEB}, $E_{\beta\text{-}month}$ and $E_{\beta\text{-}day}$ ($R^2 = 0.99$), although monthly means of E_{ECEB} were ~0.1 mm day^{-1} higher than $E_{\beta\text{-}month}$ and $E_{\beta\text{-}day}$. Rates of E_{ECEB} were similar to E_{pan}, with mean of the six months of 1.6 mm day^{-1} and 1.4 mm day^{-1}, respectively (Allen et al., in press). E estimated as $E_{ECEB\text{-}reduced}$ was higher than ECEB in summer months and lower in October and November because it did not account for ΔS or G which resulted in better agreement with E_{pan} ($R = 0.44$).

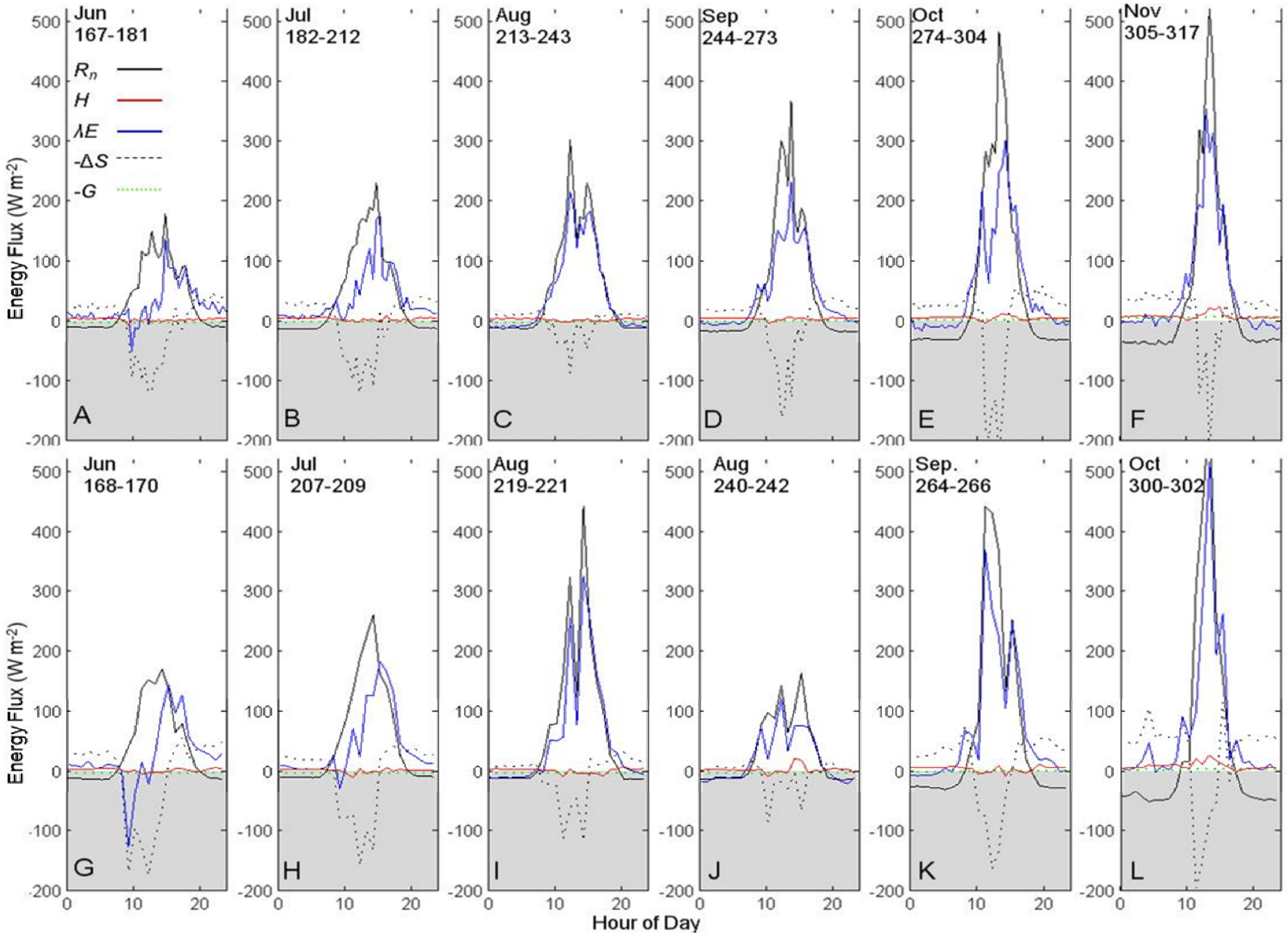

Figure 2.6 Monthly ensembles of half-hourly means (A-F) and select 3-day ensembles of hourly means (G-L) of sensible heat flux (H), latent heat flux (λE), net radiation (R_n), heat storage flux (ΔS), and ground heat flux (G). The gray area indicates negative values.

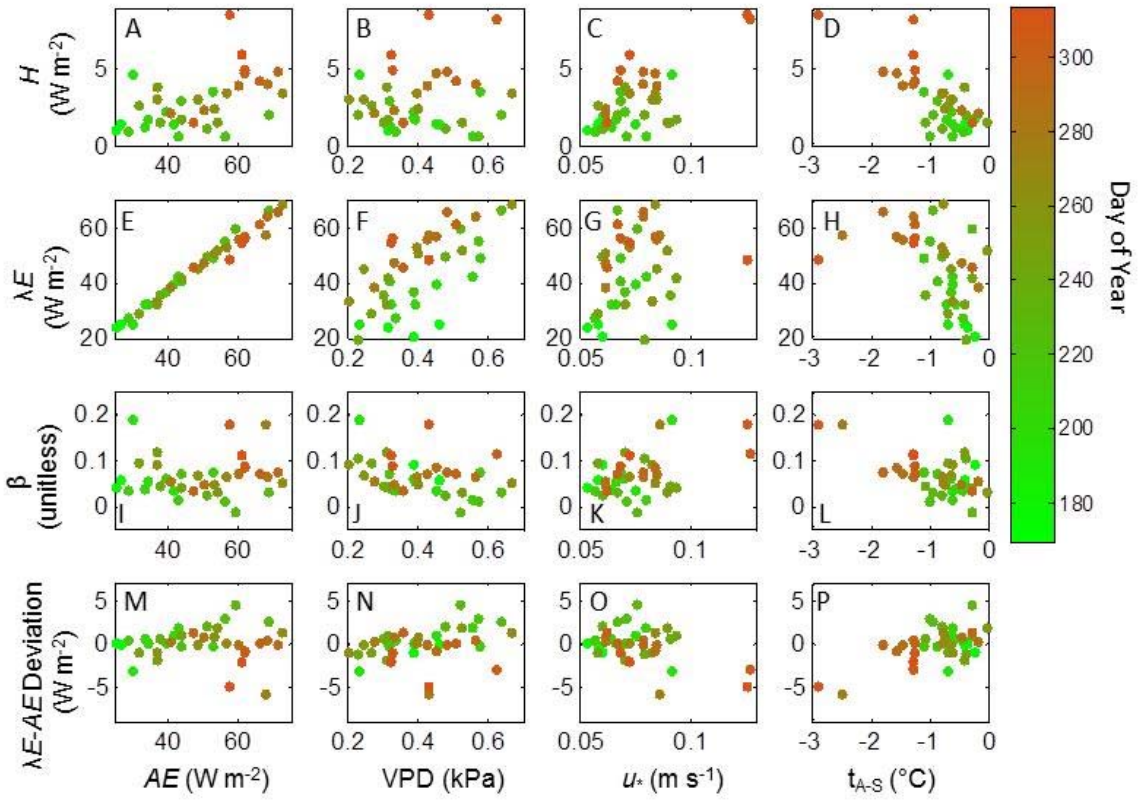

Figure 2.**7** Sensible heat flux (*H*), latent heat flux (λ*E*), Bowen Ratio (β), and deviation from a linear model of λ*E* versus available energy plotted against available energy (*AE*), vapor pressure deficit (VPD), friction velocity u_*, in m s^{-1}, and temperature difference of water surface minus air temperature. Values are means of 3-day ensembles.

Table 2.3 Mean Bowen ratios (β): β_{ECEB}, calculated by eddy covariance for sensible heat flux and energy balance for latent heat; β_{day}, calculated by daily mean vapor pressure and temperature gradients; and β_{month}, calculated by monthly mean vapor pressure and temperature gradients.

Month	β_{ECEB}	β_{day}	β_{month}
Jun[a]	0.06	0.03	0.05
Jul	0.07	0.08	0.08
Aug	0.04	0.09	0.10
Sep	0.06	0.09	0.09
Oct	0.08	0.11	0.13
Nov[a]	0.13	0.16	0.22

[a] Measurement did not include entire month (started 6 June, ended 13 November 2014)

2.3.4 Surface conductance and aerodynamic effects

Advective conditions varied seasonally. Daily mean (of 3-day ensembles) g_a was variable (Figure 2.8C; mean = 0.026 m s^{-1}) but with a slight trend of lower values in late August through September. This period of low g_a (~DOY240-268) had low mean $e_S - e_A$ too (Figure 2.8B),

conditions indicating low advective transport, yet there were some scattered periods of higher λE (DOY 253-258, 262-264). Patterns of g_s (mean = 0.007 m s^{-1}) differed from $e_S - e_A$ or g_a; g_s mostly increased throughout the entire measurement period with multiple peaks in November. Throughout, Ω was variable, but with a trend of increasing Ω until September then decreasing in fall (Figure 2.8D). Peak Ω, with evidence of expanding surface boundary layer thickness (low g_a, low $e_S - e_A$; Figure 2.8) were coincident with intermediate E rates, exceeding most E rates in June or July when there was higher g_a; this September period had many precipitation events (Figure 2.4) that may have directly decreased exchange, or indirectly by affecting water temperatures. Overall, modeled $(1-\Omega)\times E_{imp}$ was a larger fraction of E (Figure 2.8E) than was $\Omega \times E_{eq}$, and was also strongly correlated with AE ($R^2 = 0.83$).

Table 2.4 Evaporation rates (mm day^{-1}) estimated by: eddy-covariance energy-balance method with the full energy balance (E_{ECEB}), eddy-covariance energy-balance method without accounting for storage or ground heat fluxes ($E_{ECEB\text{-}reduced}$), Bowen-ratio energy balance calculations made with 3-day ensemble means ($E_{\beta\text{-}day}$), Bowen-ratio energy balance calculations made at the monthly interval ($E_{\beta\text{-}month}$), and pan water level fluctuations (E_{pan}).

Month	E_{ECEB}	$E_{ECEB\text{-}reduced}$	$E_{\beta\text{-}day}$	$E_{\beta\text{-}month}$	E_{pan} [b]
Jun[a]	0.9	1.1	0.9	0.9	NA
Jul	1.3	1.4	1.2	1.3	1.2
Aug	1.5	1.7	1.4	1.4	1.1
Sep	1.6	1.6	1.5	1.6	1.7
Oct	1.9	1.7	1.8	1.9	1.5
Nov[a]	1.9	1.3	1.8	1.8	1.1

[a] Measurement did not include entire month (started 6 June, ended 13 November 2014)
[b] from vegetated pan (Allen et al 2016)

2.4. DISCUSSION

2.4.1 Effects of energy storage and canopy phenology on available energy

Patterns in AE were largely controlled by the superimposition of patterns in canopy transmission on the progression of climate seasonality. Canopy control over radiation caused increasing R_n in October and November, despite lower sun angles, shorter day length, and likely decreased downward longwave radiation (Figure 2.2A). However, given the coincidence of canopy changes and seasonal weather changes, it was difficult to separate the underlying influences. Wilson et. al. (2000) found that R_n below a deciduous forest was 44% of above-canopy R_n in the dormant season, and 14% in the growing season, with peak R_n (~60%) and E in spring prior to leaf expansion. In a flooded wetland, it is less likely that E in spring exceeds E in fall because in spring, there there would be a net flux of energy into the water (i.e., positive ΔS) reducing AE relative to R_n where as AE is augmented by ΔS and G in fall.

Energy storage by floodwaters and the underlying soil caused seasonal patterns of AE and R_n to differ. Specifically, G and ΔS reduced early-season AE and increased late-season AE. Given the magnitudes of G and ΔS (Table 2.2) with respect to R_n, the effect was substantial (41% increase to AE in November). While the roles of G and ΔS can be ignored in many environments (Spittlehouse and Black, 1980) or over intermediate time intervals (Allen et al., 1998), it cannot be ignored in the presence of persistent standing water, even if shallow (Shoemaker et al., 2005). Most of diel energy storage and release occurred in the uppermost layer of the water, likely

because the floating vegetation prevented deeper radiation transmission. Diel variation in G was low (e.g. Figure 2.6) but the seasonal effect (Table 2.2) was more substantial. As a comparison, G in lakes is often unimportant and there can be complex thermoclines or circulation dynamics that affect ΔS (Ragotzkie, 1978). Observed sub-canopy ΔS effects on diel and seasonal variations at our study site parallel lake energy dynamics, but at a smaller amplitude because the canopy attenuates energy exchanges.

The diel mean peak and magnitude of ΔS increased in fall with canopy thinning and changing advective conditions, inferred by the covariation of H, u_*, and $t_{A\text{-}S}$. During the day, higher net radiation resulted in increased peak ΔS, but this also resulted in more negative ΔS at night; at night, R_n became increasingly negative, likely attributable to decreasing longwave re-radiated downward by the canopy. Prior to senescence, the canopy buffered radiation and advection so magnitude of all fluxes was dampened.

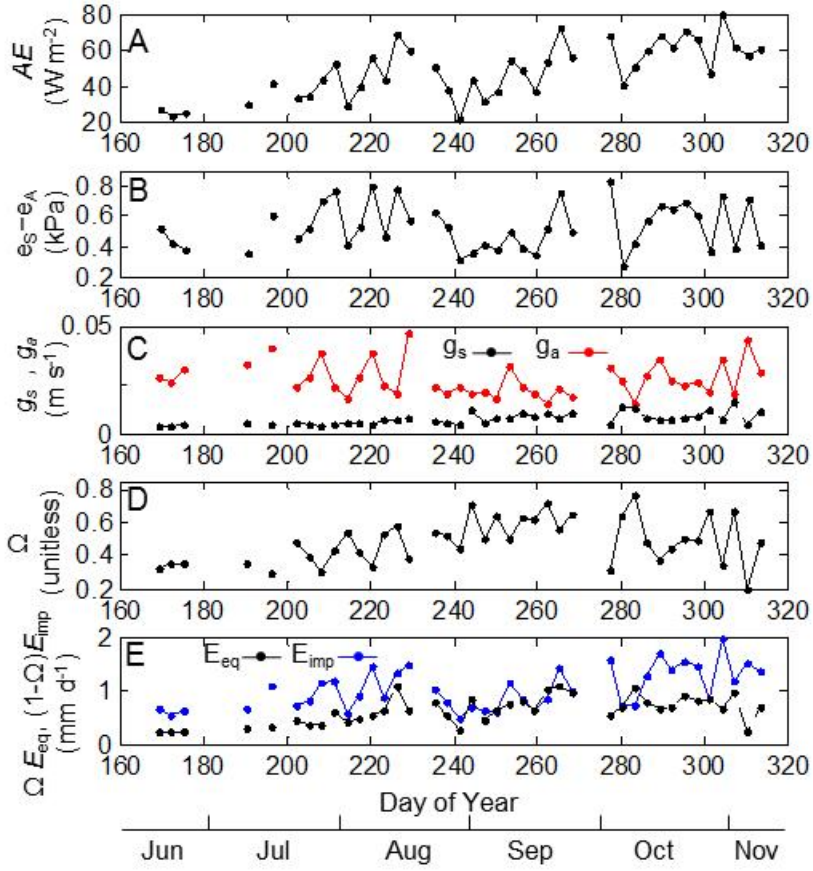

Figure 2.8 Calculations, from means of 3-day ensembles, for (A) available energy, AE, (B) vapor pressure of air subtracted from that at the surface, (C) aerodynamic conductance (g_a) and surface conductance (g_s), (D) the decoupling coefficient, Ω, and (E) contributions, as adjusted by Ω, of imposed evaporation (E_{imp}), and equilibrium evaporation (E_{eq}).

2.4.2 Factors explaining evaporation

Across the months measured, E was 0.9-1.9 mm day^{-1} and almost directly proportional to AE (Table 2.4; Figure 2.7E). Previously reportedsurface E rates in flooded forested wetlands (Brown, 1981; Liu, 1996) were similar to those of the present study, but the mechanisms driving

E were not examined. In the present case, *AE* appears be the primary driver of *E*, as calculated by ECEB. With low *H*, β was similar to or lower then that of open water (Lenters et al., 2005) which is often seen in wet areas such as marshes (Jacobs et al., 2002; Schedlbauer et al., 2011) or wet forest understory layers such as mosses (Kettridge et al., 2013). Demonstrating the effect of surface wetness on energy partitioning between *H* and λ*E*, Wilson et al. (2000) found β of 0.19 when litter was wet and 0.55 when dry, amounting to a 95% decrease in g_s. The present study showed g_s was relatively constant (the same order of magnitude) throughout, presumably because of the constant water presence and persistent vegetation mat. Although vegetation cover on the floodwater was 100%, it was < 2 cm height and had passive stomata and was thus similar to an open water surface (Allen et al. in press). While β increased in November, it was likely because of increased warming of the air by water and not by changes to the surface structure.

The various energy balance methods yielded similar estimates of *E* that were all close to *AE* in magnitude. Although eddy covariance can underestimate fluxes as compared to energy balances (Twine et al., 2000), our conclusions are relatively insensitive to even fairly large errors in estimates of *H*. For example, even with a hypothetical doubling of *H* compared to what was measured, the conclusion would remain that the majority of *AE* is partitioned to *E* and results would be that E_{ECEB} was similar to $E_{\beta\text{-day}}$ and $E_{\beta\text{-month}}$. An independent validation of the monthly trend in energy partitioning was provided by the similarity between β calculated by ECEB and β_{day} or β_{month} calculated from Δe and Δt.

The cause of incongruities between E_{ECEB} and E_{pan} is less clear. Some differences may have resulted from the pans not being entirely sunken, affecting connectivity to floodwater and *G* and Δ*S* fluxes. This would also explain the better agreement between E_{pan} and $E_{ECEB\text{-reduced}}$. E_{pan} magnitudes were similar to, but ~10-20% lower than, E_{ECEB}, but this magnitude of discrepancy is common (Foken, 2008a) and could be caused by R_n being estimated from mean of only two point measurements therefore vulnerable to spatial biases. However, spatial biases are likely lower than in other forests because of the dense and relatively homogeneous broadleaf canopy. Despite uncertainties, the pan measurements provided some validation of magnitude.

Another source of uncertainty in *E* and the energy balance was Δ*S*. Although different calculations using t_W measurements yielded similar results (section 2.3.2), more t_W measurements—with better depth-resolution and with lateral replication—may have decreased uncertainty in *E* because of the importance of the Δ*S* term.

2.4.3 Sensible heat fluxes and corresponding temperature gradients

Although *H* was low, patterns of seasonal and diel variability were likely related to t_W lagging t_A at seasonal and diel timescales. Generally, low *H* was expected because of the small temperature gradients. With $t_{A\text{-}S}$ increasing in fall, *H* and β increased also, indicating an increase in relative partitioning of *AE* towards *H*. Wilson et al. (2000) also observed β increasing with canopy senescence, which could be explained similarly. Higher g_a likely increased *H* in the fall when t_W exceeded t_A, but the effect was opposite in early summer, when g_a was high and *H* was lowest. At the diel timescale, there was a small but frequent upward *H* at night (Figure 2.6) when t_W generally always exceeded t_A (Figure 2.3).

Diel patterns of *H* were low amplitude and flux direction was variable (Figure 2.6), caused by frequent reversal of the temperature gradients. For June through August, mean daytime *H* was approximately zero. There were frequent inversions of *H* that suggest the surface was transiently heated by sunflecks. With canopy senescence in the fall, greater air temperature variability and increased frequency of direct solar radiation reaching the surface likely explains

the more stable diel patterns. Although there were still multiple reversals throughout the day, they were relatively consistent, including a mid-day positive *H* in October and November.

2.4.4 Humidity gradients and the daily development of a vapor pressure deficit

Although it might be assumed that the high humidity was related to the sub-canopy airspace being mostly stagnant, this was apparently not true. Despite high evaporation rates contributing moisture to the airspace (1-2 mm day^{-1} is sufficient to saturate the 13 m sub-canopy airspace several times over), transport out was high enough that t_{dew} generally decreased during the day (Figure 2.3) and there was a mean afternoon VPD of 1.1 kPa (not shown). The role of turbulent exchange was evident by periods of high g_a occurring with higher $e_S - e_A$, (i.e., a shrinking boundary layer; Figure 2.8). Given the large apparent contribution of E_{imp} to *E*, despite a static direct relationship between *E* and *AE*, it is likely the *AE* is driving advective exchange by buoyant forces. September had the highest Ω, when there was frequent rain which could have decreased water temperatures, increased downward Δ*S* and *H* (Figure 2.6K), and increased e_a (Figure 2.8B). Into October and November, g_a, g_s, and $e_S - e_A$ all increased with increasing evaporation from the water and apparently increasing transport from the subcanopy. Overall, Ω was surprisingly low compared to some systems (e.g., crops and grasslands ≈ 0.6-0.9; Jarvis and McNaughton 1986); that is, the flux is relatively smaller as compared to the transport out of the system than it is in grassland, despite *E* here not being controlled by active stomata.

Downward humidity gradients conditions coincided with development of high vapor pressure after sunrise, which is consistent with canopy transpiration and warming of the canopy airspace prior to direct solar radiation reaching the water surface. The water surface was relatively colder than the air during this time. While this gradient suggests flux towards the water surface, it is unclear whether condensation occurred because inversions across the gradient could have occurred. The surface temperature sensors were in the floating vegetation layer, but not at its surface and thus may not precisely represent the true skin temperature. Condensation could not be corroborated with pan data because pressure transducer temperature dependence reduced prohibited examining sub-daily patterns. While downward gradients apparently co-occurred with positive energy balances, this conclusion could be an artifact of imperfect measurement of temporally explicit energy budget components (Foken, 2008a). While the diel condensation patterns seem to be a function of the floodwater, forest humidity and temperature profiles vary substantially throughout the day (Flerchinger et al., 2015; Oke, 1988) and can result in internal water cycling (Berkelhammer et al., 2013) without floodwater.

The stability of high-humidity conditions is an important characteristic of this microclimate. With a transpiring canopy above and an evaporating surface below, saturated or near-saturated conditions were frequent. We know of no work focusing on the ecological effects of these super-humid conditions in wetland forests. While wetland vegetation is known to be hydrophytic (sensitive to root zone water availability), this environment is also conducive to hygrophytic (sensitive to vapor pressure deficits) plants. Furthermore, vapor flux upward to the canopy must affect vapor pressure deficits in the canopy, and thus affect stomatal activity of trees above. These humid conditions define a microclimate that is atypical among temperate forests that are not rainforests and potentially have unrecognized effects on many ecological processes, such as decomposition and nutrient cycling, that depend on humidity-sensitive microbial (Nagy and Macauley, 1982) or fungal activity (Daubenmire, 1974).

2.4.5 *E* as part of *ET*: Modeling and scaling

Understanding the implications of this study to whole-system hydrologic function and appropriate model representation requires considerations of (1) how to account for factors controlling *E*, and (2) how *E* relates to *ET*. Variability in *E* was almost exclusively related to *AE*, as modified by canopy phenology (i.e., R_n was out of phase with above-canopy solar irradiance) and floodwater ΔS. If *AE* can be measured or effectively estimated, an equilibrium evaporation model (i.e., Priestley and Taylor, 1972) is a simple approach:

$$E = \alpha \frac{\Delta AE}{\lambda(\Delta+\gamma)}, \quad (15)$$

where α is the scaling coefficient that would be expected to be fairly stable given the consistency of β. For the 3-day ensembles, α varied between 1.11 and 1.26 until day 288 of the year, after which it varied between 1.27 and 1.38. However, modeling understory *AE* remains problematic because, among other reasons, understory R_n is not a fixed fraction of above-canopy R_n.

The challenges in modeling sub-canopy *AE* could be bypassed with a Priestly-Taylor model combining *E* and *T* terms. This method has been applied to wetlands (Mao et al., 2002), but its application could be improved by accounting for energy storage effects. Importantly, in a flooded system, Priestly-Taylor is probably more appropriate than it is in other systems because of stability in overall *ET* due to the constant water surface (i.e., *E* increased as the canopy senesced). There are no soil-water deficits (albeit, stress responses are not well understood), and while spatial and temporal variation in canopy cover or leaf area generally affects *T* (e.g., Oren et al., 1999), senescence responses suggest that variation in *E* may compensate for these variations in T and results in better satisfaction of Priestly-Taylor assumptions. November *E*, when the canopy was mostly leafless, was comparable to nearby pan evaporation rates for November (Farnsworth and Thompson, 1982) after applying a correction coefficient of 0.75 (1.3-2.2 mm day^{-1} over 62 years of data at three sites).

Apparently *E* in the flooded forested wetlands where it has been measured (this study; Brown, 1981; Liu, 1996) is similar to *E* in forests with sparser canopies and exceeds other closed-canopy forests. In unflooded, closed-canopy forests, *T* generally far exceeds *E* (Kool et al., 2014) but relatively few studies have measured *E* in closed canopy forests because of presumed low contribution of *E* to the overall water budget. In a closed-canopy broadleafed forest in the southeastern US, *E* rarely exceeded 0.5 mm day^{-1} during the growing season and composed a mean fraction of 8% of *ET* (Wilson et al. 2000). In a dense coniferous stand in the central Netherlands, even with generally humid conditions, *E* averaged 0.19-0.38 mm day^{-1} (Schaap et al. 1997). If canopy *T* in the present study was assumed to be was 2-3 mm day^{-1}, as observed for a reasonably similar ash-sweetgum-baldcypress forest in the southeastern US (Krauss et al., 2014), *E* would be 26-40% of *ET* as assumed was 2.5 mm day^{-1} in the growing season months (June-September). This high fraction, a result of low β, is similar or greater than fractions observed in sparser semiarid forests with LAI = 0.7-1.6 and thus much more radiation at the forest floor (Baldocchi et al., 2004, 2000; Raz-Yaseef et al., 2010; Scott et al., 2003). Similarly, sparse boreal forests also have *E*/*ET* fractions ranging from 20-62% (reviewed by (Baldocchi and Ryu, 2011; Iida et al., 2009).

While wetland *E* rates are high, they are not high enough to warrant the conclusion that wetland *ET* is especially high compared to other systems. Effects of the reduced atmospheric demand by the high E fluxes could increase water use efficiency, particularly with strong boundary layer decoupling (*sensu* Jarvis and McNaughton, 1986) and important feedback between *E* and *T* terms. Rates of *E* would likely be higher in a smaller or more isolated wetlands

or in a less-humid region because both lateral and vertical advection effects increase in those circumstances (Baldocchi et al., 2016; Idso, 1981).

2.5. CONCLUSIONS

The understory environment of a flooded forested wetland is defined by high humidity, small temperature gradients, and relatively low energy—factors related to the influences of canopy above and the persistent floodwater. Saturation humidity conditions occurred nearly every day, and accordingly vapor pressure gradients were created by frequently reversing temperature profiles. These temperature and humidity gradients often resulted in apparent vapor fluxes towards the water surface, even during the day, because of the high heat capacity of the water.

Fall seasonal temperature changes and canopy senescence changes increased diel variability in radiation, air temperature, water temperature, and humidity. Sub-canopy net radiation peaked in fall, strongly out of phase with above-canopy solar radiation. The available energy was even more out of phase with solar irradiance because changes in heat fluxes into the flood water was a major component. These storage fluxes shifted the energy budget at both the sub-daily level (reducing evaporation in the morning and increasing in evening) and seasonal level, reducing available energy in June by 22% and increasing in November by 41% (as compared to available energy from net radiation). Thus, the highest evaporation rates were in October and November (1.8 to 1.9 mm day^{-1}), even though this coincided with highest and often upward sensible heat fluxes because water temperatures generally exceeded air temperatures. Sensible heat exchanges were highest when friction velocity was high and the water was warmer than the air. Otherwise, for much of the season, sensible heat flux direction varied throughout the day with fluctuating temperature gradients, and was near zero for most of the summer. Accordingly, Bowen ratios were also near zero for most of the year, peaking in the fall at 0.22.

Available energy was the best predictor of evaporation rates, with almost all energy partitioned to latent heat exchange. While the aerodynamic conductance and VPD of the system were high enough to conclude that imposed evaporation was the primary contribution to evaporation, high evaporation rates also occurred during periods of low aerodynamic conductance. These forested wetland evaporation rates were high and exceeded rates observed by others in closed canopy forests. For predicting sub-canopy evaporation rates in a wetland, the Priestly-Taylor model is generally appropriate if the magnitude and seasonality of available sub-canopy energy is adjusted to account for canopy effects and heat storage of the floodwater.

2.6 REFERENCES

Allen, R.G., Pereira, L.S., Raes, D., Smith, M., 1998. Crop evapotranspiration: Guidelines for computing crop water requirements. FAO - Food and Agriculture Organization of the United Nations, Rome, Italy.

Allen, S.T., Edward, B.L., Reba, M.L,. Keim, R.F., In press. Sub-canopy evapotranspiration from floating vegetation and open water in a swamp forest. Wetlands.

Allen, S.T., Whitsell, M.L., Keim, R.F., 2015. Leaf area allometrics and morphometrics in baldcypress. Can. J. For. Res. 45, 963–969. doi:10.1139/cjfr-2015-0039

Andersen, I.H., Dons, C., Nilsen, S., Haugstad, M.K., 1985. Growth, photosynthesis and photorespiration of Lemna gibba: response to variations in CO2 and O2 concentrations and photon flux density. Photosynth. Res. 6, 87–96. doi:10.1007/BF00029048

Baldocchi, D., Knox, S., Dronova, I., Verfaillie, J., Oikawa, P., Sturtevant, C., Matthes, J.H., Detto, M., 2016. The impact of expanding flooded land area on the annual evaporation of rice. Agric. For. Meteorol. 223, 181–193. doi:10.1016/j.agrformet.2016.04.001

Baldocchi, D.D., Law, B.E., Anthoni, P.M., 2000. On measuring and modeling energy fluxes above the floor of a homogeneous and heterogeneous conifer forest. Agric. For. Meteorol. 102, 187–206. doi:10.1016/S0168-1923(00)00098-8

Baldocchi, D.D., Ryu, Y., 2011. A Synthesis of Forest Evaporation Fluxes – from Days to Years – as Measured with Eddy Covariance, in: Levia, D.F., Carlyle-Moses, D., Tanaka, T. (Eds.), Forest Hydrology and Biogeochemistry, Ecological Studies. Springer Netherlands, pp. 101–116.

Baldocchi, D.D., Xu, L., Kiang, N., 2004. How plant functional-type, weather, seasonal drought, and soil physical properties alter water and energy fluxes of an oak–grass savanna and an annual grassland. Agric. For. Meteorol. 123, 13–39. doi:10.1016/j.agrformet.2003.11.006

Blanken, P.D., 1998. Turbulent Flux Measurements Above and Below the Overstory of a Boreal Aspen Forest. Bound.-Layer Meteorol. 89, 109–140. doi:10.1023/A:1001557022310

Bosch, D.D., Marshall, L.K., Teskey, R., 2014. Forest transpiration from sap flux density measurements in a Southeastern Coastal Plain riparian buffer system. Agric. For. Meteorol. 187, 72–82. doi:10.1016/j.agrformet.2013.12.002

Brown, S., 1981. A Comparison of the Structure, Primary Productivity, and Transpiration of Cypress Ecosystems in Florida. Ecol. Monogr. 51, 403–427. doi:10.2307/2937322

Daubenmire, R.F., 1974. Plant and Environment. A text book of Plant Autecology, Third. ed. John Wiley and Sons, Inc., London, UK.

Dolman, A.J., Gash, J.H.C., Roberts, J., Shuttleworth, W.J., 1991. Stomatal and surface conductance of tropical rainforest. Agric. For. Meteorol. 54, 303–318. doi:10.1016/0168-1923(91)90011-E

Domec, J.-C., Sun, G., Noormets, A., Gavazzi, M.J., Treasure, E.A., Cohen, E., Swenson, J.J., McNulty, S.G., King, J.S., 2012. A Comparison of Three Methods to Estimate Evapotranspiration in Two Contrasting Loblolly Pine Plantations: Age-Related Changes in Water Use and Drought Sensitivity of Evapotranspiration Components. For. Sci. 58, 497–512. doi:10.5849/forsci.11-051

dos Reis, R.J., Dias, N.L., 1998. Multi-season lake evaporation: energy-budget estimates and CRLE model assessment with limited meteorological observations. J. Hydrol. 208, 135–147. doi:10.1016/S0022-1694(98)00160-7

Farnsworth, R.K., Thompson, E.S., 1982. Mean Monthly, Seasonal, and Annual Pan Evaporation for the United States (NOAA Technical Report No. NWS 34). National Weather Service, Washington, DC.

Flerchinger, G.N., Reba, M.L., Link, T.E., Marks, D., 2015. Modeling temperature and humidity profiles within forest canopies. Agric. For. Meteorol. 213, 251–262. doi:10.1016/j.agrformet.2015.07.007

Foken, T., 2008a. Micrometeorology. Springer Publishing, New York, NY, USA.

Foken, T., 2008b. The Energy Balance Closure Problem: An Overview. Ecol. Appl. 18, 1351–1367. doi:10.1890/06-0922.1

Gay, L., W., Knoerr, K.R., 1975. The Forest Radiation Budget. Duke University of Forestry and Environmental Studies, Durham, NC, USA.

Idso, S.B., 1981. Relative Rates of Evaporative Water Losses from Open and Vegetation Covered Water Bodies1. JAWRA J. Am. Water Resour. Assoc. 17, 46–48. doi:10.1111/j.1752-1688.1981.tb02587.x

Iida, S., Ohta, T., Matsumoto, K., Nakai, T., Kuwada, T., Kononov, A.V., Maximov, T.C., Molen, V.D., K, M., Dolman, H., Tanaka, H., Yabuki, H., 2009. Evapotranspiration from understory vegetation in an eastern Siberian boreal larch forest. Agric. For. Meteorol 149, 1129-1139. doi:10.1016/j.agrformet.2009.02.003.

Jacobs, J.M., Mergelsberg, S.L., Lopera, A.F., Myers, D.A., 2002. Evapotranspiration from a wet prairie wetland under drought conditions: Paynes prairie preserve, Florida, USA. Wetlands 22, 374–385. doi:10.1672/0277-5212(2002)022[0374:EFAWPW]2.0.CO;2

Jarvis, P.G., McNaughton, K.G., 1986. Stomatal Control of Transpiration: Scaling Up from Leaf to Region, in: Ford, A.M. and E.D. (Ed.), Advances in Ecological Research. Academic Press, pp. 1–49.

Junk, W., Bayley, P.B., Sparks, R.E., 1989. The Flood Pulse Concept in River—Floodplain Systems, in: Dodge, D.P. (Ed.), Proceedings of the International Large River Symposium. Presented at the International Large River Symposium, 106, Ontario, CA, pp. 110–127.

Keim, R.F., Dean, T.J., Chambers, J.L., 2013. Flooding effects on stand development in cypress-tupelo, in: Proceedings of the 15th Biennial Southern Silvicultural Research Conference. Asheville, NC: U.S. Department of Agriculture, Forest Service, Southern Research Station, pp. 431–437.

Kettridge, N., Thompson, D.K., Bombonato, L., Turetsky, M.R., Benscoter, B.W., Waddington, J.M., 2013. The ecohydrology of forested peatlands: Simulating the effects of tree shading on moss evaporation and species composition. J. Geophys. Res. Biogeosciences 118, 422–435. doi:10.1002/jgrg.20043

Kool, D., Agam, N., Lazarovitch, N., Heitman, J.L., Sauer, T.J., Ben-Gal, A., 2014. A review of approaches for evapotranspiration partitioning. Agric. For. Meteorol. 184, 56–70. doi:10.1016/j.agrformet.2013.09.003

Krauss, K.W., Duberstein, J.A., Conner, W.H., 2014. Assessing stand water use in four coastal wetland forests using sapflow techniques: annual estimates, errors and associated uncertainties. Hydrol. Process. n/a-n/a. doi:10.1002/hyp.10130

Lenters, J.D., Kratz, T.K., Bowser, C.J., 2005. Effects of climate variability on lake evaporation: Results from a long-term energy budget study of Sparkling Lake, northern Wisconsin (USA). J. Hydrol. 308, 168–195. doi:10.1016/j.jhydrol.2004.10.028

Liu, S., 1996. Evapotranspiration from Cypress (Taxodium ascendens) Wetlands and Slash Pine (Pinus elliottii) Uplands in North-Central Florida (Dissertation). University of Florida, Gainesville, FL, USA.

Mao, L.M., Bergman, M.J., Tai, C.C., 2002. Evapotranspiration Measurement and Estimation of Three Wetland Environments in the Upper St. Johns River Basin, Florida1. JAWRA J. Am. Water Resour. Assoc. 38, 1271–1285. doi:10.1111/j.1752-1688.2002.tb04347.x

Mauder, M., Foken, T., 2004. Quality control of eddy covariance measurements (c: 0,1,2).

Meinzer, F.C., Andrade, J.L., Goldstein, G., Holbrook, N.M., Cavelier, J., Jackson, P., 1997. Control of transpiration from the upper canopy of a tropical forest: the role of stomatal, boundary layer and hydraulic architecture components. Plant Cell Environ. 20, 1242–1252. doi:10.1046/j.1365-3040.1997.d01-26.x

Moncrieff, J., Clement, R., Finnigan, J., Meyers, T., 2004. Averaging, Detrending, and Filtering of Eddy Covariance Time Series, in: Lee, X., Massman, W., Law, B. (Eds.), Handbook of Micrometeorology, Atmospheric and Oceanographic Sciences Library. Springer Netherlands, pp. 7–31.

Moncrieff, J.B., Massheder, J.M., de Bruin, H., Elbers, J., Friborg, T., Heusinkveld, B., Kabat, P., Scott, S., Soegaard, H., Verhoef, A., 1997. A system to measure surface fluxes of momentum, sensible heat, water vapour and carbon dioxide. J. Hydrol., HAPEX-Sahel 188–189, 589–611. doi:10.1016/S0022-1694(96)03194-0

Nagy, L.A., Macauley, B.J., 1982. Eucalyptus leaf-litter decomposition: Effects of relative humidity and substrate moisture content. Soil Biol. Biochem. 14, 233–236. doi:10.1016/0038-0717(82)90031-1

Oke, T.R., 1988. Boundary Layer Climates, 2 edition. ed. Routledge.

Oren, R., Phillips, N., Ewers, B.E., Pataki, D.E., Megonigal, J.P., 1999. Sap-flux-scaled transpiration responses to light, vapor pressure deficit, and leaf area reduction in a flooded Taxodium distichum forest. Tree Physiol. 19, 337–347. doi:10.1093/treephys/19.6.337

Papale, D., 2012. Data Gap Filling, in: Aubinet, M., Vesala, T., Papale, D. (Eds.), Eddy Covariance - A Practical Guide to Measurement and Data. Springer Netherlands, Netherlands, p. 438.

Perez, P.J., Castellvi, F., Ibañez, M., Rosell, J.I., 1999. Assessment of reliability of Bowen ratio method for partitioning fluxes. Agric. For. Meteorol. 97, 141–150. doi:10.1016/S0168-1923(99)00080-5

Priestley, C.H.B., Taylor, R.J., 1972. On the Assessment of Surface Heat Flux and Evaporation Using Large-Scale Parameters. Mon. Weather Rev. 100, 81–92. doi:10.1175/1520-0493(1972)100<0081:OTAOSH>2.3.CO;2

Ragotzkie, R.A., 1978. Heat Budget of Lakes, in: Lakes: Chemistry, Geology, Physics. Springer-Verlag, New York, NY, USA.

Raz-Yaseef, N., Rotenberg, E., Yakir, D., 2010. Effects of spatial variations in soil evaporation caused by tree shading on water flux partitioning in a semi-arid pine forest. Agric. For. Meteorol. 150, 454–462. doi:10.1016/j.agrformet.2010.01.010

Rouse, W.R., Oswald, C.J., Binyamin, J., Spence, C., Schertzer, W.M., Blanken, P.D., Bussières, N., Duguay, C.R., 2005. The Role of Northern Lakes in a Regional Energy Balance. J. Hydrometeorol. 6, 291–305. doi:10.1175/JHM421.1

Schaap, M.G., Bouten, W., 1997. Forest floor evaporation in a dense Douglas fir stand. J. Hydrol. 193, 97–113. doi:10.1016/S0022-1694(96)03201-5

Schedlbauer, J., Oberbauer, S., Starr, G., Jimenez, K., 2011. Controls on sensible heat and latent energy fluxes from a short-hydroperiod Florida Everglades marsh. J. Hydrol.

Schlesinger, W.H., Jasechko, S., 2014. Transpiration in the global water cycle. Agric. For. Meteorol. 189–190, 115–117. doi:10.1016/j.agrformet.2014.01.011

Scott, R.L., Watts, C., Payan, J.G., Edwards, E., Goodrich, D.C., Williams, D., James Shuttleworth, W., 2003. The understory and overstory partitioning of energy and water fluxes in an open canopy, semiarid woodland. Agric. For. Meteorol. 114, 127–139. doi:10.1016/S0168-1923(02)00197-1

Shoemaker, W.B., Lopez, C.D., Duever, M., 2011. Evapotranspiration over Spatially Extensive Plant Communities in the Big Cypress National Preserve, Southern Florida, 2007-2010

(USGS Scientific Investigations Report No. 2011–5212). United States Geological Survey.

Shoemaker, W.B., Sumner, D.M., Castillo, A., 2005. Estimating changes in heat energy stored within a column of wetland surface water and factors controlling their importance in the surface energy budget. Water Resour. Res. 41. doi:10.1029/2005WR004037

Sota, E.R. de la, Pazos, L.A.C. de, 1990. On the stomata of Salvinia herzogii (Salviniaceae, Pteridophyta). Plant Syst. Evol. 172, 119–125. doi:10.1007/BF00937802

Spittlehouse, D.L., Black, T.A., 1980. Evaluation of the Bowen ratio/energy balance method for determining forest evapotranspiration. Atmosphere-Ocean 18, 98–116. doi:10.1080/07055900.1980.9649081

Sun, X., Onda, Y., Kato, H., Otsuki, K., Gomi, T., 2014. Partitioning of the total evapotranspiration in a Japanese cypress plantation during the growing season. Ecohydrology 7, 1042–1053. doi:10.1002/eco.1428

Sun, X., Onda, Y., Otsuki, K., Kato, H., Gomi, T., 2016. The effect of strip thinning on forest floor evaporation in a Japanese cypress plantation. Agric. For. Meteorol. 216, 48–57. doi:10.1016/j.agrformet.2015.10.006

Tillberg, E., Dons, C., Haugstad, M., Nilsen, S., 1981. Effect of abscisic acid on CO2 exchange in Lemna gibba. Physiol. Plant. 52, 401–406. doi:10.1111/j.1399-3054.1981.tb02707.x

Twine, T.E., Kustas, W.P., Norman, J.M., Cook, D.R., Houser, P.R., Meyers, T.P., Prueger, J.H., Starks, P.J., Wesely, M.L., 2000. Correcting eddy-covariance flux underestimates over a grassland. Agric. For. Meteorol. 103, 279–300. doi:10.1016/S0168-1923(00)00123-4

van der Valk, A.G., 1981. Succession in Wetlands: A Gleasonian Approach. Ecology 62, 688–696. doi:10.2307/1937737

Van Wijk, W.R., de Vries, D.A., 1963. Thermal properties of soils, in: Physics of plant environment. p. 382 pp.

Webb, E.K., 1960. On estimating evaporation with fluctuating Bowen ratio. J. Geophys. Res. 65, 3415–3417. doi:10.1029/JZ065i010p03415

Wilczak, J.M., Oncley, S.P., Stage, S.A., 2001. Sonic Anemometer Tilt Correction Algorithms. Bound.-Layer Meteorol. 99, 127–150. doi:10.1023/A:1018966204465

Wilson, K., Goldstein, A., Falge, E., Aubinet, M., Baldocchi, D., Berbigier, P., Bernhofer, C., Ceulemans, R., Dolman, H., Field, C., Grelle, A., Ibrom, A., Law, B.E., Kowalski, A., Meyers, T., Moncrieff, J., Monson, R., Oechel, W., Tenhunen, J., Valentini, R., Verma, S., 2002. Energy balance closure at FLUXNET sites. Agric. For. Meteorol., FLUXNET 2000 Synthesis 113, 223–243. doi:10.1016/S0168-1923(02)00109-0

Wilson, K.B., Baldocchi, D.D., 2000. Seasonal and interannual variability of energy fluxes over a broadleaved temperate deciduous forest in North America. Agric. For. Meteorol. 100, 1–18. doi:10.1016/S0168-1923(99)00088-X

Wilson, K.B., Hanson, P.J., Baldocchi, D.D., 2000. Factors controlling evaporation and energy partitioning beneath a deciduous forest over an annual cycle. Agric. For. Meteorol. 102, 83–103. doi:10.1016/S0168-1923(00)00124-6

Wullschleger, S.D., Wilson, K.B., Hanson, P.J., 2000. Environmental control of whole-plant transpiration, canopy conductance and estimates of the decoupling coefficient for large red maple trees. Agric. For. Meteorol. 104, 157–168. doi:10.1016/S0168-1923(00)00152-0

CHAPTER 3: SUB-CANOPY EVAPOTRANSPIRATION FROM FLOATING VEGETATION AND OPEN WATER IN A SWAMP FOREST[1]

3.1 INTRODUCTION

Vegetation is a key feature distinguishing wetlands from other aquatic systems because of its role in physical, biological, and chemical processes. The water balance of a wetland can be affected by vegetation because transpiration is generally a dominant component of evapotranspiration (ET). However, despite substantial research in this area, the effect of vegetation on wetland evapotranspiration is not well constrained (Drexler et al. 2004). A fundamental question that remains unanswered is how the presence of vegetation on a body of water affects the magnitude and timing of ET (Allen et al. 1997).

Numerous approaches have been used to address this question; collectively, these have yielded a tenuous characterization of wetland ET, as reviewed by Crundwell (1986) and Abtew and Melesse (2013). Theory suggests that ET from vegetation should be similar to evaporation from open water in humid environments that are not strongly influenced by lateral advection, as demonstrated by many studies reviewed by Crundwell (1986). However, reported rates of ET from wetland vegetation range from slightly less than open water evaporation rates to several times higher (Abtew and Melesse 2013). The latter generally occurs when experimental designs allow advection to be a major energy source, as in the case of isolated lysimeters in non-representative environments (Anderson and Idso 1987).

One component of how vegetation affects wetland ET that has been minimally explored is the role of floating vegetation in flooded swamp forests. Floating vegetation is common in wetlands worldwide, spreads prolifically, and is becoming more common (Hough et al. 1989, Egertson et al. 2004, Luque et al. 2013). Because floating vegetation is extensive in the understory of forested wetlands in some regions (Mitsch and Gosselink 2007), effects of this cover on ET could account for significant variations in regional water balances. While some past studies have compared ET from floating vegetation to open water in clearings (e.g., Snyder and Boyd 1987, Rao 1988), none have compared below forest canopy with the exception a short period of measurements by Brown (1981). However, effects of floating vegetation may differ in the sub-canopy environment because ET there is largely driven by radiative energy transmitted through the canopy and absorbed at the surface (Raz-Yaseef et al. 2010).

In this study, our objective was to quantify and compare ET from floating aquatic vegetation (ET_v) and evaporation from open water (E_{ow}) below a swamp forest canopy. We compared ET_v and E_{ow} across seasonal weather and phenological variations to elucidate controls over magnitudes and differences. Measurements were made in Class A evaporation pans placed in a flooded swamp to mitigate vulnerability to biases from laterally advected energy and to understand the effect of vegetation on ET specifically in this environment (Figure 3.1).

3.2 METHODS

3.2.1 Site Description

Measurements were conducted 6 June 2014 to 13 November 2014, comprising summer and fall through senescence, in the Maurepas Swamp in southeastern Louisiana at 30° 6' 3" N,

[1] This chapter previously appeared as Allen, S.T., Edward, B.L., Reba, M.L,. Keim, R.F., In press. Sub-canopy evapotranspiration from floating vegetation and open water in a swamp forest. Wetlands. It is reprinted by permission of Springer

90° 37' 29" W (Figure 3.1), with mostly continuous, homogenous swamp for > 2.5 km in all directions. The site is permanently flooded and impounded by roads and small levees; during the study period, water depth was between 0.4 and 0.6 m, aside from during two large precipitation events. The climate is humid subtropical with monthly mean temperatures ranging from 10 to 27 °C. Mean precipitation (annual mean of 160 cm) is similar among months, although lower in fall of most years and offset by occasional tropical cyclones. The study period (Table 3.1) followed typical climate conditions, with all monthly temperatures within 2 °C of 30-year means and no consistent bias (1984-2013). There was a relatively drier fall (Table 3.1; 30-year mean precipitation for June, July, August, September, October, November = 16, 13, 15, 12, 12, 10 cm, respectively).

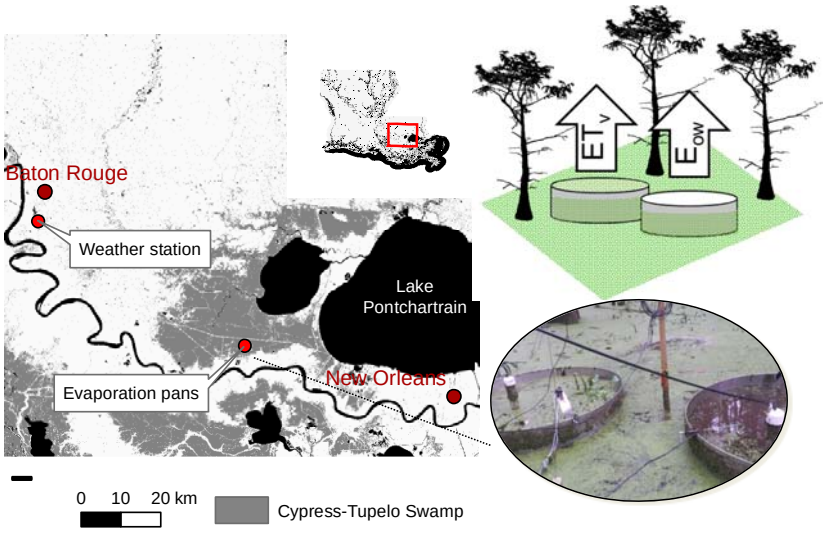

Figure 3.1 Study site photo, mapped location with respect to extent of baldcypress-ash-tupelo swamp (with cover data from Couvillion and Barras 2006), and diagram depicting site set-up for measuring evaporation from open water (E_{ow}) and evapotranspiration from floating vegetation (ET_v), which also surrounded the pans.

The forest overstory was composed of baldcypress (*Taxodium distichum*), water tupelo (*Nyssa aquatica*), and ash (*Fraxinus spp.*), with swamp red maple (*Acer rubrum* var. *drummondii*) in the midstory. Codominant tree height was 21.6 ± 0.4 m (mean ± SE), with a canopy base at 13.6 ± 0.8 m. Midstory red maple trees were scattered and were 6.0 ± 0.4 m tall with crowns extending nearly to the water surface. Heights were measured by laser hypsometer (TruPulse 200x, Laser Technology Inc., Centennial CO, USA). Basal area at the study site was 44 ± 3 m^2 ha^{-1}, measured with a BAF10 wedge prism. All trees on site are deciduous and the transition from leaf-on to leaf-off was noted with successive field visits. Baldcypress maintained most of its foliage through the end of the study. Senescence of the other species began in mid-September and they were mostly without leaves by the beginning of November.

The water surface in the swamp was nearly completely covered by floating aquatic vegetation, predominantly common salvinia (*Salvinia minima*) and duckweed (*Lemna* spp.) with few water-hyacinth (*Eichhornia crassipes*). *Salvinia* are ferns with circular fronds < 2 cm diameter, rising < 1 cm above the water, and with permanently open stomata (de la Sota and Pazos 1990). *Lemna* are monocots with fronds < 8 mm long, rising < 3 mm above the water, and also with permanently open stomata (Tillberg et al. 1981; Andersen et al. 1985).

Table 3.1 Meteorological variables during the study: daily maximum and minimum temperature (T), daily maximum and minimum relative humidity (RH), vapor pressure deficit (VPD), net radiation under canopy and over floating vegetation (R_{net}), total precipitation (P), and downward shortwave radiation (R_{sol}). Measurements were below canopy at the study site and off site in Baton Rouge, USA.

	On site, below canopy						Off site, in clearing						
Month	T Max, °C	T Min, °C	RH Max, %	RH Min, %	VPD Max, kPa	R_{net} Mean, W m^{-2}	T Max, °C	T Min, °C	RH Max, %	RH Min, %	VPD Max, kPa	P cm	R_{sol} Mean, W m^{-2}
Jun[a]	30.8	22.4	100	68	1.45	33.8	31.1	22.1	96	53	2.14	9	114
Jul	31.3	22.5	100	64	1.71	36.8	31.9	21.9	95	48	2.49	13	122
Aug	32.3	23.0	100	66	1.71	39.9	32.5	22.6	96	51	2.45	19	103
Sep	31.1	21.9	100	67	1.55	40.3	31.1	21.1	96	50	2.28	6	94
Oct	28.5	15.8	100	52	1.85	47.3	27.7	14.2	96	41	2.15	6	86
Nov[a]	20.5	8.9	99	57	1.07	33.8	20.5	7.9	91	44	1.37	2	62

[a] Measurement did not include entire month (started 6 June, ended 13 November 2014

Plants in the dense mats appeared to decline in vigor at the end of the study period, indicated by a more yellow color; we have observed this partial decline to be typical in this environment, although the cover may persist through winter. Water and soil were characteristic of an impounded blackwater swamp, with dark, tannic water and a thick, semi-fluid organic layer at the ground surface.

3.2 Instrumentation and Measurements

3.2.1 Evaporation Pans

Two standard Class A evaporation pans (254 mm depth, 1.22 meter diameter) were installed, partially submerged (Guenther et al 2012), on level wooden platforms (Fig. 1). Depth of submergence varied with swamp water level, and heights of platforms were re-adjusted periodically to maintain contact with swamp water because heat conduction is an important part of the energy balance (Shoemaker et al 2005). Pan water levels were also adjusted on a ~1-2 week interval to keep water near the rim (within 5 cm) but avoid overtopping. Under typical deployment, Class A pans provide estimates of potential ET; correction factors are required to compensate for biases related to heat storage, exposure, and advection (Dingman 2002). By submerging most of the pans and placing them in a low wind-speed environment, the biases requiring corrections are mitigated and changes in pan water levels are direct measurements of site evapotranspiration (Masoner et al 2008).

One pan contained open water and the other contained *Salvinia minima* and *Lemna* spp. at approximately 100% cover, similar to the surrounding water. Each pan contained a high-precision vented pressure transducer (Omega Engineering, Inc., model PX709GW-HH, Stamford, CT, USA), calibrated to measure a water depth range of 0-254 mm, concomitant with pan depth, with an accuracy of 0.08% of calibration range.

3.2.2 Environmental Measurements

Air temperature and humidity were measured (Campbell Scientific CS-215, Inc., Logan, UT, USA) below the canopy, at approximately 2.4 m above the mean water surface. Net radiation (R_{net}) was measured at 2 m height with a radiometer (Kipp Zonen NR-Lite 2, Delft, Netherlands) over floating vegetation. Open water R_{net} was not measured because the sensor field of view included the surrounding swamp, and not just the pans; open water R_{net} likely was different because of emissivity and reflectance differences. Outside of the pans, a thermocouple measured temperature at 40 cm above the soil surface, ranging from just under the water surface (at lowest water levels) to 20 cm below, roughly corresponding with the height of the bottom of the pan. Another thermocouple measured water temperature inside the pans, near but below the water surface. The mean of the two thermocouples were used to estimate pan water temperature and compensate for temperature dependence of the pressure transducers, which were calibrated in the laboratory. All instrumentation was scanned every five seconds and logged as five minute averages.

Ancillary meteorological measurements from 2014, including precipitation, temperature, relative humidity, and solar radiation (Table 1) were from the Louisiana Agriclimatic Information System (http://weather.lsuagcenter.com), measured at 9 m height in a clearing surrounded by agricultural fields near Baton Rouge, LA (57 km away). These data were used for reference to conditions external to wetland microclimatic influences.

3.2.3 Vegetation Reflectance

Relative reflectance spectra (325 to 1075 nm) were measured for *Salvinia*, *Lemna*, and open water to better understand differences in energy relationships which may be an important control over differences between ET_v and E_{ow}. Reflectance was measured with a portable spectroradiometer (FieldSpec Handheld2, ASD inc., Boulder, CO, USA). Measurements were taken with a 25° solid angle field of view from approximately 0.5 m above the water surface on 23 July 2014. Six 10-scan-mean spectra were measured for each vegetation type, and 12 10-scan-means for open water.

3.3 Data Processing and Analysis

Pan water levels were used to derive estimates of ET_v and E_{ow}. Data were excluded on days that received precipitation, when pans were overtopped by the surrounding water, when pan water levels were manually adjusted, or if data showed other spikes suggesting disturbance or sensor and datalogger issues. Evaporation rates were estimated as differences between start and end water levels for each disturbance-free 24 hour period, minimizing temperature effects on the pressure transducers.

For temporal replication, 24-hour sampling units were binned at both monthly and seasonal time scales. Paired t-tests were used to compare ET_v and E_{ow} for each season. Differences between months, differences between treatments, and interactions effects were compared by two-way analysis of variance (ANOVA). All analyses were performed in MATLAB (Mathworks, Inc., Natick MA, USA). Tukey HSD tests were used for multiple comparisons among months. In paired comparisons between ET_v and E_{ow} and in calculating seasonal or annual means, only matched periods (i.e., with measurements from both) were used to eliminate associated biases. All collected data were used in presentation of temporal trends.

3.3 RESULTS

Over the study period, temperature, day-time relative humidity, and precipitation decreased (Table 3.1; Figure 3.2), typical of the summer to fall transition in this region. Above-canopy solar radiation (R_{sol}) at the reference station peaked in early July and generally trended downward through the sampling period. In contrast, below-canopy R_{net} trended upward (Figure 3.2C), peaking in September-October with the onset of canopy senescence and leaf abscission despite decreasing sun angle and day length.

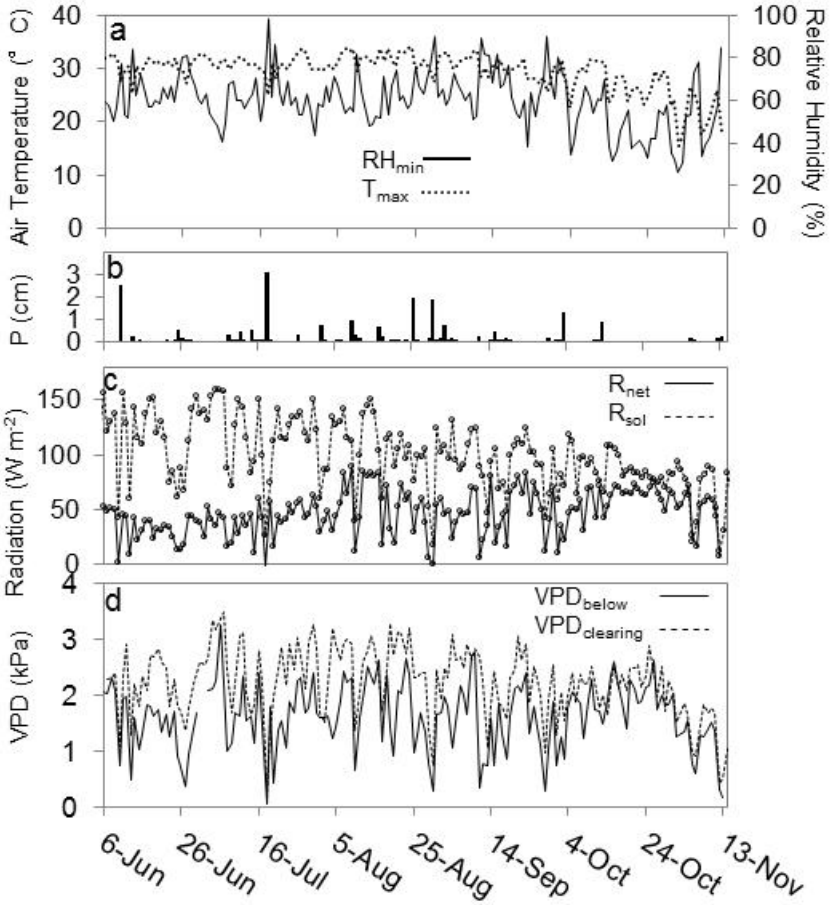

Figure 3.2 (A) Daily minimum relative humidity (RH) and daily maximum air temperature measured below canopy on site. Panel (B), daily precipitation (P) measured off site. Panel (C), mean daily solar irradiance (R_{sol}) in a clearing above an agricultural field (measured off site) and mean daily net radiation (R_{net}) under canopy in a swamp (measured on site). Panel (D), maximum daily vapor pressure deficit in a clearing above an agricultural field (measured off site; $VPD_{clearing}$) and maximum daily vapor pressure deficit under canopy in a swamp (measured on site; VPD_{below}).

Vapor pressure deficit (VPD) under the canopy was fairly stationary throughout the period. Similar to radiation, sub-canopy VPD was offset from VPD at the reference station (Figure 3.2D), but they converged towards the end of the measurement period. The ratio of VPD at the reference station (in a clearing) versus the in-situ VPD declined through the measurement period, with monthly ratios for June through November of 1.48, 1.46, 1.44, 1.47, 1.16, and 1.28, respectively.

There were 33 rainless periods used for quantifying ET, ranging from 1 to 14 continuous days (Table 3.2) with 23 periods and 74 days of matched measurements from both pans. During these periods, mean (±SE) ET_v and E_{ow} were 1.35 ± 0.10 and 1.36 ± 0.06 mm day^{-1}, respectively.

Rates of ET_v and E_{ow} generally followed similar trends over the study period with small net differences between pans. In summer (11 June – 22 September), ET_v was 1.26 ± 0.15 mm day^{-1} and E_{ow} was 1.43 ± 0.09 mm day^{-1} with no significant differences between means ($p = 0.13$). In fall (23 September – 13 November), ET_v was 1.45 ± 0.14 mm day^{-1}, which was significantly different ($p = 0.03$) from E_{ow} of 1.23 ± 0.09 mm day^{-1}. At the monthly time scale, there were significant differences among months ($p = 0.02$; Figure 3.3), but not for ET_v versus E_{ow} ($p = 0.77$) and no significant interaction effect between month and treatment ($p = 0.48$). ET was highest in September and lowest in November, which respectively corresponded with the months with highest and second lowest R_{net}.

Table 3.2 Number of contiguous 24 hour periods per month separated by commas indicate gaps between (e.g: '3,6' represents a 3 day uninterrupted measurement period, a gap of some duration, and a 6 day uninterrupted measurement period).

Month	Sample Size
June	2*, 1*, 2*, 1*, 1*, 1*
July	4, 1, 3, 2*, 2*, 4, 5
August	2, 2, 2, 2, 1, 1, 3, 1
September	1, 2*, 1, 2, 1*, 9
October	5, 1, 3, 14
November	3, 6

* data only available for one pan

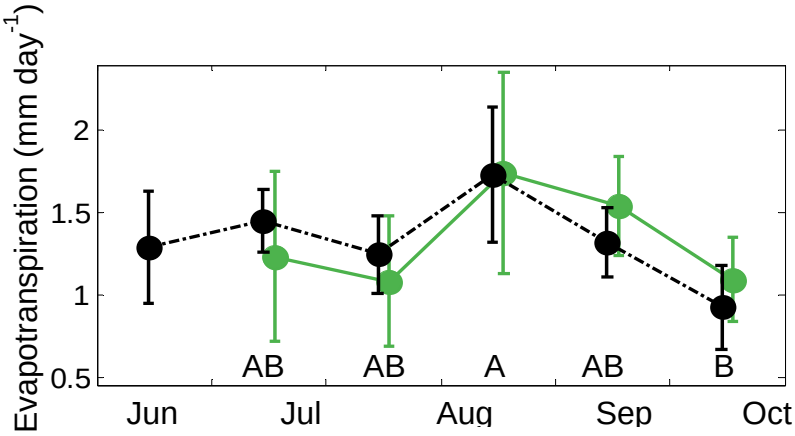

Figure 3.3 Monthly differences between evapotranspiration from open water (black, dashed line) and floating vegetation (green, solid line). Letters indicate groupings of differences among months by Tukey Honestly Significant Difference test ($\alpha = 0.05$).

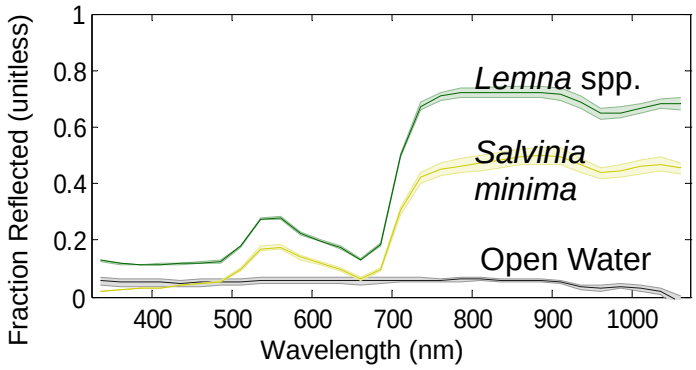

Figure 3.4 Relative reflectance spectra over visible and near IR for open water (black / gray), *Salvinia minima* (yellow), and *Lemna* spp. (green). Spectra were averaged in 25 nm bins to remove noise.

Relative reflectance spectra differed significantly between open water and vegetation (Figure 3.4). The 95% confidence intervals of reflectance rarely overlapped, except for *Salvinia* and open water at the reflectance minima for vegetation: 400-500 nm and at ~675 nm. Otherwise, vegetation had higher reflectance in mid visible range (500-650 nm), and the near-infrared (NIR) range (> 700 nm). Mean relative reflectance across the measured spectrum was 4.9 ± 0.4 % for water, 26.7 ± 0.8 % for *Salvinia*, and 42.4 ± 0.4 % for *Lemna*.

3.4 DISCUSSION

The range of monthly mean ET_v and E_{ow} of 0.9 to 1.7 mm per day is consistent with results from the two studies that have measured sub-canopy evaporation from floodwaters in forested wetlands (Brown 1981; Liu 1996). Brown (1981) used a gas exchange chamber system for 8 days in June and July and measured rates of 1.65 from *Lemna* and 1.46 mm day^{-1} from open water, both under a baldcypress canopy. Liu (1996) measured in-situ pan evaporation for open water under baldcypress; specific details were not reported but the study found that ET could be modeled from above-canopy R_{net}, yielding rates ranging from 0 to 3 mm day^{-1}. At a different site in Louisiana, an energy balance approach yielded estimates of ET_v of 0.3 to 1.4 mm day-1 from *Salvinia* under baldcypress (Allen et al. 2014). Given the climate similarity among these previous studies, similarity in ET rates is not surprising, despite variations in baldcypress canopy structure (Allen et al 2015) with potentially significant effects on understory ET (Kettridge et al 2013).

Although comparisons of ET_v and E_{ow} under flooded forest cover are rare, previous studies have found similarity between ET_v and E_{ow} in other environments (Table 3.3). Generally, past studies can be partitioned into those conducted in-situ, which generally find $ET_v \approx E_{ow}$, and those conducted off site in non-wetland environments which tended to find $ET_v > E_{ow}$ (Table 3.3). The latter (reviewed by Crundwell 1986) suggests advection of dry air into wetlands or wetland microcosms amplifies ET_v more than E_{ow} due to greater aerodynamic roughness and surface area of vegetation (Anderson and Idso 1987). These advective conditions are unlike the sub-canopy environment, where turbulent exchange is reduced because of sheltering by the canopy (Blanken 1998; Reba et al 2012) and radiation is a more prominent driver. Differences in radiation balances between vegetation and open water are likely because of differences in albedo, surface temperature, and emissivity. However, downward longwave and shortwave radiation

would be equivalent and radiative factors affected by surface cover are probably insubstantial enough in this below-canopy climate to explain the similarity between ET_v and E_{ow}.

Variations between ET_v and E_{ow}, and seasonal variation of both, coincided with climatological and phenological changes. The fall had (1) greater R_{net}, (2) lower relative humidity, and (3) canopy leaf senescence (Figure 3.2), all of which may have contributed to peak ET in September (Figure 3.3). Sub-canopy ET in wetlands has been modeled as a fraction of above canopy potential ET (Sun et al. 1998; Liu et al. 1998), but this approach would yield results different from what we observed. In our study, the increasing R_{net} and ET in September and October is likely out of phase with above-canopy R_{net}, which generally peaks near the solstice (e.g., Parkhurst et al. 1998). A likely cause for this late peak ET was canopy senescence which resulted in increased transmission of R_{sol} and greater coupling with the atmosphere (Wilson et al. 2000). With canopy senescence, longwave radiation emitted from the water surface is increasingly transmitted to the sky rather than being absorbed and largely re-emitted back to the ground surface; this would partially counteract the effects of increased transmittance of R_{sol}. Evidenced by greater similarity between below-canopy VPD and reference site VPD in October and November, the thinning canopy also increased the likelihood of advection of relatively dry air into the sub-canopy airspace. This VPD convergence suggests less decoupling (*sensu* Jarvis and McNaughton 1986) in the fall; greater coupling is associated with a higher likelihood of advection which can increase ET_v relative to E_{ow} (Anderson and Idso 1987).

Changes in radiation spectra of incoming energy may also contribute to $ET_v - E_{ow}$ differences because of the reflectance differences between the vegetated and open water surfaces. Given the lack of stomatal control by these floating plants, $ET_v - E_{ow}$ differences are probably related to morphology or energy relations. Forest canopies reduce the overall incoming radiation, but also disproportionately decrease transmission of red and blue radiation relative to green and near infrared radiation bands (Monteith and Unsworth 2008; Reifsnyder and Lull 1965). Floating vegetation has greater relative reflectance, especially in these wavelengths (i.e., visible green and NIR) than open water (Figure 3.4). With senescence, as more red and blue visible light is transmitted, the relative proportion of incoming energy in green and NIR wavelengths (those less absorbed by vegetation) decreases; this could cause a relatively greater increase in ET_v than E_{ow} during the leaf-off period. However, total reflectance of floating vegetation is likely greater than open water in all circumstances except very low sun angles.

Differences in regional water budgets between forested swamps with versus without floating vegetation are likely minor. Under closed canopy forest, mean and seasonal $ET_v - E_{ow}$ differences were small (approximately ± 0.2 mm day^{-1} difference). This is unlikely to have major effects on the total ET flux, which likely peaks around 4-6 mm day^{-1} in summer for southeastern swamp forests (Brown 1981; Ewel and Smith 1992; Krauss et al. 2014). Surface evaporation and ET represent an increasing proportion of total ET with progression into the fall, but as a component of the understory, observed $ET_v - E_{ow}$ differences remained small. However, *Salvinia* has been described as one of the world's most noxious invasive species (Luque et al. 2013), and is regionally expanding (Allen and Suir 2014). If the late season increase of ET_v over E_{ow} is caused by increased advective exchange, $ET_v - E_{ow}$ differences could be greater in conditions where lateral advection has a larger role such as non-forested or isolated wetlands such as those reviewed in Table 3.3. Identifying the specific mechanistic controls over evaporation would be beneficial to predicting changes in surface $ET_v - E_{ow}$ in different conditions; similarly, measuring $ET_v - E_{ow}$ differences across a canopy density gradient could help illustrate those controls.

Table 3.3 Comparison of some previously observed ET rates from vegetated wetlands (ET_v) versus open water (E_{ow}), comparing across methods, vegetation type, and whether the study took place in a wetland (in-situ) or not (off-site).

Study	Location	Site	Method[a]	Type	ET_v (mm/day)	E_{ow} (mm/day)	ET_v:E_{ow} Ratio
Present Study	Louisiana, USA	in-situ[b]	Lysimeter	Floating	1.4	1.4	1.0
Brown 1981	Florida, USA	in-situ[b]	Gas Exchange	Floating	1.7	1.5	1.1
Parkhurst et al 1998	North Dakota, USA	in-situ	Energy Balance	Emergent	4.3	4.2	1.0
Abtew 1996	Florida, USA	in-situ	Lysimeter	Emergent	3.5 - 3.6	3.7	0.9 - 1.0
Eisenlohr 1966	North Dakota, USA	in-situ	Water Balance	Emergent	3.0 - 3.4	4.2	0.7 - 0.8
Burba et al 1999	Nebraska, USA	in-situ	Energy Balance	Emergent	3.5 - 3.8	4.1	0.9
Abtew 2005	Florida, USA	in-situ	Energy Balance	Emergent	3.4 - 4.2	4.2 - 4.5	0.8 - 1.0
Mao et al 2002	Florida, USA	in situ	Lysimeter	Emergent	3.3 - 3.5	3.2	1.0 - 1.1
Anderson and Idso 1987	Arizona, USA	off-site	Lysimeter	Floating	NA[c]	NA[c]	0.9 - 1.4
Snyder and Boyd 1987	Alabama, USA	off-site	Lysimeter	Floating	7.3 - 10.1	5	1.5 - 2.0
Snyder and Boyd 1987	Alabama, USA	off-site	Lysimeter	Emergent	7.1 - 9.2	5	1.4 - 1.8
Rogers and Davis 1972	Alabama, USA	off-site	Lysimeter	Floating	NA[c]	NA[c]	5.3
Rao 1988	SW India	off-site	Lysimeter	Floating	4.8 - 7.8	5.6	0.9 - 1.4

[a]'Lysimeter' includes any contained unit where the water balance was monitored
[b]Study took place underneath forest canopy
[c]Not available because study reported only relative differences

3.5 CONCLUSIONS

This study shows that in a sub-tropical swamp, ET under a closed-canopy forest from floating macrophytes (ET_v) and from open water (E_{ow}) are roughly equal in the summer and fall. Overall, mean rates are similar despite differences in the surface reflectance which must affect the overall radiation budgets and may explain the minor differences in seasonal trends of ET_v versus E_{ow}. Peak rates of ET occurred in September when temperatures were high and senescence of the overlying canopy began. ET rates in September and October exceeded ET during periods when incoming solar energy above the canopy was greatest (i.e., near summer solstice).

3.6 REFERENCES

Abtew, D.W., Melesse P.D.A., 2013. Wetland evapotranspiration. Evaporation and Evapotranspiration Measurements and Estimations. Springer, Netherlands. 93-108

Abtew, W., 1996. Evapotranspiration measurements and modeling for three wetland systems in south Florida1. JAWRA Journal of the American Water Resources Association 32:465–473. doi: 10.1111/j.1752-1688.1996.tb04044.x

Abtew, W., 2005. Evapotranspiration in the Everglades; Comparison of Bowen ratio measurements and model estimations. American Society of Agricultural Engineers 2005 Annual Meeting. doi: 10.13031/2013.19812

Allen, L.H. Jr, Sinclair, T.R., Bennett, J.M., 1997. Evapotranspiration of vegetation of Florida: perpetuated misconceptions versus mechanistic processes. Proceedings - Soil and Crop Science Society of Florida 56:1–10.

Allen, S.T., Edwards B.L., Keim R.F., Reba M.L., 2014. Measurement of sub-canopy evaporation in a flooded forest. Evapotranspiration: Challenges in Measurement and Modeling from Leaf to the Landscape Scale and Beyond Conference Proceedings of the American Society of Agricultural Engineers. doi: 10.13031/et.1815545

Allen, S.T., Whitsell, M.L., Keim, R.F., 2015. Leaf area allometrics and morphometrics in baldcypress. Canadian Journal of Forest Research 45:963–969. doi:10.1139/cjfr-2015-0039

Allen, Y.C., Suir, G.M., 2014. Using high-resolution, regional-scale data to characterize floating aquatic nuisance vegetation in coastal Louisiana navigation channels. Army Corps of Engineers Vicksburg, MS, No. ERDC/TN APCRP-EA-27.

Andersen, I.H., Dons, C., Nilsen, S., Haugstad, M.K., 1985. Growth, photosynthesis and photorespiration of Lemna gibba: response to variations in CO2 and O2 concentrations and photon flux density. Photosynthesis Research 6:87–96. doi: 10.1007/BF00029048

Anderson, M.G., Idso, S.B., 1987. Surface geometry and stomatal conductance effects on evaporation from aquatic macrophytes. Water Resources Research 23:1037–1042. doi: 10.1029/WR023i006p01037

Blanken, P.D., 1998. Turbulent flux measurements above and below the overstory of a boreal aspen forest. Boundary-Layer Meteorology 89:109–140. doi: 10.1023/A:1001557022310

Brown, S., 1981. A comparison of the structure, primary productivity, and transpiration of cypress ecosystems in Florida. Ecological Monographs 51:403–427. doi: 10.2307/2937322

Burba, G.G., Verma, S.B., Kim, J., 1999. A comparative study of surface energy fluxes of three communities (Phragmites australis, Scirpus acutus, and open water) in a prairie wetland ecosystem. Wetlands 19:451–457. doi: 10.1007/BF03161776

Couvillion, B.R., Barras, J.A., 2006. Late 20th century land use / land cover changes in the northern Gulf Coast. http://ngom.usgs.gov/task3_3/.

Crundwell, M.E., 1986. A review of hydrophyte evapotranspiration. Revue d'Hydrobiologie Tropicale 19:215–232.

de la Sota, E.R., Pazos, L.A.C., 1990. On the stomata of Salvinia herzogii (Salviniaceae, Pteridophyta). Plant Systematics and Evolution 172:119–125. doi: 10.1007/BF00937802

Dingman,S.L., 2002. Physical Hydrology. Waveland Press, Inc., Long Grove, IL, USA

Drexler, J.Z., Snyder, R.L., Spano, D., Paw, U. K.T., 2004. A review of models and micrometeorological methods used to estimate wetland evapotranspiration. Hydrological Processes 18:2071–2101. doi: 10.1002/hyp.1462

Egertson, C.J., Kopaska, J.A., Downing, J.A., 2004. A century of change in macrophyte abundance and composition in response to agricultural eutrophication. Hydrobiologia 524:145–156. doi: 10.1023/B:HYDR.0000036129.40386.ce

Eisenlohr, W.S., 1966. Water loss from a natural pond through transpiration by hydrophytes. Water Resources Research 2:443–453. doi: 10.1029/WR002i003p00443

Ewel, K.C., Smith, J.E., 1992. Evapotranspiration from Florida Pondcypress Swamps. JAWRA Journal of the American Water Resources Association 28:299–304. doi: 10.1111/j.1752-1688.1992.tb03995.x

Guenther, S.M., Moore, R.D., Gomi, T., 2012. Riparian microclimate and evaporation from a coastal headwater stream, and their response to partial-retention forest harvesting. Agricultural and Forest Meteorology 164:1–9. doi: 10.1016/j.agrformet.2012.05.003

Hough, R.A., Fornwall, M.D., Negele, B.J., et al, 1989. Plant community dynamics in a chain of lakes: principal factors in the decline of rooted macrophytes with eutrophication. Hydrobiologia 173:199–217. doi: 10.1007/BF00008968

Jarvis P.G., McNaughton K.G., 1986. Stomatal control of transpiration: Scaling up from leaf to region. In: Ford AM (ed) Advances in Ecological Research. Academic Press, pp 1–49

Kettridge N., Thompson D.K., Bombonato L., et al., 2013. The ecohydrology of forested peatlands: Simulating the effects of tree shading on moss evaporation and species composition. Journal of Geophysical Research: Biogeosciences 118:422–435. doi: 10.1002/jgrg.20043

Krauss, K.W., Duberstein, J.A., Conner, W.H., 2014. Assessing stand water use in four coastal wetland forests using sapflow techniques: annual estimates, errors and associated uncertainties. Hydrological Processes. doi: 10.1002/hyp.10130

Liu, S., 1996. Evapotranspiration from cypress (Taxodium ascendens) wetlands and slash pine (Pinus elliottii) uplands in north-central Florida. Dissertation, University of Florida

Liu, S., Riekerk, H., Gholz, H.L., 1998. Simulation of evapotranspiration from Florida pine flatwoods. Ecological Modelling 114:19–34. doi: 10.1016/S0304-3800(98)00103-3

Luque, G.M., Bellard, C., Bertelsmeier, C., et al 2013. The 100th of the world's worst invasive alien species. Biological Invasions 16:981–985. doi: 10.1007/s10530-013-0561-5

Mao, L.M., Bergman, M.J., Tai, C.C., 2002. Evapotranspiration measurement and estimation of three wetland environments in the Upper St. Johns River Basin, Florida. JAWRA Journal of the American Water Resources Association 38:1271–1285. doi: 10.1111/j.1752-1688.2002.tb04347.x

Masoner, J.R., Stannard, D.I., Christenson, S.C., 2008. Differences in evaporation between a floating pan and Class A Pan on land. JAWRA Journal of the American Water Resources Association 44:552–561. doi: 10.1111/j.1752-1688.2008.00181.x

Mitsch W.J., Gosselink J.G., 2007. Wetlands, 4th edn. John Wiley & Sons, Inc., New York, NY, USA

Monteith, J., Unsworth, M., 2008. Principles of Environmental Physics, 3rd edn. Academic Press, Burlington, MA, USA

Parkhurst, R.S., Winter, T.C., Rosenberry, D.O., Sturrock, A.M., 1998. Evaporation from a small prairie wetland in the Cottonwood Lake area, North Dakota—An energy-budget study. Wetlands 18:272–287. doi: 10.1007/BF03161663

Rao, A.S., 1988. Evapotranspiration rates of Eichhornia crassipes (Mart.) Solms, Salvinia molesta d.s. Mitchell and Nymphaea lotus (L.) Willd. Linn. in a humid tropical climate. Aquatic Botany 30:215–222. doi: 10.1016/0304-377088)90052-6

Raz-Yaseef, N., Rotenberg, E., Yakir, D., 2010. Effects of spatial variations in soil evaporation caused by tree shading on water flux partitioning in a semi-arid pine forest. Agricultural and Forest Meteorology 150:454–462. doi: 10.1016/j.agrformet.2010.01.010

Reba, M.L., Pomeroy, J., Marks, D., Link, T.E., 2012. Estimating surface sublimation losses from snowpacks in a mountain catchment using eddy covariance and turbulent transfer calculations. Hydrological Processes 26:3699–3711. doi: 10.1002/hyp.8372

Reifsnyder, W.E., Lull, H.W., 1965. Radiant Energy in Relation to Forests. U.S. Department of Agriculture, Forest Service Technical Bulletin No. 1344, Washington, DC, USA

Rogers, H.H., Davis, D.E., 1972. Nutrient removal by waterhyacinth. Weed Science 20:423–428. doi: 10.2307/4042146

Shoemaker, W.B., Sumner, D.M., Castillo, A., 2005. Estimating changes in heat energy stored within a column of wetland surface water and factors controlling their importance in the surface energy budget. Water Resources Research 41. doi: 10.1029/2005WR004037

Snyder, R.L, Boyd, C.E., 1987. Evapotranspiration by Eichhornia crassipes Mart.) Solms and Typha latifolia L. Aquatic botany 27:217–227.

Sun, G., Riekerk, H., Comerford, N.B., 1998. Modeling the forest hydrology of wetland-upland ecosystems in Florida. JAWRA Journal of the American Water Resources Association 34:827–841. doi: 10.1111/j.1752-1688.1998.tb01519.x

Tillberg, E., Dons, C., Haugstad, M., Nilsen, S., 1981. Effect of abscisic acid on CO2 exchange in Lemna gibba. Physiologia Plantarum 52:401–406. doi: 10.1111/j.1399-3054.1981.tb02707.x

Wilson, K.B., Hanson, P.J., Baldocchi, D.B., 2000. Factors controlling evaporation and energy partitioning beneath a deciduous forest over an annual cycle. Agricultural and Forest Meteorology 102: 83-103.

CHAPTER 4: WETLAND TREE TRANSPIRATION MODIFIED BY RIVER-FLOODPLAIN CONNECTIVITY[1]

4.1 INTRODUCTION

Wetlands are generally defined by hypoxic soils (van der Valk 2012), but transitions from wet to dry conditions are common to many wetlands. Oscillating river flows can create a complex stress environment for floodplain ecosystems, where both flood stress and drought can occur within a single growing season (Parolin 2001). In floodplain forests where evapotranspiration (ET) may exceed precipitation (King et al. 2012), wet conditions often transition to drier but more aerobic conditions through the growing season (Dewey et al. 2006). Such variability defines many forested floodplain wetlands of the southeastern United States, (e.g., bottomland hardwood [BLH] systems), which are the most spatially extensive wetland type in the United States (Turner et al. 1981).

It is not well understood how trees respond to this transition from flooding in the early growing season to water deficits in the late growing season. Wetland tree growth can be decreased by flooding because it can reduce root function and induce stomatal closure or early senescence (Kozlowski 1997), and many large river floodplain ecosystems have reduced production during flooding (Parolin and Wittmann 2010). Alternately, the effect of the dry phase may limit vegetation through water deficit (Shankman et al. 2012) which has not been well examined in BLH wetlands. Wetter floodplain sites have less extensive root systems (Baker et al. 2001) and might be more vulnerable to droughty conditions; in general, adaptation to one stress decreases likelihood of tolerance to another (Niinemets 2010). Most knowledge of BLH tree physiological response to flooding or drought is based on sapling studies (e.g., Gardiner and Hodges 1996, Nash and Graves 1993, Pezeshki et al. 1996), which have different ecophysiological constraints than trees in forests (Krauss and Duberstein 2010). The relative influences of drought and flooding on carbon and water exchange remain mostly unexplored.

Previous studies in BLH forests showed hydrologic control over patterns of growth and productivity, but some major findings seemingly conflict. Vigor or productivity has been observed to be higher in both drier (Mitsch et al. 1991, Rodríguez-González et al. 2010, Shure and Gottschalk 1985) and wetter (Broadfoot 1967, Clawson et al. 2001) floodplain forests. Annual radial growth can correlate positively with wetter years (Mitsch et al. 1991, Gee et al. 2014), but growth may still increase with longer-term drier conditions (Gee et al. 2014). While these relationships are seemingly idiosyncratic, flooding can act as both subsidy or stress to forests (Odum et al. 1979), providing benefits of water and nutrients but detriments by stress associated with hypoxic soil conditions; ideal conditions are site-specific but often intermediate (Anderson and Mitsch 2008, Conner et al. 2011, Megonigal et al. 1997).

Floodplain hydrology (and thus ecological responses to hydrology) depends on seasonality of river flows, but also on spatiotemporal variations in connectivity of the floodplain to the river. Connectivity, broadly defined as the ease of transport of matter, organisms, and energy between distinct landscape units (Ward et al. 1999), is an important concept for

[1] This chapter previously appeared Allen, S.T., Krauss, K.W., Cochran, J.W., King, S.L., Keim, R.F., 2016. Wetland tree transpiration modified by river-floodplain connectivity. J. Geophys. Res. Biogeosciences 2015JG003208. It is reprinted by permission of John Wiley and Sons.

understanding floodplain ecosystems. Connections from the river to the floodplain facilitate transport of water and nutrients, which is important for vegetation productivity (Conner and Day 1992, Megonigal et al. 1997, Mitsch et al. 1991). Connections by surface and subsurface pathways are generally active at higher river stages, although there is considerable spatial variability in large floodplains because of heterogeneities in soil, geology, and topography. River engineering can alter river-floodplain connectivity directly or indirectly by slower processes (e.g., a lowering of river relative to the floodplain by channel incision; Bravard et al. 1997).

Understanding tree responses to hydrology can be improved by real-time examination of physiological processes with respect to water table fluctuations. Sapflow measurement enables real-time examination of the interaction between soil water and atmospheric demand as mediated by tree physiological processes (Bond et al. 2008). Stomatal aperture largely regulates this flow, thus sapflow is also related to carbon exchange in addition to transpiration (Ping et al. 2003).

In this study, we explored whether river-floodplain connectivity differences, and resulting hydrologic regime difference, are a factor controlling transpiration in a floodplain wetland. We tested this by measuring tree water use in two hydrologically distinct sites, where contrasting connectivity caused late season flooding at one site but not the other. Our second objective was to examine species differences in responses to hydrologic variability. We measured sapflow in one species that is generally considered flood tolerant (*Quercus lyrata* Walt.) and another that is considered less flood tolerant (*Celtis laevigata* Willd.) to see how flood tolerance translates to functional responses and ultimately competitive interactions.

4.2 METHODS

4.2.1 Study species

The two species, overcup oak (*Q. lyrata*) and sugarberry (*C. laevigata*) often cohabitate and are shallowly rooted in wet, floodplain soils (Baker et al. 2001, Kennedy 1990), but differ in tolerances of flooding and shade. *Q. lyrata* is highly tolerant of flooding (Hook 1984) and moderately tolerant of shade (Niinemets and Valladares 2006), is relatively slow-growing, and generally leafs out later than co-occurring species (Solomon 1990). *C. laevigata* is weakly tolerant of flooding (Hook 1984) and tolerant of shade (Battaglia and Sharitz 2006). Increasing prevalence of *C. laevigata* has been observed in floodplains of the region, likely associated with conditions becoming drier from hydrologic modifications that reduce flooding (Gee et al. 2014, Hanberry et al. 2012), which may otherwise kill *C. laevigata* (Broadfoot and Williston 1973). Drought tolerance has not been systematically investigated for either species.

4.2.2 Site descriptions

Sapflow was measured at two sites in the Dale Bumpers White River National Wildlife Refuge on the White River floodplain in southeastern Arkansas, USA, co-located with a previous study (Allen et al. *in press*). Mean discharge of White River coming into the refuge (at DeValls Bluff; USGS gauge 07077000; 14 km north at 34°47’25” N, 91°26’45” W) is 741 m^3s^{-1}, regulated by dams in the upper watershed. The floodplain of the lower river, including both study sites, is 8-14 km wide, much of which is inundated seasonally. In most years, river stage peaks between March and early June, followed by a steep recession and low stage into November. In 2013 when this study was conducted, stage was higher than typical and flooding occurred later, peaking in late June and receding through July (Figure 4.1).

One study site (Site S; 30 km south of St. Charles, Arkansas and 0.2 km from the main channel of the White River; 34°6’32” N, 91°7’31” W) is in a southern reach of the floodplain

heavily influenced by backwater flooding from the Mississippi River (Johnson 2015), leading to occasional deep flooding in the wet season but rare headwater flooding by the White River. After the primary flood waters recede, Site S loses connection to the river because the incised river is well below the site at base flow (Figure 4.1B), leading to pronounced seasonal drying. The other site (Site N; 26 km northwest of St. Charles and 2.6 km from the main river channel; 34°34'44" N, 91°15'23" W) is in a reach of the floodplain influenced mainly by headwater floods from the White River, north of the Mississippi backwater effect and the river is not incised into the floodplain. Floodplain stage at Site N is responsive to river flows during the growing season, even after the primary floodwaters have receded (Figure 4.1). A parallel study using 28 water monitoring stations on the floodplain and HEC-GeoRAS (US Army Corps of Engineers, Davis CA, USA) to model 2013 flooding found surface water connections in August extending from the river channel to Site N as well as much of the surrounding floodplain (Johnson 2015).

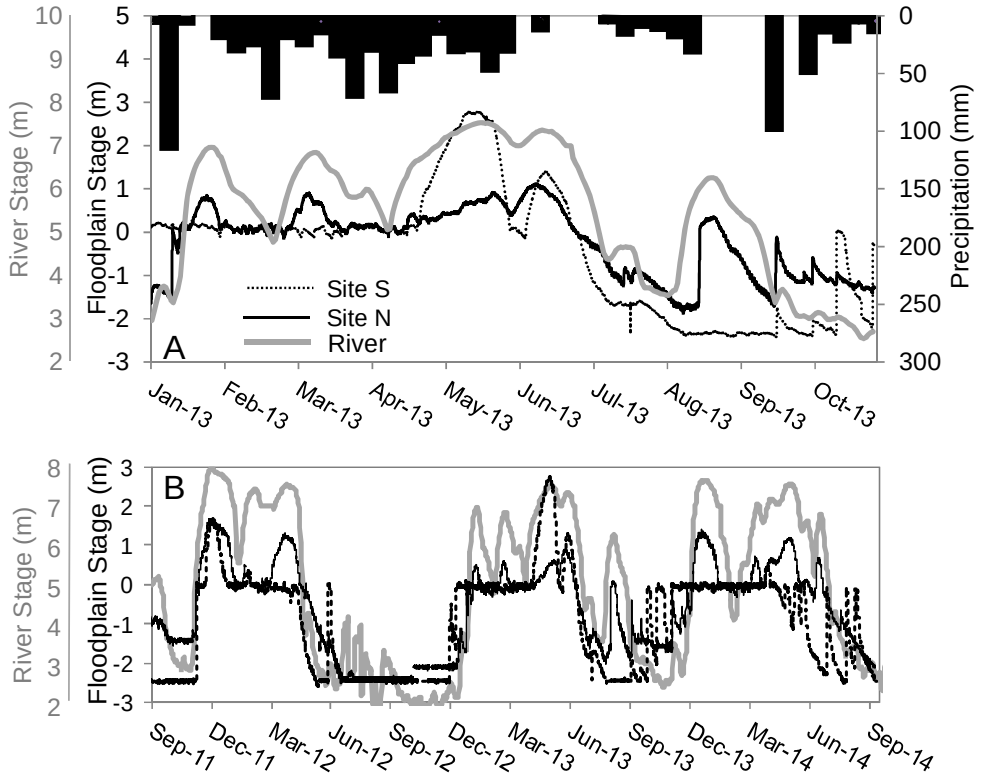

Figure 4.1 Stage of the White River at St. Charles and at the two study sites, and weekly precipitation (bars) for the 2013 growing season, and pre-growing season. (A**)** the study year through the end of growing season; (B**)** a three year record. Horizontal lines in floodplain stage indicate the water table was below the water level sensor. Stage is relative to 39.6 m AMSL for river and relative to floodplain soil surface for study sites.

Soils at both sites are fine textured alluvial soils, classified by USDA as complexes of aquerts and aquepts, depending on microtopography. Flats and swales are clayey or silty-clayey throughout the profile, and ridges are silt-loamy or silty-clay-loamy and typically finer at depth but with occasional sandy layers. Permeability of clays is extremely low, especially when wet because they are dominated by smectitic clay minerals.

Forest composition at the sites was similar and was typical of BLH of the Lower Mississippi Alluvial Valley. Tree cores showed ages from 45 to 140 years old, with similar ranges for both site. At each site, four plots (0.04 ha) were established and trees with diameter over 5.0 cm were inventoried by species and diameter (at 1.37 m height; DBH). *C. laevigata* and *Q. lyrata* were the most common species, respectively accounting for 20% and 16% of the basal area (plot total 28.6 ± 3.9 m^2 ha^{-1}; mean ± SE) at Site N and 14% and 37% at Site S (plot total 27.3 ± 2.2 m^2 ha^{-1}). Respectively, *C. laevigata* and *Q. lyrata* composed 20% and 21% of trees at site N and 27% and 40% of trees at Site S.

Relative ground elevation among trees was surveyed by autolevel in all plots. Tree base elevations of all trees ranged over 1.1 m at Site N, because of microtopography on the site created by meander scrolls. Ridges were predominantly occupied by *C. laevigata* and swales by *Q. lyrata*. Across all plots, mean elevation for *Q. lyrata* was 0.59 m lower than for *C. laevigata* (t-test, $p < 0.001$). Site S had less microtopographic variation (elevation range 0.4 m) with no significant difference in elevation between species (mean difference = 0.03 m, t-test, $p = 0.23$).

4.2.3 Measurements

4.2.3.1 Environmental measurements

Elevation of groundwater or surface water, with respect to soil surface, was measured at half hour intervals in wells by a pressure transducer (Hobo, Onset Computer Corp, Bourne, MA, USA) 2.3 m below the soil surface at each site. Pre-dawn xylem water potentials were measured in leaves collected from the canopy base, using a Scholander-type pressure bomb (PMS Instruments, Albany Oregon, USA) several times throughout the growing season. Temperature and relative humidity were measured at the canopy base in each study site half-hourly (HOBO U23 Pro v. 2, Onset Computer Corp., Bourne Massachusetts, USA); these data were used to calculate vapor pressure deficit (*D*). Photosynthetically active radiation (PAR) (LI190SA, LI-COR Environmental Inc., Lincoln Nebraska, USA), relative humidity, and temperature (HMP45C, Vaisala Oyj, Helsinki, Finland) were measured in a clearing roughly halfway between the two sites and logged at 15 minute intervals (CR800, Campbell Scientific Inc., Logan, Utah, USA). Precipitation data were from Stuttgart, Arkansas (National Climatic Data Center, Asheville NC, USA), 26 and 57 km away from sites N and S, respectively.

4.2.3.2 Sapflow measurement and analysis

Sap flux density (J_s) was measured using paired heat dissipation probes (Dynamax Inc., Houston Texas) inserted into co-dominant trees of both species at varying depths (Granier 1987). Both probes contained thermocouples; difference in temperature between the bottom, reference probe and the top, heated probe was used to calculate flow rate.

At Site N, 10 trees were instrumented with probes measuring J_s at 15 mm depth, and at Site S, 16 trees were instrumented with probes inserted to 15 mm and varying radial depths (Table 4.1) to measure variation of J_s with depth. In all study trees, J_s was measured at 15 mm and, where not otherwise specified, J_s throughout refers to J_s at 15 mm depth. Datalogger systems (CR1000, Campbell Scientific Inc., Logan, Utah, USA) regulated voltage and recorded data from probes at half hour intervals. Reflective insulation over probes and installation on north sides of trees minimized external heating.

Crown footprint area, estimated by assuming an ellipse described by the distance from stem to furthest-extending branch and crown width at 90, 180, and 270 degrees from there, was similar for the two species (64.9 ± 10.4 m^2 and 56.5 ± 5.6 m^2 for *Q. lyrata* and *C. laevigata*,

respectively). Diameters were similar for *Q. lyrata* (37.9 ± 4.0 cm) and *C. laevigata* (34.1 ± 3.3 cm). Sapwood areas (identified by color or dye injections in transpiring trees) were also similar (483 ± 70 and 519 ± 106 cm^2). Heights of *Q. lyrata* were greater than *C. laevigata* at both Site S (27.0 ± 5.2 m versus 21.5 ± 3.3 m; t-test, p = 0.002) and Site N (24.4 ± 2.9 m versus 21.0 ± 4.3 m; t-test, p = 0.03). At Site S, there was little microtopographic variation for study trees, but at Site N, only one probed *C. laevigata* was in a swale and no *Q. lyrata* were on ridges.

At half-hour intervals, sap flux density (g m^{-2} s^{-1}) was calculated at each thermocouple depth as

$$J_{s_i} = 119 \times \frac{(\Delta T_M - \Delta T_i)^{1.231}}{\Delta T_i}, \quad (4.1)$$

where ΔT_M (°C) is the reference temperature difference between the two probes at zero flow (calculated daily and verified to occur 0300 to 0600), and ΔT_i (°C) is the temperature difference between the two probes at time *i* (Clearwater et al. 1999, Granier 1987, Ping et al. 2003).

Table 4.1 Characteristics of study trees, *Celtis laevigata* (*C.l.*) and *Quercus lyrata* (*Q.l.*).

Site	Species	Sensor Depth (mm)	DBH (cm)	Sapwood Area (cm^2)	Height (m)	Crown Area (m^2)
N	*C.l.*	15	55.0	1395	25.8	83
N	*C.l.*	15	17.4	168	15.9	28
N	*C.l.*	15	34.3	565	20.6	81
N	*C.l.*	15	17.4	235	18.0	62
N	*C.l.*	15	38.5	653	24.9	59
N	*Q.l.*	15	42.7	704	28.0	87
N	*Q.l.*	15	19.7	138	20.7	15
N	*Q.l.*	15	33.6	373	23.7	84
N	*Q.l.*	15	24.7	245	23.1	31
N	*Q.l.*	15	40.1	654	26.6	91
S	*C.l.*	15/25	19.9	215	16.0	36
S	*C.l.*	15/25	21.9	207	18.9	29
S	*C.l.*	15	35.8	269	22.0	41
S	*C.l.*	15	42.6	1124	25.5	87
S	*C.l.*	15/70	44.6	707	19.3	45
S	*C.l.*	15/70	37.4	474	25.2	55
S	*C.l.*	15/50/90	33.8	176	20.9	73
S	*C.l.*	15/50/90	44.8	561	24.0	57
S	*Q.l.*	15/25	24.0	285	23.9	24
S	*Q.l.*	15/25	48.0	781	29.2	76
S	*Q.l.*	15	22.6	190	19.5	19
S	*Q.l.*	15	19.1	150	22.6	19
S	*Q.l.*	15/70	54.9	676	32.7	94
S	*Q.l.*	15/70	48.7	582	23.5	83
S	*Q.l.*	15/50/90	54.7	718	32.2	94
S	*Q.l.*	15/50/90	59.4	775	32.5	126

Tree water use (F; l day^{-1}) was calculated by scaling sap flux density by effective sapwood area. Scaling from point measurements of J_s to F requires consideration of the reduction of J_s with depth into the sapwood through xylem bands of increasing age, integrating across the sapwood cross sectional area. We used 15 mm probes as our reference depth because greatest J_s generally occurred at this depth in trees with multiple probes; probes at other depths (Table 4.1) were used to parameterize species-specific attenuation functions. The attenuation curve was a second-degree polynomial step function of J_s by depth, normalized to reference J_s (with a fixed minimum of 0 and maximum of 1), yielding a similar shape to the Gaussian functions used by Ford et al. (2004). This function was integrated over the flow field for each tree and multiplied by J_s to determine F. Alternative attenuation functions were constructed, based on the measured sapwood width per tree, and they yielded estimates of F similar to the simpler, empirical J_s attenuation function.

Data were processed for comparison of means across sites over coincident time domains (i.e., removing sampling dates that did not overlap). Analyses focused on temporal trends of J_s in outer sapwood (15 mm) to mitigate uncertainties associated with scaling to F. We compared temporal trends in sapflow to remove effects of tree-specific magnitude differences. To test for effects of hydrologic differences between sites, we compared J_s from August to September: a flood event occurred at Site N in late August but not at Site S.

To analyze differences between species, data were z-transformed for each tree; that is, for each tree, temporal mean J_s was subtracted from each daily value and divided by the standard deviation of J_s. This yielded time series for each tree of anomalies in units of standard deviations; these were averaged for each species for each site, yielding four time series for comparison without biases from tree size effects.

Analysis of covariance (ANCOVA) was used to test for differences in J_s or F with tree size by species. Statistical analyses were performed using MATLAB (Mathworks, Natick, MA).

4.3 RESULTS

4.3.1 Hydrologic Connectivity and Environmental Factors

Precipitation in March, April, and May was 125, 147, and 110 mm, followed by a drier summer with 26, 16, 46, and 94 mm for June, July, August, and September, respectively. There were two major flood pulses in the growing season that caused overbank flooding in much of the floodplain; the first in May and June, and the second in August (Figure 4.1). At the precipitation measurement location, there was no measureable rain for 37 days from mid-August to mid-September.

Floodplain stage responded to the river differently at each site: the water table at Site N varied closely with river stage, whereas at Site S it only responded to extremely high river stage (Figure 4.1A). At Site N, there was shallow flooding (< 1 m) in the early growing season that receded prior to sapflow measurements, and a late-season (16-28 Aug) flood pulse yielded shallow surface flooding. At Site S, there was deeper flooding (up to 2.7 m) prior to sapflow measurement, but the water table receded rapidly beneath the surface during July when measurement began and remained more than 2 m below the surface, even during the late-season flood pulse.

Pre-dawn water potential measurements indicated soil water status differences between sites and species (Table 4.2). Pre-dawn water potential was more negative in *C. laevigata* than *Q. lyrata* for the entire study except on 11-July at Site S. Water potential in *Q. lyrata* was more negative at Site S than at Site N in mid-July ($p = 0.009$) and in late July ($p < 0.001$). Water

potential in *C. laevigata* was more negative at Site N than Site S mid-July ($p < 0.001$), and the opposite in late July, ($p < 0.001$). The most negative water potential in the study was in *C. laevigata* in August at Site S, when the water table was more than 2 m below the surface.

Table 4.2 Pre-dawn xylem water potential (Ψ) (mean ± standard error) and results of *t* tests of species differences by date.

Date	Site	Ψ (MPa)		t-test
		Q. lyrata	*C. laevigata*	*p*
11 July	S	-0.23 ± 0.06	-0.12 ± 0.02	0.072
14 July	N	-0.09 ± 0.00	-0.40 ± 0.03	<0.001
21 July	S	-0.21 ± 0.02	-0.36 ± 0.01	<0.001
26 July	N	-0.06 ± 0.01	-0.28 ± 0.02	<0.001
16 August	S	-0.12 ± 0.01	-0.43 ± 0.02	<0.001

4.3.2 Site effects on sap flux density

Across both sites and both species, much variation in J_s was controlled by meteorological conditions (Table 4.3). Daily mean J_s was most strongly related to PAR, accounting for 65-78% of variation. In general, correlation of J_s with meteorological variables was stronger at Site N than at Site S for both species. This was especially true for *D*, which explained 65% and 38% of the variability in J_s at Site N for *Q. lyrata* and *C. laevigata*, respectively, but only 16% and 8% at Site S. Between sites, *D* was similar (slope = 1.01, $R^2 = 0.82$). Correlations between J_s and environmental variables at monthly intervals (Table 4.3) were similar between July and August but notably lower in September.

Table 4.3 Pearson correlation coefficients between daily (24 hour) mean sap flux density (J_s) and daily mean environmental variables: Stage of groundwater table, air temperature, relative humidity (RH), photosynthetically active radiation (PAR), and vapor pressure deficit (*D*).

Site	Species	Period	Correlation with J_s				
			Stage[a]	Temperature[a]	RH[a]	PAR[b]	*D*[a]
S	*Q. lyrata*	July	0.24	0.38	-0.76	0.79	0.79
S		Aug.	0.31	0.38	-0.73	0.78	0.72
S		Sept.	-0.22	0.01	-0.50	0.61	0.62
S		All	0.23	0.31	-0.33	0.83	0.39
S	*C. laevigata*	July	0.23	0.41	-0.84	0.80	0.87
S		Aug.	0.18	0.18	-0.76	0.77	0.70
S		Sept.	0.14	-0.23	-0.11	0.63	0.15
S		All	0.39	0.22	-0.26	0.80	0.29
N	*Q. lyrata*	Aug.	0.24	0.19	-0.88	0.81	0.92
N		Sept.	0.11	0.15	-0.52	0.52	0.59
N		Oct.	0.37	-0.31	-0.85	0.85	0.91
N		All	0.38	0.40	-0.74	0.88	0.81
N	*C. laevigata*	Aug.	0.19	0.12	-0.80	0.81	0.84
N		Sept.	0.28	0.35	-0.43	0.52	0.67
N		Oct.	0.17	-0.32	-0.74	0.81	0.83
N		All	0.43	0.59	-0.46	0.87	0.62

[a] Measured at study sites, and at canopy base for meteorological variables
[b] Measured in a clearing in St. Charles, Arkansas, halfway between the sites

There were differences in the relationship between J_s and D by site that were apparently related to site water table stage. Max J_s occurred with higher D (0.4−0.8 kPa) at site N, whereas J_s at Site S tended to be lower when D was 0.6−0.8 kPa than it was when D was 0.4−0.6 kPa. At Site S, decline of J_s from the expected plateau in relationship with D at high D (Bond et al., 2008) coincided with periods of lower water table (Figure 4.2); this pattern was evident for both species. In contrast, the water table was not as low at Site N and periods of lower water table did not correspond with reduced J_s. Site S daily J_s explained 45% and 64% of the variability in site N daily J_s, for *Q. lyrata* and *C. laevigata* respectively, but residuals were related to water levels. Water level differences between sites concurrent with positive residuals (i.e., when Site N measured J_s > Site N modeled as a function of Site S J_s) were significantly higher than water levels when negative residuals were observed; this was true for both *Q. lyrata* (1.46 versus 0.86 m; two sample t-test, p = 0.002) and *C. laevigata* (1.51 versus 0.91 m; p = 0.002).

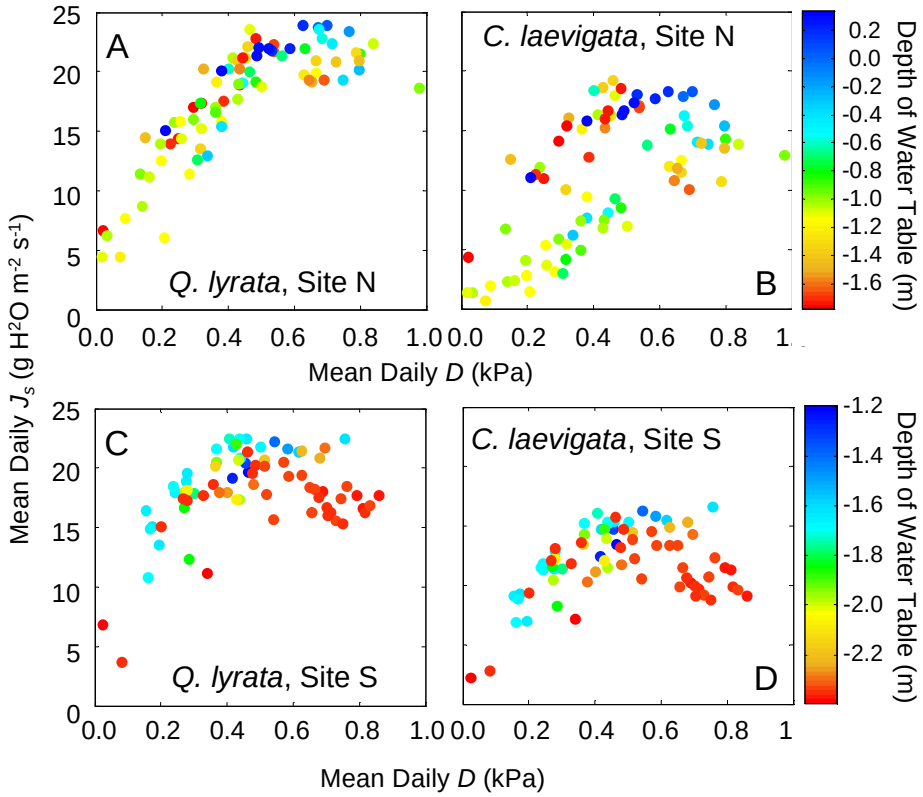

Figure 4.2 Sap flux density (J_s) related to vapor pressure deficit (D) for *Quercus lyrata* (A and C) and *Celtis laevigata* (B and D) at sites N (A and B) and S (C and D). Water table height is defined as zero at the soil surface, at each study site; color scales differ between plots.

Site differences in temporal patterns of J_s reflected water table differences between sites. At the time of sustained peak J_s at Site N (late Aug through Sept) with high water table, J_s began a general downward trend at Site S (Figure 4.3) where there was a low water table. The August rise in the water table at Site N was followed by a period with the highest J_s for *Q. lyrata*. At Site S, where water table declined during August and remained low in September, J_s was

significantly ($p < 0.05$) lower in September than in August in six of eight probed *C. laevigata*, and in five of eight *Q. lyrata* (Figure 4.4). In contrast, at site N, where water table was higher, J_s was lower in September ($p < 0.05$) in only two of five *C. laevigata* and in zero of five *Q. lyrata*. For Site S, the percent change in J_s (Figure 4.4) for *C. laevigata* was negatively correlated with size variables (DBH: R = -0.98, p = 0.003; Height: R= -0.80, p = 0.017); *Q. lyrata* showed no trend, although, in contrast, the three largest *Q. lyrata* (by height and by DBH) had the three least negative changes in J_s from August to September.

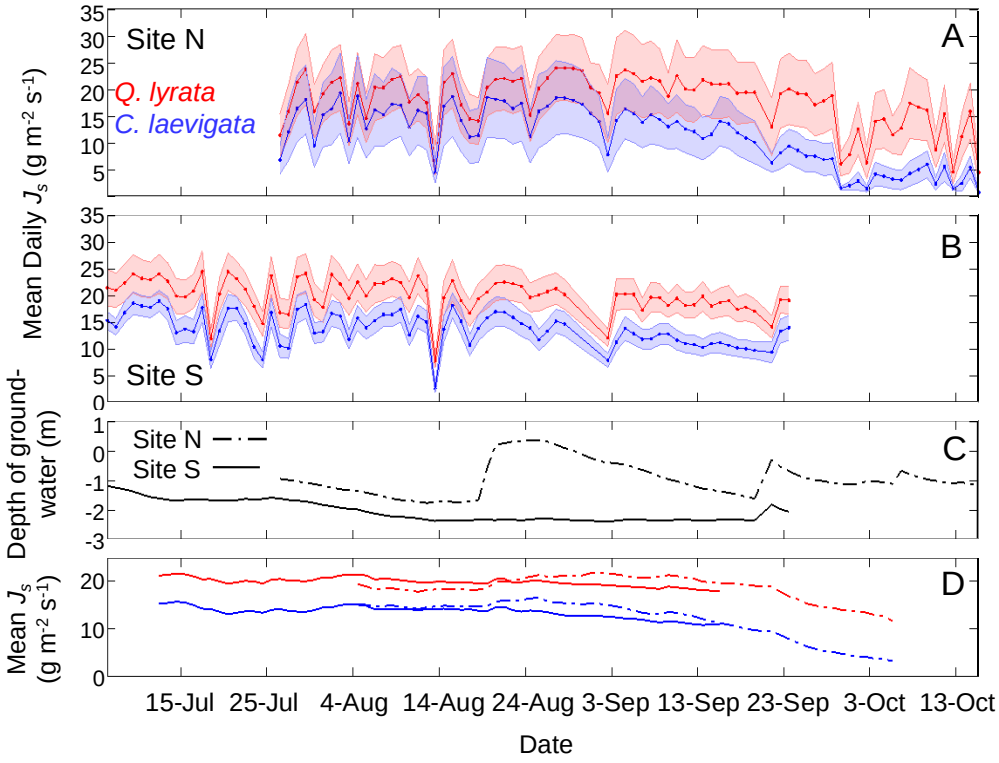

Figure 4.3 Mean daily sapflux density (J_s) at (A) Site N and (B) Site S for *C. laevigata* (blue) and *Q. lyrata* (red), compared to (C) water table variations and (D) low-pass filtered (14-day window) trends. Lines are species means and shaded widths indicate ± one standard error.

Temporal patterns were more similar between species than between sites (Figure 4.3D). Species-mean daily mean J_s was more highly correlated between species at the same site (R^2 = 0.60 at Site N and 0.84 at Site S) than for the same species between sites (R^2 = 0.47 for *Q. lyrata* and 0.62 for *C. laevigata*).

4.3.3 Species differences in sapflux density and tree water use

Despite similarities between species, there were some species differences in J_s by site (Figure 4.5). Through late July into September, normalized J_s in *C. laevigata* decreased with respect to *Q. lyrata* at both sites (Figure 4.5); this also continued into October at Site N (Figure 4.3). The difference between species at Site N increased beginning with the August flood pulse. At the intra-day timescale, *Q. lyrata* showed a wider diurnal signal (Figure 4.6); the ratio of daily maximum J_s to daily mean J_s was higher in *C. laevigata* than *Q. lyrata* (paired t-test, $p < 0.0001$) for both Site S (3.7 ± 0.6 versus 2.9 ± 0.58; mean ± SD) and Site N (4.0 ± 0.5 versus 3.5 ± 0.9).

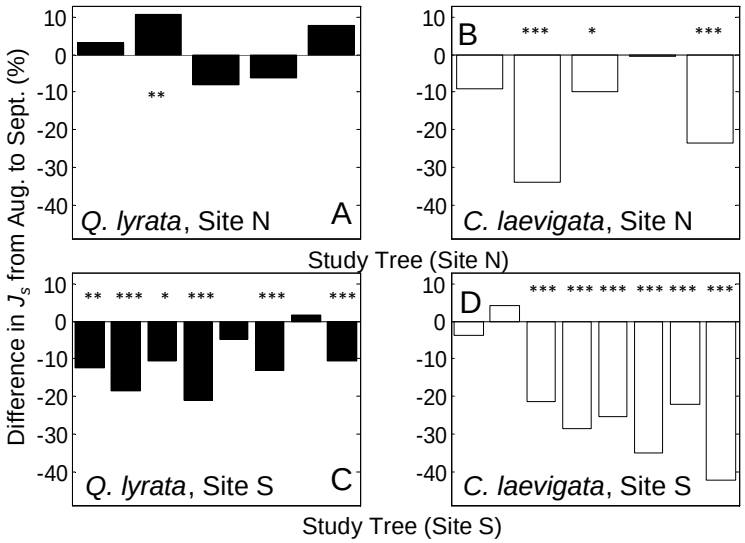

Figure 4.4 Difference of sap flux density (J_s) for individual trees from August to September for (A and B) Site N and(C and D) Site S for both species. Statistically significant differences between months for each tree are denoted by * ($p < 0.1$), ** ($p < 0.05$), and *** ($p < 0.01$).

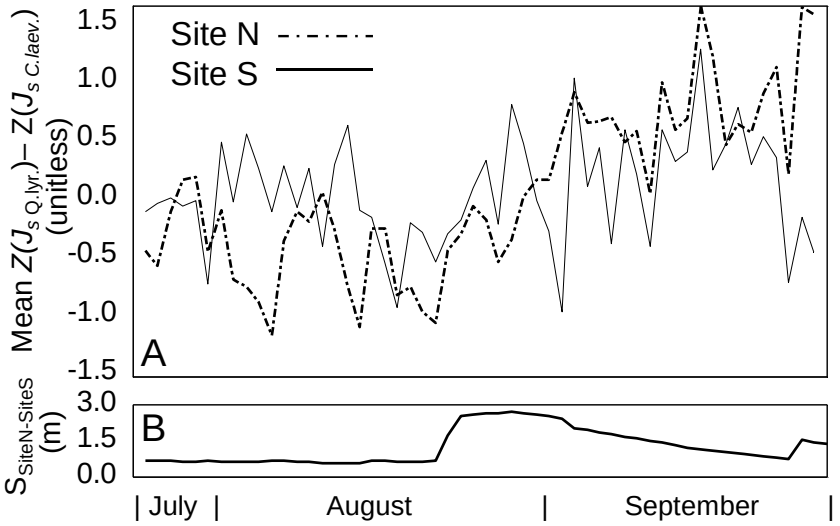

Figure 4.5 (A) Differences in mean normalized (Z-transformed) J_s between species, and (B) differences in water table stage (S) between sites for the period of complete data at both sites.

There were some indications that microtopographic position of trees affected J_s, but species stratification by position limits the strength of comparisons. Reduction in J_s from August to September at Site N was related (t-test, $p < 0.001$) to whether trees were on ridges (17 ± 7% reduction) or swales (1 ± 3% reduction), although this finding is confounded because *Q. lyrata* were in swales and all but one *C. laevigata* were on ridges. At Site S, there was no species stratification by elevation (t-test, $p = 0.46$), so regression analysis was used and showed no significant effect of elevation on J_s ($R^2 = 0.14$, $p = 0.15$).

Both J_s and F increased with tree size for *Q. lyrata* (quantified by diameter, height, crown area, and sapwood basal area) but were almost independent of tree size for *C. laevigata* (Table

4.4). Tree water use for *Q. lyrata* was best explained (Table 4.4) by sapwood basal area. For *C. laevigata*, J_s was independent of size and *F* was only weakly dependent on tree diameter and height (Table 4.4). Both J_s and *F* were generally greater for *Q. lyrata* than *C. laevigata* when compared as a function of size, with significant species differences (ANCOVA; $\alpha = 0.05$) in relationship to sapwood area for J_s and *F*, and to diameter for *F*.

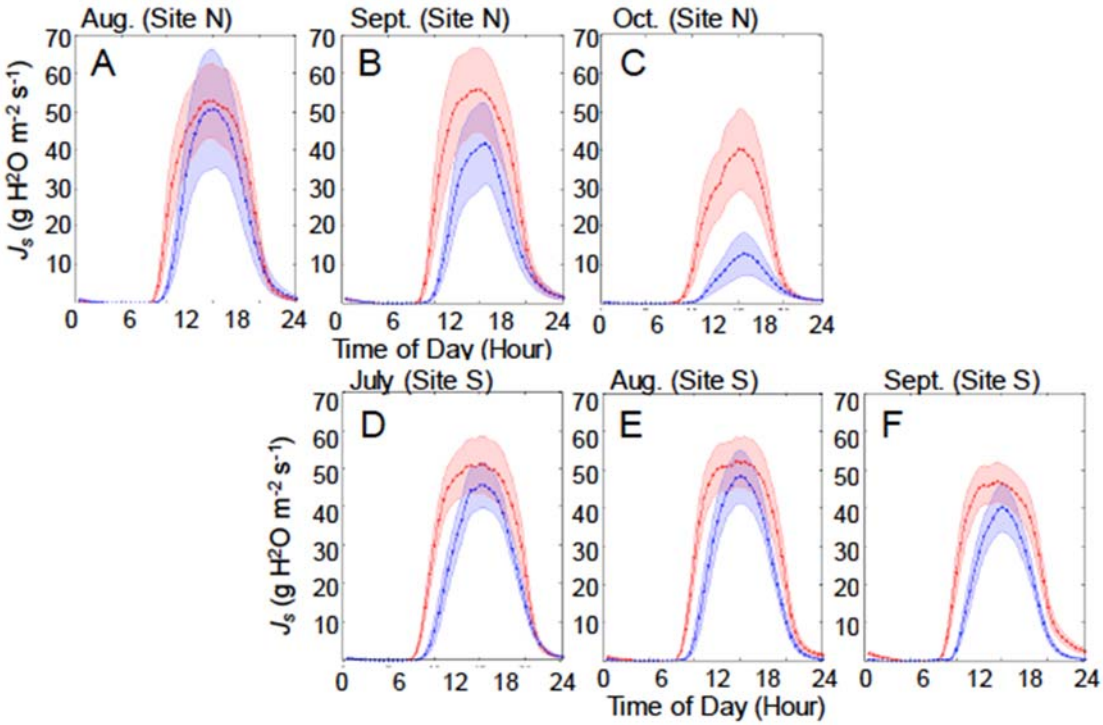

Figure 4.6 Ensemble-averaged, half-hourly sap flux density (J_s) at (A-C) Site N and (D-F) Site S for *Q. lyrata* (red) and *C. laevigata* (blue). Lines are species means and shaded widths indicate ± one standard error.

Table 4.4 Correlations (R^2) and regression coefficients (*b*) between tree-mean seasonal sap flux density (J_s) or tree water use (*F*) and tree characteristics for *Quercus lyrata* (*Q.l.*) and *Celtis laevigata* (*C.l.*). Units of *b* are g m^{-2} s^{-1}(independent variable)$^{-1}$ for significant regressions of J_s and l d^{-1} (independent variable)$^{-1}$ for regressions of *F*. Statistically significant correlations are denoted by * ($p < 0.1$), ** ($p < 0.05$), and *** ($p < 0.01$).

		Independent Variable							
		Diameter (cm)		Height (m)		Crown area (m^2)		Sapwood area (cm^2)	
Dependent Variable	Species	R^2	*b*	R^2	*b*	R^2	*b*	R^2	*b*
J_s	*Q. l.*	0.43^{**}	0.43	0.33^{**}	1.40	0.47^{***}	0.17	0.68^{***}	0.03
J_s	*C. l.*	0.04		0.09		0.03		0.01	
F	*Q. l.*	0.76^{***}	3.53	0.51^{***}	10.9	0.72^{***}	1.34	0.88^{***}	0.22
F	*C. l.*	0.29^{*}	1.22	0.30^{*}	4.16	0.15		0.17	

4.4 DISCUSSION

4.4.1 Transpiration reduced with declining groundwater

Despite wetland conditions and inundation during much of the growing season, drier conditions resulted in reduced water use. With essentially equivalent weather conditions between sites but differences in stage and soil moisture, spatial differences in function (sap flow, and thus inferred stomatal control and gas exchange) can be attributed to hydrologic conditions. After the water table had dropped at Site S in summer, J_s also dropped; this pattern in J_s did not occur similarly in the wetter Site N, which suggests that this response was neither solely meteorological nor phenological. Meteorological variables (e.g., D and PAR) were more strongly correlated with J_s than was water table (Table 4.3), but all correlations declined in September suggesting a change in controlling processes.

The apparent dependence on water table may be related to the relatively rapid transition from wet to dry. Some tree traits are associated with both water excess and deficit (e.g., lower specific leaf area (Poorter et al. 2009)), but an extensive root system is inhibited by hypoxia, so root systems in BLH forests are typically shallow (Pezeshki 2001). Riparian cottonwoods in arid regions rely on slow river recession so root growth can keep pace with water table lowering or they experience drought stress (Mahoney and Rood 1998); similar processes may occur in BLH forests, where the high soil moisture capacity of silty or clayey soils matters less because of the limited root system.

The effects of dry conditions are noteworthy here because, unlike in upland systems, hydrologic control over wetland ecosystem structure is usually attributed to flooding (e.g., classifications by flood tolerances (Hook 1984)). We did not observe direct reductions in J_s associated with flooding, possibly because site conditions were never sufficiently hypoxic or the mature trees were resistant to flood stress because of large resource reserves (Waring and Running 2010). As Megonigal et al. (1997) explains, conceptualizing flooding as either ‘subsidy’ (increased water availability) or ‘stress’ (hypoxia and flood stress) is inadequate because of the complexity of biological responses to conditions.

Transpiration patterns not only have implications for tree function, but also control soil-water availability and groundwater elevation. Declining sapflow (and thus transpiration) when water tables were low (Figure 4.2) and increased with flooding is a negative feedback between flooding and water use; others have shown evidence that this interaction may be a positive feedback in other wetland systems (Krauss et al. 2007 and others reviewed in: Kozlowski 1997, Pezeshki 2001).

4.4.2 Hydrologic connectivity maintains late season transpiration

The differences by study site in flooding and water table connectivity to the river provided a means for comparing responses to water table variations, but also provided a test of the ecophysiological importance of connectivity in general. Hydrologic connectivity and associated water delivery to Site N supported high transpiration rates through September, while sapflow concurrently trended downward at Site S without the connectivity. Previous studies have observed stand productivity trends are associated with indices of connectivity (Conner and Day 1992, Megonigal et al. 1997, Mitsch et al. 1991). However, the finer temporal resolution provided by sapflow in this study showed how connectivity differences lead to differing ecophysiological responses.

This case study contributes to an under-developed research area linking ecophysiological responses to floodplain geomorphology and resulting patterns of connectivity (Ward and Stanford 1995). This topic is highly important because river engineering has extensively altered connections between rivers and floodplains (Hupp et al. 2009), often reducing frequent, shallow flood pulses (Ward and Stanford 1995) which are here demonstrated to be ecologically important. The extent of these changes in the White River are known: our observed site differences were consistent with general connectivity differences between these two reaches of the lower White River floodplain (Johnson 2015) caused by geomorphic processes related to both management and underlying geology (Schumm and Spitz 1996). HEC-GeoRAS modeling demonstrated that this August event flooded much of the floodplain in the northern reach but flooding was minimal in the southern reach where the river is incised into its floodplain. The extent of connectivity in the northern reach likely exceeds that driven by surface flooding alone because groundwater connections have a larger zone of influence (Jung et al. 2004, Lewandowski et al. 2009). Although clayey low-conductivity soils can limit lateral fluxes, groundwater recession rates at Site N (Figure 4.1) exceeded reasonable ET rates, demonstrating substantial subsurface connectivity.

The importance of the August flooding, which occurred during an extended rainless period at the sites, is illustrated by the soil water balance. For a coarse estimate of stand transpiration, F can be estimated for each tree in study plots, which were predominantly oaks, by the relationship between basal area (BA; cm^2) and F for *Q. lyrata* ($F = 0.0562 \times BA + 11.2$), then summed for all trees and divided by the plot area for an estimate of mean canopy transpiration of 2.4 ± 0.5 mm day^{-1} over the July-October measurement period. Assuming that fine roots, and thus water uptake, are primarily in the top 30 cm of soil (Baker et al. 2001) and that the clayey soil has an available moisture content of roughly 17% by volume (Brady and Weil 2007), transpiration would deplete available moisture within 21 days, neglecting hydraulic redistribution and that some roots likely extend deeper. The rainless period from 14-August to 19-September (37 days) was thus likely long enough to develop water limitations and may explain differences between Site S−where groundwater was likely inaccessible by roots−and Site N.

In general, precipitation alone could not have supplied evaporative demands so water deficit may be common unless offset by water subsidy from the river or groundwater sources. Given an estimate of ET of 3.5 to 4.0 mm day^{-1} (reasonable if canopy transpiration is 2.4 mm day^{-1} and the remainder is surface and understory ET; (Oren et al. 1998)), and roughly 105 to 120 mm of ET per month, ET exceeds mean monthly precipitation every month June through October, and nearly doubles mean August precipitation. Others have arrived at similar conclusions with respect to river subsidies allowing ET to exceed precipitation for extended periods (Bosch et al. 2014), which may be an important control of the geographic extent of bottomland hardwood species (Shankman et al. 2012).

4.4.3 Differences between *Q. lyrata* and *C. laevigata*

Despite its well-known association with drier zones within floodplains (Battaglia and Sharitz 2006, Hook 1984), *C. laevigata* did not demonstrate drought tolerance superior to *Q. lyrata*. Instead, J_s of both *Q. lyrata* and *C. laevigata* decreased at the drier Site S from August to September, and *C. laevigata* decreased more rapidly during this dry time of year and was mostly inactive by October (Figure 4.6). This greater reduction in late-season J_s of *C. laevigata* suggests phenological avoidance of drought stress and not a stress response because it was observed at

both the dry and wet sites. The majority of radial growth for *C. laevigata* occurred before July on these sites and ceased earlier at drier sites (Allen et al. *in press*). With earlier leafout than *Q. lyrata*, *C. laevigata* benefits from less light competition but must be tolerant of any flooding usually occurring in spring.

In contrast, there was a late-shifted growing season for *Q. lyrata*. For this species, J_s declined more slowly into the dry period and it maintained steady radial growth into late August (Allen et al. *in press*). This later growing season, coinciding with the drier period, is a less conservative water use habit because conditions are drier, but the increased J_s of *Q. lyrata* in September at Site N suggests that the later growing season enabled benefits from the late-season flood waters. This response to hydrology in the late season, and assumed stomatal activity affecting carbon exchange, may justify why *Q. lyrata* growth, as assessed by tree ring analysis at this site, correlates with fall water levels of the previous year (Gee 2012).

In accordance with apparent differences in tolerance to flooding and drought, the two species co-occur but with phenological offsets. This offset between the species demonstrates some temporal separation in water usage, which is common in more arid regions (e.g., West et al. 2007) but not as well described in humid floodplain forests. This may decrease competition and potentially facilitate the co-occurrence of *C. laevigata* and *Q. lyrata*. Furthermore, with timing differences in water use, community transpiration must differ from that of monotypic stands.

Light competition may explain species differences in the shape of daily sapflow curves. While peak J_s was similar between the two species, the broader J_s signal (i.e., more gradual diurnal increase and decrease) of *Q. lyrata* resulted in higher daily flux compared to the narrower signal of *C. laevigata*. These differences in curve shape are unlike those associated with water limitations (e.g., Kume et al. 2007), and we are not aware of others finding similar differences in J_s curves between species. Despite all monitored trees having co-dominant canopy positions, the slightly lower canopy position of *C. laevigata* may have reduced light at lower sun angles. Lower canopy position may also explain why tree size in *C. laevigata* was not as strongly related to J_s or F as it was for *Q. lyrata.* Implications of this finding for carbon and water relations are unclear.

Pre-dawn water potential, as a proxy for the availability of water to roots (Hinckley et al. 1978), suggested differences in rooting habits across microtopography. At Site N (with microtopography), *C. laevigata* was more prevalent on ridges and *Q. lyrata* in swales, and *Q. lyrata* accessed lower-tension water than did *C. laevigata*. For comparison, at Site S (with little microtopography), *C. laevigata* transitioned from lower-tension water (July 11) to greater-tension water (Aug. 16) compared to *Q. lyrata*. As the water table lowered, *Q. lyrata* apparently gained connection with lower tension water by either increasing root density for better access to less bound water, or by accessing the water table (*sensu* Mahoney and Rood 1998). This is consistent with a previous study of BLH rooting that found *Q. lyrata* rooting habits were less affected by flooding than other species (Burke and Chambers 2003). It may follow, then, that *C. laevigata* may have less well-developed roots after flooded conditions and therefore be more vulnerable to subsequent drought. This is of particular interest because *C. laevigata* is becoming increasingly abundant in hydrologically disconnected BLH systems (Gee et al. 2012), which may decrease the relative advantage *Q. lyrata* would have in wetter conditions.

4.5 CONCLUSIONS

Water limitations can control forest function in floodplain forests, particularly in floodplains with altered hydrology. Sapflow indicated the importance of short-term, late-season flooding and shallow groundwater as a net water subsidy to floodplain trees. River flood pulses generated responses by floodplain trees only where there was connectivity to the floodplain. The greater positive response to flooding by *Q. lyrata* as compared to *C. laevigata* suggests a physiological advantage in wetter conditions. In dry floodplain sites where there is no connectivity to the river, sapflow techniques did not strongly indicate any differences between *Q. lyrata* and *C. laevigata*. Both of the studied species are responsive to dry conditions, as demonstrated by site differences. Drought appears an important control on trees even in humid floodplain wetlands.

4.6 REFERENCES

Allen, S. T., J. W. Cochran, K. W. Krauss, R. F. Keim, S. L. King, 2016. Hydrologic effects on diameter growth phenology for Celtis leavigata and Quercus lyrata in the floodplain of the lower White River, Arkansas, in Proceedings of the 18th Biennial Southern Silvicultural Research Conference, USFS, Knoxville, TN.

Anderson, C. J., and W. J. Mitsch, 2008. Tree basal growth response to flooding in a bottomland hardwood forest in central Ohio, J. Am. Water Resour. Assoc., 44(6), 1512–1520, doi:10.1111/j.1752-1688.2008.00255.x.

Baker, T. T., W. H. Conner, B. G. Lockaby, J. A. Stanturf, M. K. Burke, 2001. Fine root productivity and dynamics on a forested floodplain in South Carolina, Soil Sci. Soc. Am. J., 65(2), 545-556, doi:10.2136/sssaj2001.652545x.

Battaglia, L. L., R. R. Sharitz, 2006. Responses of floodplain forest species to spatially condensed gradients: a test of the flood–shade tolerance tradeoff hypothesis, Oecologia, 147(1), 108–118, doi:10.1007/s00442-005-0245-7.

Bond, B. J., F. C. Meinzer, J. R. Brooks, 2008. How trees influence the hydrological cycle in forest ecosystems, in Hydroecology and Ecohydrology, edited by P. J. W. S. Lecturer, D. M. H. S. Lecturer, and J. P. S. Reader, pp. 7–35, John Wiley & Sons, Ltd.

Bosch, D. D., L. K. Marshall, R. Teskey, 2014. Forest transpiration from sap flux density measurements in a Southeastern Coastal Plain riparian buffer system, Agric. For. Meteorol., 187, 72–82, doi:10.1016/j.agrformet.2013.12.002.

Brady, N., R. Weil, 2007. The Nature and Properties of Soils, 14th Edition, 14 edition., Prentice Hall, Upper Saddle River, N.J.

Bravard, J.-P., C. Amoros, G. Pautou, G. Bornette, M. Bournaud, M. Creuzé des Châtelliers, J. Gibert, J.-L. Peiry, J.-F. Perrin, H. Tachet, 1997. River incision in south-east France: morphological phenomena and ecological effects, Regul. Rivers Res. Manag., 13(1), 75–90, doi:10.1002/(SICI)1099-1646(199701)13:1<75::AID-RRR444>3.0.CO;2-6.

Broadfoot, W. M., 1967. Shallow-water impoundment increases soil moisture and growth of hardwoods, Soil Sci. Soc. Am. J., 31(4), 562-56, doi:10.2136/sssaj1967.03615995003100040036x.

Broadfoot, W. M., H. L. Williston, 1973. Flooding effects on southern forests, J. For., 71(9), 584–587.

Burke, M. K., J. L. Chambers, 2003. Root dynamics in bottomland hardwood forests of the Southeastern United States Coastal Plain, Plant Soil, 250(1), 141–153, doi:10.1023/A:1022848303010.

Clawson, R. G., B. G. Lockaby, and B. Rummer, 2001. Changes in production and nutrient cycling across a wetness gradient within a floodplain forest, Ecosystems, 4(2), 126–138, doi:10.1007/s100210000063.

Clearwater, M. J., F. C. Meinzer, J. L. Andrade, G. Goldstein, N. M. Holbrook, 1999. Potential errors in measurement of nonuniform sap flow using heat dissipation probes, Tree Physiol., 19(10), 681–687, doi:10.1093/treephys/19.10.681.

Conner, W. H., J. W. Day, 1992. Water level variability and litterfall productivity of forested freshwater wetlands in Louisiana, Am. Midl. Nat., 128(2), 237–245, doi:10.2307/2426457.

Conner, W. H., B. Song, T. M. Williams, J. T. Vernon, 2011. Long-term tree productivity of a South Carolina coastal plain forest across a hydrology gradient, J. Plant Ecol., 4(1-2), 67–76, doi:10.1093/jpe/rtq036.

Dewey, J. C., S. H. Schoenholtz, J. P. Shepard, M. G. Messina, 2006. Issues related to wetland delineation of a Texas, USA bottomland hardwood forest, Wetlands, 26(2), 410–429, doi:10.1672/0277-5212(2006)26[410:IRTWDO]2.0.CO;2.

Ford, C. R., M. A. McGuire, R. J. Mitchell, R. O. Teskey, 2004. Assessing variation in the radial profile of sap flux density in Pinus species and its effect on daily water use, Tree Physiol., 24(3), 241–249, doi:10.1093/treephys/24.3.241.

Gardiner, E., J. Hodges, 1996. Physiological, morphological and growth responses to rhizosphere hypoxia by seedlings of North American bottomland oaks, Ann. Sci. For., 53(2-3), 303–316, doi:10.1051/forest:19960213.

Gee, H, 2012. The effects of hydrologic modifications on floodplain forest tree recruitment and growth in the Mississippi River Alluvial Valley, USA. Dissertation, Louisiana State University, Baton Rouge, LA, 29 May 2015.

Gee, H. K. W., S. L. King, R. F. Keim, 2014. Tree growth and recruitment in a leveed floodplain forest in the Mississippi River Alluvial Valley, USA, For. Ecol. Manag., 334, 85–95, doi:10.1016/j.foreco.2014.08.024.

Granier, A., 1987. Evaluation of transpiration in a Douglas-fir stand by means of sap flow measurements, Tree Physiol., 3(4), 309–320, doi:10.1093/treephys/3.4.309.

Hanberry, B. B., J. M. Kabrick, H. S. He, B. J. Palik, 2012. Historical trajectories and restoration strategies for the Mississippi River Alluvial Valley, For. Ecol. Manag., 280, 103–111, doi:10.1016/j.foreco.2012.05.033.

Hinckley, T. M., J. P. Lassoie, S. W. Running, 1978. Temporal and spatial variations in the water status of forest trees, For. Sci., 24(3), a0001–z0001.

Hook, D. D., 1984. Waterlogging tolerance of lowland tree species of the south, South. J. Appl. For., 8(3), 136–149.

Hupp, C. R., A. R. Pierce, G. B. Noe, 2009. Floodplain geomorphic processes and environmental impacts of human alteration along Coastal Plain rivers, USA, Wetlands, 29(2), 413–429, doi:10.1672/08-169.1.

Johnson, E., 2015. Effects of hydrologic modification on flooding in bottomland hardwoods, Thesis, Louisiana State University, Baton Rouge, LA, 29 May 2015.

Jung, M., T. P. Burt, P. D. Bates, 2004. Toward a conceptual model of floodplain water table response, Water Resour. Res., 40(12), doi:10.1029/2003WR002619.

Kennedy, H., 1990. Celtis laeviga Willd., sugarberry, in Silvics of North America, vol. 2 (Hardwoods), edited by R. M. Burns and B. H. Honkala, U.S. Department of Agriculture, US Forest Service, Washington, DC.

King, S. L., L. L. Battaglia, C. R. Hupp, R. F. Keim, B. G. Lockaby, 2012. Floodplain Wetlands of the Southeastern Coastal Plain, in Wetlands of North America: Ecology and Conservation Concerns, edited by D. Batzer and A. H. Baldwin, pp. 253–266, University of California Press, Berkeley, CA.

Kozlowski, T. T., 1997. Responses of woody plants to flooding and salinity, Tree Physiol., 17(7), 490–490, doi:10.1093/treephys/17.7.490.

Krauss, K. W., J. A. Duberstein, 2010. Sapflow and water use of freshwater wetland trees exposed to saltwater incursion in a tidally influenced South Carolina watershed, Can. J. For. Res., 40(3), 525–535, doi:10.1139/X09-204.

Krauss, K. W., P. J. Young, J. L. Chambers, T. W. Doyle, R. R. Twilley, 2007. Sap flow characteristics of neotropical mangroves in flooded and drained soils, Tree Physiol., 27(5), 775–783, doi:10.1093/treephys/27.5.775.

Kume, T., H. Takizawa, N. Yoshifuji, K. Tanaka, C. Tantasirin, N. Tanaka, M. Suzuki, 2007. Impact of soil drought on sap flow and water status of evergreen trees in a tropical monsoon forest in northern Thailand, For. Ecol. Manag., 238(1-3), 220–230.

Lewandowski, J., G. Lischeid, G. Nützmann, 2009. Drivers of water level fluctuations and hydrological exchange between groundwater and surface water at the lowland River Spree (Germany): field study and statistical analyses, Hydrol. Process., 23(15), 2117–2128, doi:10.1002/hyp.7277.

Mahoney, J. M., and S. B. Rood, 1998. Streamflow requirements for cottonwood seedling recruitment—An integrative model, Wetlands, 18(4), 634–645, doi:10.1007/BF03161678.

Megonigal, J. P., W. H. Conner, S. Kroeger, R. R. Sharitz, 1997. Aboveground production in southeastern floodplain forests: A test of the subsidy–stress hypothesis, Ecology, 78(2), 370–384, doi:10.1890/0012-9658(1997)078[0370:APISFF]2.0.CO;2.

Mitsch, W. J., J. R. Taylor, K. B. Benson, 1991. Estimating primary productivity of forested wetland communities in different hydrologic landscapes, Landsc. Ecol., 5(2), 75–92, doi:10.1007/BF00124662.

Nash, L. J., and W. R. Graves, 1993. Drought and flood stress effects on plant development and leaf water relations of five taxa of trees native to bottomland habitats, J. Am. Soc. Hortic. Sci., 118(6), 845–850.

Niinemets, Ü., F. Valladares, 2006. Tolerance to shade, drought, and waterlogging of temperate northern hemisphere trees and shrubs, Ecol. Monogr., 76(4), 521–547, doi:10.1890/0012-9615(2006)076[0521:TTSDAW]2.0.CO;2.

Odum, E. P., J. T. Finn, E. H. Franz, 1979. Perturbation theory and the subsidy-stress gradient, BioScience, 29(6), 349–352, doi:10.2307/1307690.

Oren, R., N. Phillips, G. Katul, B. E. Ewers, D. E. Pataki, 1998. Scaling xylem sap flux and soil water balance and calculating variance: a method for partitioning water flux in forests, Ann. Sci. For., 55(1-2), 191–216, doi:10.1051/forest:19980112.

Parolin, P., 2001. Morphological and physiological adjustments to waterlogging and drought in seedlings of Amazonian floodplain trees, Oecologia, 128(3), 326–335, doi:10.1007/s004420100660.

Parolin, P., F. Wittmann, 2010. Struggle in the flood: tree responses to flooding stress in four tropical floodplain systems, AoB Plants, 2010, doi:10.1093/aobpla/plq003.

Pezeshki, S. R., 2001. Wetland plant responses to soil flooding, Environ. Exp. Bot., 46(3), 299–312, doi:10.1016/S0098-8472(01)00107-1.

Pezeshki, S. R., J. H. Pardue, R. D. DeLaune, 1996. Leaf gas exchange and growth of flood-tolerant and flood-sensitive tree species under low soil redox conditions, Tree Physiol., 16(4), 453–458, doi:10.1093/treephys/16.4.453.

Ping, L., L. Urban, Z. Ping, 2003. Granier's thermal dissipation probe (TDP) method for measuring sap flow in trees: theory and practice, Acta Bot. Sin., 46(6), 631–646.

Poorter, H., Ü. Niinemets, L. Poorter, I. J. Wright, and R. Villar, 2009. Causes and consequences of variation in leaf mass per area (LMA): a meta-analysis, New Phytol., 182(3), 565–588, doi:10.1111/j.1469-8137.2009.02830.x.

Rodríguez-González, P. M., J. C. Stella, F. Campelo, M. T. Ferreira, and A. Albuquerque, 2010. Subsidy or stress? Tree structure and growth in wetland forests along a hydrological gradient in Southern Europe, For. Ecol. Manag., 259(10), 2015–2025, doi:10.1016/j.foreco.2010.02.012.

Schumm, S. A., W. J. Spitz, 1996. Geological influences on the Lower Mississippi River and its alluvial valley, Eng. Geol., 45(1–4), 245–261, doi:10.1016/S0013-7952(96)00016-6.

Shankman, D., C. W. Lafon, B. D. Keim, 2012. Western range boundaries of floodplain trees in the southeastern United States, Geogr. Rev., 102(1), 35–52, doi:10.1111/j.1931-0846.2012.00129.x.

Shure, D. J., M. R. Gottschalk, 1985. Litter-fall patterns within a floodplain forest, Am. Midl. Nat., 114(1), 98–111, doi:10.2307/2425245.

Solomon, J. D., 1990. Quercus lyrata Walt., overcup oak, in Silvics of North America, vol. 2 (Hardwoods), edited by R. M. Burns and B. H. Honkala, U.S. Department of Agriculture, US Forest Service, Washington, DC.

Turner, R. E., S. W. Forsythe, N. J. Craig, 1981. Bottomland hardwood forest land resources of the southeastern United States, in Wetlands of Bottomland Hardwood Forests, vol. 11, edited by J. R. Clark and J. Benforado, pp. 13–28, Elsevier, Amsterdam, Netherlands.

van der Valk, A. G., 2012. The Biology of Freshwater Wetlands, 2 edition., Oxford University Press, Oxford ; New York.

Ward, J. V., J. A. Stanford, 1995. Ecological connectivity in alluvial river ecosystems and its disruption by flow regulation, Regul. Rivers Res. Manag., 11(1), 105–119, doi:10.1002/rrr.3450110109.

Ward, J. W., K. Tockner, F. Schiemer, 1999. Biodiversity of floodplain river ecosystems: ecotones and connectivity, Regul. Rivers Res. Manag., 15(1-3), 125–139, doi:10.1002/(SICI)1099-1646(199901/06)15:1/3<125::AID-RRR523>3.0.CO;2-E.

Waring, R. H., S. W. Running, 2010. Forest Ecosystems: Analysis at Multiple Scales, Elsevier, Burlington, MA.

West, A. G., K. R. Hultine, K. G. Burtch, and J. R. Ehleringer, 2007. Seasonal variations in moisture use in a piñon–juniper woodland, Oecologia, 153(4), 787–798, doi:10.1007/s00442-007-0777-0.

4.7 APPENDIX: RADIAL GROWTH PHENOLOGY[2]

4.7.1 Measurements

Timing of intra-annual diameter growth of overcup oak, *Q. lyrata* and sugarberry, *C. laevigata* respectively) were measured by dendrometer bands and were compared among sites and species. Eight plots in the Dale Bumpers White River National Wildlife Refuge on the White River floodplain in southeastern Arkansas, USA. Similar to the two plots used for sapflow analysis, they differed by connectivity to the main river channel and experienced different flood regimes (Figure 4.7). Four plots were in the disconnected, entrenched reach, and four plots were in the more connected reach.

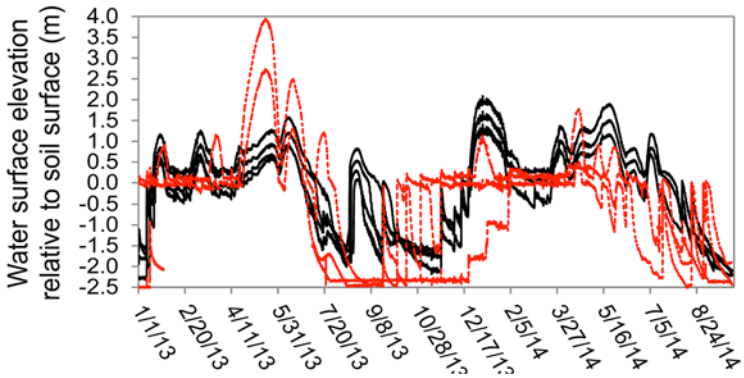

Figure 4.7 Water levels in plots on the White River floodplain for 2013 and 2014 (study year). The four black lines are for plots on the northern zone of the floodplain and the three red lines are wells in plots in the southern zone.

In each plot, four subplots (0.04 ha) were established for assessing stand characteristics and selecting measurement trees. Species and diameter (DBH) were recorded for every tree with DBH > 5.0 cm. Stainless steel dendrometer bands were installed at 1.4 m height on 216 trees (70 overcup oak and 140 sugarberry). Sizes of banded trees varied considerably (table 1) to represent the range of trees found within the stands. Bands were installed in the summer of 2012 and allowed to settle for a year for accurate measurements. Bands were measured with vernier calipers to the nearest 0.1 mm in 2013 and 2014. Measurements were zeroed at the beginning of the 2014 growing season, and we report data from five increments throughout the 2014 growing season (June 25, July 13, August 6, August 23, October 1).

Each plot had a ~2.5 m deep well for monitoring depth to water table, logged hourly. Relative surface elevation for trees was surveyed with respect to a co-located monitoring well.

4.7.2 Analyses

Trees that did not show substantial growth (minimum 0.25 cm in circumference) were excluded because of poor data resolution, which left 42 overcup oak and 86 sugarberry trees remaining. Excluded trees were mostly small and suppressed. Tree diameter increment was

[2]Content previously appeared Allen, S.T., Cochran, J.W., Krauss, K.W., Keim, R.F., King, S.L. 2016. Hydrologic effects on diameter growth phenology for Celtis leavigata and Quercus lyrata in the floodplain of the lower White River, Arkansas, in Proceedings of the 18th Biennial Southern Silvicultural Research Conference, USFS, Knoxville, TN, but is not copyrighted.

compared between species by t-test and compared to diameter for each species by simple correlation. For each tree, data from the dendrometer bands were converted to cumulative fractional growth through the season to examine seasonal diameter growth curves; curve shape indicates timing but not magnitude of differences among trees (i.e., high values do not indicate more growth). Trees were partitioned by size as 'small' (< 20 cm for sugarberry, < 35 cm for overcup oak) versus 'large' (> 20 cm for sugarberry, > 35 cm for overcup oak) to determine size effects on growth curves. Different criteria were used for each species because of different size distributions. Location within plots was separated based on microtopography. The highest 50 percent of trees were classified as 'Higher' and the lower 50 percent as 'Lower' with the exception of one site that was classified entirely as 'Higher' because it had minimal microtopography and was the least flooded site. These stratifications of the data were used as treatments, with differences tested for each measurement date by 2-sample t-tests ($\alpha = 0.05$). We estimated the growing season started with day of year (DOY) 100, corresponding with the approximate leaf out date estimated from satellite imagery (MODIS phenology products, http://phenology.cr.usgs.gov/), although the actual leaf out date was likely later for overcup oak (Solomon 1990). All analyses were conducted in MATLAB (Mathworks Inc., Natick, MA).

Table 4.5 Sample sizes (N) and tree sizes (diameter at breast height; DBH) and growth (diameter increment; DI) for *C. laevigata* and *Q. lyrata* trees with dendrometer measurements from the North (wetter) and South (drier) zones of the White River floodplain. Small, Med[ium] and Large refers to trees with DBH < 20 cm, 20-35 cm, and > 35 cm, respectively.

		Celtis laevigata			*Quercus lyrata*		
Site	*Size*	*N*	*DBH (cm)*	*DI (cm yr^{-1})*	*N*	*DBH (cm)*	*DI (cm yr^{-1})*
North	Small	14	16.0 ± 1.0	0.6 ± 0.4	0	No Data	
North	Med	18	27.0 ± 0.9	0.6 ± 0.4	3	31.6 ± 5.2	0.7 ± 0.4
North	Large	5	43.3 ± 3.4	0.8 ± 0.5	12	54.3 ± 14.0	2.2 ± 1.3
South	Small	29	3.9 ± 4.2	0.6 ± 0.3	9	20.9 ± 2.4	1.1 ± 0.3
South	Med	14	26.1 ± 4.8	0.8 ± 0.5	3	28.2 ± 4.2	1.3 ± 0.7
South	Large	7	44.3 ± 5.7	0.8 ± 0.5	15	59.7 ± 12.9	1.5 ± 0.5

4.7.3 Results and Conclusions

Despite different hydrogeomorphic settings, stand structure was similar across all study areas. All plots had multi-cohort, closed canopy forests (basal area of 30.4 ± 10.2 m^2 ha^{-1}; mean ± SD). Dominant species were *Celtis laevigata, Quercus lyrata, Carya aquatica, Liquidambar styraciflua, Fraxinus* spp.*, Quercus texana,* and *Ulmus americana.* The study species, sugarberry and overcup oak, accounted for 17 and 27 percent of basal area, and 20 and 13 percent of all stems (605 ± 215 stems ha^{-1} for trees with DBH > 5 cm), respectively, together accounting for 16 to 92 percent of all stems per plot.

The magnitude of annual diameter increment and its relationship with size differed between species. The 2014 diameter increment for overcup oak exceeded sugarberry ($p < 0.0001$). For sugarberry, diameter increment was not related to tree diameter ($r = 0.11$, $p = 0.33$), but for overcup oak, diameter increment was positively correlated to tree size ($r = 0.36$, $p = 0.024$). These relationships held across both northern and southern plots (Table 4.5).

Dendrometer data indicated differences in growth trends between species and hydrogeomoprhic setting. Upon the first dendrometer measurements (DOY 176), 75 ± 17 percent

(mean ± SD) of annual growth had occurred in sugarberry trees (Figure 4.8). In contrast, only 56 ± 18 percent of overcup oak growth had occurred by this time. Accordingly, a lower proportion of late-season growth occurred in sugarberry compared to overcup oak. Growth increments in overcup oak remained steady until DOY 235. Neither species had substantial growth in the last measurement period (DOY 235 to DOY 273). Growth trends were not size dependent for either species (Figure 4.8A), and showed minor, statistically insignificant effects of microtopographic position (Figure 4.8B). Stratifying the data by river reaches (north versus south) resulted in separation among means (Figure 4.8C). For multiple periods, t-tests indicated significant differences in cumulative fractional growth between the northern and southern sites for overcup oak (DOY 176, $p = 0.0082$; DOY 217, $p = 0.0027$) and sugarberry (DOY 176, $p = 0.03$; DOY 194, $p = 0.01$, DOY 217, $p = 0.01$). While our results may suggest that the northern site has a longer growing season, lack of precise north/south leaf-out dates prevents inferring total length.

Dendrometer data from 128 trees on the White River floodplain suggest that sugarberry grows rapidly in the early growing season while overcup oak grows more steadily and later into the growing season. For both, growth decreases earlier in drier sites.

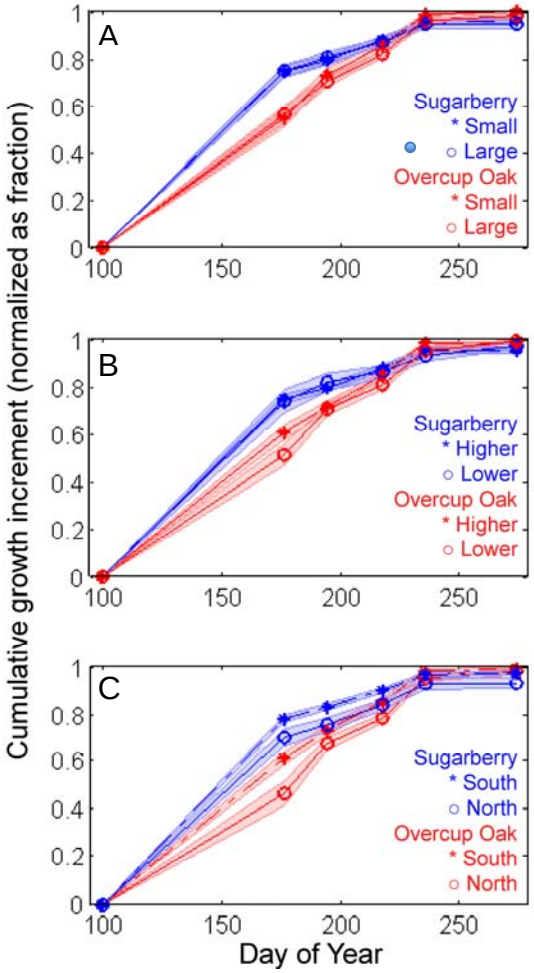

Figure 4.8. Cumulative fractionational growth curves from dendrometer band measurements of sugarberry (*Celtis laevigata*) and overcup oak (*Quercus lyrata*) trees on the White River floodplain from the 2014 growing season. Comparisons are of (a) tree diameters, (b) tree relative elevations within plots, and (c) plot location on the wetter, northern plots or drier, southern plots.

CHAPTER 5: ELUCIATING WETLAND-TREE GROWTH RESPONSES TO HYDROLOGY THROUGH DEVELOPMENT AND OPTIMIZATION OF A NON-LINEAR RADIAL GROWTH MODEL

5.1 INTRODUCTION

The interaction between vegetation and hydrological variability underlies wetland ecosystem structure and function (e.g., Junk et al., 1989; van der Valk, 1981). However, it is difficult to infer details about the nature of vegetation responses to this hydrologic variability (Rodriguez-Iturbe et al., 2007). Central to this is the challenge of linking multiscale ecological responses to patterns of hydrological variability. Even disregarding ecological responses, hydrologic variability itself is difficult to characterize qualitatively or quantitatively (Nuttle, 1997). Despite these hurdles, we need intersite and interstudy comparisons to formulate a generalized understanding of vegetation responses.

In wetlands, a particularly important and recurrent question is when flooding becomes stressful to vegetation. At the ecosystem scale, several studies (e..g, Megonigal et al., 1997; Mitsch et al., 1991; Odum et al., 1979; Rodríguez-González et al., 2010) have concluded that pulsed shallow floods enhance production, and stagnant or deep flooding limits stand production. Studies of seedlings in controlled environments have shown both flood-stress and drought-stress effects, such as reduced stomatal conductance, growth, and leaf area (Nash and Graves, 1993; Pezeshki and Chambers, 1986), with effects exacerbated by high temperatures (McLeod et al., 1986). Especially interesting is the finding that detrimental effects from flooding may be reduced by preconditioning, demonstrating acclimation to stress (Anderson and Pezeshki, 2001). Fewer direct measurements of gas exchange have been measured in mature trees, but the few have shown a general insensitivity of wetland trees to flooding these seedling-level findings seem to conflict with in-situ studies of mature trees that show improved water status with flooding (Allen et al., 2016; Krauss et al., 2007; Krauss and Duberstein et al., 2013). Tree rings have been another source of information on mature tree responses to water levels, often showing that growth correlates positively with wetter years (Day et al., 2012; Ford and Brooks, 2002; Keim et al., 2012), but longer periods of high water lead to lower growth (Keim et al., 2012; Keim and Amos, 2012; Young et al., 1995). The inconsistencies within this knowledge-base establish a need for further investigation.

While tree ring records contain a wealth of ecological information, conventional dendrochronological methods may not be ideal for interpreting flooding effects on wetland tree growth. Conventional approaches involve regressing ring chronologies against potentially dozens monlthy, seasonal, annual climate metrics and finding the best fit (Speer 2010). This can produce spurious results (Meko et al., 2011), which is partially mediated by using trees in water limited systems, enabling the assumption that wetter years should yield more growth (Fritts, 2001). This assumption may generally be valid in terrestrial systems because presumably water excess and deficit are common in wetlands, warranting representation by non-monotonic relationship (Mitsch and Gosselink, 2007). Indeed many variables likely have non-monotonic responses (e.g., pH, nutrient concentrations, temperature) across many forest types. Another limitation of linear regressions may not adequately represent each trees ring integrating responses over a whole growing season (Vaganov et al., 2006a), interactions among inhibiting factors (known to exist for temperature and flooding effects McLeod et al., 1986), and non-stationarity in the relationships between environmental factors and growth responses (e.g., by morphological adjustment to flooding; Anderson and Pezeshki, 2001; Kozlowski, 1997).

Deterministic models are an alternative method for analyzing tree rings, providing a framework where radial growth can be examined with respect to varying non-linear responses, interactions among drivers, and sub-annual variations can be considered (Tolwinski-Ward et al., 2011). Thus models avoid many drawbacks associated with linear statistics (Hughes, 2002). However, model development must be done cautiously to avoid overly complex model structures that may yield equifiniality and reduce interpretability. Tolwinski-Ward et al., (2011) presented a dendrochronological model (VS-Lite) to simplify the mechanistic Vaganov-Shashkin model (Vaganov et al., 2006a, 2006b). The Vaganov-Shashkin model aggregates growth as a product of responses to monthly meteorological inputs that modify both the production rate (growth, division) and physical attributes of xylem elements (e.g., size) in the cambium, with months added annually to construct a single ring. VS-Lite forgoes the cell processes by employing direct growth response functions to temperature and soil water availability. In both V-S and VS-Lite, the lower of the two growth factors is multiplied by an insolation-derived (from latitude and month) growth factor for a monthly growth index; indices are summed over the growing season (Tolwinski-Ward et al., 2011; Vaganov et al., 2006a).

In this study, the VS-Lite framework is used to develop a model of radial growth responses to monthly environmental conditions specific to wetlands (VSL-Wet). Our overarching objective is to better understand the nature of wetland tree responses to water level variations. This is approached by seeking the simplest form for a mechanstic model that can effectively simulate tree growth variations in wetlands and examining optimal parameter values. The model development process was conducted by comparing measured data to model outputs with model form varied by iteratively including and omitting of parameters representing concepts that we hypothesize may be important to explaining growth in wetlands. Through this heuristic approach, we examined model performance with respect to (1) non-linear versus linear growth responses, (2) water level and temperature independently controlling growth, or with interaction effects, and (3) static thresholds defining growth responses to water level versus ones varying with past hydrologic conditions showing response plasticity. VSL-Wet performance was compared to linear-regression models, with respect to overall fit (with penalties by number of parameters) and by comparison of parameter set generalizability across different stands and different sites. VSL-Wet was calibrated and performance was assessed with six baldcypress (*Taxodium distichum* (L.) Rich. var *distichum*) chronologies across two wetlands—one connected and one disconnected from the Atchafalaya River, USA resulting in distinctly different water level variability.

5.2 VSL-WET MODEL

5.2.1 Theory and Development

VSL-Wet was designed similarly to the upland oriented VS-Lite—monthly radial growth responses directly to two non-linear growth response functions with threshold values but modified to wetland considerations:

$$G(y) = \sum_{m=1}^{12} g_E(m) \times f[g_W(m,y)\ ,\ g_T(m,y)]\ , \qquad (5.1)$$

where $G(y)$ is radial growth increment (ring width) of year y, g_E is a solar energy function for latitude and for month m (Tolwinski-Ward et al., 2011), g_W is a growth response function to water depth, and g_T is a growth response function to temperature. Values of g_W, g_E, and g_T range from zero to one. The primary differences between eq. 5.1 of VSL-Wet and that of the VS and VSL models are that, in VSL-Wet, the interaction of g_W and g_T is not fixed (section 2.2) and that the growth response function of soil moisture was replaced by a growth response function of

water level (Figure 5.1) because the study sites are mostly permanently flooded. Baldcypress is deciduous with an assigned winter leaf-off period of mid-November to mid-March (Eggler, 1955; MacClurkin, 1965), so g_E was zerofor December through February and half of potentials for March and November yielding values from 0.25 in November to 1 in June.

Both high and low water depths (W) and temperatures (T) may limit growth. Thus, g_W was defined with lower (*W2*) and upper (*W3*) thresholds beyond which growth is reduced and lower (*W1*) and upper (*W4*) thresholds beyond which growth is zero (Figure 5.1), consistent with previous similar models (Vaganov et al., 2006b), as

$$g_W(m,y) = \begin{cases} 0, & \text{if } W(m,y) \le W1 \\ 0, & \text{if } W(m,y) \ge W4 \\ 1, & \text{if } W2 \le W(m,y) \le W3 \\ \frac{W(m,y)-W3}{W1-W3}, & \text{if } W1 \le W(m,y) \le W2 \\ \frac{W(m,y)-W2}{W4-W2}, & \text{if } W3 \le W(m,y) \le W4 \end{cases}, \quad (5.2)$$

where *W* is water level of month *m* and year *y*, and, in parallel, g_T was defined as

$$g_T(m,y) = \begin{cases} 0, & \text{if } T(m,y) \le T1 \\ 0, & \text{if } T(m,y) \ge T4 \\ 1, & \text{if } T2 \le T(m,y) \le T3 \\ \frac{T(m,y)-T3}{T1-T3}, & \text{if } T1 \le T(m,y) \le T2 \\ \frac{T(m,y)-T2}{T4-T2}, & \text{if } T3 \le T(m,y) \le T4 \end{cases}. \quad (5.3)$$

Uppercase terms *W1*, *W2*, *W3*, *W4*, *T1*, *T2*, *T3*, and *T4* are the thresholds with respect to the g_T and g_W. These threshold values are defined by a function of lowercase terms *w1*, *w2*, *w3*, *w4*, *t1*, *t2*, *t3*, *t4* that each represents a free parameter (Figs 5.1, 5.2, Tables 5.1 and 5.2). Benefits of the piece-wise trapezoidal function include the flexibility to take on many shapes including the full range of triangular and monotonic functions (Vaganov et al., 2006a).

5.2.2 Candidate models and associated hypothesis tests

Candidate models were explored to best represent the measured data, but not all combinations of potential model structures were investigated (Table 5.2; Figure 5.2). The interaction of growth functions was tested by comparing models using the product of g_T and g_W, addition of g_T and g_W weighted by *c1*, minimum of g_T and g_W, and univariate models of g_T or g_W alone:

$$G_{mult}(y) = \sum_{m=1}^{12} g_E(m) \times [g_W(m,y) \times g_T(m,y)], \quad (5.4)$$

$$G_{add}(y) = \sum_{m=1}^{12} g_E(m) \times [c_1 g_W(m,y) + (1-c_1) g_T(m,y)], \quad (5.5)$$

$$G_{min}(y) = \sum_{m=1}^{12} g_E(m) \times \min\{g_W(m,y), g_T(m,y)\}, \quad (5.6)$$

$$G(y) = \sum_{m=1}^{12} g_E(m) \times g_W(m,y), \text{ and} \quad (5.7)$$

$$G(y) = \sum_{m=1}^{12} g_E(m) \times g_T(m,y). \quad (5.8)$$

The importance of acclimation in growth responses to W was tested by considering two models: one in which *W1*, *W2*, *W3*, and *W4* did not vary in time (fixed; Table 5.2, Figure 5.2), and another where values varied (var; Table 5.2, Figure 5.2) with respect to mean W over the previous *n1* years as,

$$W2(y) = w2 + \frac{1}{n1} \sum_{y-n1}^{y} \overline{W(y)}, \quad (5.9)$$

where $\overline{W(y)}$ is the annual mean of W(*m*,*y*). Threshold *W3* followed the same form. Thus, the thresholds were deviations from a low-pass filtered time series of water levels with window

width of *n1* years. In contrast, thresholds in fixed models were explicit water depths, although an explicit depth could equivalently be stated as a deviation from mean depth.

Table 5.1 Abbreviations and symbols

Response Curves	
g_W	Growth response to water level (eq.1)
g_T	Growth response to temperature (eq. 5.2)
g_E	Growth response to solar energy
T(*m,y*)	monthly temperature
W(*m,y*)	monthly water level, unique to each plot
m	month
y	year
W1, W2, W3, W4	water levels defining g_W (eq. 5.2; Table 5.2)
T1, T2, T3, T4	temperatures defining g_T (eq. 5.3; Table 5.2)
w1,w2,w3,w4	free parameters defining *W1, W2, W3, W4*, respectively (Table 5.2)
t1, t2, t3, t4	free parameters defining T1, T2, T3, T4, respectively (Table 5.2)
s1	free parameter defining the monthly window shift (eq. 5.10)
n1	free parameter defining the number of years over which mean W is calculated for defining varying thresholds (eq. 5.9)
Candidate Models	
G	the relative ring width proxy annual output of VSL-Wet model
G_{mult}	model using g_T and g_W multiplied (eq. 5.4); G_{mult} is used if unspecified
G_{add}	model using g_T and g_W added (eq. 5.5)
G_{min}	model using minimum of g_T and g_W (eq. 5.6)
G__*-shift*	Model using shift parameter s1 (eq. 5.10)
T__	Model including g_T
W__	Model including g_W
__4	Model with g_T or g_W thresholds defined by four free parameters
__2	Model with g_T or g_W thresholds defined by two free parameters
__fixed	model with fixed W1,2,3,4 thresholds over the time series
__var	Model with *W* thresholds varying as fixed deviations from mean W over past *n1* years
Research Sites	
Verret	Verret Basin site
Atch	Atchafalaya Basin site at Grand Lake
AT	Attakapas landing, one of the two deeper plots in Verret
GC	Godchaux Canal, one of the two deeper plots in Verret
EH	Elm Hall Wildlife Management area, the shallower plots in Verret
SM	Six Mile Lake, in Atch
VU	Verdunville landing, in Atch
GH	Gray Horse Island, in Atch

Simpler, 2-free-parameter forms of g_W (eq. 5.2) and g_T (eq. 5.3) were tested, in which the lower (*W1*, *T1*) and upper thresholds (*W4*, *T4*) respectively equaled the minima and maxima of monthly W and T. Consequently, there were four months of each chronology with g_W or g_T forced to zero.

Similar to VS-Lite, we tested a growing-season window shift to account for part of one year's growth to be a product of the previous year's conditions and responses (Tolwinski-Ward et al., 2011). A free parameter, *s1*, defined the fixed-width 12-month window defining the growing period contributing to each ring,

$$G_{mult-shift}(y) = \sum_{m=1-s1}^{12-s1}[g_W(m,y) \times g_T(m,y)] \times g_E(m) \quad . \qquad (5.10)$$

Accounting for senescence, *s1* from zero to four months defined the contributing intervals as: Mar$_y$ to Nov$_y$, Nov$_{y-1}$ to Oct$_y$, Octy$_{y-1}$ to Sept$_y$, or Sept$_{y-1}$ to Aug$_y$.

5.3 METHODS

5.3.1 Study Sites and Environmental Data

Six study plots were in two hydrologically distinct sites—the Atchafalaya Basin (Atch) at Grand Lake and Verret Basin—that are extensive baldcypress-tupelo swamps in southern Louisiana (Figure 5.3). While both are within the former Atchafalaya River basin, now levees disconnect Lake Verret plots from Atchafalaya River flows (Figure 5.3), decreasing water level variability and sediment and nutrient inputs (DeLaune et al., 1987). Sampled stands established between 1798 and 1902 (Keim and Amos, 2012).

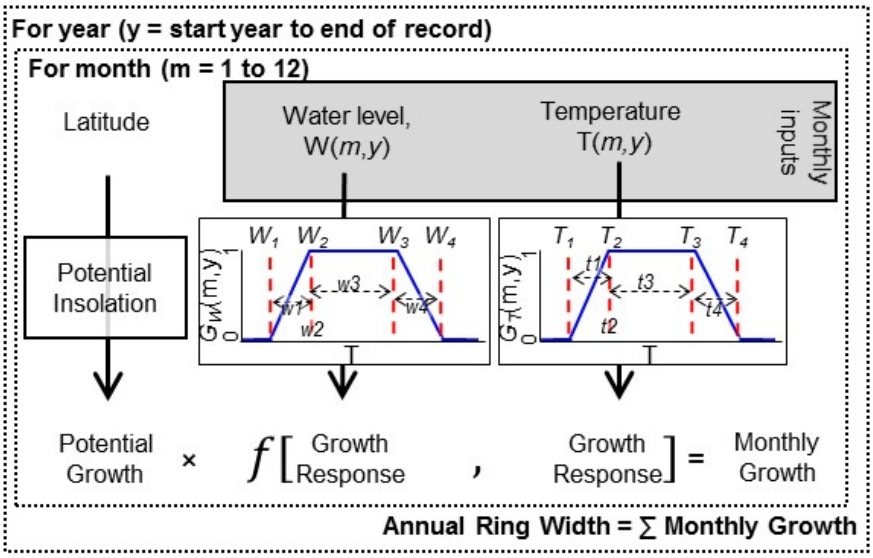

Figure 5.1 Diagrammatic representation of VSL-Wet.

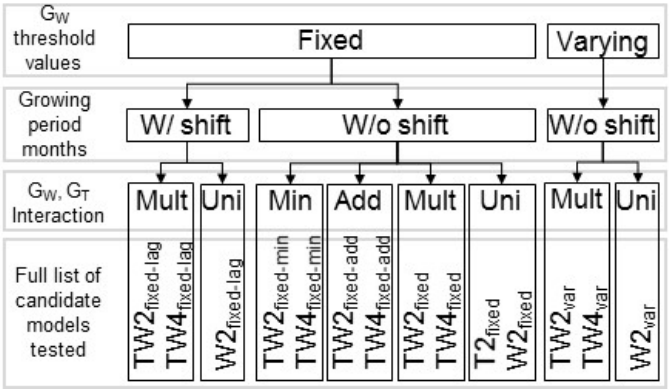

Figure 5.2 Hierarchical diagram of VSL-Wet candidate models. Models considered whether water response thresholds were fixed or varying in time, whether there was a shift term allowing growth contribution from the previous year, whether one or both growth response functions (g) for water levels (W) or temperature (T) were included and how they interacted, and whether growth response functions were defined by two parameters or four.

Table 5.2 Candidate models as defined by number of free parameters and interaction effects, and the g_W (eq. 5.2) and g_T (eq. 5.3) thresholds (uppercase letters) defined in terms by free parameters (lowercase letters), where the inputs ranges, in notation [maximum, minimum], were: w1 [0.0,1.5]; w2 [W_{min},W_{max}] for fixed models and *w2*[$W_{min}-\overline{W_{y-n1\ to\ y}}$], $W_{max}-\overline{W_{y-n1\ to\ y}}$] for var models; *w3*[0.0,$W_{min}-W_{max}$]; *w4*[0.0,1.5]; *t1*[0.0,10.0]; *t2*[0.0 ,30.0]; *t3*[0.0 ,10.0]; *t4*[0.0 ,10.0]; *s1*[0, 4]; and, *n1*[1,10].

Model	Free params	Inter-action	Response function thresholds								Month shift	Lag W mean
			W1	*W2*	*W3*	*W4*	*T1*	*T2*	*T3*	*T4*		
$TW4_{fixed}$	8	G_{mult}	*w2 – w1*	*w2*	*w2 + w3*	*w3 + w4*	*t2 – t1*	*t2*	*t2 + t3*	*t3 + t4*	NA	NA
$TW4_{fixed}$	8	G_{min}	—"—	—"—	—"—	—"—	—"—	—"—	—"—	—"—	NA	NA
$TW4_{fixed}$	11	G_{add}	—"—	—"—	—"—	—"—	—"—	—"—	—"—	—"—	NA	NA
$TW4_{fixed\text{-}shift}$	9	G_{mult}	—"—	—"—	—"—	—"—	—"—	—"—	—"—	—"—	*s1*	NA
$TW2_{fixed}$	4	G_{mult}	Min(W)	—"—	—"—	Max(W)	0.0	—"—	—"—	Max(T)	NA	NA
$TW2_{fixed}$	4	G_{min}	—"—	—"—	—"—	—"—	—"—	—"—	—"—	—"—	NA	NA
$TW2_{fixed}$	6	G_{add}	—"—	—"—	—"—	—"—	—"—	—"—	—"—	—"—	NA	NA
$TW2_{fixed\text{-}shift}$	5	G_{mult}	—"—	—"—	—"—	—"—	—"—	—"—	—"—	—"—	*s1*	NA
$T2_{fixed}$	2	NA	NA	NA	NA	NA	—"—	—"—	—"—	—"—	NA	NA
$W2_{fixed}$	2	NA	Min(W)	*w2*	*w2 + w3*	Max(W)	NA	NA	NA	NA	NA	NA
$W2_{fixed\text{-}shift}$	3	NA	—"—	—"—	—"—	—"—	NA	NA	NA	NA	*s1*	NA
$TW4_{var}$	9	G_{mult}	*w2 – w1*	$\frac{1}{n1}\sum_{y-n1}^{y}\overline{W(y)}$ + *w2*	*w2 + w3*	*w3 + w4*	*t2 – t1*	*t2*	*t2 + t3*	*t3 + t4*	NA	*n1*
$TW2_{var}$	5	G_{mult}	Min(W)	—"—	—"—	Max(W)	0.0	—"—	—"—	Max(T)	NA	*n1*
$W2_{var}$	3	NA	—"—	—"—	—"—	—"—	NA	NA	NA	NA	NA	*n1*

Elevation differed among plots, resulting in differences in flood frequency, depth, and duration within sites (Figures 5.4, 5.5). We developed plot-specific hydrographs from long term water level records in nearby lakes; this was possible because standing water extended from plots to the gauges most of the time (Keim and Amos, 2012). We used records from 1966 to 2004 for the Atch plots and 1959 to 2004 for the Verret plots. Temperature data (Figure 5.5C) were from the National Climatic Data Center. All environmental data were monthly means of daily mean values. More details on sites, water level records, and climate records were described by Keim and Amos (2012).

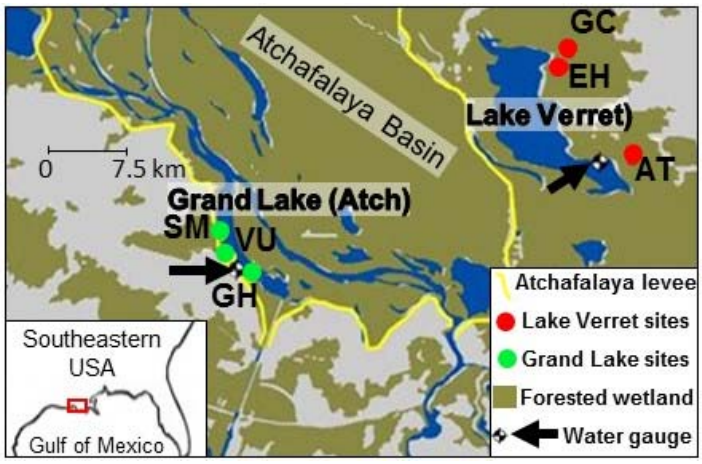

Figure 5.3 Map of study region, Atchafalaya (Atch) plots in Grand Lake–Six Mile Lake (SM), Verdunville landing (VU), and Gray Horse Island–and Lake Verret Sites–Godchaux Canal (GC), Elm Hall Wildlife Management Area (EH), and Attakapas Landing (AT)

5.3.2 Tree Ring Analysis

Baldcypress is among the most flood tolerant trees (Mitsch and Gosselink, 2007) and is responsive to climate variations (Stahle et al., 1985). The specific trees, cores, measurements, and cross dating statistics are all the same as presented by (Keim and Amos, 2012). For each of the six plots, 10 or 11 co-dominant baldcypress trees were sampled, with two cores from each tree at 3 m above ground level to be above stem buttressing. Conventional methods were used for preparing and measuring cores, and Cofecha used to verify cross-dating (Speer, 2010).

Ring data were detrended with a high-pass filter using ARSTAN (Cook, 1985) with autoregressive signals removed and detrended; a 20-year spline with spline parameter of 0.5 was selected because of the short hydrologic record (39 and 46 years) and our interest in annual responses rather than long term signals. This removed remove the low frequency signal present in both raw ring width and RCS chronologies used by Keim and Amos (2012; Figure 5.6). All ARSTAN chronologies were also normally distributed (Shapiro-Wilk test; α=0.05) and were normalized by subtracting the mean (over the 46 and 39 year periods) and dividing by the standard deviation so that both VSL-Wet output and normalized chronologies to have the same distribution and domain (mean of zero, standard deviation of one). From here forward, all analyses were only applied to the processed 1959-2004 (Verret) and 1966-2004 (Atch) segments referred to as site chronologies.

5.3.3 Model assessment and analysis

The model sensitivity and parameterizations was analyzed through Monte-Carlo iteration of random parameter sets bounded by a range of realistic values (Table 5.2). The Pearson correlation coefficient, *R*, was used as an objective function for consistency with common dendroclimatological approaches (Speer, 2010). Although *R* is insensitive to both proportional and additive differences between measurements and model outputs (Legates and McCabe, 1999), these limitations are not problematic because results were normalized to the same scales. In describing relative model performance, we qualify “better” models as those with lower AIC or higher *R*.

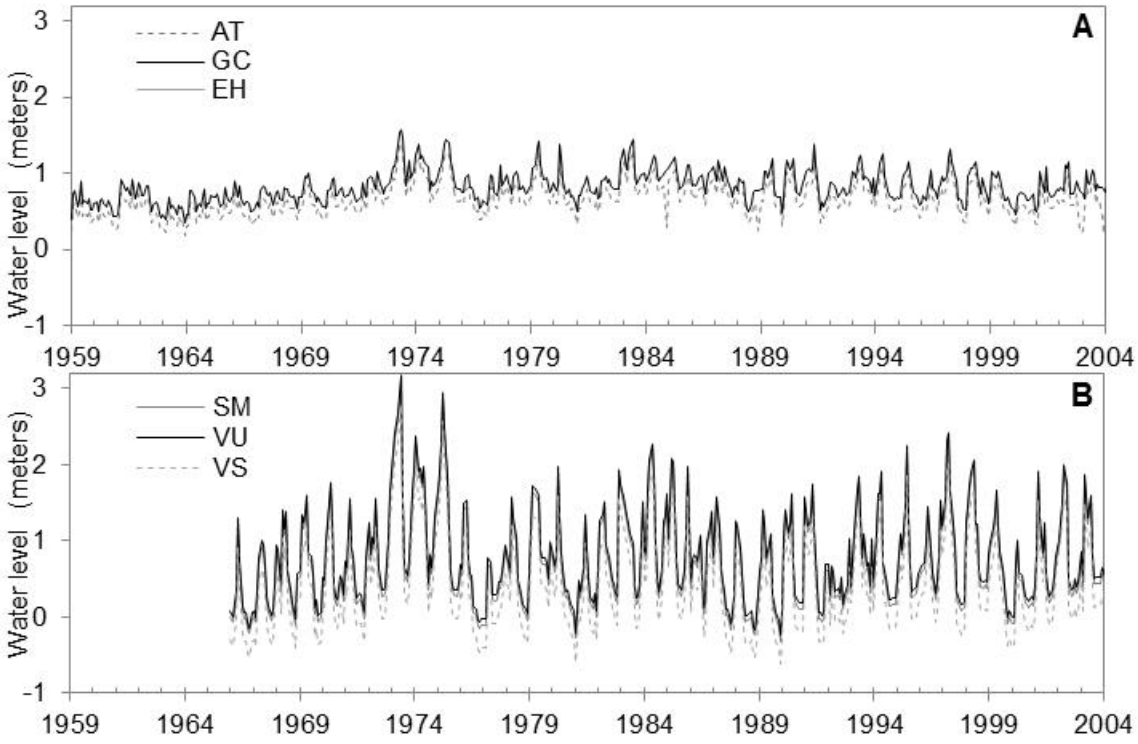

Figure 5.4 Site-specific hydrographs

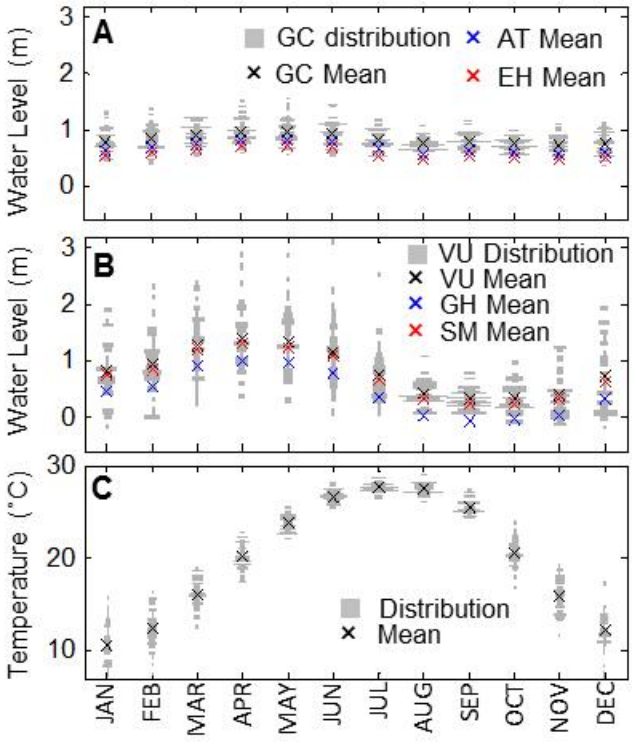

Figure 5.5 Violin plots and means of monthly water levels for 46 years at Verret sites (A) and 39 years at Atch sites (B), and temperature (C).

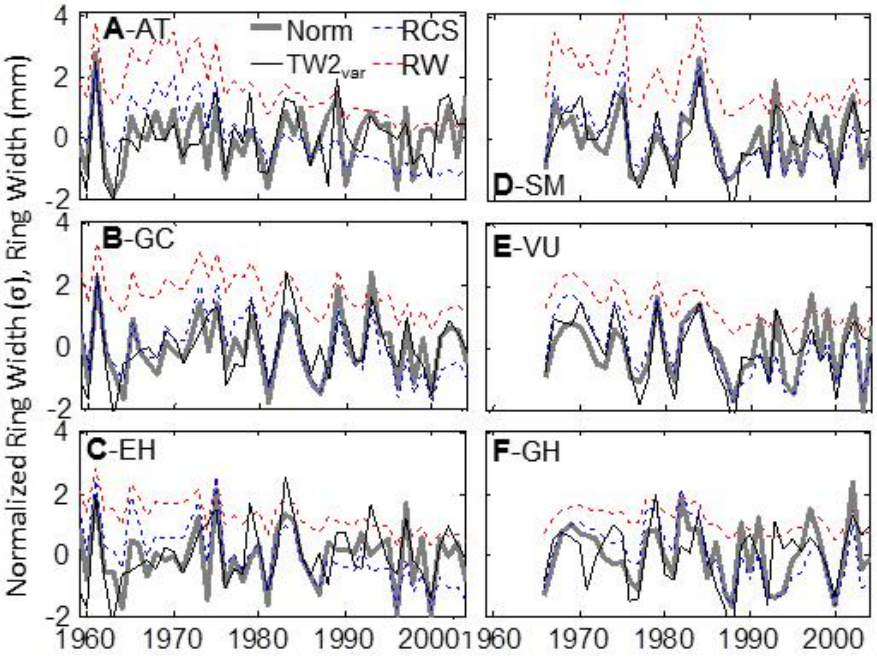

Figure 5.6 Tree ring chronologies for the Verret (A-C) and Atch (D-F) sites, showing the normalized chronology (Norm) from Arstan, as used in model calibration and validation, the raw ring widths (in mm), the RCS detrended ring widths described by Keim and Amos (2012), and, one example VSL-Wet output from the $TW2_{var}$ model.

Both the Akaike Information Criterion (AIC), as a model performance statistic penalizing for the number of parameters, and the dotty plot approach, drawn from generalized likelihood uncertainty estimation (GLUE; Beven and Freer, 2001), was used to identify the best model forms. Dotty plots compare values of the objective function, *R* to candidate parameter values from the Monte-Carlo process, indicating which terms the model performance is sensitive to. Dotty plots also serve as a tool for visualizing optimal zones of parameters rather an individual optimal values

To assess its relative utility, model fits for VSL-Wet were compared to performance of simple correlation with monthly temperatures and water levels (two free parameters), multiple regression of mean annual temperature and water level (three free parameter), and multiple regression of monthly water levels (13 free parameter).

Cross-site model validation was by applying best-fit parameter sets from each site to all other sites. This same approach was applied to test the efficacy of multiple regression models in predicting growth at other sites to compare to VSL-Wet.

5.4 RESULTS

5.4.1 Model Assessment

Of the fixed-parameter models, $TW4_{fixed\text{-}mult\text{-}shift}$ showed relatively high AIC (Table 5.3) and high *R* (Table 5.4), but varriations in *R* were unaffected by most parameter values, suggesting it was over-parameterized; thus it was selected for analyzing effects of the nine parameters (Figure 5.7). Univariate dotty plots for $TW4_{fixed}$ (Figure 5.7) showed sensitivity to *w2*, *t2*, and *t4* parameters. Fits were better for Atch sites than Verret sites (Table 5.4), and the model

fit was more sensitive to parameter values at VU than GC. At GC, *w2* and *t2*, there was a plateau of *R* over much of the domain but poor correlations at lower values. At VU, there was a distinct peak in *R* for both *w2* and *t2*. In bivariate space, sensitivity to *w3* was also evident (Figures 5.8, 5.9 for model $W2_{fixed}$), and it co-varied with *w2* because they define the location and width of the "plateau" region of g_W.

Table 5.3 Model AIC for all sites and for all candidate models. Where model response function interaction is not specified, models are G_{mult}. Lowest values are in bold.

Model	AT	GC	EH	SM	VU	GH	Mean
$TW4_{fixed}$	6.6	0.1	9.2	-6.3	-9.6	6.6	1.1
$TW4_{fixed}$ (G_{min})	5.7	2.3	**3.5**	-2.2	-9.4	8.6	1.4
$TW4_{fixed}$ (G_{add})	7.8	4.0	10.2	-10.5	-11.6	6.6	1.1
$TW4_{fixed\text{-}shift}$	6.2	0.2	11.1	-0.5	-9.8	6.4	2.3
$TW2_{fixed}$	6.5	-0.7	11.4	-10.9	**-13.3**	7.4	0.1
$TW2_{fixed}$ (G_{min})	6.7	-1.1	12.0	-7.7	-7.4	7.2	1.6
$TW2_{fixed}$ (G_{add})	5.9	-1.3	10.7	-10.2	-5.7	9.7	1.5
$TW2_{fixed\text{-}shift}$	9.1	1.3	13.4	-9.1	-12.4	9.2	1.9
$T2_{fixed}$	9.6	13.9	16.2	18.1	19.8	22.2	16.6
$W2_{fixed}$	17.1	3.6	14.3	-7.1	-2.8	6.7	5.3
$W2_{fixed\text{-}shift}$	19.5	5.4	16.6	-5.4	-1.2	8.7	7.3
$TW4_{var}$	4.4	-14.5	8.0	-4.0	-2.4	10.1	0.3
$TW2_{var}$	**-1.5**	**-20.7**	3.6	**-17.6**	-12.0	5.4	**-7.1**
$W2_{var}$	7.9	-11.9	8.8	-14.8	-6.1	**2.5**	-2.3

Models including response function interactions (G_{mult} and G_{add}) performed better than those that did not versus G_{min} or single response functions models (Tables 5.3, 5.4). For $TW4_{fixed}$, G_{mult} and G_{add}, AIC was similar. Mean AIC for TW2 was lower for G_{mult} than for G_{add} *or* G_{min}. All models including both g_T and g_W performed better than respective single response function models (i.e., $TW2_{fixed}$ versus $T2_{fixed}$ or $W2_{fixed}$ and $TW2_{var}$ versus $W2_{var}$; Tables 5.3, 5.4).

In general, inclusion of a shift parameter (*s1*) did not substantially improve model fits (Table 5.4), and AIC suggested it was not justified on average (Table 5.3). The exception was that inclusion of *s1* resulted in a lower AIC for EH for $TW4_{fixed}$, with an optimal window of Nov(*y-1*) to Oct(*y*). Overall, inclusion of *s1* affected *R* by < 0.01 for both $TW2_{fixed}$ and $W2_{var}$, and the optimal value of *s1* was always either zero or one [i.e., Mar(*y*)-Nov(*y*) or Nov(*y-1*)-Oct(*y*)].

Inclusion of *n1* parameter for varying thresholds (Tables 5.2, 5.3) effectively improved model performance. Both AIC and *R* were almost universally better for $W2_{var}$, $TW2_{var}$, and $TW4_{var}$ than $W2_{fixed}$ $TW2_{fixed}$, and $TW4_{fixed}$.

Consistent with insensitivity to multiple TW4 parameters (i.e., *w1,w4, t1 t4*; Figure 5.7) and better fits with growth response function interactions, the TW2 models performed best for both fixed-parameter and varying-parameter candidate models. $TW2_{fixed}$ was the best fixed model with respect to AIC (Table 5.3) and had only slightly lower *R* than did $TW4_{fixed}$. $T2_{fixed}$ performed worst of all models and $W2_{fixed}$ was intermediate, but both are useful because of their simplicity and interpretability as 2-parameter models. $W2_{var}$ was substantially better than $W2_{fixed}$, and by mean AIC was the second best model, behind $TW2_{var}$.

Table 5.4 Model *R* for all sites and for all candidate models, simple linear regression with monthly temperature (T) and water levels (W), and correlation with multiple regression models of mean W(*m,y*) and T(*m,y*) and model of multiple regression of all months W. Where model model response function interaction not specified, models are G_{mult}.

Candidate Model	AT	GC	EH	SM	VU	GH	Mean
$TW4_{fixed}$	0.58	0.64	0.55	0.71	0.73	0.60	0.64
$TW4_{fixed}$ (G_{min})	0.59	0.64	0.53	0.66	0.74	0.60	0.63
$TW4_{fixed}$ (G_{add})	0.59	0.62	0.56	0.75	**0.76**	**0.62**	0.65
$TW4_{fixed\text{-}shift}$	0.61	0.64	0.62	0.69	0.75	0.60	0.65
$TW2_{fixed}$	0.50	0.58	0.44	0.68	0.70	0.49	0.57
$TW2_{fixed}$ (G_{min})	0.50	0.58	0.43	0.66	0.65	0.50	0.55
$TW2_{fixed}$ (G_{add})	0.53	0.60	0.47	0.69	0.66	0.49	0.57
$TW2_{fixed\text{-}shift}$	0.50	0.58	0.44	0.69	0.71	0.50	0.57
$T2_{fixed}$	0.42	0.37	0.32	0.26	0.23	0.18	0.30
$W2_{fixed}$	0.32	0.49	0.35	0.61	0.57	0.45	0.47
$W2_{fixed\text{-}shift}$	0.31	0.50	0.34	0.62	0.57	0.45	0.47
$TW4_{var}$	**0.62**	**0.75**	0.58	0.71	0.70	0.58	**0.66**
$TW2_{var}$	0.60	0.74	0.55	**0.75**	0.71	0.54	0.65
$W2_{var}$	0.47	0.65	0.45	0.70	0.62	0.53	0.57
simp reg (W, indiv. *m*)[1]	0.32	0.47	0.42	0.51	0.42	0.35	0.42
Corr (T, indiv. *m*)[2]	-0.40	-0.32	-0.25	0.42	0.35	0.39	0.36
Mult. Reg. ($T_{mean,}$, W_{mean})	0.41	0.51	0.38	0.52	0.48	0.36	0.44
Mult. Reg. ($W_{monthly}$)	0.38	0.67	**0.63**	0.64	0.64	0.60	0.59

[1]Highest *R* were for Sept, Apr, Mar, May, May, Apr
[2]Highest *R* were for June, Apr, Apr, Oct, Oct, Oct. Mean is of absolute values.

Linear regression models mostly performed worse than VSL-Wet models. In simple linear regression models, water levels were positively correlated with growth for some months and negatively correlated for others, with maximum single-month *R* varying by site from 0.32 to 0.51 (Table 5.4). Temperature best fits were both positively and negatively corrrelcted (Table 5.4). While *R* was low for the multiple regression of annual mean T and W, the 12-parameter multiple regression of monthly W(*m,y*) yielded *R* = 0.60, exceeding *R* for all VSL-Wet candidate models except $TW4_{fixed}$, $TW4_{var}$, and $TW2_{var}$; however, the VSL-Wet models all had fewer free parameters.

Parameterized VSL-Wet models were effective at modeling responses across plotsand sites; it far outperformed regression models in cross validation (Table 5.5). The cross validation was particularly strong within sites, with parameters from other Verret plots often yielding equivalent *R* values to those achieved by site-specific optimization and was particularly high for varying-threshold models (Table 5.4). While Atch plots also effectively cross-validated for both fixed and varying threshold models, the similarity in fit among plots was less than at Verret.

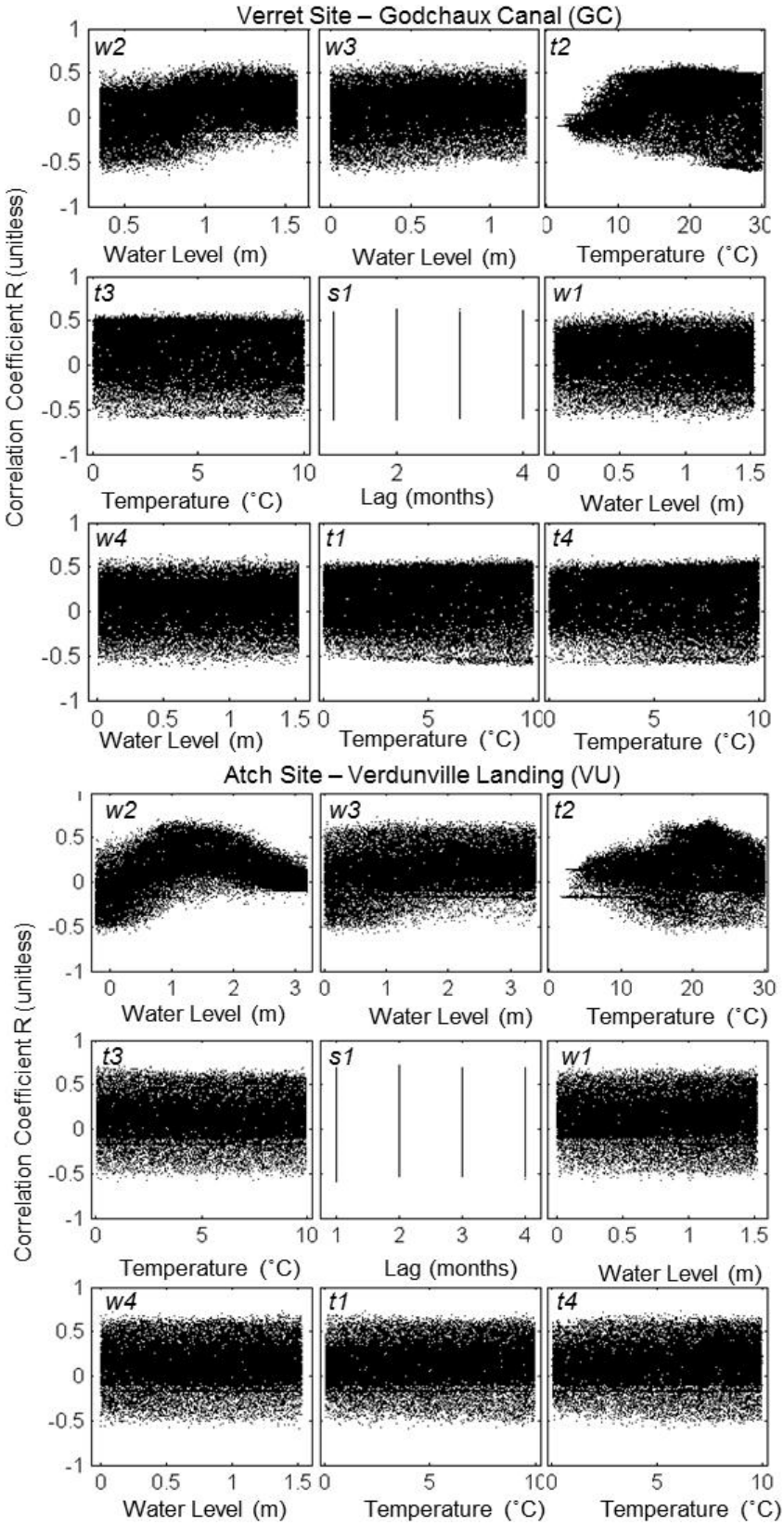

Figure 5.7 Univariate dotty plots of free parameters (Table 5.2) for $TW4_{fixed\text{-}mult\text{-}shift}$ for GC and VU. The top row and first panel of second row are the same as in the TW2 models.

Table 5.5 Cross-site correlations with parameters optimized for one training chronology.

Model	Training Chronology	Tested Chronology					
		AT	GC	EH	SM	VU	GH
Multiple Regression, monthly stage, 12 parameters	AT	**0.38**	0.61	0.47	0.41	0.34	0.24
	GC	0.34	**0.67**	0.55	0.28	0.27	0.23
	EH	0.28	0.59	**0.63**	0.25	0.18	0.21
	SM	0.19	0.36	0.28	**0.64**	0.58	0.44
	VU	0.12	0.28	0.20	0.58	**0.64**	0.49
	GH	-0.07	0.00	0.02	0.47	0.53	**0.60**
$TW2_{fixed}$	AT	**0.50**	0.23	0.27	0.32	0.33	0.41
	GC	0.40	**0.58**	0.44	0.59	0.61	0.38
	EH	0.39	0.57	**0.44**	0.46	0.55	0.40
	SM	0.41	0.55	0.41	**0.68**	0.65	0.42
	VU	0.41	0.54	0.41	0.65	**0.70**	0.45
	GH	0.43	0.43	0.36	0.58	0.61	**0.49**
$W2_{fixed}$	AT	**0.32**	-0.15	0.15	0.27	0.28	0.41
	GC	0.32	**0.49**	0.35	0.54	0.56	0.42
	EH	0.32	0.49	**0.35**	0.52	0.55	0.43
	SM	0.32	0.49	0.35	**0.61**	0.55	0.39
	VU	0.32	0.49	0.35	0.58	**0.57**	0.42
	GH	0.29	0.34	0.27	0.50	0.51	**0.45**
$W2_{fixed}$** mean-adjusted	AT	**0.32**	0.24	0.12	0.33	0.40	0.32
	GC	0.32	**0.49**	0.35	0.51	0.56	0.44
	EH	0.32	0.49	**0.35**	0.55	0.56	0.44
	SM	0.32	0.49	0.35	**0.61**	0.55	0.41
	VU	0.31	0.49	0.34	0.57	**0.57**	0.45
	GH	0.30	0.48	0.31	0.56	0.57	**0.45**
$TW2_{var}$	AT	**0.60**	0.67	0.43	0.44	0.46	0.33
	GC	0.57	**0.74**	0.54	0.59	0.61	0.43
	EH	0.55	0.73	**0.55**	0.60	0.61	0.43
	SM	0.48	0.62	0.48	**0.75**	0.67	0.49
	VU	0.52	0.65	0.50	0.72	**0.71**	0.51
	GH	0.41	0.58	0.39	0.64	0.61	**0.54**
$W2_{var}$	AT	**0.47**	0.60	0.40	0.48	0.49	0.45
	GC	0.46	**0.65**	0.44	0.60	0.57	0.49
	EH	0.45	0.65	**0.45**	0.48	0.50	0.42
	SM	0.38	0.55	0.40	**0.70**	0.61	0.47
	VU	0.40	0.57	0.41	0.69	**0.62**	0.50
	GH	0.38	0.57	0.39	0.65	0.61	**0.53**

**The fixed parameter terms were defined as a difference from the full period mean

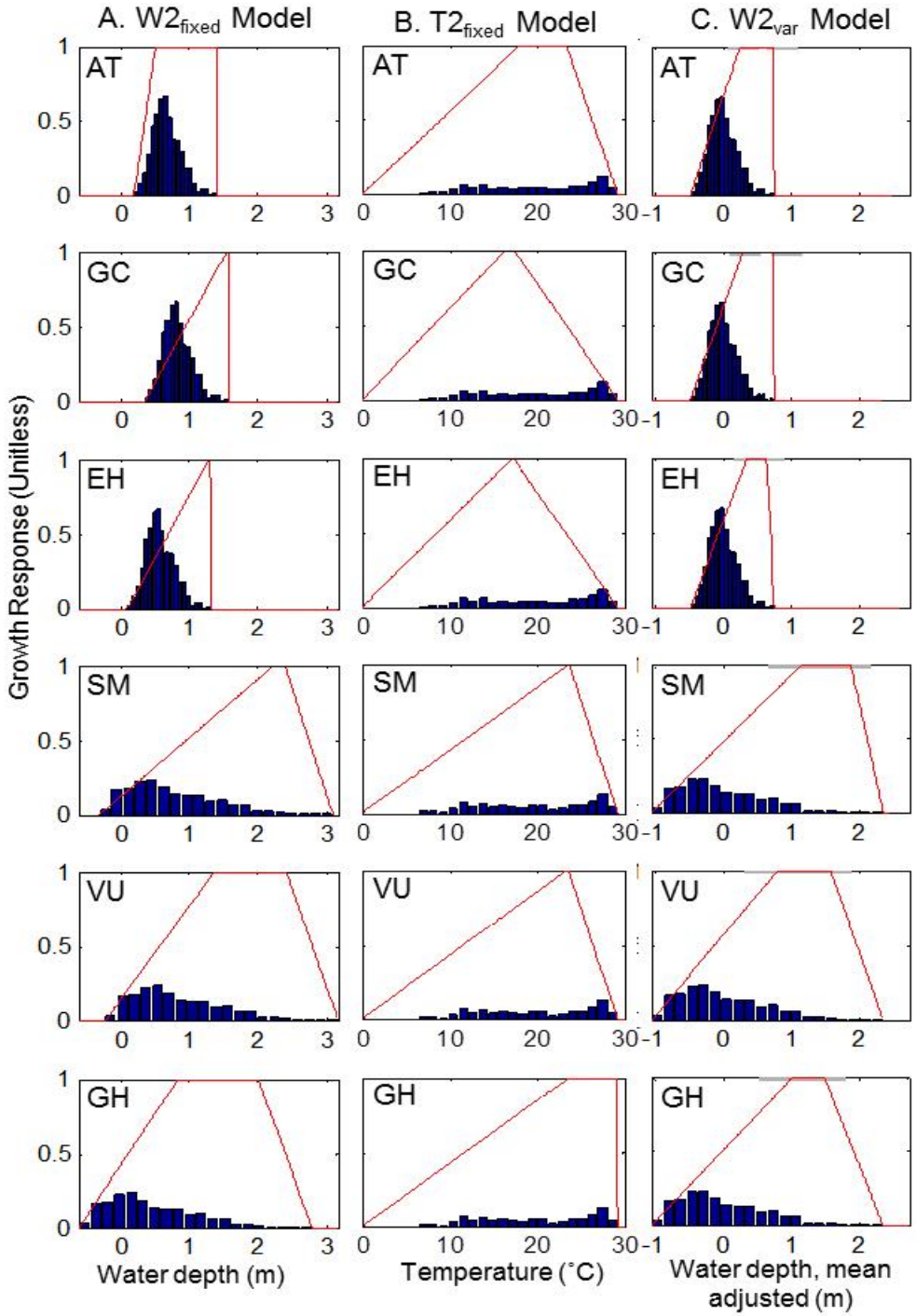

Figure 5.8 Example water (W) and temperature (T) growth response functions (red lines), as optimized for all six sites for $W2_{fixed}$ (Column A), for $T2_{fixed}$ (Column B), and for $W2_{var}$ (Column C). Blue bars compose histograms of water levels and temperatures. Dotted gray lines intercepts zero for all water level plots. For column C, since thresholds and data are plotted with respect to site mean W, red lines indicate mean g and grey bars at the top represent the range of variation for the *W2* and *W3* parameters (as described in Table 5.2).

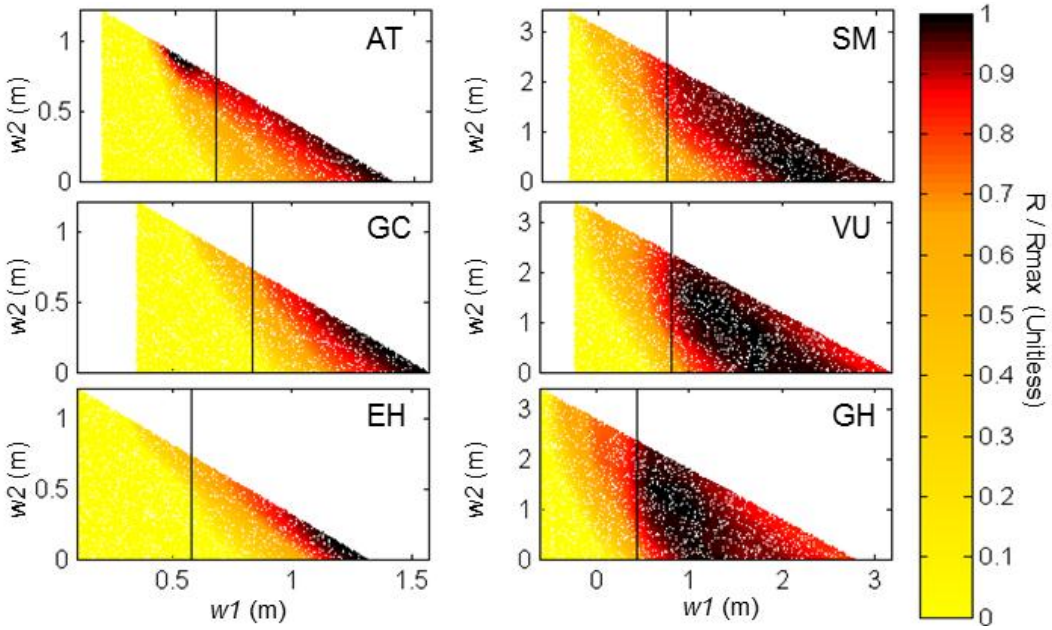

Figure 5.9 Bivariate dotty plots for *w1* and *w2* parameters in the $W2_{fixed}$ model.

5.4.2 Optimal parameter sets

The best-fit $W2_{fixed}$ parameterizations of g_W were similar across sites and plots. While the best-fit curves were not identical (Figure 5.8), the dotty plots demonstrated substantial overlap in optimal zone of the parameter spaces (Figure 5.9). The optimal growth response curves showed increasing growth with increasing water levels over much of the domain for the Verret plots (Figures 5.8, 9). Differences in g_W among Verret plots were consistent in magnitude with differences in plot water levels (Figure 5.8); that is, *w2* was approximately 0.5 to 0.75 m above plot mean W, and *w3* covaried inversely with *w2*, ranging from 0 to 0.5 m. The Atch plots, despite varying elevation and water depths among plots, were more similar to each other with respect to absolute depth (rather than depth relative to mean W), resulting in substantial overlap of optimal zones (Figure 5.9) from roughly 1 to 1.5 m for *w2* and 0.5 to the upper limit for *w3*. Across all sites, parameter space for *w2* had similarities with respect to mean W (Figures 5.8, 9).

The optimal parameter zone for $W2_{var}$ was less distinct than for $W2_{fixed}$, because of noise introduced by a third parameter (*nl*). As with $W2_{fixed}$, the optimal zone was more similar within sites than among sites (Figure 5.10). Compared to g_W for $W2_{fixed}$, the optimal g_W for $W2_{var}$ showed a larger range of W over which growth was reduced by high water levels in Verret plots. While *n1*—the length of time over which W was averaged and thresholds defined with respect to—was the same for both $W2_{Var}$ and $TW2_{Var}$ models for all plots but AT, values were inconsistent within or between sites; optimal values of *n1* were 7, 3, 3, 6, 6, and 2 years (for $W2_{var}$) or 1, 3, 3, 6, 6 and 2 years (for $TW2_{var}$) respectively for AT, GC, EH, SM, VU, GH.

Optimal parameters for g_T differed between Verret and Atch plots. Growth in the Verret plots was generally more related to T than in the Atch plots (Table 5.4), with optimal *t2* between roughly 15-20 °C for EH and GC, and slightly higher for AT (Figures 5.8, 5.11). As with *w2* and *w3*, *t3* value varied inversely with *t2*. The zone of optimality was smaller for Atch sites, with *t2* ranging between 22 to 24 °C for SM, VU, and GH, and *t3* of 0-2 °C for SM and VU. However, in both, g_T parameters describe growth reduction over much of domain. Unlike the others sites, the optimal T range for GH was limited such that there were high temperatures with maximum growth response and otherwise growth is only reduced by lower temperatures (Figure 5.8).

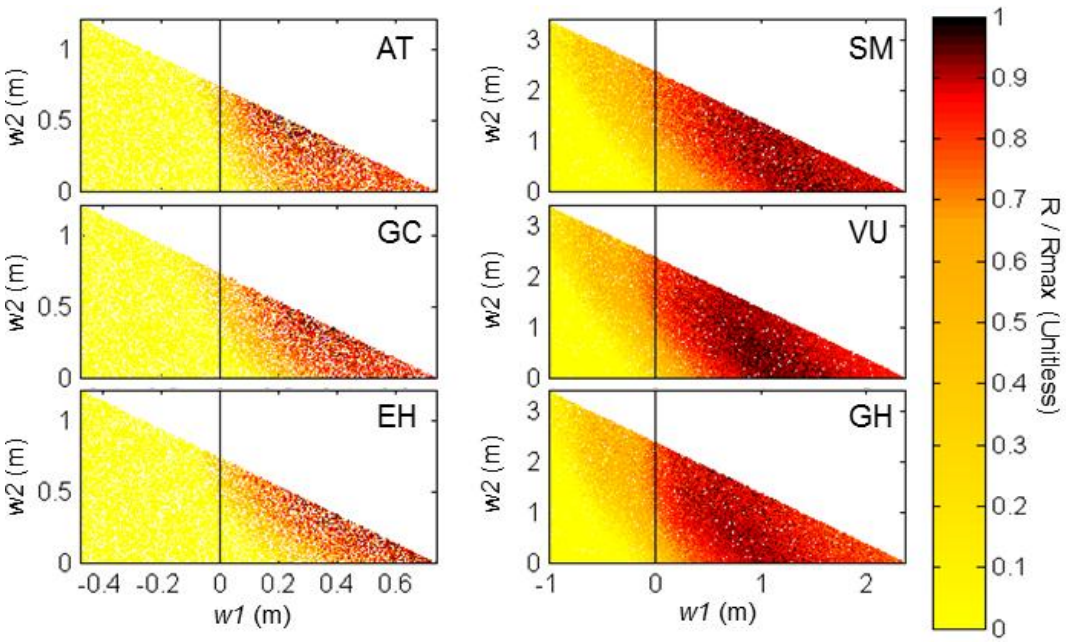

Figure 5.10 Bivariate dotty plots for *w1* and *w2* parameters in the $W2_{var}$ model.

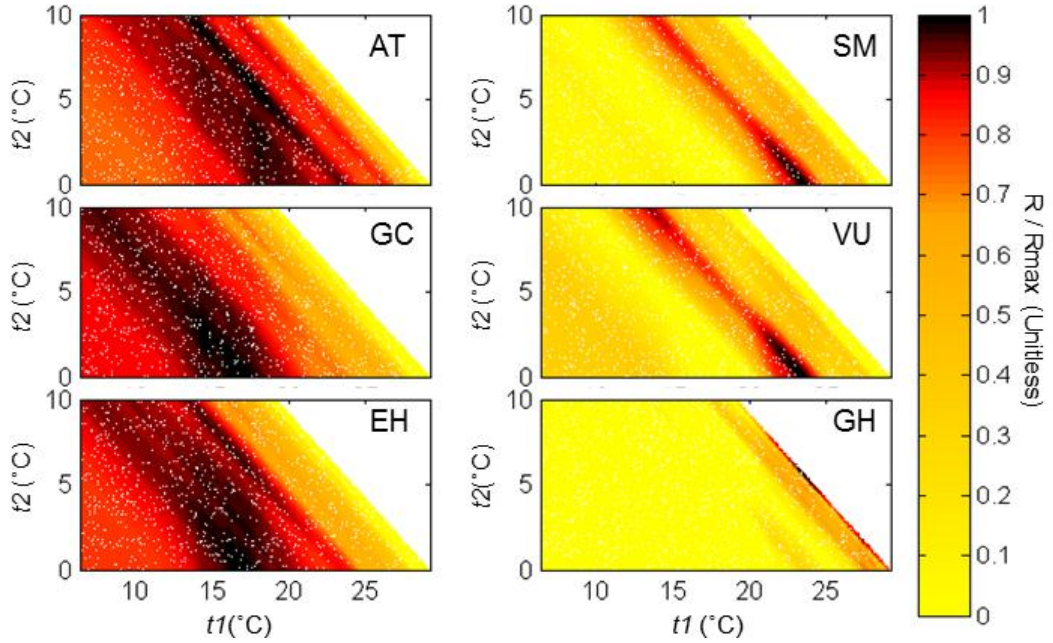

Figure 5.11 Bivariate dotty plots for *t1* and *t2* parameters in the $T2_{fixed}$ model

5.5 DISCUSSION

5.5.1 Model performance

In these wetlands, VSL-Wet often modeled ring width variability more effectively than simple regression approaches. The better performance is consistent with empirical observations that trees respond to conditions (whether temperature or water level) sub-annually and non-monotonically. Keeland and Sharitz (1997) empirically showed that baldcypress growth responses to weekly water levels and climate variability. There is a large evidence base that both spatial and temporal variations in wetland tree growth is non-linearly related to water levels and

intermediate conditions are often optimal (reviewed by Mitsch and Gosselink, 2007). Performance of VSL-Wet was particularly superior to regression for predicting growth in plots other than the site of calibration, demonstrating greater generalizability and indicating that superior performance was not a consequence of overfitting. The poor cross-site performance for regression models was not surprising because of differences in site water level ranges, inevitably leading to different best-fit parameters. While linear regression is better suited for climate reconstruction because the non-linear and sub-annual responses in VS models (Vaganov et al., 2006a), in this study, VSL-Wet was better for interpreting tree growth responses.

Best-fit growth response functions g_T and especially g_W are instructive for interpreting environmental controls over tree growth. The strong spatial cross-site validation performance of best-fit VSL-Wet models is especially important because it shows similarities of g_W and g_T among sites (section 5.4.2). Additionally, these parameters have physical meaning (i.e., depth), which is useful for inter-site comparisons and examining the generalizability of the responses represented by g_W. In general, a major obstacle to inter-site comparison is identifying what elements constituting a wetland "hydroperiod" are important. For example, many hydrologic metrics of Atch and Verret sites are similar but others are different: VU and AT are permanently flooded with mean depths of 0.82 m and 0.83 m, but mean intra-annual variability is 1.60 m and 0.47 m respectively. Importantly, an optimized g_W curve from VSL-Wet is a transferrable metric for comparing growth responses among sites that circumvents the need to also characterize and contrast site water-level variability, either qualitatively, or quantitatively with unavoidable simplifications.

While model performance was developed using mean monthly water levels and temperatures, increased temporal resolution or substitution of more direct drivers of growth may increase physiological interpretability (Vaganov et al., 2006a). However, long datasets other than temperature and water levels may be difficult to acquire. While temperature and water level have physiological relevance to wetland trees (Allen et al., 1996; Anderson and Pezeshki, 2001; McLeod et al., 1986; Nash and Graves, 1993) the VSL-Wet model form is suitable for integration of additional growth response functions to predictors others have found to control wetland tree growth, such as number of days of flooding (Anderson and Mitsch, 2008; Mitsch and Rust, 1984) or Palmer drought severity index (Conner et al., 2014; Keim et al., 2012; Keim and Amos, 2012; Stahle et al., 1985).

5.5.2 Ecological implications of best-fit models and parameters

An examination of the $TW4_{fixed}$ dotty plots as well as comparison of $TW4_{fixed}$ and $TW2_{fixed}$ models showed that performance was largely driven by the *t2* and *w2* parameters (and thus *W2* and *T2*). The more physiologically realistic 4-parameter response curves improved model fits but not AIC, so the omitted parameters are apparently not critical drivers. TW4 was especially not well justified for Verret sites where strong fits did not include reduced growth at high water levels (i.e., *W3=W4*). However, inclusion of the W3 at least was necessary to allow the optimization process to explore effects of a non-linear growth response curve.

Models allowing growth response function interactions performed better than models with single limiting factors, which is consistent with ecological principles but uncommon in dendrochronological practice. Modeling based on one limiting factor is common in dendroecology (principle of limiting factors; Fritts, 2001; Speer, 2010). Interaction of stressors can increase effects of (Mooney et al., 1991; Niinemets, 2010). To wetland trees, aggregate stress effects have been observed specifically for temperature and flooding, in that flooding

effects that are conditional on temperature effects (McLeod et al., 1986). Reasons for this could be that flooding inhibits trees by rhizosphere hypoxia (Pezeshki, 2001), and dissolved oxygen is inversely related to temperature (Joyce et al., 1985). Alternately, limited water uptake by degraded root systems (Kozlowski, 1997) may reduce transpiration and exacerbate temperature stress at the foliage (Larcher, 1995). If salinity were a factor in this study, a multiplicative or additive interaction of flooding and salinity would also be justified because those effects have been shown to interact also (Allen et al., 1996). Despite poor performance and lack of physiological relevance, the single limiting factor concept does facilitate parameter interpretation. Considering that temperature varies more within years than it does among years, the better performance of G_{mult} could have been due to g_T acting as a secondary (in addition to g_E) seasonal adjustment, reweighting g_W effects, and thus not indicate anything about the nature of stressors interactions.

Inclusion of a seasonal shift term (*s1*) had little effect on model performance. It is known that the growth in one year is directly a function of photosynthesis in the previous (e.g., late-season photosynthate allocated to early root and shoot growth in the next year; (Kozlowski, 1991). In baldcypress, photosynthesis occurs later into the year than does radial growth (Conner et al., 1981; Eggler, 1955). Thus, optimized shifts showing Mar(y)-Nov(y) or Nov($y-1$)-Oct(y) growth years are a departure from known tree behavior. However, this mismatch may just reflect that late season water levels are least variable (Figure 5.5) or that they contribute a fairly small fraction to the annual growth because of low g_E. Another possible limitation to this representation is the lack of interaction between *s1* and W, (i.e., the growing season is determined by the water level; Allen et al., 2016; Keeland and Sharitz, 1995). Longer-term lagged effects were also omitted, but could be modeled by, for example, including growth-response decay rates controlled by free parameters.

The model performed substantially better when it included time-varying growth responses to water level, which may relate to model better representing tree acclimation to environmental conditions. While the best-fit window of response, *n1,* varied among plots (one to seven years), it was short relative to the 39- or 46-year periods of record. Plants show phenotypic plasticity at multiple spatial and temporal scales (De Kroon et al., 2005), but plasticity is particularly important in trees that are adapted to be long-lived, spanning highly variable conditions (Kramer, 1995; Magnani et al., 2002). Baldcypress are highly flood tolerant, partially due to responsiveness to flooding: low oxygen in the rhizosphere reduces root growth but also stimulates the development of aerenchyma, which can facilitate greater oxygen transport in wood (Megonigal and Day, 1992; Pezeshki, 1991), and adventitious roots (Megonigal and Day, 1992; Pezeshki and Anderson, 1996), which allow access to shallower water that is generally less anoxic.

The similarity in *w2* and *w3* across sites (Figures 8, 9, 10), despite varying hydrology and chronologies, indicates the functional relevance of g_W. Obviously inferences from model results have limitations, but the conceptually more appropriate process representation of VSL-Wet may be a better source of insight than less generalizable regression models. At these sites, particularly Verret, best fits showed mostly linearly increasing growth response to water levels. This was particularly true in Verret where the zone of optimality (Figure 5.9) yielded $W2_{fixed}$ thresholds that extended to the upper limit of W variability. The models perform better in the higher W variability Atch sites when g_W attained a trapezoidal shape with reduced growth at extreme high water level (Figures 9, 10). Depths at which growth was reduced were rare; e.g., at Atch sites, depth was >1.0 m above mean 8% of the time and >2.0 m above mean 1% of time. Drier

conditions were frequently limiting in all plots, with optimal *w2* exceeding the mean W(*m,y*) nearly universally (except AT in $W2_{fixed}$; Figures 9, 10). Even if assumed that flood stress is atypical, it may still seem surprising that the permanently flooded plots (AT, GC, and VU) benefit from deeper flooding. Simple regression analysis has previously showed flooded trees benefit from deeper flooding (Keim et al., 2012). One potential explanation is flooded trees develop water roots that could lose function when less flooded. Another potential explanation is that lower water levels result in more areas of exposed soils regionally (even if not at the tree), thereby increasing sensible heat fluxes—especially with dark organic soils (Oke, 1988) —and yielding greater vapor pressure deficits that can decrease canopy carbon exchange.

Studies at both coarse resolution (yearly resolution; Conner et al., 2014; Keim and Amos, 2012) and fine resolution (< weekly resolution; Duberstein et al., 2013; Keeland and Sharitz, 1997) have shown baldcypress stimulated by flooding, but water levels alone may not explain increased growth. Water levels often relate to precipitation, and thus lower vapor pressure deficits, but water level was unrelated to monthly precipitation in both Verret (R^2 = 0.08) and Atch (R^2=0.01). Atchafalaya River stage and water quality are mostly controlled by the Mississippi River (Pasco et al., 2015) and river pulses cause high water levels but also other beneficial inputs, like nutrients (Junk et al., 1989; Tockner et al., 1999). The discharge-water-quality relationship could explain why deeper flooding is beneficial in even the permanently flooded plots; dissolved oxygen in Grand Lake where the sites are located responds to river flow (Sabo et al., 1999). However, Verret is more stagnant (Keim and Amos, 2012). Thus, our results showing increasing growth with increasing water level are inconsistent with the common position that stagnant flooding results in reduced growth (Mitsch, 1988), as has been concluded in the Verret Basin (Keim and Amos, 2012; Megonigal et al., 1997).

5.6 CONCLUSIONS

Calibration and cross-site validation showed that VSL-Wet explained much of the inter-annual variation in six baldcypress chronologies from plots with different flooding depths in two hydrologically distinct wetlands in south Louisiana, USA.

The VSL-Wet model performance reflects how well the model formulations—a series of hypotheses on wetland tree growth responses—represents actual inter-annual growth variability. Model performance was better than conventional approaches and exceeded performance often reported in dendroecological studies. This overall performance suggests modeling wetland tree ring indices as the sum of monthly responses to temperature and water levels is effective. The particularly high explanatory power—in some cases, 50% of the variance in inter-annual ring width variability—was enabled by accounting for interacting temperature and water response functions and by allowing the thresholds in the water response function to vary with respect to recent water levels. The improvement incurred by including these two components may reflect the ecophysiological roles of interacting stressors and plasticity in responses to stressors.

Optimal parameters defining the growth response functions to water levels were similar among sites, despite difference in flooding characteristics. Specifically, the growth response function that best explained growth variations were defined by increasing growth up to 0.5-0.75 m above the mean water level, or up to 1 m above mean for the more deeply flooded sites. This suggests shallower water levels reduce growth, which is a rational possibility when considering that these trees are morphologically adjusted to these permanently flooded conditions. Due to the nature of VSL-Wet, the parameters may have a literal meaning; that is, they define the thresholds defining shifts in growth response to environmental conditions. Transferability of parameters

across sites may demonstrate that these growth functions have ecological meaning instead of being a product of overfitting. Optimal growth response functions to water level obtained from VSL-Wet may serve as a useful tool for inter-site comparison, which is otherwise a great challenge because of hydrological differences among sites.

5.7 REFERENCES

Allen, J.A., Pezeshki, S.R., Chambers, J.L., 1996. Interaction of flooding and salinity stress on baldcypress (Taxodium distichum). Tree Physiol. 16, 307–313.

Allen, S.T., Krauss, K.W., Cochran, J.W., King, S.L., Keim, R.F., 2016. Wetland tree transpiration modified by river-floodplain connectivity. J. Geophys. Res. Biogeosciences 2015JG003208. doi:10.1002/2015JG003208

Anderson, C.J., Mitsch, W.J., 2008. Tree basal growth response to flooding in a bottomland hardwood forest in central Ohio. J. Am. Water Resour. Assoc. 44, 1512–1520. doi:10.1111/j.1752-1688.2008.00255.x

Anderson, P.H., Pezeshki, R., 2001. Effects of flood pre-conditioning on responses of three bottomland tree species to soil waterlogging. J. Plant Physiol. 158, 227–233. doi:10.1078/0176-1617-00267

Beven, K., Freer, J., 2001. Equifinality, data assimilation, and uncertainty estimation in mechanistic modelling of complex environmental systems using the GLUE methodology. J. Hydrol. 249, 11–29. doi:10.1016/S0022-1694(01)00421-8

Bond, B.J., Meinzer, F.C., Brooks, J.R., 2008. How trees influence the hydrological cycle in forest ecosystems, in: Lecturer, P.J.W.S., Lecturer, D.M.H.S., Reader, J.P.S. (Eds.), Hydroecology and Ecohydrology. John Wiley & Sons, Ltd, pp. 7–35.

Conner, W.H., Duberstein, J.A., Jr, J.W.D., Hutchinson, S., 2014. Impacts of Changing Hydrology and Hurricanes on Forest Structure and Growth Along a Flooding/Elevation Gradient in a South Louisiana Forested Wetland from 1986 to 2009. Wetlands 34, 803–814. doi:10.1007/s13157-014-0543-0

Conner, W.H., Gosselink, J.G., Parrondo, R.T., 1981. Comparison of the vegetation of three Louisiana swamp sites with different flooding regimes. Am. J. Bot. 68, 320. doi:10.2307/2442768

Cook, E.R., 1985. A time series analysis approach to tree ring standardization (Dissertation). University of Arizona, Tucson, AZ, USA.

Day, J., Hunter, R., Keim, R.F., DeLaune, R., Shaffer, G., Evers, E., Reed, D., Brantley, C., Kemp, P., Day, J., Hunter, M., 2012. Ecological response of forested wetlands with and without Large-Scale Mississippi River input: Implications for management. Ecol. Eng. 46, 57–67. doi:10.1016/j.ecoleng.2012.04.037

De Kroon, H., Huber, H., Stuefer, J.F., Van Groenendael, J.M., 2005. A modular concept of phenotypic plasticity in plants. New Phytol. 166, 73–82. doi:10.1111/j.1469-8137.2004.01310.x

DeLaune, R. d., Patrick, W.H. jun, Pezeshki, S. r., 1987. Foreseeable Flooding and Death of Coastal Wetland Forests. Environ. Conserv. 14, 129–133. doi:10.1017/S0376892900011486

Duberstein, J.A., Krauss, K.W., Conner, W.H., Jr, W.C.B., Shelburne, V.B., 2013. Do hummocks provide a physiological advantage to even the most flood tolerant of tidal freshwater trees? Wetlands 33, 399–408. doi:10.1007/s13157-013-0397-x

Eggler, W.A., 1955. Radial growth in nine species of trees in southern Louisiana. Ecology 36, 130–136. doi:10.2307/1931438

Ford, C.R., Brooks, J.R., 2002. Detecting forest stress and decline in response to increasing river flow in southwest Florida, USA. For. Ecol. Manag. 160, 45–64. doi:10.1016/S0378-1127(01)00440-6

Fritts, H., 2001. Tree Rings and Climate, 2nd ed. Blackburn Press, Caldwell, NJ, USA.

Hughes, M.K., 2002. Dendrochronology in climatology – the state of the art. Dendrochronologia 20, 95–116. doi:10.1078/1125-7865-00011

Joyce, K., Todd, R.L., Asmussen, L.E., Leonard, R.A., 1985. Dissolved oxygen, total organic carbon and temperature relationships in southeastern U.S. coastal plain watersheds. Agric. Water Manag. 9, 313–324. doi:10.1016/0378-3774(85)90041-1

Junk, W., Bayley, P.B., Sparks, R.E., 1989. The Flood Pulse Concept in River—Floodplain Systems, in: Dodge, D.P. (Ed.), Proceedings of the International Large River Symposium. Presented at the International Large River Symposium, 106, Ontario, CA, pp. 110–127.

Keeland, B.D., Sharitz, R.R., 1997. The Effects of Water-Level Fluctuations on Weekly Tree Growth in a Southeastern USA Swamp. Am. J. Bot. 84, 131–139. doi:10.2307/2445890

Keeland, B.D., Sharitz, R.R., 1995. Seasonal growth patterns of Nyssasylvatica var biflora, Nyssaaquatica, and Taxodiumdistichum s affected by hydrologic regime. Can. J. For. Res. 25, 1084–1096. doi:10.1139/x95-120

Keim, R.F., Amos, J.B., 2012. Dendrochronological analysis of baldcypress (Taxodium distichum) responses to climate and contrasting flood regimes. Can. J. For. Res. 42, 423–436. doi:10.1139/x2012-001

Keim, R.F., Izdepski, C.W., Jr, J.W.D., 2012. Growth Responses of Baldcypress to Wastewater Nutrient Additions and Changing Hydrologic Regime. Wetlands 32, 95–103. doi:10.1007/s13157-011-0248-6

Kozlowski, T.T., 1997. Responses of woody plants to flooding and salinity. Tree Physiol. 17, 490–490. doi:10.1093/treephys/17.7.490

Kozlowski, T.T., 1991. Environmental stresses to deciduous trees, in: Mooney, H.A., Winner, W.E., Pell, E.J. (Eds.), Response of Plants to Multiple Stresses. Academic Press, San Diego, CA, pp. 391–411.

Kramer, K., 1995. Phenotypic plasticity of the phenology of seven European tree species in relation to climatic warming. Plant Cell Environ. 18, 93–104. doi:10.1111/j.1365-3040.1995.tb00356.x

Krauss, K.W., Young, P.J., Chambers, J.L., Doyle, T.W., Twilley, R.R., 2007. Sap flow characteristics of neotropical mangroves in flooded and drained soils. Tree Physiol. 27, 775–783. doi:10.1093/treephys/27.5.775

Larcher, W., 1995. Physiological plant ecology. Springer-Verlag.

Legates, D.R., McCabe, G.J., 1999. Evaluating the use of "goodness-of-fit" Measures in hydrologic and hydroclimatic model validation. Water Resour. Res. 35, 233–241. doi:10.1029/1998WR900018

MacClurkin, D.C., 1965. Diameter growth and phenology of trees on sites with high water tables. Southern Forest Experiment Station, Forest Service, U.S. Dept. of Agriculture.

Magnani, F., Grace, J., Borghetti, M., 2002. Adjustment of tree structure in response to the environment under hydraulic constraints. Funct. Ecol. 16, 385–393. doi:10.1046/j.1365-2435.2002.00630.x

McLeod, K.W., Donovan, L.A., Stumpff, N.J., Sherrod, K.C., 1986. Biomass, photosynthesis and water use efficiency of woody swamp species subjected to flooding and elevated water temperature. Tree Physiol. 2, 341–346. doi:10.1093/treephys/2.1-2-3.341

Megonigal, J.P., Conner, W.H., Kroeger, S., Sharitz, R.R., 1997. Aboveground production in southeastern floodplain forests: A test of the subsidy–stress hypothesis. Ecology 78, 370–384. doi:10.1890/0012-9658(1997)078[0370:APISFF]2.0.CO;2

Megonigal, J.P., Day, F.P., 1992. Effects of Flooding On Root and Shoot Production of Bald Cypress in Large Experimental Enclosures. Ecology 73, 1182–1193. doi:10.2307/1940668

Meko, D.M., Touchan, R., Anchukaitis, K.J., 2011. Seascorr: A MATLAB program for identifying the seasonal climate signal in an annual tree-ring time series. Comput. Geosci. 37, 1234–1241. doi:10.1016/j.cageo.2011.01.013

Mitsch, W.J., 1988. Productivity-Hydrology-Nutrient Models of Forseted Wetlands, in: Mitsch, W.J., Straškraba, M., Jorgensen, S.E. (Eds.), Wetland Modelling. Elsevier, Amsterdam, Netherlands.

Mitsch, W.J., Gosselink, J.G., 2007. Wetlands, 4th ed. John Wiley & Sons, Inc., New York, NY, USA.

Mitsch, W.J., Rust, W.G., 1984. Tree growth responses to flooding in a bottomland forest in northeastern Illinois. For. Sci. 30, 499–510.

Mitsch, W.J., Taylor, J.R., Benson, K.B., 1991. Estimating primary productivity of forested wetland communities in different hydrologic landscapes. Landsc. Ecol. 5, 75–92. doi:10.1007/BF00124662

Mooney, H.A., Winner, W.E., Pell, E.J. (Eds.), 1991. Response of Plants to Multiple Stresses. Academic Press, San Diego, CA.

Nash, L.J., Graves, W.R., 1993. Drought and flood stress effects on plant development and leaf water relations of five taxa of trees native to bottomland habitats. J. Am. Soc. Hortic. Sci. 118, 845–850.

Niinemets, Ü., 2010. Responses of forest trees to single and multiple environmental stresses from seedlings to mature plants: Past stress history, stress interactions, tolerance and acclimation. For. Ecol. Manag. 260, 1623–1639.

Nuttle, W.K., 1997. Measurement of wetland hydroperiod using harmonic analysis. Wetlands 17, 82–89. doi:10.1007/BF03160720

Odum, E.P., Finn, J.T., Franz, E.H., 1979. Perturbation theory and the subsidy-stress gradient. BioScience 29, 349–352. doi:10.2307/1307690

Oke, T.R., 1988. Boundary Layer Climates, 2 edition. ed. Routledge.

Pasco, T.E., Kaller, M.D., Harlan, R., Kelso, W.E., Rutherford, D.A., Roberts, S., 2015. Predicting Floodplain Hypoxia in the Atchafalaya River, Louisiana, USA, a Large, Regulated Southern Floodplain River System. River Res. Appl. n/a-n/a. doi:10.1002/rra.2903

Pezeshki, S.R., 2001. Wetland plant responses to soil flooding. Environ. Exp. Bot. 46, 299–312. doi:10.1016/S0098-8472(01)00107-1

Pezeshki, S.R., 1991. Root responses of flood-tolerant and flood-sensitive tree species to soil redox conditions. Trees 5, 180–186. doi:10.1007/BF00204341

Pezeshki, S.R., Anderson, P.H., 1996. Responses of three bottomland species with different flood tolerance capabilities to various flooding regimes. Wetl. Ecol. Manag. 4, 245–256. doi:10.1007/BF02150538

Pezeshki, S.R., Chambers, J.L., 1986. Variation in Flood-Induced Stomatal and Photosynthetic Responses of Three Bottomland Tree Species. For. Sci. 32, 914–923.

Rodríguez-González, P.M., Stella, J.C., Campelo, F., Ferreira, M.T., Albuquerque, A., 2010. Subsidy or stress? Tree structure and growth in wetland forests along a hydrological gradient in Southern Europe. For. Ecol. Manag. 259, 2015–2025. doi:10.1016/j.foreco.2010.02.012

Rodriguez-Iturbe, I., D'Odorico, P., Laio, F., Ridolfi, L., Tamea, S., 2007. Challenges in humid land ecohydrology: Interactions of water table and unsaturated zone with climate, soil, and vegetation. Water Resour. Res. 43, W09301. doi:10.1029/2007WR006073

Sabo, M.J., Bryan, C.F., Kelso, W.E., Rutherford, D.A., 1999. Hydrology and aquatic habitat characteristics of a riverine swamp: II. Hydrology and the occurrence of chronic hypoxia. Regul. Rivers Res. Manag. 15, 525–544. doi:10.1002/(SICI)1099-1646(199911/12)15:6<525::AID-RRR554>3.0.CO;2-Q

Speer, J.H., 2010. Fundamentals of tree-ring research. University of Arizona Press, Tucson.

Stahle, D.W., Cleaveland, M.K., Hehr, J.G., 1985. A 450-year drought reconstruction for Arkansas, United States. Nature 316, 530–532. doi:10.1038/316530a0

Teskey, R.O., Sheriff, D.W., Hollinger, D.Y., Thomas, R.B., 1995. External and internal factors regulating photosynthesis, in: Resource Physiology of Conifers: Acquisition, Allocation, and Utilization. Academic Press, San Diego, CA, pp. 105–140.

Tockner, K., Pennetzdorfer, D., Reiner, N., Schiemer, F., Ward, J.V., 1999. Hydrological connectivity, and the exchange of organic matter and nutrients in a dynamic river–floodplain system (Danube, Austria). Freshw. Biol. 41, 521–535. doi:10.1046/j.1365-2427.1999.00399.x

Tolwinski-Ward, S.E., Evans, M.N., Hughes, M.K., Anchukaitis, K.J., 2011. An efficient forward model of the climate controls on interannual variation in tree-ring width. Clim. Dyn. 36, 2419–2439. doi:10.1007/s00382-010-0945-5

Vaganov, E.A., Hughes, M.K., Shashkin, A.V., 2006a. Modeling External Influence on Xylem Development, in: Growth Dynamics of Conifer Tree Rings, Ecological Studies. Springer Berlin Heidelberg, pp. 189–243.

Vaganov, E.A., Hughes, M.K., Shashkin, A.V., 2006b. Simulation of tree-ring growth dynamics in varying and changing climates, in: Growth Dynamics of Conifer Tree Rings, Ecological Studies. Springer Berlin Heidelberg, pp. 244–280.

van der Valk, A.G., 1981. Succession in Wetlands: A Gleasonian Approach. Ecology 62, 688–696. doi:10.2307/1937737

Young, P.J., Keeland, B.D., Sharitz, R.R., 1995. Growth response of baldcypress [Taxodium distichum (L.) Rich.] to an altered hydrologic regime. Am. Midl. Nat. 133, 206–212. doi:10.2307/2426385

CHAPTER 6: LEAF AREA ALLOMETRICS AND MORPHOMETRICS IN BALDCYPRESS TREES[3]

6.1 INTRODUCTION

Leaf area index (LAI), the one-sided leaf area per ground area, and tree leaf area (LA) are primary controls over stand and tree growth. In-situ measurements of LAI of forests generally use allometric relationships between sapwood basal area (SBA) and LA scaled up to stand level LAI, or use optical sensing by, for example, canopy photo analysis or light attenuation (Weiss et al., 2004). Allometric scaling relationships require species specific calibration (Waring and Running, 2010). Optical methods also require calibration, often by comparison with LAI estimated independently by allometric relationships (Gower and Norman, 1991) to compensate for biases associated with LA clumping at the leaf, branch, and tree scales (Smith et al., 1993). Accordingly, substantial preliminary work is required to reliably measure LAI.

Techniques for LAI estimation have not previously been developed for baldcypress (*Taxodium distichum* var. *distichum*), despite its ecological importance to many wetlands of the southern and eastern United States. In general, measurements of LAI in wetlands are rare (Asner et al., 2003). Baldcypress commonly occurs in pure stands or with *Nyssa* spp. with variable stand structure, ranging from sparse stands to dense, closed-canopy stands. Flooding limits regeneration (Effler and Goyer, 2006) and contributes to low stand density, but tree growth can be high in some flooded conditions (Keeland and Young, 1997). In general, stand density may not be a good index of tree vigor or stand productivity (Long and Smith, 1990), so LAI may be more useful for evaluating stand vigor for baldcypress. Also, because leaves are the fundamental unit controlling carbon assimilation and water use, LAI is a key term for modeling forest growth, productivity, and hydrology (Waring and Running, 2010). Thus, knowledge of LAI and LAI measurement techniques for baldcypress is important.

Direct LA measurements generally use a tree-scale SBA:LA relationship developed by felling trees, weighing all foliage, and scaling mass to area accounting for variability in leaf morphometrics (i.e, specific leaf area, SLA; Stenberg et al., 1994). Quantifying leaf morphometrics is important to LAI measurement because they vary with height, light, and site quality (Poorter et al., 2009), and especially in baldcypress, for which there is substantial variation in leaf morphology (Neufeld, 1983). At the tree scale, LA and SBA are generally related because the area of conducting wood tissue required to support leaves is often nearly constant (i.e., pipe-model; Shinozaki et al., 1964), although non-linearities result from differences in xylem conductance (Pothier et al., 1989). This SBA:LA relationship can be used to estimate of LAI independent of optical analysis methods.

In this study, we made the first measurements of LA and LAI in a baldcypress forest by methods that account for varying tree and stand structure. Our objective was to develop methods for estimating baldcypress leaf area by allometric relationships with SBA and diameters and by optical methods, identifying and accounting for morphological variations at the leaf, tree, and stand scales. Specifically, we (1) measured SLA as it varied by morphology, (2) developed tree-level SBA:LA relationships for estimating LA, (3) calibrated and compared stand-level optical LAI measurements across plots with contrasting structure.

---

[3] This chapter previously appeared as Allen, S.T., Whitsell, M.L., Keim, R.F., 2015. Leaf area allometrics and morphometrics in baldcypress. Canadian Journal of Forest Research 45:963–969. doi:10.1139/cjfr-2015-0039. It is reprinted by permission of NRC Research Press.

6.2 METHODS

6.2.1 Species Description

Baldcypress is a large, long-lived deciduous conifer that is adapted to flooded or waterlogged soils of forested wetlands of the coastal plains of both the Gulf of Mexico and southeastern Atlantic, and inland within floodplains, particularly in the Mississippi Alluvial Valley. Baldcypress has an excurrent growth habit without whorled branching. The photosynthetically active unit of baldcypress is a feather-like branchlet consisting of a deciduous stem with flat, needle-like leaves spirally arranged on the stem but often displayed in a pseudo-distichous arrangement; however the morphology varies within and among individuals, and leaves can be partially or fully appressed to stems (Coulter, 1889). Branchlets are generally lateral shoots, but sometimes are the terminal, actively elongating stem (Cross, 1939); the latter tend to have smaller leaves appressed to stems, and are not always deciduous. Stomata are dominantly on the abaxial leaf surfaces (Sharma and Madsen, 1978) but amphistomatic leaves have been reported with generally fewer stomata on the adaxial surface (Qing-Wen et al., 2004).

6.2.1 Study Site

This study took place at Bluff Swamp (30.31,-91.01°), a backswamp at the margin of the Mississippi Alluvial Valley, 24 km southeast of Baton Rouge, Louisiana, USA. Mean monthly temperatures range from 10 to 27°C and mean precipitation of 160 cm is mostly evenly distributed throughout the year. Lower evapotranspiration in winter and spring results in generally higher water levels. Historically, Mississippi River floodwaters occasionally occupied the site, but levees have mostly prevented this for more than 200 years. Soils are vertic clays (mostly Schriever and Fausse series) formed from Mississippi River sediments.

Eleven study plots were established over a range of crown densities over a range in elevation of ~30 cm. The sparser plots were in deeper water, had trees with open-grown crowns, often with live branches nearly to the water level, and an understory of floating aquatic vegetation (*Salvinia* spp*., Lemna* spp*., Eichhornia crassipes*), typical of permanently flooded wetlands. The denser plots were less flooded, had trees with crowns typical of forest-grown trees, and the understory was mostly not vegetated, typical of transiently flooded wetlands. Overstory trees at all plots were predominantly baldcypress, with few individuals of *Nyssa aquatica*, *Planera aquatica*, and *Salix nigra*; baldcypress was 97% of basal area over all plots, with a plot minimum of 80%. Baldcypress trees were generally 50-85 years old as estimated from ring counts.

6.2.2 Field and Lab Measurements

For tree-level and leaf-level allometrics, nine trees were felled and dissected in July through August 2013, which is at least three months after leaf out and three months before fall senescence. Damage by pests and pathogens was not apparent. Sapwood area and diameter were measured 0.9 m above the stem buttress. Total height was measured after each tree was felled. Crowns were stratified into thirds: top, middle, and bottom sections. All branches containing foliage were clipped at < 1 cm thickness (less than 100 g) to eliminate large woody elements and create a linear relationship between branch and leaf masses. Samples were bagged, and weighed immediately in the field with a digital hanging balance. From each crown section of each tree, 10 branches and 10 branchlets were randomly selected and brought to the lab for immediate processing. Mass of the 10 branches was measured immediately, then all branchlets were removed from branches, air dried in a convection oven at least 96 hours at 50°C, and mass of dry

branchlets measured. These data were used to calculate foliar mass per fresh branch mass. The 10 branchlet samples were measured on an area meter (LI-3100; LiCOR, Lincoln, NE), then air dried and weighed. These data were used to calculate projected specific leaf area (SLA_{proj}; $cm^2\ g^{-1}$).

Morphologies of sampled branchlets were categorized into classes by degree of leaf appression for separate analysis of leaf allometrics by class. The relative abundances of each morphologic class within and among trees were recorded for the branch subsamples brought to lab. A conversion from SLA_{proj} to one sided leaf area (SLA) for each class was developed from 86 measurements of leaf cross sectional shapes, photographed at 100x magnification (MZFLIII; Leica, Wetzlar, Germany) and analyzed with ImageJ (National Institute of Health, Bethesda, MD, USA). The resulting ratio of projected to surface-area was multiplied by SLA_{proj} to yield SLA for each morphologic class.

For plot-level analyses, eleven 250 m^2 sampling plots were established. For statistical comparison between plots, we grouped the five densest plots as high density / high elevation plots (HPs) and the five lowest as low density / low elevation plots (LPs). Diameters of all trees in plots were measured 0.9 m above stem buttresses. Within each plot, sapwood depth was measured in two cores taken from three co-dominant trees (5.15 mm increment borer, Hagloff; Mora, Sweden). The sapwood-heartwood boundary was determined by color and abrupt change in light transmittance (Kaufmann and Troendle, 1981). An LAI proxy was measured ($LAI_{LAI-2000}$) for each plot using an optical canopy analyzer (LAI-2000, LI-COR Inc., Lincoln, Nebraska) with 106° view angle at five points (plot center and 5 m from center at cardinal directions). Measurements were taken under diffuse light conditions and paired with simultaneous measurements taken in an adjacent opening. Dominant tree height was measured on a 40 m grid encompassing the plots at 38 points (16 near LPs and 22 points near HPs) with a clinometer.

6.2.3 Analysis

Tree leaf area (LA) was determined for the felled trees using multi-scale allometric relationship as did Gower and Norman (1991) and Smith et al. (1993). Crown-section-specific SLA was determined by multiplying relative abundance of branchlet morphologic classes in each crown section by class-specific SLA to obtain weighted-mean SLA for each crown section. The ratio of dry foliage mass to fresh branch mass obtained from linear regression was multiplied by the total fresh branch mass to obtain total foliar mass for each crown section. Foliar mass was then multiplied by weighted-mean SLA to obtain LA for each crown section of each felled tree, then crown-section estimates were summed to estimate LA for the entire crown of felled trees.

For each tree in the 250 m^2 plots, LA was estimated from diameters, using the relationship between diameter and SBA derived from both cored and felled trees and the relationship between SBA and LA from the felled trees. For each plot, LAI was calculated (LAI_{calc}) as the sum of LA for all trees in the plot divided by plot area. We then compared LAI_{calc} to $LAI_{LAI-2000}$ as a calibration to $LAI_{LAI-2000}$.

All statistical analyses were performed in MATLAB (Mathworks Inc., Natick, MA, USA). Conversion factors for SLA_{proj} to SLA were normally distributed within each morphometric class (Shapiro Wilk test, $p > 0.05$) and were compared among classes with one-way analysis of variance tests (ANOVA) with separation of means determined using Tukey Honestly Significant Difference comparisons at $\alpha = 0.05$. Branchlet SLA, branchlet area, and the ratio of dry foliage mass to fresh branch mass were not normally distributed so non-parametric Kruskal-Wallis tests with Turkey HSD tests of rank-transformed values were used to test mean

differences. To compare branchlet morphologic categories among trees and within crowns, a foliage index was calculated as the mean class, weighted by respective abundances in each section. Individual tree variables (height, diameter, foliage index, sapwood area, and leaf area) and plot variables (number of trees, BA_{plot}, LAI_{calc}, and $LAI_{LAI\text{-}2000}$) were normally distributed (Shapiro Wilk, $p > 0.05$ for all), and analyzed using ANOVA and Tukey tests.

6.3 RESULTS

6.3.1 Branchlet-level morphology and area relations

Morphology, area, and SLA_{proj} varied among branchlets (Table 6.1). The four forms (Figure 6.1) were: broad open branchlets with flat, distichously arranged leaves (Class I); a form similar to Class I but with shorter leaves and less distichous (Class II); having short leaves, more appressed and not distichous (Class III); and almost fully scaled (Class IV). Class IV branchlets were commonly branched and Class III branchlets were occasionally branched.

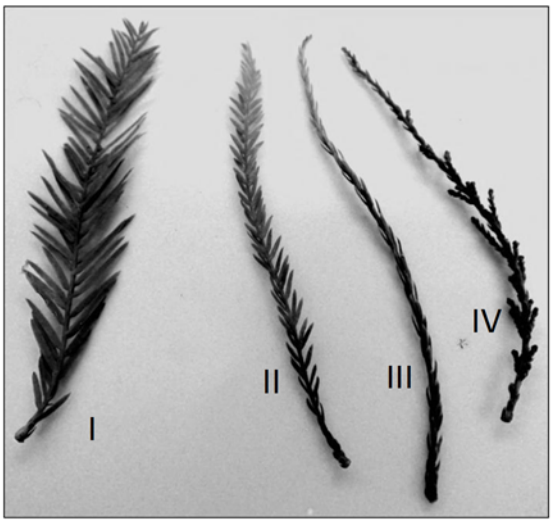

Figure 6.1 Classes of leaf morphology from non-appressed (I) to fully appressed (IV).

Leaf cross sectional shape also differed by morphology; Class I and II leaf cross-sections were pointed ellipses, while III and IV cross-sections varied and were triangular, crescent-shaped, or elliptical. The cross sectional shapes yielded different ratios of SLA_{proj} to SLA (Table 6.1); Class I branchlets were flattest and the SLA was nearly equal to SLA_{proj}, whereas the SLA of Class IV branchlets was 29% greater than SLA_{proj}.

There was a higher abundance of branchlets with more appressed leaves in the top crown section (Table 6.2). The bottom and middle crown sections of felled trees were majority Class I (92% and 66%, respectively) while the top sections were mostly Class II (42%) and III (37%). The abundance of appressed leaves increased in taller trees, both for entire crowns and considering the top crown section only (Figure 6.2).

6.3.2 Tree-level leaf area allometric scaling

There were strong allometric relationships at the branch and branchlet levels in the felled and dissected trees (Table 6.3). Relative abundance of branchlet classes and ratio of branch mass to dry foliar mass were similar among trees but not among crown sections (Table 6.3). Tree LA allometric relationships were developed by summing of branch mass in each crown section.

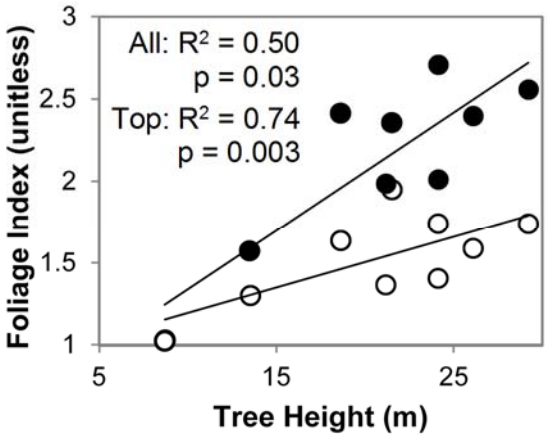

Figure 6.2 Foliage index for felled trees, calculated as the mean morphology class, weighted by relative abundance. Open circles are for tree foliage index across all sections and filled circles are for the top crown section foliage index.

Tree SBA was linearly related with LA ($R^2 = 0.85$, $p < 0.001$; Figure 6.3); a second-order, two-parameter polynomial ($R^2 = 0.93$, $p < 0.0001$) and a third order, three-parameter polynomial ($R^2 = 0.98$, $p < 0.0001$) inevitably provided better fits (Figure 6.3). The first order was applied to calculate plot LAI (section 3.3). For data pooled across all plots, a power law curve related BA_{tree} and SBA (Figure 6.4).

Table 6.1 Branchlet morphometrics for baldcypress, where branchlet morphologies are: (I) open branchlets with distichous leaves, (II) shorter leaves and less distichous, (III) more appressed and radial leaves, and (IV) almost fully appressed.

Class	n	Projected Area[1,2] (cm^2)	Projected SLA[1,2] (cm^2g^{-1})	SLA:SLA_{proj}[1,3,4]	SLA[1,2] (cm^2g^{-1})
I	116	3.7 ± 2.2a	81.5 ± 30.7a	1.07 ± 0.02a	87.3 ± 32.8a
II	41	1.2 ± 0.9b	49.1 ± 31.3b	1.12 ± 0.06a	55.0 ± 35.1b
III	23	0.8 ± 0.4b	30.0 ± 6.9 bc	1.29 ± 0.11b	38.7 ± 8.9 b
IV	10	0.7 ± 0.5b	19.1 ± 8.4 c	1.38 ± 0.12c	26.3 ± 11.5b

[1] Values are mean ± 1 SD
[2] Groupings indicates differences significant at α = 0.05 by Tukey HSD test of rank-transformed data.
[3] Groupings indicates differences significant at α = 0.05 by Tukey HSD test.
[4] Sample size differs from other columns: N = 17, 14, 40, 15 for I, II, III, and IV respectively

6.3.3 Stand structure and LAI

In contrast to SBA:LA allometrics and branchlet morphometrics, which were similar across plots, stand structure and LAI varied among plots (Table 6.4). The LPs had fewer trees (373 ± 62 ha^{-1}; mean ± SE), lower BA_{plot} (25.5 ± 6.1m^2 $ha^{-1)}$, and shorter dominant trees (18.0 ± 0.6 m) compared to the HPs (736 ± 57 ha^{-1}, 72.1 ± 4.5 m^2 $ha^{-}1$, and 25.9 ± 0.8 m; t tests, p <

0.005 for all). The LPs also had lower LAI_{calc} (3.6 ± 0.62) and $LAI_{LAI\text{-}2000}$ (2.9 ± 0.29) compared to HPs (8.4 ± 0.62 and 4.2 ± 0.13; t tests, $p < 0.005$ for both); this resulted in higher LA per basal area in LPs (0.143 ± 0.013 $m^2\ cm^{-2}$) than in HPs (0.117 ± 0.002 $m^2\ cm^{-2}$; t test, $p < 0.0001$). The LA per tree in the LPs (96.4 ± 4.9) was generally less, but not significantly (α =0.05) than in HPs (116 ± 8; t test, $p = 0.06$).

Table 6.2 Branchlet morphometric class abundance (%) for baldcypress by crown section (values are means ± 1 SD) with letters indicating mean separations of classes for each crown position by Tukey HSD test ($\alpha = 0.05$) of rank transformed data (Kruskal-Wallis tests; $p < 0.001$ for each crown section).

	Crown Position		
Branchlet Class	Bottom	Middle	Top
I	92 ± 17a	66 ± 20a	18 ± 16ab
II	6 ± 14b	27 ± 14ab	42 ± 18a
III	2 ± 4 b	6 ± 8 bc	37 ± 22a
IV	0 ± 0 b	0 ± 0 c	3 ± 3 b

Table 6.3 Allometric relationships between fresh branches (clipped to 1 cm diameter maximum) and branchlet mass from those branches for each crown section, and specific leaf area (SLA) composites derived from weighting branchlet class SLA by relative abundance of each branchlet morphology class in each crown section (values are mean ± 1 SD).

Crown Section	Branch Mass[1] (g)	Branch : Dry Branchlets[2] ($g\ g^{-1}$)	R^2, Branch v. Dry Branchlets	SLA[2] ($cm^2 g^{-1}$)
Bottom	23.3 ± 17.8	0.18 ± 0.06a	0.82	84.0 ± 6.2a
Middle	22.6 ± 16.0	0.21 ± 0.05b	0.89	74.6 ± 8.1ab
Top	20.4 ± 16.9	0.25 ± 0.04c	0.97	51.5 ± 9.0b
Mean	21.5 ± 16.8	0.22 ± 0.05	0.86	63.9 ± 9.9

[1]Branches sample sizes are N = 90, 80, 80, and 250, for bottom, top, middle and all, respectively.
[2]Groupings indicates differences significant at $\alpha = 0.05$ by Tukey HSD test of rank transformed data.

Across plots and sites, $LAI_{LAI\text{-}2000}$ was nonlinearly related to and generally lower than LAI_{calc} (Figure 6.5, Table 6.4). The ratios LAI_{calc}:$LAI_{LAI\text{-}2000}$ for HPs (2.03 ± 0.36; mean ± st. dev.) and LPs (1.25 ± 0.36) were significantly different (t test, $p < 0.01$) because of the apparently nonlinear relationship between LAI_{calc} and $LAI_{LAI\text{-}2000}$. The ratio LAI_{calc}:$LAI_{LAI\text{-}2000}$ was positively related to BA_{plot} ($R^2 = 0.86$).

6.4 DISCUSSION

6.4.1 Branchlet morphometric variation

Branchlet and leaf morphology of baldcypress vary within the canopy in ways similar to other *Taxodium* taxa and other genera of *Cupressaceae*. Appressed branchlets of baldcypress are

similar to those of pondcypress (*T. distichum* var. *imbricarium*), which are typically more appressed (Neufeld, 1983), less pseudo-distichous, and more vertically oriented (Neufeld, 1986) than baldcypress. The SLA of baldcypress branchlets with appressed leaves is similar to other species in *Cupressaceae* with scale leaves such as *Juniperus ashei* (Hicks and Dugas, 1998), *J. monosperma* (Reich et al., 1998), *J. virginiana*, and *J. scopulorum* (Cregg 1992), but higher than *Sequioa sempervirens* stems with appressed leaves (Koch et al., 2004). The SLA of baldcypress branchlets with open leaves is lower than that of *Metasequoia glyptostroboides* (Zhang et al., 2011), regardless of canopy position (Jagels and Day, 2004). In general, SLA in baldcypress is similar to other tree species in its native biome across all families (Reich et al., 1998). Compared to 597 species reviewed by (Niinemets, 1999), baldcypress Class IV branchlets (most appressed) are near the minimum SLA_{proj} (7% higher) and Class I (least appressed) SLA_{proj} is close to the mean across all species.

Table 6.4 Plot level stand metrics and comparison of leaf area estimated using allometry from sapwood basal area (LAI_{calc}) and a LI-COR canopy analyzer ($LAI_{LAI-2000}$) with five denser plots compared to six less dense plots; for all variables, means for high elevation plots are significantly different from low elevation plots (two-sample t tests; $p < 0.01$).

Elevation & Crown Density	Plot	Number of Trees (ha^{-1})	BA_{plot} (m^2/ha)	LAI_{calc} (unitless)	$LAI_{LAI-2000}$ (unitless)	LAI:BA (m^2/cm^2)	LAI_{calc}:$LAI_{LAI-2000}$ (unitless)
High	1	800	83.0	9.5	4.0	0.11	2.4
High	2	720	56.5	6.9	4.6	0.12	1.5
High	3	840	89.2	10.2	4.4	0.11	2.3
High	4	800	66.3	8.2	3.8	0.12	2.1
High	5	520	65.4	7.4	4.1	0.11	1.8
High	Mean	736	72.1	8.4	4.2	0.12	2.0
Low	1	360	29.2	4.1	2.5	0.14	1.7
Low	2	440	30.3	4.3	2.9	0.14	1.5
Low	3	240	12.2	1.8	2.2	0.15	0.8
Low	4	240	16.7	2.4	2.2	0.14	1.1
Low	5	320	21.8	3.1	3.6	0.14	0.9
Low	6	640	42.8	6.0	3.8	0.14	1.6
Low	Mean	373	25.5	3.6	2.9	0.14	1.3

Leaf variation with height is common across many species and many biomes, and higher leaves are generally thicker with less area (Poorter et al., 2009). While some leaf morphological variations are apparently most affected by light (e.g., Coble and Cavaleri, 2014), recent work suggests morphology better corresponds with hydraulic gradients that reduce foliar expansion at the top of crowns, affecting SLA (Koch et al., 2004) and other anatomical characteristics (Carins Murphy et al., 2012). We observed branchlet classes with lower SLA were more common in the

upper crown (Table 6.2), and that taller trees generally had greater abundance of branchlets with Class II, III and IV (more appressed) morphology, particularly in the top section (Figure 6.2).

While our data alone are not sufficient to differentiate between hydraulic and light controls over morphology, related work suggests hydraulic effects are more likely than light effects. For example, Neufeld (1983) found that baldcypress branchlet morphology did not vary with light environment in saplings. Also, leaves of the closely related *Metasequoia glyptostroboides* also vary by canopy position (Jagels and Day, 2004), and the same variation also exists in response to water stress in seedlings (Zhang et al., 2011). Leaves of trees growing in more stressful sites generally have lower SLA; both drought (Eamus, 2003) and waterlogging (Poorter et al., 2009) reduce SLA, consistent with hydraulic effects. Stiller (2009) found that baldcypress growing with drought and salinity stress both had reduced SLA and stem conductance.

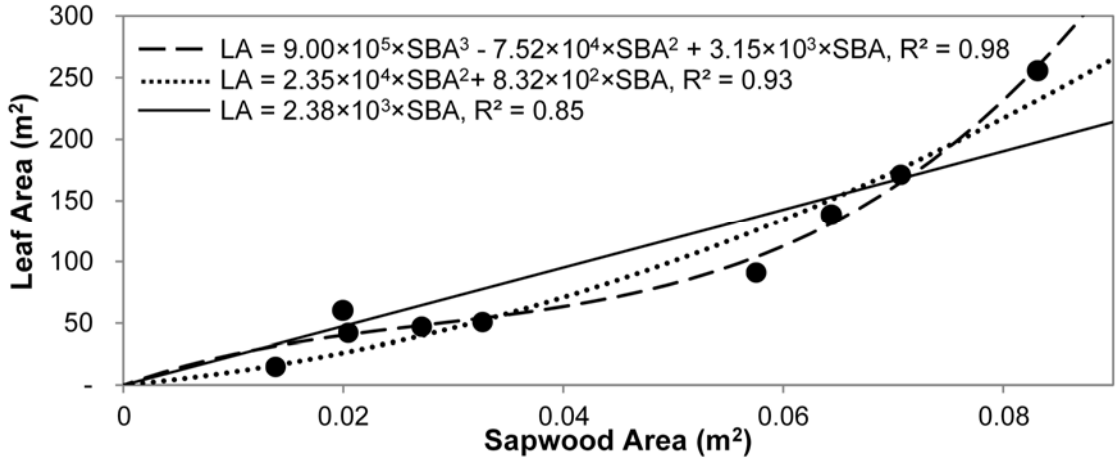

Figure 6.3 Relationship between sapwood basal area (SBA) and leaf area (LA) of felled trees.

Productivity and species composition of forested wetlands are affected by temporally and spatially varying water levels and other stressors (e.g., Megonigal et al., 1997); other aspects of baldcypress morphology are also well documented to respond to stressors and their temporal variability. Both buttressing (Varnell, 1998) and development of knees (Kernell and Levy, 1990) respond to variability in flooding, but integrate over longer periods of time than is likely for leaf morphology. Given the branchlet morphologic variability we observed, and the general relationship between leaf morphology and site conditions observed by others, research into the utility of baldcypress branchlet morphology as an indicator of site stress may be worthwhile.

6.4.2 Allometric Estimates of tree leaf area

The SBA:LA relationship may be the best method for estimating LAI in the field because clumping of leaves, branches, or stems causes problems for optical methods (Smith et al., 1993). The benefit of the allometric method is that it can be applied using only diameter measurements and the BA:SBA relationship. This is a simple, non-destructive method for measuring leaf area that requires no specialized instrumentation.

While the pipe model theory (Shinozaki et al., 1964) and some empirical evidence (e.g., Waring et al., 1977) suggest the relationship between LA and SBA is linear, most field data indicate the relationship is generally nonlinear, affected by stand structure (Long and Smith 1988), crown length (Dean and Long, 1986), canopy position (Shelburne et al., 1993), and variations in sapwood permeability (Pothier et al., 1989). Generally, LA:SBA increases with tree

SBA (Long and Smith, 1988) because larger trees have greater sapwood permeability (Pothier et al., 1989); this coheres with our observed fit line.

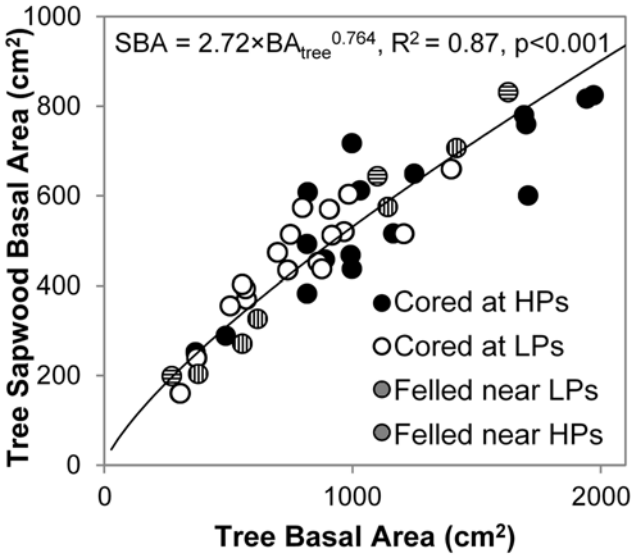

Figure 6.4 Tree basal area versus sapwood basal area from cored trees and felled trees.

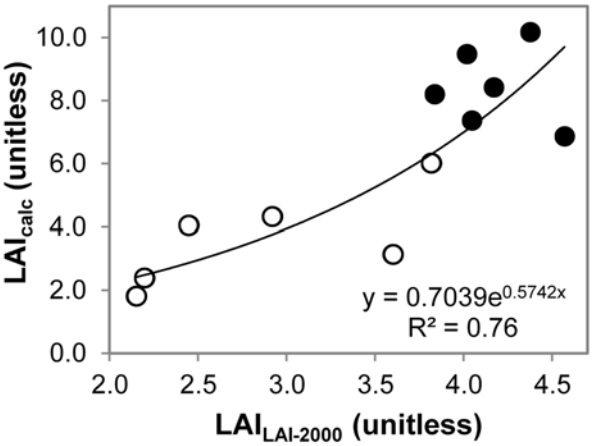

Figure 6.5 Leaf area index (LAI) estimated by LI-COR 2000 canopy analyzer ($LAI_{LAI-2000}$) compared to LAI calculated by allometric relations with sapwood area (LAI_{calc}). Open circles are lower elevation / lower density plots and filled are higher elevation / higher density plots.

The observed strength of relationship between SBA and LA (and sample size) were within the range of SBA:LA regression coefficients reported by others. Examples show LA predicted from SBA or diameter for: five tropical species was linear with R^2 ranging from 0.41 to 0.97, N = 11-14 (Calvo-Alvarado et al., 2008); six tropical species were related by 2nd order polynomial, power law, and logarithmic functions with R^2 ranging from 0.9 to 0.99, N = 4 (Arias et al., 2007) ;for four continental montane species was linear with R^2 ranging from 0.93 to 0.99, N = 8-11 (Kaufmann and Troendle, 1981); four maritime humid species in Oregon, USA, was linear or log-log with R^2 ranging from 0.8 to 0.99, N = 12-19 (Waring et al., 1977); lodgepole

pine in Wyoming, USA with varying density was linear with R^2 from 0.63 to 0.95 and N = 80 over six sites (Pearson et al., 1984).

Within a species, the SBA:LA relationship can vary with site quality and stand density, so this ratio is an index of growth potential (Long and Smith, 1988). Trees in water limited environments generally have higher SBA:LA to avoid low xylem water potential (Martínez-Vilalta et al., 2009). Similarly, baldcypress seedling exposed to salinity or drought have higher wood density and lower conductance (Stiller, 2009). Accordingly, we expect that conditions, and the resulting water limitations caused by waterlogging effects (Kozlowski, 1997), likely cause variations in SBA:LA across sites.

6.4.3 LAI and optical calibration and their respective implications

Across all plots, LAI_{calc}:$LAI_{LAI\text{-}2000}$ was 1.7 ± 0.6 (mean ± SD), which is similar to values observed for other conifers: 1.35-2.02 in Douglas-fir (Barclay and Trofymow, 2000); 2.63 in Douglas-fir (Smith et al., 1993); 1.75 in Scots pine (Stenberg et al. 1994); and 1.54-1.67 in red pine, European larch, Norway spruce, and white pine (Gower and Norman, 1991). Conifers have higher correction factors in general (e.g., Gower and Norman 1991) due to non-flat leaves (Chen and Black, 1992) and greater clumping at multiple scales, further necessitating calibrating canopy analyzer outputs (Weiss et al., 2004).

The non-linearity of the relationship between LAI_{calc} and $LAI_{LAI\text{-}2000}$ is likely related to differences in distribution of foliage. Open canopy structure and tree clumping is common in baldcypress because flooding can restrict regeneration of species to microtopographic highs (Jones et al., 1994). Clumping is a multi-scale structural component of forests that conflicts with the assumption of randomly distributed foliage associated with optical techniques (Weiss et al., 2004); higher overlap among canopy elements and lower proportional area of woody elements results in higher ratio of LAI_{calc}:$LAI_{LAI\text{-}2000}$ for denser stands (Smolander and Stenberg, 1996). Thus, tree overlap may explain why plots with higher $LAI_{LAI\text{-}2000}$ have a relatively higher conversion factor (Table 6.4). While others have successfully estimated this clumping factor through measuring branch, leaf, or even stand architectural traits (Gower and Norman, 1991), this approach would not account for the present non-uniform pattern of stems from baldcypress tending to establish on microtopographic highs. Thus empirical factors of conversion from $LAI_{LAI\text{-}2000}$ to LAI_{calc} are more appropriate (Smith et al., 1993). Because the generality of the relationship depends on tree clumping and stand openness, variation in stand structure caused by flooding inherently adds uncertainty to LAI estimation.

6.4.4 Implications for baldcypress ecology

Stand-level measurements of baldcypress leaf area have not been previously reported. At this site, observed LAI at HPs (mean = 8.4) exceeded all natural biome means (e.g., temperature broadleaf forest, shrubland, etc.), and is only exceeded by forest plantation means (compared to the >1000 studies reviewed by Asner et al., 2003). Mean LAI at the HPs equals the highest of six previously reported for wetland ecosystems (Asner et al. 2003). High LAI suggests high site quality leading to high productivity (Waring and Running, 2010). Baldcypress-tupelo above ground net primary productivity has been estimated to be as high as 1166 g m^{-2} yr^{-1} (Conner et al., 1981); these values are comparable to biome means for subtropical/warm temperature coniferous forests (Gower et al., 1995).

Although LAI is generally a good indicator of stand vigor and productivity (Waring and Running, 2010), stand vigor or health is a difficult concept for baldcypress because flooding may

affect forest structure without reducing tree growth. While stand openness may indicate tree stress in baldcypress, studies have sometimes observed greater tree growth rates in more flooded conditions, especially when flood induced mortality of less tolerant species reduces competition (Keeland and Young, 1997). Accordingly, baldcypress LAI and LA together may provide diagnostic utility for comparing trees or stands among sites.

Unlike most open forests where competition for limited water drives spacing between plants (Phillips and MacMahon, 1981), forested wetlands are different because water is not limited but may still be limiting because of flood stress, particularly with respect to regeneration (Jones et al., 1994). It is unclear whether the lower LAI in the LPs reflects lower maximum LAI as a result of hydrologic limitations on stem density via seedling exclusion, or whether it reflects a delay in attainment of maximum LAI. At the time of measurements, the leaf area was differently allocated over available stems between LPs and HPs in that LAI:BA was higher in the LPs (Table 6.4). Keim et al. (2013a) found that baldcypress-tupelo stands in wetter, lower elevation sites generally develop more slowly but that tree competition is not fundamentally changed by flooding. Considering the size and longevity of baldcypress, it is possible that the sparser sites will approach a comparable LAI to the denser plots, following typical forest development of long-term approach to a dynamic (theoretical) maximum LAI (McDowell et al., 2007). However, with lower stem density and larger trees, canopy architecture is likely less efficient (Long and Smith, 1990) and such limitations may prevent lower elevation stands from ever reaching the same maximum as observed in the HPs.

6.5. CONCLUSIONS

Branchlet morphology and morphometrics vary substantially among trees and leaves are generally more appressed to branchlets in the upper portions of crowns. There is a strong relationship between leaf area and sapwood area in baldcypress that allows sapwood area to serve as a non-destructive proxy for tree leaf area that can be scaled up to stand LAI. Plot-level LAI estimated from these allometrics differed from LAI estimated by light attenuation by a factor ranging of 0.8 to 2.4, from low to high density. These initial insights into baldcypress leaf area show LAI is high compared to the global range of LAI. Stem density, decreased by deeper flooding, apparently either decreases maximum LAI or delays attainment of LAI observed in higher elevation stands

6.6 REFERENCES

Arias, D., Calvo-Alvarado, J., Dohrenbusch, A., 2007. Calibration of LAI-2000 to estimate leaf area index (LAI) and assessment of its relationship with stand productivity in six native and introduced tree species in Costa Rica. For. Ecol. Manag. 247, 185-193. doi: 10.1016/j.foreco.2007.04.039.

Asner, G.P., Scurlock, J.M.O., Hicke, J., 2003. Global synthesis of leaf area index observations: implications for ecological and remote sensing studies. Glob. Ecol. Biogeogr. 12, 191–205. doi: 10.1046/j.1466-822X.2003.00026.x.

Barclay, H.J., Trofymow, J.A., 2000. Relationship of readings from the LI-COR canopy analyzer to total one-sided leaf area index and stand structure in immature Douglas-fir. For. Ecol. Manag. 132, 121–126. doi: 10.1016/S0378-1127(99)00222-4.

Calvo-Alvarado, J.C., McDowell, N.G., Waring, R.H., 2008. Allometric relationships predicting foliar biomass and leaf area:sapwood area ratio from tree height in five Costa Rican rain forest species. Tree Physiol. 28, 1601–1608. doi: 10.1093/treephys/28.11.1601.

Carins Murphy, M.R., Jordan, G.J., Brodribb, T.J., 2012. Differential leaf expansion can enable hydraulic acclimation to sun and shade. Plant Cell Environ. 35, 1407–1418. doi: 10.1111/j.1365-3040.2012.02498.x.

Chen, J.M., Black, T.A., 1992. Defining leaf area index for non-flat leaves. Plant Cell Environ. 15, 421–429. doi: 10.1111/j.1365-3040.1992.tb00992.x.

Coble, A.P., Cavaleri, M.A., 2014. Light drives vertical gradients of leaf morphology in a sugar maple (Acer saccharum) forest. Tree Physiol. 34, 146–158. doi: 10.1093/treephys/tpt126.

Conner, W.H., Gosselink, J.G., Parrondo, R.T., 1981. Comparison of the vegetation of three Louisiana swamp sites with different flooding regimes. Am. J. Bot. 68, 320. doi: 10.2307/2442768.

Coulter, S., 1889. Histology of the leaf of Taxodium. Bot. Gaz. 14, 76–81.

Cregg, B.M., 1992. Leaf area estimation of mature foliage of Juniperus. For. Sci. 38, 61–67.

Cross, G.L., 1939. A note on the morphology of the deciduous shoot of Taxodium distichum. Bull. Torrey Bot. Club 66, 167–172. doi: 10.2307/2481227.

Dean, T.J., Long, J.N., 1986. Variation in sapwood area-leaf area relations within two stands of lodgepole pine. For. Sci. 32, 749–758.

Eamus, D., 2003. How does ecosystem water balance affect net primary productivity of woody ecosystems? Funct. Plant Biol. 30, 187–205.

Effler, R.S., Goyer, R.A., 2006. Baldcypress and water tupelo sapling response to multiple stress agents and reforestation implications for Louisiana swamps. For. Ecol. Manag. 226, 330–340. doi: 10.1016/j.foreco.2006.02.011.

Gower, S.T., Isebrands, J.G., Sheriff, D.W., 1995. Carbon allocation and accumulation in conifers. In Resource Physiology of Conifers: Acquisition, Allocation, and Utilization. Academic Press, San Diego, CA. pp. 217 – 254.

Gower, S.T., Norman, J.M., 1991, Rapid estimation of leaf area index in conifer and broad-Leaf plantations. Ecology 72, 1896–1900. doi: 10.2307/1940988.

Hicks, R.A., Dugas, W.A., 1998. Estimating ashe juniper leaf area from tree and stem characteristics. J. Range Manag. Arch. 51, 633–637.

Jagels, R., Day, M.E., 2004. The adaptive physiology of Metasequoia to Eocene high-latitude environments. The Evolution of Plant Physiology. Academic Press, London, UK. pp. 401–421.

Jones, R.H., Sharitz, R.R., Dixon, P.M., Segal, D.S., Schneider, R.L., 1994. Woody plant regeneration in four floodplain forests. Ecol. Monogr. 64, 345–367. doi: 10.2307/2937166.

Kaufmann, M.R., Troendle, C.A., 1981. The relationship of leaf area and foliage biomass to sapwood conducting area in four subalpine forest tree species. For. Sci. 27, 477–482.

Keeland, B.D., Young, P.J., 1997. Long-term growth trends of baldcypress (Taxodium distichum (L.) rich.) at Caddo Lake, Texas. Wetlands 17, 559–566.

Keim, R.F., and Amos, J.B, 2012. Dendrochronological analysis of baldcypress (Taxodium distichum) responses to climate and contrasting flood regimes. Can. J. For. Res. 42, 423–436. doi: 10.1139/x2012-001.

Keim, R.F., Dean, T.J., Chambers, J.L., 2013a. Flooding effects on stand development in cypress-tupelo. Proceedings of the 15th biennial southern silvicultural research conference. Asheville, NC: U.S. Department of Agriculture, Forest Service, Southern Research Station. pp. 431–437.

Keim, R.F., Zoller, J.A., Braud, D.H., Edwards, B.L., 2013b. Classification of forested wetland degradation using ordination of multitemporal reflectance. Wetlands, 1–13. doi: 10.1007/s13157-013-0466-1.

Kernell, J.L., Levy, G.F., 1990. The relationship of bald cypress (Taxodium distichum (L.) Richard) knee height to water depth. Castanea 55,217-222.

Koch, G.W., Sillett, S.C., Jennings, G.M., and Davis, S.D, 2004. The limits to tree height. Nature 428: 851–854. doi: 10.1038/nature02417.

Kozlowski, T.T., 1997. Responses of woody plants to flooding and salinity. Tree Physiol. 17, 490–490. doi: 10.1093/treephys/17.7.490.

Long, J.N., Smith., F.W, 1988. Leaf area - sapwood area relations of lodgepole pine as influenced by stand density and site index. Can. J. For. Res. 18, 247–250. doi: 10.1139/x88-036.

Long, J.N., Smith., F.W, 1990. Determinants of stemwood production in Pinus contorta var. Latifolia Forests: The influence of site quality and stand Structure. J. Appl. Ecol. 27, 847–856. doi: 10.2307/2404381.

Martínez-Vilalta, J., Cochard, H., Mencuccini, M., Sterck, F., Herrero, A., Korhonen, J.F.J., Llorens, P., Nikinmaa, E., Nolè, A., Poyatos, R., Ripullone, F., Sass-Klaassen, U., and Zweifel, R, 2009. Hydraulic adjustment of Scots pine across Europe. New Phytol. 184, 353–364. doi: 10.1111/j.1469-8137.2009.02954.x.

McDowell, N.G., Adams, H.D., Bailey, J.D., Kolb, T.E., 2007. The role of stand density on growth efficiency, leaf area index, and resin flow in southwestern ponderosa pine forests. Can. J. For. Res. 37, 343–355. doi: 10.1139/X06-233.

Megonigal, J.P., Conner, W.H., Kroeger, S., Sharitz, R.R., 1997. Aboveground production in southeastern floodplain forests: A test of the subsidy-stress hypothesis. Ecology 78, 370-384. doi: 10.2307/2266014.

Neufeld, H.S., 1983. Effects of light on growth, morphology, and photosynthesis in baldcypress (Taxodium distichum (L.) Rich.) and pondcypress (T. ascendens Brongn.) seedlings. Bull. Torrey Bot. Club 110, 43–54. doi: 10.2307/2996516.

Neufeld, H.S., 1986. Ecophysiological implications of tree architecture for two cypress taxa, Taxodium distichum (L.) Rich. and T. ascendens Brongn. Bull. Torrey Bot. Club 113, 118–124. doi: 10.2307/2995934.

Niinemets, Ü., 1999. Research review: Components of leaf dry mass per area – thickness and density – alter leaf photosynthetic capacity in reverse directions in woody plants. New Phytol. 144, 35–47. doi: 10.1046/j.1469-8137.1999.00466.x.

Pearson, J.A., Fahey, T.J., and Knight, D.H., 1984. Biomass and leaf area in contrasting lodgepole pine forests. Can. J. For. Res. 14, 259–265. doi: 10.1139/x84-050.

Phillips, D.L., and MacMahon, J.A., 1981. Competition and spacing patterns in desert shrubs. J. Ecol. 69, 97–115. doi: 10.2307/2259818.

Poorter, H., Niinemets, Ü., Poorter, L., Wright, I.J., Villar, R., 2009. Causes and consequences of variation in leaf mass per area (LMA): a meta-analysis. New Phytol. 182, 565–588. doi: 10.1111/j.1469-8137.2009.02830.x.

Pothier, D., Margolis, H.A., Waring, R.H., 1989. Patterns of change of saturated sapwood permeability and sapwood conductance with stand development. Can. J. For. Res. 19, 432–439. doi: 10.1139/x89-068.

Qing-Wen, M., Fenglan, L., Chengsen, L., 2004. Leaf epidermal structure and stomatal parameters of the genus Taxodium (Taxodiaceae). Acta Phytotaxon. Sin. 43, 517–525.

Reich, P.B., Walters, M.B., Ellsworth, D.S., Vose, J.M., Volin, J.C., Gresham, C., Bowman, W.D., 1998. Relationships of leaf dark respiration to leaf nitrogen, specific leaf area and leaf life-span: a test across biomes and functional groups. Oecologia 114, 471–482. doi: 10.1007/s004420050471.

Shelburne, V.B., Hedden, R.L., Allen, R.M., 1993. The effect of site, stand density, and sapwood permeability on the relationship between leaf area and sapwood area in loblolly pine (Pinus taeda L.). For. Ecol. Manag. 58, 193–209. doi: 10.1016/0378-1127(93)90145-D.

Shinozaki, K., Yoda, K., Hozumi, K., Kira, T., 1964. A quantitative analysis of plant form: the pipe model theory,1 Basic analyses. Jpn. J. Ecol. 14, 97–105.

Smith, N.J., Chen, J.M., Black, T.A., 1993. Effects of clumping on estimates of stand leaf area index using the LI-COR LAI-2000. Can. J. For. Res. 23, 1940–1943. doi: 10.1139/x93-244.

Smolander, H., Stenberg, P., 1996. Response of LAI-2000 estimates to changes in plant surface area index in a Scots pine stand. Tree Physiol. 16, 345–349. doi: 10.1093/treephys/16.3.345.

Stenberg, P., Linder, S., Smolander, H., Flower-Ellis, J., 1994. Performance of the LAI-2000 plant canopy analyzer in estimating leaf area index of some Scots pine stands. Tree Physiol. 14, 981–995. doi: 10.1093/treephys/14.7-8-9.981.

Stiller, V., 2009. Soil salinity and drought alter wood density and vulnerability to xylem cavitation of baldcypress (*Taxodium disticum* (L.) Rich.) seedlings. Environ. Exp. Bot. 67, 164-171. Doi: 10.1016/j.envexpbot.2009.03.12.

Varnell, L.M., 1998. The relationship between inundation history and baldcypress stem form in a Virginia floodplain swamp. Wetlands 18,176-183.

Waring, R.H., Gholz, H.L., Grier, C.C., Plummer, M.L., 1977. Evaluating stem conducting tissue as an estimator of leaf area in four woody angiosperms. Can. J. Bot. 55, 1474–1477. doi: 10.1139/b77-173.

Waring, R.H., Running, S.W., 2010. Forest Ecosystems: Analysis at Multiple Scales. Elsevier, Burlington, MA.

Weiss, M., Baret, F., Smith, G.J., Jonckheere, I., Coppin, P., 2004. Review of methods for in situ leaf area index (LAI) determination: Part II. Estimation of LAI, errors and sampling. Agric. For. Meteorol. 121, 37–53. doi: 10.1016/j.agrformet.2003.08.001.

Zhang, Y., Equiza, M.A., Zheng, Q., Tyree, M.T., 2011. The impact of long-term water stress on relative growth rate and morphology of needles and shoots of Metasequoia glyptostroboides seedlings: research toward identifying mechanistic models. Physiol. Plant. 143, 10–20. doi: 10.1111/j.1399-3054.2011.01482.x.

CHAPTER 7: PARTITIONING TREE GROWTH FROM STAND DISTURBANCE IN THE WETLAND SUBSIDY-STRESS CONCEPT: A CASE STUDY IN FLOODED BALDCYPRESS WETLANDS

7.1. INTRODUCTION

Wetlands have frequent disturbance and many interacting stressors, yet are well known to have high primary production (Mitsch and Gosselink, 2007). It has been argued that flooding can represent a "subsidy" to growth with intermediate flooding or a "stress" with severe flooding (Odum et al., 1979). This concept was been developed and propagated under the premise that stress can be considered at the ecosystem level (Megonigal et al., 1997; Odum et al., 1979), a concepted that has long been debated (Jax, 2006; Odum, 1969; Pickett et al., 1989). Regardless, many subsequent studies in forested wetlands have followed this convention of using ecosystem measurements to assess flood effects on stress in wetland forests (e.g., Anderson and Mitsch, 2008; Clawson et al., 2001; Effler et al., 2007; Megonigal et al., 1997; Middleton and McKee, 2004). However, these studies must be interpreted with recognition that individual-level effects cannot be inferred from ecosystem-level effects (i.e., ecological fallacy; Robinson, 1950; Thorndike, 1939) and thus so-called ecosystem stress may be entirely unrelated to the common concept of physiological stress that is experienced by individuals (e.g., Kozlowski, 1991; Lambers et al., 2006; Larcher, 1995).

The potential for fallacy in inferring tree stress from stand production is evident in an example where severe stress was concluded from low production by Megonigal et al. (1997); baldcypress tree stress was implied as the cause of reduced production by suggesting lower production was due to by tree-level responses. However, at that site, originally Conner et al. (1993) noted that some species showed signs of stress, but that baldcypress was particularly productive there. A third study at the same sites (Conner et al., 2014) showed that increased flooding resulted in mortality but also increases in production of the baldcypress increased over the past two decades with greater production per tree. These baldcypress trees should not be considered stress, even if the stand was referred to as stressed.

More knowledge is needed regarding the ecological and ecophysiological consequences of flooding. It is well known that flooding limits regeneration (Chambers et al., 2005; Conner et al., 1986; Effler et al., 2007; Keeland and Conner, 1999; Middleton, 2008; Souther and Shaffer, 2000) and can cause mortality of less flood-tolerant tree species (Broadfoot and Williston, 1973; Conner et al., 2014; Keeland and Young, 1997). Deep or sustained flooding is often associated with relatively sparse, open-canopy forests (Brown, 1981; Faulkner et al., 2007; Krauss et al., 2009) at the wetter end of the spectrum, such as in baldcypress (*Taxodium distichum* var. *distichum*) swamps. Accordingly, the open stand structure in swamps may be best described as a function of disturbance (*sensu* Grime, 1977), although it is likely trees (mature or seedlings) that died were stressed prior to mortality; in fact Kolasa and Pickett (1992) suggested that Odum et al. (1979) and others' conceptions of ecosystem stress are often indistinguishable from disturbance. Physiological stress from flooding has been documented mostly in controlled experiments of seedlings (Allen et al., 1996; Anderson and Pezeshki, 2001; McLeod et al., 1986; Nash and Graves, 1993; Pezeshki and Chambers, 1986), but flood stress responses have not always been apparent with in-situ physiological measurements (Allen et al., 2016; Duberstein et al., 2013). While it is clear that severe flooding, particularly when stagnant (Brown, 1981; Conner et al., 1981; Megonigal et al., 1997), reduces production, we need to distinguish whether

reduced production is a consequence of tree-level reduced production, or a consequence of low-density arising from prior disturbance.

Due to the basic ecological principle that higher density, and thus higher competition, reduces the resources available to individuals (Gause, 1934), we may expect disturbance and tree growth to be opposite. In fact, it is a fundamental silvical principle that reductions in stand density may reduce total production but increase growth and vigor of individuals (Long, 1985), and this seems to hold true in forested wetlands. For example, as reported by Eggler and Moore (Eggler and Moore, 1961), impoundment (i.e., increased stagnant flooding) resulted in mortality for most trees but greater growth for those remaining. Similarly, others have measured higher tree growth, especially for baldcypress, in more heavily flooded sites (Brown and Peterson, 1983; Conner et al., 1981; Visser and Sasser, 1995) or during more flooded periods (Ford and Brooks, 2002; Keim and Amos, 2012; Mitsch and Rust, 1984). There are also examples of reduced tree growth despite disturbance, particularly after large changes to a system such that trees appear poorly adjusted to new physical conditions (Day et al., 2012; Harms et al., 1980; Keim et al., 2012; Young et al., 1995). In cases where individual tree growth increases following disturbance, it is likely a function of reduced competition (likely for light) associated with disturbance. If stress from flooding is exceeded by the benefits of reduced competition, and there is a resulting net benefit from the total environment, it should not be said these trees are more stressed.

This study examines relationship between growth and stand structure as affected by flooding in baldcypress dominated wetlands. To compare tree growth with accounting for size biases, we quantify growth per leaf area, also called growth efficiency (GE_{tree}; Waring et al., 1980). Leaf area is an important correlate with growth (Long et al., 2004)—although minimally examined in wetlands (Asner et al., 2003)—because it largely determines the light interception capability. Thus, GE_{tree} is a measure of the degree to which that capability is realized as growth of the tree stem, and serves as a useful concept examining controls over and trajectory of growth (e.g., Binkley et al., 2002; Kaufmann, 1996; Long and Smith, 1990; McDowell et al., 2011; Roberts and Long, 1992; Vose and Allen, 1988). Specifically, we determine whether conditions for tree growth are more favorable in trees of open stands created by flood disturbance, or in trees of less flooded, closed stands. We hypothesize that GE_{tree} is greater in more flooded sites because stand sparseness reduces competition, as seen in uplands (Brix, 1983; Waring et al., 1981), and the benefits of reduced competition outweigh the detrimental impact of flood stresses on trees.

7.2. METHODS

7.2.1 Sites

Data were collected in two forested wetlands in southern Louisiana. For this region, mean monthly temperatures ranged from 10 to 27°C, with mean annual precipitation of 160 cm evenly distributed throughout the year (National Climatic Data Center, Asheville, NC). Within each wetland, we sampled from sites of varying canopy density corresponding with different hydrology. All sites were majority baldcypress and canopy dominant or codominant trees were almost exclusively baldcypress.

Bluff Swamp is a backswamp in the Mississippi Alluvial Valley 24 km southeast of Baton Rouge, Louisiana, USA. Soils are clays (mapped as Fausse series; NRCS, 2016) formed from Mississippi River sediments. Levees have prevented any Mississippi River floodwater influence for more than 200 years, making the site water levels primarily influenced by rainfall

with minor influence of a small tributary stream from the adjacent upland. Two sites that differed in elevation by about 30 cm were selected such that one was shallowly and transiently flooded with rain events ($Bluff_{shallow}$; 30° 16' 56" N, 90° 59' 54" W) and one was semi-permanently and more deeply flooded ($Bluff_{deep}$; 30° 18' 44" N, 91° 00' 43" W). $Bluff_{deep}$ had sparser forest with crowns typical of open-grown trees, often with live branches nearly at the water level. The $Bluff_{deep}$ understory was floating aquatic vegetation (*Salvinia* spp*., Lemna* spp*., Eichhornia crassipes*) or was unvegetated in the infrequent locations and times when ground was above water, typical of semi-permanently flooded wetlands in this area. $Bluff_{shallow}$ had mostly unvegetated understory, but crowns were typical of forest-grown trees. At $Bluff_{deep}$, there were extensive and abundant canopy gaps, but regeneration was restricted to hummocks of decomposing old-growth baldcypress logs and stumps. At $Bluff_{shallow}$, there were few gaps, and there was regeneration in those gaps. Tree rings indicated that both stands were established in the early 1900s, although with some much older trees and distinct younger cohorts too.

Bayou Pigeon is an area over 30 km^2 of nearly continuous, seasonally flooded baldcypress-tupelo and bottomland hardwood backswamp within the Atchafalaya Basin in southern Louisiana, one of the largest wetlands in the contiguous U.S (5700 km^2). Water levels are highly variable because of fluctuations of the Atchafalaya River, varying several meters annually and typically peaking in the spring. Because it is a backswamp, the site fills by overbank or backwater flooding, and then drains slowly. When not flooded, these Fausse (NRCS, 2016) clay soils typically remain moist due to a high water table but can become dry and cracked. Three sites were established along an elevation gradient. The highest elevation, and thus least flooded site, $Pigeon_{shallow}$ (30° 04' 20" N, 91° 18' 36" W), is typically flooded for 249 days of the year (Keim et al., 2010) from January through August, potentially several meters deep and resulting in little understory vegetation. While flooded, floating aquatic vegetation (*Salvinia* spp*., Lemna* spp.) primarily covers the wetland. $Pigeon_{deep}$ was lower in the same swamp, approximately 5 km south of $Pigeon_{shallow}$ (30° 01' 29" N, 91° 16' 49" W). Exact duration of flooding and relative elevation are unknown, but this plot is in the same wetland at lower elevation than as a site that Dicke and Tolliver (1990) referred to as a "permanently flooded" that Keim et al. (2006) estimated to be unflooded for mean 35 days of the growing season. We expect it dries in occasional years with low river stages. Compared to $Pigeon_{shallow}$, $Pigeon_{deep}$ had a more-developed floating aquatic understory, composed of dense *Eichornia crassipes*. The intermediate site, $Pigeon_{int,}$ (30° 03' 51" N, 91° 18' 02" W) had understory vegetation and was also a semi-permanently flooded site like $Pigeon_{deep}$ with elevation estimated be a meter lower $Pigeon_{shallow}$ by comparison to simultaneous floodwater depths in $Pigeon_{shallow}$. None of the Pigeon sites had many baldcypress saplings, suggesting recruitment limitations although they were not clearly related to flooding at $Pigeon_{shallow}$ due to the largely closed canopy. Canopy gaps at $Pigeon_{shallow}$ were associated with permanently ponded depressional areas. There were extensive gaps at $Pigeon_{int}$ and $Pigeon_{deep}$, not seemingly associated with microtopographically deeper locations.

7.2.2 Measurements

To measure tree growth efficiency and stand density, tree cores were collected and four to six study plots (25 total) were established at each site for stand measurements. Measurements varied by site (Table 7.1), but data at all plots included canopy height, tree density (trees per hectare; TPH), basal area, and increment cores extracted from at least three trees. Additional cores were taken at some sites from trees outside of plots ($Pigeon_{shallow}$; $Bluff_{deep}$; $Bluff_{shallow}$), for

a total of 190. Diameter (*D*) measurements and cores were taken at 0.9 m above the stem buttress for all trees > 10 cm *D* by diameter tape or Wheeler pentaprism. Heights of at least 15 codominant trees per site were measured by clinometer and tape or by laser hypsometer (Laser Technology Inc., Centennial CO, USA).

Two increment cores from each tree were taken using a 5.15-mm increment borer (Hagloff, Mora, Sweden). The sapwood-heartwood boundary was identified in each core by color change and differential light transmission, and sapwood width was measured by vernier calipers in the field. Growth increments of the past 10 years were measured with a 0.01-mm-precision measurement system (Velmex Inc., Bloomfield NY) after cross dating to identify false or missing rings under 10-100 × magnification. Tree ages (from the time the tree reached height of coring) were estimated from ring counts.

There were some differences in measurements among sites (Table 7.1). Larger study plots were used at $\text{Pigeon}_{\text{deep}}$ because of wider spacing between trees. While $\text{Bluff}_{\text{deep}}$ also had sparse vegetation, small plots were used because of channels crossing the site. In four out of five sites, leaf area index (LAI) measurements were taken with a canopy analyzer (LAI-2000, LI-COR Biosciences, Lincoln, NE, USA) providing $\text{LAI}_{\text{LI-COR}}$ with the assumption of uniform radiation attenuation by the canopy. These measurements were taken in summer of 2013 for the Bluff sites and summer of 2006 for the Pigeon sites. The $\text{Pigeon}_{\text{deep}}$ site LAI measurements were slightly distant (~300 m) from the study plots and associated with another study (Keim et al., 2013a) and likely overestimate the canopy at $\text{Pigeon}_{\text{deep}}$. $\text{LAI}_{\text{corrected}}$ was also estimated using the relationship between $\text{LAI}_{\text{LI-COR}}$ and $\text{LAI}_{\text{corrected}}$ developed by Allen et al. (Allen et al., 2015) at the Bluff sites; this corrections likely overestimates $\text{LAI}_{\text{corrected}}$ in plots with more broadleaf trees (Gower and Norman, 1991).

Table 7.1 Samples and plot sizes per site.

Site	Samples Sizes				Plot size (m^2)
	LAI	Heights	Cores	Plots	
$\text{Bluff}_{\text{shallow}}$	25	22	48	5	250
$\text{Bluff}_{\text{deep}}$	30	16	42	6	250
$\text{Pigeon}_{\text{shallow}}$	27	15	42	5	314
$\text{Pigeon}_{\text{int}}$	—	15	30	5	314
$\text{Pigeon}_{\text{deep}}$	9	16	32	4	707

7.2.3 Analysis

At the tree level, the cross sectional basal area (BA_{tree}), 10-year basal area growth increment (BAI_{tree}), and sapwood basal area (SBA_{tree}) were calculated. To calculate SBA_{tree}, the heartwood area of elliptical shape calculated from sapwood widths was subtracted from BA_{tree}. Mean annual growth over the previous ten years was estimated as the mean between the two cores. Tree radial growth was converted to BAI_{tree} assuming circular geometry.

For site characteristics, (BA_{stand}) and stem density were calculated at plot scale and averaged for sites. Tree data were reported at the site or plot level with means and standard deviations calculated across individuals. Mean height, LAI, and BA_{prism} are only presented at the site level. Stand density was calculated as a stand metric to represent tree size and density (Reineke 1933),

$$\text{SDI} = n\left(\frac{D_q}{25}\right)^{1.6}, \quad (1)$$

where n = number of trees per hectare (TPH), and D_q is the site quadratic mean D.

We calculated GE_{tree} in two ways. By assuming that tree sapwood basal area (SBA_{tree}) is a surrogate for leaf area, $GE_{B:S}$ was calculated as tree basal area increment (BAI_{tree}) divided by SBA_{tree} (Waring, 1983). The non-linear relationships between SBA_{tree} and tree leaf area (LA_{tree}) and between BAI_{tree} and tree volume increment (VI_{tree}) may bias interpretations made from $GE_{B:S}$ (Dean et al., 1988; McDowell et al., 2007); to avoid these biases, also calculated was $GE_{V:L}$ from LA_{tree} and VI_{tree}. An allometric equation developed at the Bluff sites was used to calculate LA_{tree} from SBA_{tree} (Allen et al., 2015):

$$LA_{tree} = 2.35\times104\times SBA^2 + 8.32\times10^2\times SBA_{tree}. \quad (2)$$

Since height was not measure, VI_{tree} was the difference in tree volumes estimated for the current diameter and the diameter from 10 years prior using an allometric equation, (Parresol, 1998):

$$\text{Volume} = 0.0283\ e^{-3.0658 + 2.4019 \times \ln(0.394D)}; \quad (3)$$

volume estimates with D were consistent ($R^2 = 0.94$) with estimates calculted with both D and height (Hotvedt et al., 1985) for a subsample of trees with height measurements. We estimated GE at the stand level (Waring et al., 1981) as $GE_{stand} = BAI_{stand} / SBA_{stand}$, which can only be done coarsely because GE was not measured for all trees there are scaling challenges from sources of variation among trees (Dean, 2004; Roberts and Long, 1992; Waring et al., 1981) and canopy characteristics (Dean et al., 1988; McDowell et al., 2007; Waring et al., 1981).

Statistical analyses were performed to test for both tree and stand differences among sites, and the relationship between tree-level and stand-level characteristics by one way analysis of variance (ANOVA) and covariance (ANCOVA).

Multiple regression analysis was used with to test effects of tree variables (age and SBA_{tree}) and stand variables (SDI, BA_{stand}, and TPH) on GE_{tree}. Simple linear regressions were also calculated independently for each site for individual independent variables. The significant variables from the multiple regression analysis were treated as random covariates in a linear, mixed model with maximum likelihood estimator to test null hypotheses of no differences in the least-square means (LSM) of GE_{tree} between deep versus shallow for each wetland (Bluff versus Pigeon) with a nested design. Our null hypothesis is that GE_{tree} is not different for trees in more and less flooded sites. The alternate hypotheses are that (1) GE_{tree} is lower in more flooded swamps, indicating that the total environment is more limiting, or (2) GE_{tree} is greater in more flooded sites, indicating the opposite. Further, to test our hypothesis that site and flooding effects on GE_{tree} are related to stand density, the same test was run with SDI as a fixed effect with the expectation that this would fail to reject the null hypothesis that density-corrected LSM of GE_{tree} varied by flooding. Tests were conducted with both omission and inclusion of three age outliers (~200 year old).

Regression and ANOVA and regression tests were performed in MATLAB (Mathworks, Natick, MA, USA). Mixed-model analysis was performed in SAS (version 9.4, SAS Institute, Cary NC, USA).

Table 7.2 Site-level metrics for trees, stands, and sites shown as mean ± sd. Analysis of variance (ANOVA) showed differences among means for all metrics (all $p < 0.01$) and separations among site means by Tukey HSD are marked by letters.

Site	Tree Measurements		Plot Measurements				Site Measurements	
	D (cm)	Height (m)	Stem Density (trees ha^{-1})	BA_{stand} (m^2 ha^{-1})	$BA_{stand\text{-}cypress}$ (m^2 ha^{-1})	SDI (SI Units)	LAI_{LICOR} (m^2 m^{-2})	$LAI_{corrected}$ (m^2 m^{-2})
$Bluff_{shallow}$	34.5±3.1A	25.9 ± 3.8B	736 ± 128A	74.2 ± 12.4A	67.7 ± 7.3A	1306 ± 208A	4.2	7.7
$Bluff_{deep}$	28.7 ± 2.5B	18.0 ± 2.3C	373 ± 151B	25.5 ± 11.0C	24.6 ± 10.7C	485 ± 206B	2.9	3.6
$Pigeon_{shallow}$	28.8 ± 2.8B	29.2 ± 3.1A	822 ± 132A	55.7 ± 4.0B	50.5 ± 3.5B	1062 ± 66A	4.0	7.0
$Pigeon_{int}$	31.0 ± 3.4AB	23.2 ± 3.1B	382 ± 119B	29.2 ± 6.3C	20.8 ± 4.3C	543 ± 118B	——	——
$Pigeon_{deep}$	27.5 ± 1.5B	17.9 ± 2.1C	329 ± 72B	20.9 ± 5.4C	12.7 ± 3.7C	404 ± 100B	2.5*	3.0*

* LAI was measured at a nearby site within the same area but slightly uphill on a natural levee, and likely is an overestimate.

7.3. RESULTS

The more flooded sites had sparser forest by all stand metrics (i.e., TPH, BA_{stand}, SDI, and LAI; Table 7.2). Tree heights followed this same trend, with shorter trees at the more flooded, sparser sites. Arithmetic mean *D* varied by site but not following the flood gradient (Table 7.2). While nearly all codominant trees were baldcypress, water tupelo constituted 29% and 39% of the basal area in $Pigeon_{int}$ and $Pigeon_{deep}$ (Table 7.2). However, most water tupelo trees had broken crowns and low leaf area (Keim et al. 2013a), so their influence by light interception was assumed minimal.

Allometric relationships were calculated to predict SBA_{tree} and LA_{tree} from *D* (Figure 7.1A,E). Across all measured trees, SBA_{tree} was strongly related to *D*, best fit by a power model (Figure 7.1A), but given the relatively small range of tree sizes, was also well fit by the linear model, $SBA_{tree} = 20.1\ D - 225\ cm^2$ ($R^2 = 0.82$, $p < 0.001$). Slopes did not differ among sites (ANCOVA failed to reject H_0; $F = 2.21$, $p = 0.074$). The relationships between *D* and LA_{tree} was similarly strong (Figure 7.1E), but more curvilinear , $LA_{tree} = 5.88\ D - 108$ ($R^2 = 0.76$). Similarly, slopes did not differ among sites (ANCOVA failed to reject H_0; $F = 1.87$, $p = 0.12$.

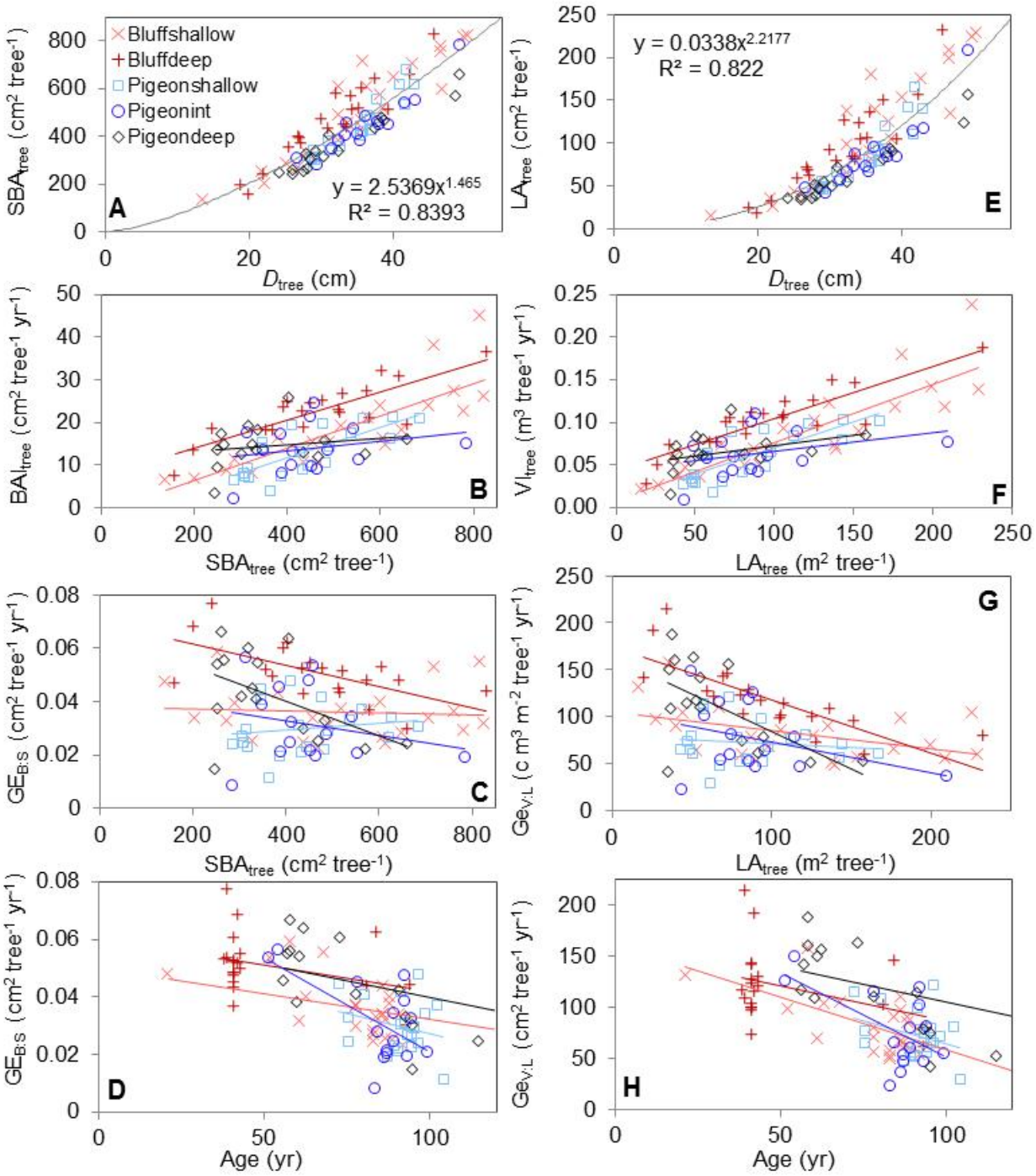

Figure 7.1 Tree-level relationships for each site for (A) tree sapwood area (SBA_{tree}) versus tree basal area (BA_{tree}), (B) tree basal area growth increment (BAI_{tree}) averaged over 10 years versus SBA_{tree}, (C) tree growth efficiency ($GE_{B:S}$), calculated as BAI_{tree} / SBA_{tree} versus SBA_{tree}, (D) $GE_{B:S}$ versus age, (E) tree leaf area (LA_{tree}) versus BA_{tree}, (F) tree Volume growth increment (VI_{tree}) averaged over 10 years versus LA_{tree}, (G) tree growth efficiency ($GE_{V:L}$) calculated as VI_{tree} / LA_{tree} versus LA_{tree}, and (H) tree growth efficiency ($GE_{V:L}$). Site-specific best fit lines are plotted in B, C, D, and F, while A and B are fit for all trees (Table 7.3). All plots, but not regressions, omit one large tree (D = 66 cm, SBA = 1253 cm^2) for improved figure resolution.

There was a modest relationship between SBA_{tree} and BAI_{tree} across all trees in all sites, where BAI = 0.032SBA+2.4 cm^2 ($R^2 = 0.43$, $p < 0.0001$). There were strong relationships between SBA_{tree} and BAI_{tree} for $Bluff_{shallow}$, $Pigeon_{shallow}$, and $Bluff_{deep}$ (Figure 7.1B; Table 7.3). In contrast, BAI_{tree} was independent of SBA_{tree} at the other two sites (Figure 7.1B; Table 7.3), which were the less dense than the shallow sites (Table 7.2). Similarly, LA_{tree} and VI_{tree} were correlated at all sites, but a larger effect of LA_{tree} on VI_{tree} was apparent in the shallow and intermediate sites (Figure 7.1F) while the effect of LA_{tree} on $GE_{V:L}$ was greater in the deep sites (Figure 7.1G).

Linear regression models showed that, across all sites, tree age and SDI were predictors of GE_{tree}. For $GE_{B:S}$, the best-fit model was

$$GE_{B:S} = -8.6\times10^{-6}\times SDI - 3.8\times10^{-6}\times SBA_{tree} - 2.9\times10^{-4}\times age + 0.07, \quad (4)$$

with $R^2 = 0.44$ ($p < 0.001$) and $p < 0.01$ for all coefficients except for SBA_{tree} ($p = 0.56$). The best-fit model for $GE_{V:L}$ was

$$GE_{V:L} = -0.022\times SDI - 0.23\times LA_{tree} - 0.67\times age + 182, \quad (5)$$

with $R^2 = 0.49$ ($p < 0.001$) and $p < 0.01$ values for all four terms. The age effect was apparent in all sites, although not always significant (not shown) because of presence of multiple age cohorts (Figure 7.2).

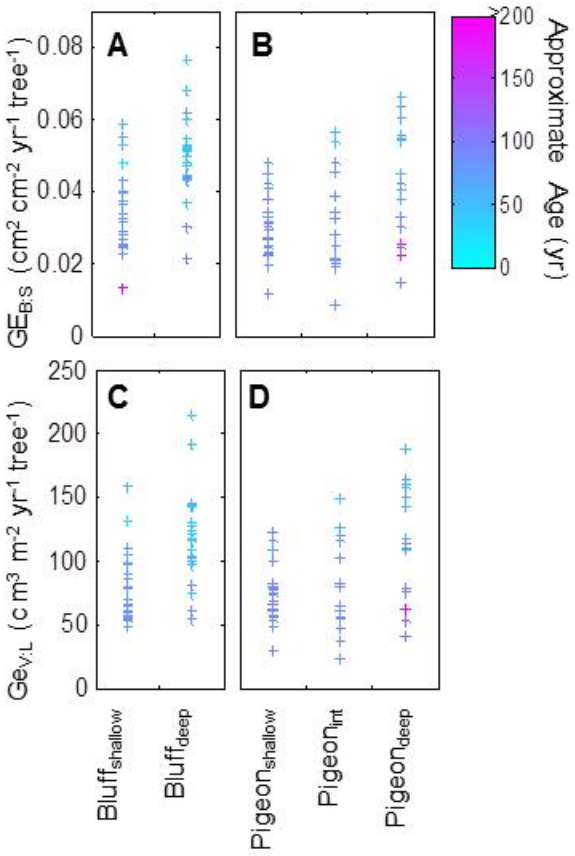

Figure 7.2 Tree growth efficiency, calculated as tree basal area increment per sapwood area, ($GE_{B:S}$; A and B), or as tree volume increment per leaf area, ($GE_{V:L}$; C and D) for the Bluff (A and C) and Pigeon (B and D) gradients. Each symbol is one tree, with color identifying age.

The mixed-model analysis showed that trees at deeper sites had significantly higher GE_{tree} than trees at shallower sites. Models omitting outliers indicated GE_{tree} was higher in more flooded sites for $GE_{B:S}$ (LSM difference of deep − shallow = 0.014 $cm^2\ cm^{-2}\ yr^{-1}$; p = 0.01) and $GE_{V:L}$ (LSM = 37 $cm^3\ m^{-2}\ yr^{-1}$; p = 0.008). Similar results were shown for models including outliers with for $GE_{B:S}$ (LSM = 0.021; p < 0.0001) and $GE_{V:L}$ (LSM = 56; p < 0.0001). However, models additionally accounting for fixed effects of SDI on GE_{tree} showed no significant differences (failure to reject H_0) between shallow and deep $GE_{B:S}$ or $GE_{V:L}$ (respectively, LSM = 37 $cm^3\ m^{-2}\ yr^{-1}$, p = 0.008 and LSM = 37 $cm^3\ m^{-2}\ yr^{-1}$, p = 0.008). There was no statistically significant site effect (Bluff versus Pigeon) on $GE_{B:S}$ or $GE_{V:L}$ of trees (p > 0.05 in all tests).

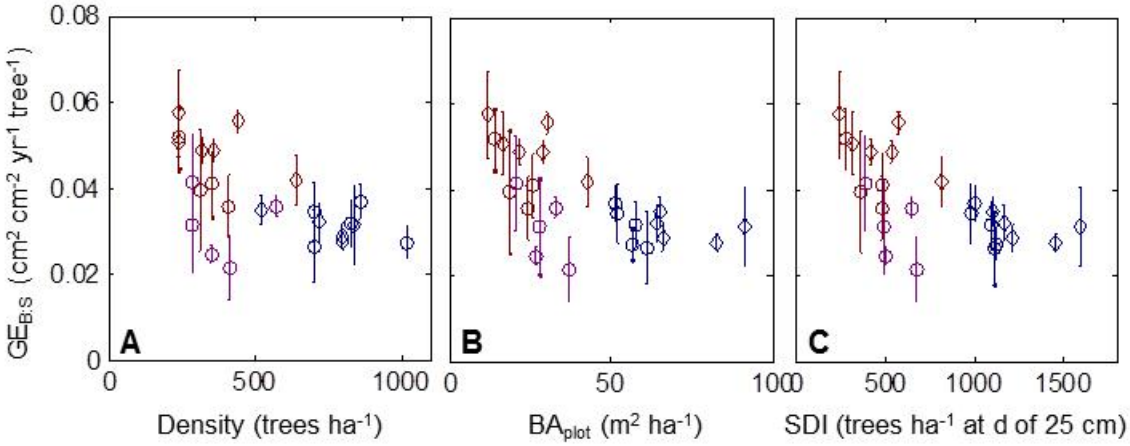

Figure 7.3 Mean and standard errors of tree growth efficiency (GE_{tree}) for plots versus stand characteristics for plots: (A) stem density (of trees < 10 cm diameter), (B) plot basal area, and (C) stand density index (SDI). Red symbols are deep sites, purple is intermediate, and blue is shallow. Diamonds are Bluff sites, and circles are Pigeon sites.

7.4. DISCUSSION

7.4.1 Flooding effects on stands and trees

Site differences, including both flooding variations and stand density, resulted in variations in tree-level growth efficiency. Stand density variations from hydrology were in agreement with the many studies that have shown that deep, long-duration flooding often yields or maintains (e.g., Brown, 1981; Conner et al., 1986; Effler et al., 2007; Effler and Goyer, 2006; Eggler and Moore, 1961; Keeland and Young, 1997; Keim et al., 2013b) sparser stands. Regeneration obstacles were readily apparent in the more flooded $Pigeon_{int}$, $Pigeon_{deep}$, and $Bluff_{deep}$, where even gaps lacked regeneration. While tree mortality is reducing stand density over time at the shallow sites (Keim et al., 2013a), it was not clearly related to flooding because self-thinning is a reasonable expectation in stands where SDI > 60% of maximum SDI (Long, 1985), with maximum SDI found to be roughly ~1200 for baldcypress (Keim et al 2010).

Our primary interest was how trees respond to the combined effect of flooding and the stand variations associated with flooding. GE_{tree} was higher at more flooded sites, suggesting a net benefit of the total environment that includes both presumed detrimental flood effects and reduced competition for light or other resources. The importance of density in this relationship was demonstrated by the failure to reject the H_0 when accounting for fixed effects of SDI. Given the environment of these trees and the stand density effects, we infer that the reduced light

competition associated with lower density explains the higher GE_{tree} in the more deeply flooded sites. Thus, across these sites, light limitations are a more dominant control over growth than flooding. This importance of shading is further demonstrated at the tree scale in that the sparser sites more strongly show reduced GE_{tree} with increasing SBA_{tree} or LA_{tree}, suggesting self-shading (Gersonde and O'Hara, 2005).

Table 7.3 Tree allometrics for by-site: basal area increment (BAI_{tree}) as a function of sapwood basal area (SBA_{tree}) and tree growth efficiency as a ratio bewteen BAI and SBA ($GE_{B:S}$), allometrically derived tree volume increment (VI_{tree}) as a function of allometrically derived tree leaf area (LA_{tree}) and GE_{tree} defined as a ratio between VI_{tree} and LA_{tree} ($GE_{V:L}$).

Site	BAI_{tree} = f (SBA_{tree}); R^2 (p)	$GE_{B:S}$ ($cm^2\ cm^{-2}\ yr^{-1}$)	VI_{tree} = f (LA_{tree}); R^2 (p)	$GE_{V:L}$ ($m^3\ m^{-2}\ yr^{-1}$)
$Bluff_{shallow}$	0.038SBA-1.2; 0.67 (<0.001)	0.036 ± 0.02	68SBA-796; 0.75 (<0.001)	82 ± 27
$Bluff_{deep}$	0.032SBA+7.5; 0.66 (<0.001)	0.051 ± 0.01	629SBA+3917; 0.71 (<0.001)	47± 23
$Pigeon_{shallow}$	0.034SBA-1.7; 0.54 (<0.001)	0.030 ± 0.01	62SBA+920; 0.65 (<0.001)	117 ± 38
$Pigeon_{int}$	0.011SBA+8.7; 0.06 (0.39)	0.032 ± 0.014	218SBA+4420; 0.11 (0.23)	78 ± 37
$Pigeon_{deep}$	0.008SBA+11.7; 0.04 (0.45)	0.042 ± 0.02	240SBA+4850; 0.16 (0.13)	111 ± 47
ALL	0.032SBA + 2.5 0.43(<0.001)	0.038 ± 0.01	58SBA + 2347; 0.56(<0.001)	92 ± 38

If we estimate BAI_{stand}, we find that patterns of BAI_{stand} are roughly the inverse of GE_{tree}. Assuming the *D*:SBA relationship is constant across all trees (Figure 7.1A) and $GE_{B:S}$ is constant across all trees in each site (Table 7.3), we can estimate SBA_{stand} as 34, 13, 29, 15, and 11 $m^2\ ha^{-1}$, and BAI_{stand} as 1.22, 0.67, 0.85, 0.46, and 0.45 $m^2\ ha^{-1}\ yr^{-1}$, $Bluff_{shallow}$, $Bluff_{deep}$, $Pigeon_{shallow}$, $Pigeon_{int}$, and $Pigeon_{deep}$ respectively. None of the more flooded sites had higher BAI_{stand} than paired drier, denser sites, although estimated BAI_{stand} at $Bluff_{deep}$ was surprisingly close to that of $Pigeon_{shallow}$ despite lower stem density. Observations in other forests indicate it is possible for stands with lower LAI or fewer stems to result in higher stand production through a more efficient canopy structure (Roberts et al., 1993; Waring et al., 1981).

Definitions of stress vary, but a common one is any environmental factor that limits a physiological process of an individual to below maximum (Kozlowski, 1991; Lambers et al., 2006; Larcher, 1995). By this definition, GE_{tree} is a could be considered a measure of stress (Waring, 1983), at the tree-level accounting for the total influence of the environment (biotic and abiotic). Interpreted this way, our results show less-stressed trees in the more deeply flooded plots that we estimate are lower productivity. A tree having low LA or SBA per tree in a sparse stand could be considered another dimension of stress, but morphologic adjustment can be a slow process for trees. It is possible that these sparser sites can later achieve canopy closure because baldcypress trees are large and long-lived (Whilhite and Toliver, 1990).

This interpretation that more flooded sites provide more favorable conditions for trees does not mean that flooding was beneficial to trees as an independent factor; rather, the net effect of combined flooding and stand differences yielded more favorable conditions than in less

flooded sites. In fact, deep flooding is likely a stressor, evident by lower tree height, which reflects site quality (Carmean, 1972; Ryan and Yoder, 1997). Consistent with this, Keim et al (2013a) found lower growth in the more flooded stand of a pair of dense baldcypress-tupelo stands at the Pigeon site. Similarly, deeper flooding of open-grown trees result in more stressed trees, inferable from controlled studies where density can be fixed, enabling testing of univariate gradients (Powell et al., 2016). Following this logic, in sites more deeply flooded than in this study, the benefits of stand openness may be outweighed by physiological stress of high water (e.g., Keim et al., 2012; Mitsch and Ewel, 1979). Other stresses that were not factors in our study, such as salinity, can exceed benefits of openness for baldcypress (Day et al., 2012), but over our study domain, light limitation was likely more important, explaining the higher GE_{tree} at the more flooded sites.

7.4.2 A more literal subsidy-stress model

The classic subsidy-stress concept holds that deeper flooding creates stresses that outweigh the subsidy of abundant water. Our conclusion—more heavily flooded sites, and resulting sparseness, reduces total stress—are in agreement with the common finding that flooding and resulting sparse forest structure yields lower production (Conner et al., 2014, 2011; Megonigal et al., 1997; Mitsch et al., 1991). We conclude that measurements of stand-level production without standardizing for tree density or age are especially inappropriate for inferring stress in forested wetlands because openness is a common consequence of flooding. This conclusion is likely particularly prominent in wetlands compared to other open stands because the openness is the result of disturbance and not a function of competition for over limited resources. This is in contrast to, for example, arid or semi-arid systems where the same resource largely limit both the density and physiological functions of individuals (Caylor et al., 2003; Rietkerk et al., 2004).

Disturbance is a better descriptor than stress for the circumstances that result in low stand production in forested wetlands. Flooding results in sparseness by preventing establishment in gaps and removal of competing trees in the canopy, in agreement with conventional descriptions of disturbance (*sensu* Grime, 1977; Pickett et al., 1989). These disturbances may involve a transition from individuals in a state of stress (e.g., in the case of dying trees). This deep end of the wetland gradient differs from shallower wetlands with seasonal or periodic flooding because there is not always regeneration potential, so disturbances lacks the successional 'reset' function common with disturbance (Pickett and White, 1985). However, even in these permanently flooded sites, multi-age cohorts existed, but separated by several decades (e.g., ~45 and ~90 year old trees at $Bluff_{deep}$, ~75 and ~90 year old trees at $Pigon_{shallow}$, ~55 and ~90 year old trees at $Pigeon_{deep}$ and $Pigeon_{int}$; Figure 7.1D). Systems with continuous or nearly continuous disturbances warrant consideration as different ecosystems (Noble and Slatyer, 1980), and sparseness is likely a frequent state of forested wetlands in more flooded areas.

We propose an alternate model to the subsidy-stress concept that separates stress (of the individual) from disturbance affecting stand density (Figure 7.4). As opposed to subsidy-stress gradient concepts, we recognize that flooding decreases stand production while contemporaneously increasing tree growth. This distinction decomposes the classic subsidy-stress production model into one function of flood effects on stand density, and one function of flood effects on tree stress. When considering stand-level effects as disturbances instead of assuming stress, the link between disturbance and stand production is in agreement with the "subsidy-stress" model. However, this model should be applied cautiously at the drier end of the

wetland forest gradient, where more tree niches overlap and gaps may be readily replaced (Battaglia and Sharitz, 2005; Conner and Brody, 1989).

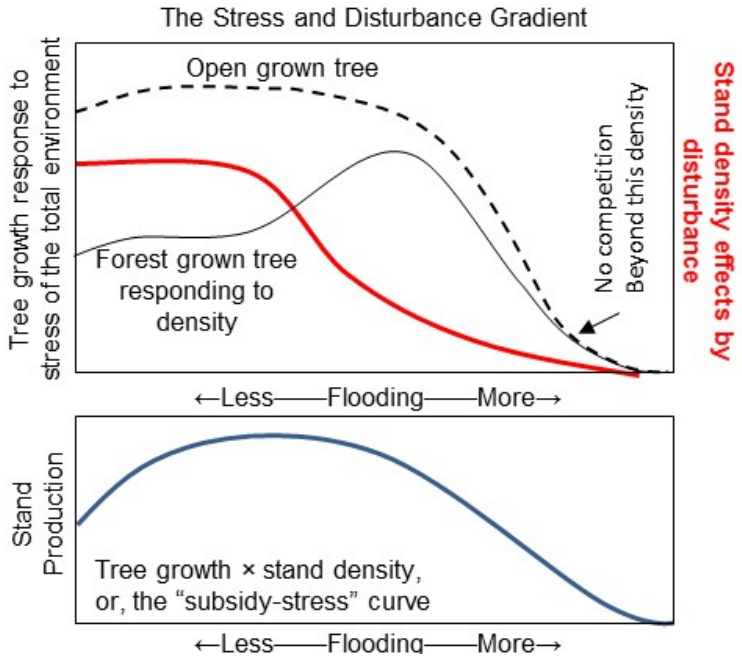

Figure 7.4 Conceptual responses of wetland trees (in black) and stands (in red) to flooding. The *solid red line* is stand density, with minor flooding allowing a dense stand, but more flooding reduces density (by mortality or recruitment limitation). The *solid black line* represents trees in that stand, where trees benefit from density until the flood stress overwhelms the benefit of reduced competition. The *dashed black line* is an open grown tree, responding only to flooding. The lines merge where stand density is low enough that trees are not in competition. Stand-level productivity is the product of stand density and tree growth curves.

Although many metrics may apply in this proposed concept suitable (Figure 7.4), both SDI and GE_{tree} are well justified because production is a linear function of SDI × GE_{stand}. Production is the product of resource supply, capture, and efficiency of use (Binkley et al., 2004; Monteith and Moss, 1977). GE reflects supply and use efficiency and density accounts for capture. Complementing GE defined per SBA, SDI is probably the appropriate metric because it is linearly related to SBA_{stand} (SBA_{stand} [cm^2 ha^{-1}]= $1.44 \times TPH \times D_q^{1.6}$) and has been intensively validated across four upland species ((Long and Dean, 1986). Among the Bluff and Pigeon SBA_{stand} estimates, the slope of this relationship is similar, at 1.53 (data not shown). Thus GE_{tree} responses to stress and SDI responses to disturbance probably serve as a more literal representation of flooding controls over stand production than the original subsidy-stress concept.

7.5 CONCLUSION

The data showed that trees in more flooded sites had higher growth efficiency, that is, higher basal area or volumetric increment per sapwood area or leaf area. In these more deeply flooded sites, the trees composed lower-density stands, which is consistent with increased growth efficiency because of decreased competition. Thus, conditions in open stands were less limiting to tree growth than in closed stands. Deeper flooding with associated sparseness can result in

overall more favorable conditions for individual trees, likely due to lower competition. This relationship requires a modification to the classic subsidy-stress concept to differentiate between stress effects on individual trees and disturbance effects on stand structure and productivity.

7.6 REFERENCES

Allen, J.A., Pezeshki, S.R., Chambers, J.L., 1996. Interaction of flooding and salinity stress on baldcypress (Taxodium distichum). Tree Physiol. 16, 307–313.

Allen, S.T., Krauss, K.W., Cochran, J.W., King, S.L., Keim, R.F., 2016. Wetland tree transpiration modified by river-floodplain connectivity. J. Geophys. Res. Biogeosciences 2015JG003208. doi:10.1002/2015JG003208

Allen, S.T., Whitsell, M.L., Keim, R.F., 2015. Leaf area allometrics and morphometrics in baldcypress. Can. J. For. Res. 45, 963–969. doi:10.1139/cjfr-2015-0039

Anderson, C.J., Mitsch, W.J., 2008. Tree basal growth response to flooding in a bottomland hardwood forest in central Ohio. J. Am. Water Resour. Assoc. 44, 1512–1520. doi:10.1111/j.1752-1688.2008.00255.x

Anderson, P.H., Pezeshki, R., 2001. Effects of flood pre-conditioning on responses of three bottomland tree species to soil waterlogging. J. Plant Physiol. 158, 227–233. doi:10.1078/0176-1617-00267

Asner, G.P., Scurlock, J.M.O., A. Hicke, J., 2003. Global synthesis of leaf area index observations: implications for ecological and remote sensing studies. Glob. Ecol. Biogeogr. 12, 191–205. doi:10.1046/j.1466-822X.2003.00026.x

Battaglia, L.L., Sharitz, R.R., 2005. Effects of natural disturbance on bottomland hardwood regeneration, in: Frederickson, L.H., King, S.L., Kaminski, R.M. (Eds.), Ecology and Management of Bottomland Hardwood Systems: The State of Our Understanding. University of Missouri-Columbia.

Binkley, D., Stape, J.L., Ryan, M.G., 2004. Thinking about efficiency of resource use in forests. For. Ecol. Manag., Synthesis of the physiological, environmental, genetic and silvicultural determinants of the growth and productivity of eucalypts in plantations. 193, 5–16. doi:10.1016/j.foreco.2004.01.019

Binkley, D., Stape, J.L., Ryan, M.G., Barnard, H.R., Fownes, J., 2002. Age-related Decline in Forest Ecosystem Growth: An Individual-Tree, Stand-Structure Hypothesis. Ecosystems 5, 58–67. doi:10.1007/s10021-001-0055-7

Brix, H., 1983. Effects of thinning and nitrogen fertilization on growth of Douglas-fir: relative contribution of foliage quantity and efficiency. Can. J. For. Res. 13, 167–175. doi:10.1139/x83-023

Broadfoot, W.M., Williston, H.L., 1973. Flooding effects on southern forests. J. For. 71, 584–587.

Brown, S., 1981. A Comparison of the Structure, Primary Productivity, and Transpiration of Cypress Ecosystems in Florida. Ecol. Monogr. 51, 403. doi:10.2307/2937322

Brown, S., Peterson, D.L., 1983. Structural Characteristics and Biomass Production of Two Illinois Bottomland Forests. Am. Midl. Nat. 110, 107–117. doi:10.2307/2425216

Carmean, W.H., 1972. Site Index Curves for Upland Oaks in the Central States. For. Sci. 18, 109–120.

Caylor, K.K., Shugart, H.H., Dowty, P.R., Smith, T.M., 2003. Tree spacing along the Kalahari transect in southern Africa. J. Arid Environ. 54, 281–296. doi:10.1006/jare.2002.1090

Chambers, J.L., Day, J.W., Faulkner, S.P., Gardiner, E.S., Hughes, M.S., Keim, R.F., King, S.L., McLeod, K.W., Miller, C.A., Nyman, J.A., Shaffer, G.P., 2005. Conservation, protection and utilization of Louisiana's Coastal Wetland Forests. (Final Report to the Governor of Louisiana). Coastal Wetland Forest Conservation and Use Science Working Group.

Clawson, R.G., Lockaby, B.G., Rummer, B., 2001. Changes in production and nutrient cycling across a wetness gradient within a floodplain forest. Ecosystems 4, 126–138. doi:10.1007/s100210000063

Conner, W.H., Brody, M., 1989. Rising water levels and the future of southeastern Louisiana swamp forests. Estuaries 12, 318–323. doi:10.2307/1351909

Conner, W.H., Duberstein, J.A., Jr, J.W.D., Hutchinson, S., 2014. Impacts of Changing Hydrology and Hurricanes on Forest Structure and Growth Along a Flooding/Elevation Gradient in a South Louisiana Forested Wetland from 1986 to 2009. Wetlands 34, 803–814. doi:10.1007/s13157-014-0543-0

Conner, W.H., Gosselink, J.G., Parrondo, R.T., 1981. Comparison of the vegetation of three Louisiana swamp sites with different flooding regimes. Am. J. Bot. 68, 320. doi:10.2307/2442768

Conner, W.H., Song, B., Williams, T.M., Vernon, J.T., 2011. Long-term tree productivity of a South Carolina coastal plain forest across a hydrology gradient. J. Plant Ecol. 4, 67–76. doi:10.1093/jpe/rtq036

Conner, W.H., Toliver, J.R., Sklar, F.H., 1986. Natural regeneration of baldcypress (Taxodium distichum (L.) Rich.) in a Louisiana swamp. For. Ecol. Manag. 14, 305–317. doi:10.1016/0378-1127(86)90176-3

Day, J., Hunter, R., Keim, R.F., DeLaune, R., Shaffer, G., Evers, E., Reed, D., Brantley, C., Kemp, P., Day, J., Hunter, M., 2012. Ecological response of forested wetlands with and without Large-Scale Mississippi River input: Implications for management. Ecol. Eng. 46, 57–67. doi:10.1016/j.ecoleng.2012.04.037

Dean, T.J., 2004. Basal Area Increment and Growth Efficiency as Functions of Canopy Dynamics and Stem Mechanics. For. Sci. 50, 106–116.

Dean, T.J., Long, J.N., Smith, F.W., 1988. Bias in leaf area — sapwood area ratios and its impact on growth analysis in Pinus contorta. Trees 2, 104–109. doi:10.1007/BF00196756

Dicke, S.G., Toliver, J.R., 1990. Growth and development of bald-cypress/water-tupelo stands under continuous versus seasonal flooding. For. Ecol. Manag. 33–34, 523–530. doi:10.1016/0378-1127(90)90215-W

Duberstein, J.A., Krauss, K.W., Conner, W.H., Jr, W.C.B., Shelburne, V.B., 2013. Do hummocks provide a physiological advantage to even the most flood tolerant of tidal freshwater trees? Wetlands 33, 399–408. doi:10.1007/s13157-013-0397-x

Effler, R.S., Goyer, R.A., 2006. Baldcypress and water tupelo sapling response to multiple stress agents and reforestation implications for Louisiana swamps. For. Ecol. Manag. 226, 330–340. doi:10.1016/j.foreco.2006.02.011

Effler, R.S., Shaffer, G.P., Hoeppner, S.S., Goyer, R.A., 2007. Ecology of the Maurepas Swamp: Effects of Salinity, Nutrients, and Insect Defoliation, in: Ecology of Tidal Freshwater Forested Wetlands of the Southeastern United States. Springer Netherlands, pp. 349–384.

Eggler, W.A., Moore, W.G., 1961. The Vegetation of Lake Chicot, Louisiana, after Eighteen Years Impoundment. Southwest. Nat. 6, 175. doi:10.2307/3669331

Faulkner, S.P., Chambers, J.L., Conner, W.H., Keim, R.F., Day, J.W., Gardiner, E.S., Hughes, M.S., King, S.L., McLeod, K.W., Miller, C.A., Nyman, J.A., Shaffer, G.P., 2007. Conservation and Use of Coastal Wetland Forests in Louisiana, in: Ecology of Tidal Freshwater Forested Wetlands of the Southeastern United States. Springer Publishing, Berlin, DE, pp. 447–460.

Ford, C.R., Brooks, J.R., 2002. Detecting forest stress and decline in response to increasing river flow in southwest Florida, USA. For. Ecol. Manag. 160, 45–64. doi:10.1016/S0378-1127(01)00440-6

Gause, G.F., 1934. The Struggle for Existence. Williams and Wilkins Co., Baltimore.

Gersonde, R.F., O'Hara, K.L., 2005. Comparative tree growth efficiency in Sierra Nevada mixed-conifer forests. For. Ecol. Manag. 219, 95–108. doi:10.1016/j.foreco.2005.09.002

Gower, S.T., Norman, J.M., 1991. Rapid estimation of leaf area index in conifer and broad-Leaf plantations. Ecology 72, 1896. doi:10.2307/1940988

Grime, J.P., 1977. Evidence for the Existence of Three Primary Strategies in Plants and Its Relevance to Ecological and Evolutionary Theory. Am. Nat. 111, 1169–1194.

Harms, W.R., Schreuder, H.T., Hook, D.D., Brown, C.L., 1980. The Effects of Flooding on the Swamp Forest in Lake Ocklawaha, Florida. Ecology 61, 1412. doi:10.2307/1939050

Hotvedt, J.E., Cao, Q.V., Parresol, B.R., 1985. Tree-Volume and Stem-Profile Functions for Baldcypress. South. J. Appl. For. 9, 227–232.

Jax, K., 2006. Ecological Units: Definitions and Application. Q. Rev. Biol. 81, 237–258. doi:10.1086/506237

Kaufmann, M.R., 1996. To live fast or not: growth, vigor and longevity of old-growth ponderosa pine and lodgepole pine trees. Tree Physiol. 16, 139–144. doi:10.1093/treephys/16.1-2.139

Keeland, B.D., Conner, W.H., 1999. Natural regeneration and growth ofTaxodium distichum (L.) Rich. in Lake Chicot, Louisiana after 44 years of flooding. Wetlands 19, 149–155. doi:10.1007/BF03161743

Keeland, B.D., Young, P.J., 1997. Long-term growth trends of baldcypress (Taxodium distichum (L.) rich.) at Caddo Lake, Texas. Wetlands 17, 559–566.

Keim, R.F., Amos, J.B., 2012. Dendrochronological analysis of baldcypress (Taxodium distichum) responses to climate and contrasting flood regimes. Can. J. For. Res. 42, 423–436. doi:10.1139/x2012-001

Keim, R.F., Dean, T.J., Chambers, J.L., 2013a. Flooding effects on stand development in cypress-tupelo, in: Proceedings of the 15th Biennial Southern Silvicultural Research Conference. Asheville, NC: U.S. Department of Agriculture, Forest Service, Southern Research Station, pp. 431–437.

Keim, R.F., Dean, T.J., Chambers, J.L., Conner, W.H., 2010. Stand Density Relationships in Baldcypress. For. Sci. 56, 336–343.

Keim, R.F., Izdepski, C.W., Jr, J.W.D., 2012. Growth Responses of Baldcypress to Wastewater Nutrient Additions and Changing Hydrologic Regime. Wetlands 32, 95–103. doi:10.1007/s13157-011-0248-6

Keim, R.F., Zoller, J.A., Braud, D.H., Edwards, B.L., 2013b. Classification of forested wetland degradation using ordination of multitemporal reflectance. Wetlands 1–13. doi:10.1007/s13157-013-0466-1

Kolasa, J., Pickett, S.T.A., 1992. Ecosystem stress and health: an expansion of the conceptual basis. J. Aquat. Ecosyst. Health 1, 7–13. doi:10.1007/BF00044404

Kozlowski, T.T., 1991. Environmental stresses to deciduous trees, in: Mooney, H.A., Winner, W.E., Pell, E.J. (Eds.), Response of Plants to Multiple Stresses. Academic Press, San Diego, CA, pp. 391–411.

Krauss, K.W., Duberstein, J.A., Doyle, T.W., Conner, W.H., Day, R.H., Inabinette, L.W., Whitbeck, J.L., 2009. Site condition, structure, and growth of baldcypress along tidal/non-tidal salinity gradients. Wetlands 29, 505–519. doi:10.1672/08-77.1

Lambers, H., Chapin, F.S., Pons, T.L., 2006. Plant Physiological Ecology. Springer Publishing, New York, NY, USA.

Larcher, W., 1995. Physiological plant ecology. Springer-Verlag.

Long, J.N., 1985. A Practical Approach to Density Management. For. Chron. 61, 23–27. doi:10.5558/tfc61023-1

Long, J.N., Dean, T.J., 1986. Sapwood area ofPinus contorta stands as a function of mean size and density. Oecologia 68, 410–412. doi:10.1007/BF01036747

Long, J.N., Dean, T.J., Roberts, S.D., 2004. Linkages between silviculture and ecology: examination of several important conceptual models. For. Ecol. Manag. 200, 249–261. doi:10.1016/j.foreco.2004.07.005

Long, J.N., Smith, F.W., 1990. Determinants of Stemwood Production in Pinus contorta var. Latifolia Forests: The Influence of Site Quality and Stand Structure. J. Appl. Ecol. 27, 847–856. doi:10.2307/2404381

McDowell, N.G., Adams, H.D., Bailey, J.D., Kolb, T.E., 2007. The role of stand density on growth efficiency, leaf area index, and resin flow in southwestern ponderosa pine forests. Can. J. For. Res. 37, 343–355. doi:10.1139/X06-233

McDowell, N.G., Beerling, D.J., Breshears, D.D., Fisher, R.A., Raffa, K.F., Stitt, M., 2011. The interdependence of mechanisms underlying climate-driven vegetation mortality. Trends Ecol. Evol. 26, 523–532. doi:10.1016/j.tree.2011.06.003

McLeod, K.W., Donovan, L.A., Stumpff, N.J., Sherrod, K.C., 1986. Biomass, photosynthesis and water use efficiency of woody swamp species subjected to flooding and elevated water temperature. Tree Physiol. 2, 341–346. doi:10.1093/treephys/2.1-2-3.341

Megonigal, J.P., Conner, W.H., Kroeger, S., Sharitz, R.R., 1997. Aboveground production in southeastern floodplain forests: A test of the subsidy–stress hypothesis. Ecology 78, 370–384. doi:10.1890/0012-9658(1997)078[0370:APISFF]2.0.CO;2

Middleton, B.A., 2008. Regeneration potential of Taxodium distichum swamps and climate change. Plant Ecol. 202, 257–274. doi:10.1007/s11258-008-9480-4

Middleton, B.A., McKee, K.L., 2004. Use of a latitudinal gradient in bald cypress (Taxodium distichum) production to examine physiological controls of biotic boundaries and potential responses to environmental change. Glob. Ecol. Biogeogr. 13, 247–258. doi:10.1111/j.1466-822X.2004.00088.x

Mitsch, W.J., 1988. Productivity-Hydrology-Nutrient Models of Forseted Wetlands, in: Mitsch, W.J., Straškraba, M., Jorgensen, S.E. (Eds.), Wetland Modelling. Elsevier, Amsterdam, Netherlands.

Mitsch, W.J., Ewel, K.C., 1979. Comparative Biomass and Growth of Cypress in Florida Wetlands. Am. Midl. Nat. 101, 417–426. doi:10.2307/2424607

Mitsch, W.J., Gosselink, J.G., 2007. Wetlands, 4th ed. John Wiley & Sons, Inc., New York, NY, USA.

Mitsch, W.J., Rust, W.G., 1984. Tree growth responses to flooding in a bottomland forest in northeastern Illinois. For. Sci. 30, 499–510.

Mitsch, W.J., Taylor, J.R., Benson, K.B., 1991. Estimating primary productivity of forested wetland communities in different hydrologic landscapes. Landsc. Ecol. 5, 75–92. doi:10.1007/BF00124662

Monteith, J.L., Moss, C.J., 1977. Climate and the Efficiency of Crop Production in Britain [and Discussion]. Philos. Trans. R. Soc. Lond. B. Biol. Sci. 281, 277–294.

Nash, L.J., Graves, W.R., 1993. Drought and flood stress effects on plant development and leaf water relations of five taxa of trees native to bottomland habitats. J. Am. Soc. Hortic. Sci. 118, 845–850.

Noble, I.R., Slatyer, R.O., 1980. The Use of Vital Attributes to Predict Successional Changes in Plant Communities Subject to Recurrent Disturbances. Vegetatio 43, 5–21.

NRCS, 2016. Web Soil Survey. United States Department of Agriculture.

Odum, E.P., 1969. The Strategy of Ecosystem Development. Science 164, 262–270. doi:10.1126/science.164.3877.262

Odum, E.P., Finn, J.T., Franz, E.H., 1979. Perturbation theory and the subsidy-stress gradient. BioScience 29, 349–352. doi:10.2307/1307690

Oliver, C.D., Larson, B.C., 1996. Forest Stand Dynamics. John Wiley & Sons, Inc., New York, NY, USA.

Parresol, B.R., 1998. Prediction and Error of Baldcypress Stem Volume from Stump Diameter. South. J. Appl. For. 22, 69–73.

Pezeshki, S.R., Chambers, J.L., 1986. Variation in Flood-Induced Stomatal and Photosynthetic Responses of Three Bottomland Tree Species. For. Sci. 32, 914–923.

Pickett, S.T.A., Kolasa, J., Armesto, J.J., Collins, S.L., 1989. The Ecological Concept of Disturbance and Its Expression at Various Hierarchical Levels. Oikos 54, 129–136. doi:10.2307/3565258

Pickett, S.T.A., White, P.S., 1985. The Ecology of Natural Disturbance and Patch Dynamics. Academic Press Inc, San Diego, CA.

Powell, A.S., Jackson, L., Ardón, M., 2016. Disentangling the effects of drought, salinity, and sulfate on baldcypress growth in a coastal plain restored wetland. Restor. Ecol.. doi:10.1111/rec.12349

Reineke,L. H., 1933. Perfecting a stand-density index for even-aged forests. J. Agr. Res. 46, 627-638.

Rietkerk, M., Dekker, S.C., Ruiter, P.C. de, Koppel, J. van de, 2004. Self-Organized Patchiness and Catastrophic Shifts in Ecosystems. Science 305, 1926–1929. doi:10.1126/science.1101867

Roberts, S.D., Long, J.N., 1992. Production efficiency of Abieslasiocarpa: influence of vertical distribution of leaf area. Can. J. For. Res. 22, 1230–1234. doi:10.1139/x92-164

Roberts, S.D., Long, J.N., Smith, F.W., 1993. Canopy stratification and leaf area efficiency: a conceptualization. For. Ecol. Manag. 60, 143–156. doi:10.1016/0378-1127(93)90028-L

Robinson, W., 1950. Ecological Correlations and the Behavior of Individuals. Am. Sociol. Rev. 15, 351–357. doi:10.2307/2087176

Ryan, M.G., Yoder, B.J., 1997. Hydraulic Limits to Tree Height and Tree Growth. BioScience 47, 235–242. doi:10.2307/1313077

Souther, R.F., Shaffer, G.P., 2000. The effects of submergence and light on two age classes of baldcypress (Taxodium distichum (L.) Richard) seedlings. Wetlands 20, 697–706. doi:10.1672/0277-5212(2000)020[0697:TEOSAL]2.0.CO;2

Thorndike, E.L., 1939. On the Fallacy of Imputing the Correlations Found for Groups to the Individuals or Smaller Groups Composing Them. Am. J. Psychol. 52, 122–124. doi:10.2307/1416673

Visser, J.M., Sasser, C.E., 1995. Changes in tree species composition, structure and growth in a bald cypress-water tupelo swamp forest, 1980–1990. For. Ecol. Manag. 72, 119–129. doi:10.1016/0378-1127(94)03471-8

Vose, J.M., Allen, H.L., 1988. Leaf Area, Stemwood Growth, and Nutrition Relationships in Loblolly Pine. For. Sci. 34, 547–563.

Waring, R.H., 1983. Estimating forest growth and efficiency in relation to canopy leaf area, in: MacFadyen, A., Ford, E.D. (Eds.), Advances in Ecological Research. Academic Press, London, UK, pp. 327–354.

Waring, R.H., Newman, K., Bell, J., 1981. Efficiency of Tree Crowns and Stemwood Production at Different Canopy Leaf Densities. Forestry 54, 129–137. doi:10.1093/forestry/54.2.129

Waring, R.H., Thies, W.G., Muscato, D., 1980. Stem Growth per Unit of Leaf Area: A Measure of Tree Vigor. For. Sci. 26, 112–117.

Wharton, C.H., Kitchens, W., Pendleton, E.C., Sipe, T.W., 1982. Ecology of bottomland hardwood swamps of the southeast: a community profile, FWS/OBS-81/37. US Department of the Interior, Washington, DC.

Whilhite, L.P., Toliver, J.R., 1990. Taxodium distichum (L.)Rich. baldcypress, in: Burns, R.M., Honkala, B.H. (Eds.), Silvics of North America, Vol. 1: Conifers, Agricultural Handbook 654. US Department of Agriculture, Washington, DC., pp. 563–572.

Young, P.J., Keeland, B.D., Sharitz, R.R., 1995. Growth response of baldcypress [Taxodium distichum (L.) Rich.] to an altered hydrologic regime. Am. Midl. Nat. 133, 206–212. doi:10.2307/2426385

CHAPTER 8: CONCLUSIONS

8.1 SYNTHESIS

The studies in this dissertation spanned two ecosystem types (floodplain bottomland hardwood forest and deep-water swamp) with physical, biological, and ecological measurements at various temporal and spatial scales. Throughout, a measurable and significant effect of water variability was evident.

Chapters 2 and 3 are among the first studies of the understory energy balance in flooded wetlands, aside from flood irrigated crops (e.g., Yan et al., 2011). In addition to characterizing evaporation rates—which were high for a forest (Baldocchi et al., 2000; Iida et al., 2009) yet similar to others measured in wetlands (Brown, 1981; Liu, 1996)—these measurements demonstrated that seasonality was asynchronous with solar angle. The complementary patterns of canopy senescence and floodwater energy storage shifted the timing of peak fluxes. Unlike understories of upland forests, nearly all energy was partitioned to evaporation, regardless of weather variations. Associated with these fluxes was high humidity, but apparently also with efficient transport of humid air out of the understory.

The examination of controls over tree function—specifically, transpiration and carbon exchange inferred by growth—showed responses to hydrologic variability that were generally positive, which is unlike much of published knowledge. The many sapling studies that have been conducted generally suggest immediate and prolonged detrimental responses to flooding (Pezeshki, 2001), but there was no evidence of this in the baldcypress tree-ring chronologies or the bottomland hardwood sap flow measurements. The many prior studies that posited reduced production arising from deeper flooding (reviewed by Megonigal et al., 1997) were consistent with the baldcypress stands I measured, although my interpretation differed. Spatially, deeper flooding resulted in a more favorable growing environment, although there were also signs of suppressed growth there too (e.g., lower height). Together, Chapters 4, 5, 6, and 7 generally showed beneficial responses to more water.

To relate carbon and water, process must be considered; that is the cause of variation in plant carbon and watch fluxes must be known to assume they are related. In water-limited systems, it is typical for ring width to be related to water availability and therefore water use (Fritts, 1974); as discussed in Chapter 5, those assumptions are not transferrable to wetlands and it is unclear how ring width might relate to transpiration. Sapflow measurements in Chapter 4 convey differences in water fluxes by site, indicating differences at the stomata and thus exchanges in carbon differences can be inferred. However, it is difficult to comment on species flux differences because of biases related to position in the growing space. The phenological differences observed (Chapter 4) are likely important to relative differences in carbon and water flux patterns. Among the baldcypress stands, canopy leaf area differences reflect differences in canopy radiation interception, which controls both carbon and water exchange. In the sparser canopy sites, trees had higher growth efficiency, inferred as a result of greater light interception; this would cause higher evaporative demand at the leaf. If transpiration is higher for individual trees in the sparse sites, site transpiration is lower due to lower canopy leaf area. However, lower transpiration in sparser stands would be counter-balanced by increased evaporation with more radiation intercepted by the water.

We re-examine the hypothesized feedback cycle: if flooding causes stress that results in lower total evapotranspiration in a wetland and evapotranspiration is a control over water levels in a wetland, we must conclude there is potential for an unstable feedback cycle with a trajectory

towards wetter conditions. There are many different natural or anthropogenic hydrogeomorphic settings in which water level is controlled by ET (e.g., within levees, depressional areas and others reviewed in Batzer and Baldwin, 2012). However, we did not observe stress responses that would result in reduced transpiration to be common. Also, evaporation rates rapidly increased upon canopy senescence, and may respond similarly to a stress event resulting in leaf area reduction or stomatal closure.

While the work here presented does not represent the full range of stand structures, tree conditions, stressors, and patterns of hydrologic variability (e.g., low productivity stands with low productivity trees [Mitsch and Ewel, 1979; Brown, 1981], or flooding where high water levels are limiting to baldcypress [Young et al., 1995]), the progress made is broadly relevant. There are also cases in which water level variability results in changes in water fluxes (Wu et al., 2016). In a design similar to classic paired watershed studies (Stednick et al., 2004), Ewel and Smith (1992), concluded that ET decreased with clearcutting; however, the opposite interpretation from these data could also be justified by the results. Others have measured increases or decreases in wetland water levels after logging (reviewed in Lockaby et al., 1997). Progress in understanding these responses in upland watershed research was largely made by examining independent effects of ET components to understand how they work and contribute to the whole system (Harr and McCorison, 1979; Pearce et al., 1980). This sort of work ultimately allowed transitioning from empiricism to physically based models (Nemani et al., 1993; Tague and Band, 2004; Wigmosta et al., 1994), which should be an objective for the field of wetland ecohydrology. I believe that the empirical and conceptual progress made in this dissertation has applications towards this same mission—towards a more process-based understanding of wetland ecohydrologic processes.

8.2 REFERENCES

Baldocchi, D.D., Law, B.E., Anthoni, P.M., 2000. On measuring and modeling energy fluxes above the floor of a homogeneous and heterogeneous conifer forest. Agric. For. Meteorol. 102, 187–206. doi:10.1016/S0168-1923(00)00098-8

Batzer, D.P., Baldwin, A.H., 2012. Wetland Habitats of North America: Ecology and Conservation Concerns. University of California Press.

Brown, S., 1981. A Comparison of the Structure, Primary Productivity, and Transpiration of Cypress Ecosystems in Florida. Ecol. Monogr. 51, 403–427. doi:10.2307/2937322

Ewel, K.C., Smith, J.E., 1992. Evapotranspiration from Florida Pondcypress Swamps1. JAWRA J. Am. Water Resour. Assoc. 28, 299–304. doi:10.1111/j.1752-1688.1992.tb03995.x

Fritts, H.C., 1974. Relationships of Ring Widths in Arid-Site Conifers to Variations in Monthly Temperature and Precipitation. Ecol. Monogr. 44, 411–440. doi:10.2307/1942448

Harr, R.D., McCorison, F.M., 1979. Initial effects of clearcut logging on size and timing of peak flows in a small watershed in western Oregon. Water Resour. Res. 15, 90–94. doi:10.1029/WR015i001p00090

Iida, S. ’ichi, Ohta, T., Matsumoto, K., Nakai, T., Kuwada, T., Kononov, A.V., Maximov, T.C., Molen, V.D., K, M., Dolman, H., Tanaka, H., Yabuki, H., 2009. Evapotranspiration from understory vegetation in an eastern Siberian boreal larch forest. Agric. For. Meteorol.

Liu, S., 1996. Evapotranspiration from Cypress (Taxodium ascendens) Wetlands and Slash Pine (Pinus elliottii) Uplands in North-Central Florida (Dissertation). University of Florida, Gainesville, FL, USA.

Lockaby, B.G., Stanturf, J.A., Messina, M.G., 1997. Effects of silvicultural activity on ecological processes in floodplain forests of the southern United States: a review of existing reports. For. Ecol. Manag., Harvesting Impacts on Bottomland Hardwood Ecosystems 90, 93–100. doi:10.1016/S0378-1127(96)03897-2

Megonigal, J.P., Conner, W.H., Kroeger, S., Sharitz, R.R., 1997. Aboveground production in southeastern floodplain forests: A test of the subsidy–stress hypothesis. Ecology 78, 370–384. doi:10.1890/0012-9658(1997)078[0370:APISFF]2.0.CO;2

Mitsch, W.J., Ewel, K.C., 1979. Comparative Biomass and Growth of Cypress in Florida Wetlands. Am. Midl. Nat. 101, 417–426. doi:10.2307/2424607

Nemani, R., Pierce, L., Running, S., Band, L., 1993. Forest ecosystem processes at the watershed scale: sensitivity to remotely-sensed Leaf Area Index estimates. Int. J. Remote Sens. 14, 2519–2534. doi:10.1080/01431169308904290

Pearce, A.J., Rowe, L.K., Stewart, J.B., 1980. Nighttime, wet canopy evaporation rates and the water balance of an evergreen mixed forest. Water Resour. Res. 16, 955–959. doi:10.1029/WR016i005p00955

Pezeshki, S.R., 2001. Wetland plant responses to soil flooding. Environ. Exp. Bot. 46, 299–312. doi:10.1016/S0098-8472(01)00107-1

Stednick, J.D., Troendle, C.A., Ice, G.G., 2004. Lessons for watershed research in the future. Century For. Wildland Watershed Lessons George G Ice John Stednick Ed.

Tague, C.L., Band, L.E., 2004. RHESSys: Regional Hydro-Ecologic Simulation System—An Object-Oriented Approach to Spatially Distributed Modeling of Carbon, Water, and Nutrient Cycling. Earth Interact. 8, 1–42. doi:10.1175/1087-3562(2004)8<1:RRHSSO>2.0.CO;2

Wigmosta, M.S., Vail, L.W., Lettenmaier, D.P., 1994. A distributed hydrology-vegetation model for complex terrain. Water Resour. Res. 30, 1665–1679. doi:10.1029/94WR00436

Wu, C.-L., Shukla, S., Shrestha, N.K., 2016. Evapotranspiration from drained wetlands with different hydrologic regimes: Drivers, modeling, and storage functions. J. Hydrol. 538, 416–428. doi:10.1016/j.jhydrol.2016.04.027

Yan, H., Oue, H., Zhang, C., 2011. Predicting water surface evaporation in the paddy field by solving energy balance equation beneath the rice canopy. Paddy Water Environ. 10, 121–127. doi:10.1007/s10333-011-0273-3

Young, P.J., Keeland, B.D., Sharitz, R.R., 1995. Growth response of baldcypress [Taxodium distichum (L.) Rich.] to an altered hydrologic regime. Am. Midl. Nat. 133, 206–212. doi:10.2307/2426385

APPENDIX: COPYRIGHT PERMISSIONS

SPRINGER LICENSE
TERMS AND CONDITIONS

May 25, 2016

This Agreement between Scott T Allen ("You") and Springer ("Springer") consists of your license details and the terms and conditions provided by Springer and Copyright Clearance Center.

License Number	3876160075105
License date	May 25, 2016
Licensed Content Publisher	Springer
Licensed Content Publication	Wetlands
Licensed Content Title	Sub-canopy Evapotranspiration from Floating Vegetation and Open Water in a Swamp Forest
Licensed Content Author	Scott T. Allen
Licensed Content Date	Jan 1, 2016
Type of Use	Thesis/Dissertation
Portion	Full text
Number of copies	1
Author of this Springer article	Yes and you are the sole author of the new work
Order reference number	None
Title of your thesis / dissertation	Ecological-Hydrological Feedback in Forested Wetlands
Expected completion date	Jul 2016
Estimated size(pages)	300
Requestor Location	Scott T Allen Louisiana State University 227 Renewable Natural Resources Bldg. BATON ROUGE, LA 70803 United States Attn: Scott T Allen
Billing Type	Invoice
Billing Address	Scott T Allen Louisiana State University 227 Renewable Natural Resources Bldg. BATON ROUGE, LA 70803 United States Attn: Scott T Allen
Total	0.00 USD
Terms and Conditions	

JOHN WILEY AND SONS LICENSE TERMS AND CONDITIONS

May 25, 2016

This Agreement between Scott T Allen ("You") and John Wiley and Sons ("John Wiley and Sons") consists of your license details and the terms and conditions provided by John Wiley and Sons and Copyright Clearance Center.

License Number	3876160925760
License date	May 25, 2016
Licensed Content Publisher	John Wiley and Sons
Licensed Content Publication	Journal of Geophysical Research: Biogeosciences
Licensed Content Title	Wetland tree transpiration modified by river-floodplain connectivity
Licensed Content Author	Scott T. Allen,Ken W. Krauss,J. Wesley Cochran,Sammy L. King,Richard F. Keim
Licensed Content Date	Mar 5, 2016
Pages	14
Type of use	Dissertation/Thesis
Requestor type	Author of this Wiley article
Format	Print and electronic
Portion	Full article
Will you be translating?	No
Title of your thesis / dissertation	Ecological-Hydrological Feedback in Forested Wetlands
Expected completion date	Jul 2016
Expected size (number of pages)	300
Requestor Location	Scott T Allen Louisiana State University 227 Renewable Natural Resources Bldg. BATON ROUGE, LA 70803 United States Attn: Scott T Allen
Billing Type	Invoice
Billing Address	Scott T Allen Louisiana State University 227 Renewable Natural Resources Bldg. BATON ROUGE, LA 70803 United States Attn: Scott T Allen
Total	0.00 USD
Terms and Conditions	

TERMS AND CONDITIONS

This copyrighted material is owned by or exclusively licensed to John Wiley & Sons, Inc. or

NRC RESEARCH PRESS LICENSE
TERMS AND CONDITIONS

May 25, 2016

This is a License Agreement between Scott T Allen ("You") and NRC Research Press ("NRC Research Press") provided by Copyright Clearance Center ("CCC"). The license consists of your order details, the terms and conditions provided by NRC Research Press, and the payment terms and conditions.

All payments must be made in full to CCC. For payment instructions, please see information listed at the bottom of this form.

License Number	3876151340983
License date	May 25, 2016
Licensed content publisher	NRC Research Press
Licensed content publication	Canadian Journal of Forest Research
Licensed content title	Leaf area allometrics and morphometrics in baldcypress
Licensed content author	Scott T. Allen, Margaret L. Whitsell, Richard F. Keim
Licensed content date	Aug 1, 2015
Volume number	45
Issue number	8
Type of Use	Thesis/Dissertation
Requestor type	Author (original work)
Format	Electronic
Portion	Full article
Order reference number	None
Title of your thesis / dissertation	Ecological-Hydrological Feedback in Forested Wetlands
Expected completion date	Jul 2016
Estimated size(pages)	300
Total	0.00 USD
Terms and Conditions	

VITA

Scott T. Allen is a Baltimore-area native. Scott attended University of Maryland, College Park from 2005-2009, receiving his Bachelor of Science degree from the College of Behavioral and Social Sciences, majoring in Environmental Science and Policy with a concentration in climatology. Scott received his Master of Science degree in Water Resource Engineering through the Water Resources Graduate Program and College of Forestry at Oregon State University in 2012 with thesis research focused on the evaporation of precipitation intercepted by forest canopies, advised by Barbara J. Bond and Jeffrey J. McDonnell. Following, Scott began his doctoral program at Louisiana State University (2012-2016). He plans to pursue a research career at the intersection of physical hydrology and ecosystem ecology.